

博士論文

**Long term behavior of improved surplus soils with  
low binder contents under groundwater**

(水浸した低改良率改良土の長期挙動)

**Digala Mudiyanseelage Dayani Nadeesha Sanjeewani**

ディガラ ムディヤンセラゲ ダヤニ ナディーシャ サンジーワニ

A thesis submitted in partial fulfilment of the requirements for the degree of

**Doctor of Philosophy**

Department of Civil Engineering

The University of Tokyo

Tokyo, Japan

**September, 2019**

論文の内容の要旨  
**Thesis Summary**

**Long term behavior of improved surplus soils with low binder contents  
under groundwater**

(水浸した低改良率改良土の長期挙動)

In Japan, it is promoted to reutilize surplus soils which are generated by earthworks such as cutting and excavations due to the limitation of reclamation sites and their capacities. All the surplus soils are not suitable for direct use in earthworks. The surplus soils with less strength or trafficability which are categorized under type 3, 4 or muddy (according to surplus soil classification) need to be improved with special installation or stabilization technique due to high water content and fine content. Generally, the engineering properties of those low-quality surplus soils are improved using cement or lime with low binder contents considering cost-effectiveness and the feasibility of the project and those improved soils are frequently used as fill materials of road embankments. In such a case, those embankments are susceptible to penetration of rainwater or groundwater due to low strength. Mechanism of strength gaining/reduction of improved surplus soils with low binder contents under groundwater is not clearly understood up to date. This study was organized to increase the awareness of long-term behavior of those improved soils.

There were several objectives in this study. First was to discuss the influential factors on the progression of deterioration under soaking curing. The second was to identify the deterioration mechanism under each exposure condition. Finally, to propose a prediction methodology on long term tendency of deterioration of improved surplus soils under groundwater.

In this study, an actual surplus soil called Miho sand which contained fines around 50 % and natural water content of 31 % was improved by using cement or lime. The contents of lime were set to 1.2, 2.5 and 3.8 % by dried weight of Miho sand, while those of the cement was set to 1.7, 3.5 and 5.3 %. Cylindrical specimens with 50 mm in diameter and 100mm in height were prepared by setting dry density as of 1.4 g/cm<sup>3</sup>. All specimens were cured under two different curing conditions as sealed and soaked. In sealed curing, specimens were cured under constant temperature room tested under saturated condition by applying saturation one day before testing. To evaluate the effect of soaking from early curing period on the strength, the

second set of specimens were cured under artificially made acidic water (immature) with pH of 4.5, after applying sealed curing for initial 3 days. In addition to that additional two sets of specimens were prepared for each cement 3.5 % and lime 2.5 % contents. First sets of specimens were soaked under pure water (immature) after 3 days of their preparation to see the effect of acidity and the second sets of specimens were cured under sealed condition for initial 6 months (168 days) and soaked under the acidic water (mature) to see the effect of maturity before soaking on the strength. Unconfined compression tests and needle penetration tests were conducted periodically for up to 2 years. To understand the mechanism of long-term behavior in the aspect of chemistry X-ray Fluorescence spectrometer (XRF), Electron probe microanalyzer (EPMA) and X-ray diffractometer (XRD) were applied to the improved soil. In addition to that soaking water was analyzed.

From the unconfined compression test results, it was found a clear reduction in unconfined compressive strength,  $q_u$ , in all the cases under soaked conditions compared to the strength of specimens cured under sealed condition. Under the sealed condition,  $q_u$  values were gradually increased with curing time. Therefore, in this study, the “deterioration” at a given curing period was defined as the reduction in strength of soaked specimen with respect to the sealed specimen. In order to quantify the deterioration, strength ratio was defined as the ratio of the averaged  $q_u$  value in each soaked condition to the averaged  $q_u$  value in sealed condition. When plot the strength ratio against soaking period, it was found that there are two stages in deterioration of cement-treated soil soaked in the immature state as primary deterioration (0-25 days) and secondary deterioration (25- 672 days). Deterioration due to primary deterioration was reduced when increasing the cement content. When increasing the maturity before soaking primary deterioration did not appear. In the case of lime treatment, no primary deterioration appeared in any of the cases. Further, it was found that there was no effect of acidity on the deterioration in both cement and lime treated soil. In the cases of cement 1.7 % and lime 1.2 % cases, it was difficult to evaluate the reason for deterioration accurately due to changes in the physical properties and further analysis were not conducted.

In order to find out the reason for the appearance of two stages in deterioration, localized strength distribution along the radius of the specimen was evaluated based on needle penetration test results for each soaking case. From that analysis, it could observe two actions which were appeared in the specimen along the radius as internal deterioration and the deterioration driven from the exposed surface in cement-treated soil soaked in the immature state. In all other cases, deterioration appeared only from the action deterioration driven from

the surface. In cement-treated immature case, it was understood that primary deterioration appeared as a result of the internal deterioration. Secondary deterioration was a combined result of deterioration driven from exposed surface and recovery of internal deterioration. In the case of all lime treated soils and the cement-treated mature case secondary deterioration was due to deterioration driven from the exposed surface.

In order to find out the mechanism of appearing internal deterioration and the deterioration driven from the surface in the aspect of chemical behavior calcium ion distributions were evaluated from XRF and EPMA analysis. It was observed a clear reduction in Ca ions near the exposed surface of the specimens. However, it could not be explained the internal deterioration with Ca leaching as there was a clear reduction in strength ratio while there was a slight reduction in Ca ratio. It was suggested that internal deterioration was a result of the mobilization of ions from pore water to soaking water. However, the deterioration observed near the surface of cement-treated immature specimens were due to leaching of calcium ions. In the case of cement-treated soil in a mature state and all cases of lime treated soil, Ca leaching was identified as the reason for the deterioration driven from the surface. Ca ratio and the strength ratio throughout the specimen showed a polynomial relationship. From XRD analysis on cement-treated soil under soaked condition, it was observed the disappearance of ettringite near the exposed surface while they remained in the centre. It was suggested that Ca leaching from ettringite also contributed to strength reduction.

A methodology was developed to predict strength distribution along with the specimen after a given soaking period based on five parameters (i.e. upper bound deterioration depth, lower bound deterioration depth, upper bound localized strength ratio, lower bound strength ratio and  $q_u$  of the sealed specimen at the given time). From detailed analysis on each parameter, it was found all parameters behaved similarly against time in logarithmically and could express by a general equation.



## Acknowledgment

First and foremost, I would like to express my deepest and sincerest gratitude to my supervisor Professor Reiko Kuwano, for her sincere guidance and motivation which helped me to achieve this research successfully. Her understanding, encouraging and warm-hearted care made this research a reality.

Besides, I am deeply grateful to my Co-advisor Prof. Kenichiro Nakarai, The University of Hiroshima for his valuable guidance, suggestions, comments, and commitment given upon this study. Without him, it would be impossible for me to complete my research. I would also like to acknowledge my other Co-advisors: Prof. Junichi Koseki, Associate Prof. Kenji Watanabe, Associate Professor Takashi Kiyota, The University of Tokyo, for their valuable suggestions and support given to this research.

I wish to express my special gratitude for the department of Civil engineering in the University of Tokyo, for providing me the necessary financial assistance through SEUT-RA scholarship during my doctoral studies and believing me and my abilities.

I am grateful to Dr. Yukika Miyashita, Mr. Takashi Oota and all members in the construction technology team of Public Works Research Institute, Tsukuba for their all support given through this journey. My special appreciation goes to Dr. Shusaku Yamazaki from CERI, Hokkaido, Mr. Atsunori Negishi from Ando Hazama co-operation and Mr. Izuo from Japan cement Association for their kind support and the guidance on chemical analysis.

My special appreciation goes to Dr. Masahide Otsubo for his kind helps for the smooth progress of this study and laboratory life.

I am also very much grateful to Ms. Satoko Kichibayashi for her kind support in handling the administrative aspects during my study. Her cheerful attitude and warm-hearted care are highly appreciated.

I would like to convey my heartiest gratitude all lab members in Kuwano Laboratory for helping me in every way. Without your friendship and support, I would not be able to be a success in this research.

I would like to give my special thanks to Dr. Nalin de Silva, University of Moratuwa and Dr. Fowze, Central Engineering Consultancy Bureau who recommended me to the University of Tokyo for believing me and inspiring me.

I would love to give my heartiest gratitude to my dearest husband Dr. Chamila Rankoth for his continuous support and encouragement during this journey. This thesis is dedicated to him for standing near me as a shadow until I fulfil my dream. Finally, my special gratitude is directed to my parents, family members for their kind support.

At last but not least, I am grateful to all the people who met me so far in life and helped me even by a single smile.

**Dayani Sanjeewani**

September 2019

Tokyo, Japan

## Table of Contents

<b>1</b>	<b>Introduction</b> .....	1-1
1.1	Background.....	1-1
1.2	Significance of the study.....	1-2
1.3	Objective and Scope .....	1-3
1.4	Methodology.....	1-3
1.5	Structure of dissertation .....	1-4
1.6	Reference.....	1-5
<b>2</b>	<b>Literature review</b> .....	2-1
2.1	Cement Stabilization.....	2-1
2.1.1	Chemical reaction and treatment mechanism .....	2-1
2.1.2	Effect of Cement treatment on the geotechnical properties of soil.....	2-4
2.2	Lime Stabilization.....	2-5
2.2.1	Chemical reactions and their effect on geotechnical properties .....	2-5
2.3	Long term behavior of improved soils.....	2-6
2.4	Evaluation method of deterioration .....	2-8
2.4.1	Empirical models .....	2-8
2.5	Reference .....	2-10
<b>3</b>	<b>Material, Apparatus and testing procedures</b> .....	3-1
3.1	Introduction.....	3-1
3.2	Material properties .....	3-1
3.2.1	Miho sand.....	3-1
3.2.2	Cement .....	3-2
3.2.3	Lime .....	3-2
3.3	Mixing proportions and specimen preparation method .....	3-2
3.4	Curing method .....	3-3
3.5	Unconfined compression test.....	3-4

3.5.1	Apparatus .....	3-4
3.5.2	Devices for measuring stress .....	3-5
3.5.3	Device for measuring strain .....	3-5
3.5.4	Testing procedure.....	3-6
3.6	Needle penetration test.....	3-6
3.6.1	Apparatus .....	3-7
3.6.2	Testing procedure.....	3-7
3.7	Electron probe micro analysis (EPMA).....	3-7
3.7.1	Apparatus .....	3-7
3.7.2	Specimen preparation.....	3-8
3.7.3	Testing procedure.....	3-8
3.8	X-ray Fluorescence spectrometer analysis (XRF) .....	3-9
3.8.1	Apparatus .....	3-9
3.8.2	Specimen preparation.....	3-9
3.8.3	Testing procedure.....	3-9
3.9	X-ray diffractometer analysis (XRD) .....	3-9
3.9.1	Apparatus .....	3-9
3.9.2	Specimen preparation.....	3-10
3.9.3	Testing procedure.....	3-11
3.10	Soaking water measurement .....	3-12
3.12	Reference .....	3-13
<b>4</b>	<b>Influential factors on the progression of deterioration .....</b>	<b>4-1</b>
4.1	Introduction.....	4-1
4.2	Unconfined compression test results .....	4-1
4.2.1	Stress strain relationship .....	4-1
4.2.2	Relationship between curing period and $q_u$ , $E_{50}$ in sealed and soaked conditions. .....	4-1

4.3	Progression of deterioration .....	4-5
4.3.1	Definition of deterioration and its stages .....	4-5
4.3.2	Influence of soaking water type .....	4-5
4.3.3	Influence of binder content .....	4-6
4.3.4	Influence of gained strength before soaking .....	4-6
4.3.5	Influence of binder type .....	4-7
4.3.6	Summary on influential factors on progression of deterioration .....	4-7
4.4	Needle Penetration test results .....	4-7
4.4.1	Evaluation method for localized strength .....	4-9
4.4.2	Localized strength ratio distribution along depth .....	4-9
4.4.3	Definition of parameters to describe localized strength distribution .....	4-10
4.4.4	Variation of deterioration depths ( $D_U$ and $D_L$ ), localized strength ratios ( $S_U$ and $S_L$ ) with soaking period.....	4-11
4.5	Summary and conclusion .....	4-12
4.6	Reference .....	4-14
<b>5</b>	<b>Mechanism of deterioration .....</b>	<b>5-1</b>
5.1	Introduction.....	5-1
5.2	Soaking water analysis results .....	5-1
5.3	Ca ion distribution in specimen .....	5-2
5.3.1	EPMA analysis results .....	5-2
5.3.2	XRF analysis results .....	5-3
5.4	Mechanism of internal deterioration and its recovery .....	5-3
5.5	Mechanism of deterioration driven from surface.....	5-4
5.5.1	Cement treated soil (immature) soaking .....	5-4
5.5.2	Cement treated soil (mature) soaking .....	5-5
5.5.3	Lime treated all soaked cases.....	5-5
5.6	Mineral identification.....	5-6

5.7	Summary and conclusions .....	5-7
5.8	Reference .....	5-8
<b>6</b>	<b>Prediction methodology for long term durability of improved surplus soils with low binder contents .....</b>	<b>6-1</b>
6.1	Introduction to propose methodology .....	6-1
6.2	Definition of parameters .....	6-1
6.3	Deterioration depths.....	6-2
6.3.1	Cement treated soil .....	6-2
6.3.2	Lime treated soil .....	6-2
6.3.3	Factors influencing deterioration rate coefficient .....	6-3
6.4	Localized strength ratios .....	6-3
6.4.1	Cement treated soil .....	6-3
6.4.2	Lime treated soil .....	6-4
6.4.3	Factors influencing localized strength rate coefficient .....	6-4
6.5	Unconfined compressive strength of sealed curing .....	6-5
6.5.1	Factors influencing deterioration rate coefficient .....	6-5
6.6	Summary of parameters and influential factors .....	6-5
6.7	Limitation of the proposed model.....	6-6
<b>7</b>	<b>Conclusions and Recommendations .....</b>	<b>7-1</b>
<b>Annex A</b>	.....	<b>An-1</b>
<b>Annex B</b>	.....	<b>An-6</b>
<b>Annex C</b>	.....	<b>An-29</b>
<b>Annex D</b>	.....	<b>An-41</b>
<b>Appendix 1</b>	.....	<b>Ap-1</b>
<b>Appendix 2</b>	.....	<b>Ap-11</b>

## List of figures

Figure 1:1 Flow of surplus soil generation and utilization in 2012 (Katsumi et al 2015) .....	1-7
Figure 1:2 Utilization of surplus soils in earthworks .....	1-7
Figure 1:3 Japanese standard classification for surplus soils (Shimazu, 2002).....	1-8
Figure 1:4 Strength gained under-groundwater after 9 years of an embankment constructed with surplus soils (Miyashita and Inoue, 2018) .....	1-9
Figure 1:5 Methodology .....	1-10
Figure 2:1 Compressive strength development in pastes of pure cement compounds .....	2-14
Figure 2:2 Microstructure of hydration products.....	2-14
Figure 2:3 Porosity changes with time.....	2-14
Figure 2:4 Rate of heat evolution during hydration of Portland cement .....	2-15
Figure 2:5 Ion equilibrium in solid phase and pore solution (Yamada 2015) .....	2-15
Figure 2:6 pH and ionic strength variation of cement pastes (Rothstein et al. 2002).....	2-15
Figure 2:7 SI of (a) Portlandite (b) Gypsum (c) Ettringite (d) Monosulphate in the cement paste (Rothstein et al. 2002).....	2-16
Figure 2:8 Factors affecting on the properties of cement treated soil.....	2-16
Figure 2:9 Strength increase model of cement Katoh, 2018) .....	2-17
Figure 2:10 Cation exchange (Smith et al. 2014) .....	2-17
Figure 2:11 Particle restructuring -Flocculation and agglomeration (Smith et al. 2014) ....	2-18
Figure 2:12 Increase of silicon and aluminum solubility in high pH environment (Cuisinier 2010) .....	2-18
Figure 2:13 Strength change model for quick lime (Katoh, 2018).....	2-19
Figure 2:14 Parameters on prediction methodology of deterioration depth (Jilai,2013).....	2-19
Figure 3:1 Methodology .....	3-17
Figure 3:2 Location where Miho sand was taken .....	3-17
Figure 3:3 Particle size distribution of Miho sand.....	3-18
Figure 3:4 Amorphous content in Miho sand .....	3-18
Figure 3:5 Minerals identified by XRD analysis- Miho sand.....	3-19
Figure 3:6 Minerals identified by XRD -Quick lime.....	3-19
Figure 3:7 Mineral identified by XRD -Cement.....	3-19
Figure 3:8 Specimen preparation method (a) Mixture (b) Standard Mold (c) Dimensions of specimen .....	3-20

Figure 3:9 Standard proctor compaction curve (a) cement treated soil (b) Lime treated soil .....	3-20
Figure 3:10 Curing conditions (a) Sealed condition (b) Soaked condition (c) Systematic figure of an road embankment which simulate each curing conditions .....	3-21
Figure 3:11 Change of acidity of precipitation .....	3-21
Figure 3:12 Setting up of tap lines for changing soaking water .....	3-21
Figure 3:13 Unconfined compression test apparatus .....	3-22
Figure 3:14 Load cell .....	3-22
Figure 3:15 Calibration curves for load cell (a) 2 kN (b) 10 kN .....	3-23
Figure 3:16 (a) External Displacement Transducer (EDT) (b) Calibration curve of EDT ..	3-23
Figure 3:17 Range of applicability of Needle penetration test .....	3-24
Figure 3:18 Needle penetration test apparatus setup .....	3-24
Figure 3:19 Needle penetration test- method 1 .....	3-25
Figure 3:20 (a) Needle penetration test -method 2 (b) Illustration of needle penetrated depth and the location .....	3-25
Figure 3:21 (a) cross section from middle height of specimen (b) EPMA apparatus.....	3-26
Figure 3:22 Configuration of EPMA .....	3-26
Figure 3:23 XRF apparatus .....	3-27
Figure 3:24 (a) Powdered sample collected location (b) Whitish deposition at outermost layer .....	3-27
Figure 3:25 Compacted soil specimen for XRF analysis.....	3-28
Figure 3:26 XRD apparatus .....	3-28
Figure 3:27 Acetone application .....	3-28
Figure 3:28 (a) Heavy liquid (b) mixing proportion (c) separation using centrifugal rotation....	3-29
Figure 3:29 After separation of lighter particles by heavy liquid method.....	3-29
Figure 3:30 (a) Agate mill (b) leveling of specimen (c) prepared specimen for XRD analysis .....	3-29
Figure 3:31 apparatus for measuring pH of soaking water .....	3-30
Figure 4:1 Stress strain relationship after curing of 672 days (a) cement 3.5 % (b) Lime 2.5 % .....	4-16
Figure 4:2 Calculation method for deformation modulus, $E_{50}$ .....	4-17



Figure 4:3 relationship between $q_u$ and curing period of cement treated soil -sealed condition .....	4-17
Figure 4:4 Relationship between $q_u$ and curing period for lime treated soil- sealed condition .....	4-18
Figure 4:5 Relationship between unconfined compressive strength and curing period of cement treated soil .....	4-19
Figure 4:6 Relationship between deformation modulus and curing time of cement treated soil .....	4-20
Figure 4:7 Relationship between unconfined compressive strength and curing period of lime treated soils .....	4-21
Figure 4:8 Relationship between deformation modulus and curing period of lime treated soil .....	4-22
Figure 4:9 Relationship between unconfined compressive strength and deformation modulus (a) cement treated soil (b) lime treated soil .....	4-23
Figure 4:10 Stages in deterioration of soaked C3.5 acid (immature) .....	4-24
Figure 4:11 Influence of soaking water type - C3.5 soaked (immature) .....	4-24
Figure 4:12 Variation of pH with soaking period- C3.5 soaked (immature).....	4-25
Figure 4:13 Influence of cement content- soaked (immature).....	4-25
Figure 4:14 Influence of maturity before soaking -C3.5 .....	4-26
Figure 4:15 Influence of binder type soaked (immature) .....	4-26
Figure 4:16 Influence of soaking water type -L2.5 soaked (immature) .....	4-27
Figure 4:17 Variation of pH with soaking period- L2.5 (immature) .....	4-27
Figure 4:18 Influence of lime content- soaked (immature) .....	4-28
Figure 4:19 Influence of maturity before soaking -L2.5 acid.....	4-28
Figure 4:20 Relationship between E50 ratio and soaking period (a) cement treated soil (b) Lime treated soil.....	4-29
Figure 4:21 Needle penetration test results- C3.5 sealed and soaked (immature).....	4-30
Figure 4:22 Needle penetration test results- C3.5 sealed and soaked (mature).....	4-31
Figure 4:23 Needle penetration test results C5.3 sealed and soaked (immature) .....	4-32
Figure 4:24 Needle penetration test results - L2.5 sealed and soaked (immature) .....	4-33
Figure 4:25 Needle penetration test results- L2.5 sealed and soaked (matured) .....	4-34
Figure 4:26 Needle penetration test results- L3.8 sealed and soaked (immature).....	4-35
Figure 4:27 Evaluation method of needle penetration resistance rate .....	4-36

Figure 4:28 Relationship between needle penetration resistance ratio and unconfined compressive strength of sealed specimens.....	4-36
Figure 4:29 Relationship of UCS and NPRR recommended by previous researchers .....	4-37
Figure 4:30 Comparison of existing empirical models and the results obtained in this study to predict UCS from NPR .....	4-37
Figure 4:31 Estimated UCS for sealed and soaked specimens based on the relationship between NPRR and UCS.....	4-38
Figure 4:32 Relationship between localized strength ratio and the distance from exposed surface- C3.5 acid (immature) .....	4-38
Figure 4:33 Relationship between localized strength ratio and the distance from exposed surface- C3.5 pure (immature).....	4-39
Figure 4:34 Relationship between localized strength ratio and the distance from exposed surface -C5.3 acid (immature) .....	4-39
Figure 4:35 Relationship between localized strength ratio and the distance from exposed surface- C3.5 acid (mature).....	4-40
Figure 4:36 Relationship between localized strength ratio and the distance from exposed surface- L2.5 acid (immature).....	4-40
Figure 4:37 Relationship between localized strength ratio and the distance from exposed surface- L2.5 pure (immature) .....	4-41
Figure 4:38 Relationship between localized strength ratio and the distance from exposed surface- L3.8 acid (immature).....	4-41
Figure 4:39 Relationship between localized strength ratio and the distance from exposed surface -L2.5 acid (mature).....	4-42
Figure 4:40 General distribution of localized strength ratio at a given soaking period.....	4-42
Figure 4:41 Relationship between estimated UCS and experimental UCS for soaked specimens (a) cement treated soil (b) Lime treated soil .....	4-43
Figure 4:42 C3.5Soak-acid (immature) (a) variation of deterioration depth (b) variation of localized strength ratio .....	4-44
Figure 4:43 C3.5-Soak Pure (immature) (a) variation of deterioration depth (b) variation of localized strength ratio .....	4-45
Figure 4:44 C5.3-Soaked (immature) (a) Variation of deterioration depth (b) Variation of localized strength ratio .....	4-46
Figure 4:45 C3.5-Soak acid (mature) (a) Variation of deterioration depth (b) Variation of localized strength ratio .....	4-47

Figure 4:46 L2.5 Soak acid (immature) (a) deterioration depth (b) localized strength ratio	4-48
Figure 4:47 L2.5 Soak Pure (immature) (a) Deterioration depth (b) localized strength ratio .....	4-49
Figure 4:48 L3.8 Soak acid (immature) (a) deterioration depth (b) Localized strength ratio .....	4-50
Figure 4:49 L2.5- Soak acid (immature) (a) deterioration depths (b) Localized strength ratios.	4-51
Figure 5:1 pH of soaking water (a) Lime treated soil (b) Cement treated soil .....	5-11
Figure 5:2 Cumulative amount of leached Ca (a) Lime treated soil (b) Cement treated soil .....	5-12
Figure 5:3 Cumulative amount of leached sulphate (a) Lime treated soil (b) Cement treated soil .....	5-13
Figure 5:4 Elimination method of voids and soil particles .....	5-14
Figure 5:5 Averaging method along radius .....	5-15
Figure 5:6 EPMA-Ca ion distribution C3.5-Acid (immature).....	5-16
Figure 5:7 EPMA- Ca ion distribution L3.8-Acid (immature) .....	5-17
Figure 5:8 EPMA-Ca ion distribution L2.5 Soak acid (immature) .....	5-18
Figure 5:9 XRF-Ca ion distribution-Cement treated soil .....	5-19
Figure 5:10 XRF-Ca ion distribution- Cement treated soil (change vertical scale) .....	5-20
Figure 5:11 XRF-Ca ion distribution-Lime treated soil .....	5-21
Figure 5:12 XRF-Ca ion distribution- Lime treated soil (change vertical axis).....	5-22
Figure 5:13 Thin CaCO <sub>3</sub> layer precipitated after 672 days soaking of (a) C 5.3 (b) L3.8...	5-23
Figure 5:14 Variation of S <sub>U</sub> of C3.5- soak acid (immature) .....	5-23
Figure 5:15 Ca ratio and Strength ratio relationship with soaking period-.....	5-24
Figure 5:16 Ca ratio and Strength ratio relationship with soaking period- C3.5 Pure (immature) .....	5-24
Figure 5:17 Ca ratio and Strength ratio relationship with soaking period- C5.3 Acid (immature) .....	5-25
Figure 5:18 Leaching of sulphate ions with soaking period-C3.5 Soak acid (immature) ...	5-25
Figure 5:19 Relationship with Ca ratio and S <sub>L</sub> at 0-5mm.....	5-26
Figure 5:20 Relationship between Ca ratio and localized strength ratio- C3.5 Soaked acid (mature).....	5-27
Figure 5:21 L2.5-Soaked acid (immature).....	5-28
Figure 5:22 L2.5- Soaked Pure (immature) .....	5-29

Figure 5:23 L2.5- Soaked acid (mature).....	5-30
Figure 5:24 L3.8- Soaked acid (immature).....	5-31
Figure 5:25 Dual pore model.....	5-32
Figure 5:26 XRD results – C 5.3 Selaed-7 days.....	5-33
Figure 5:27 XRD results-C5.3 Sealed-28 days.....	5-34
Figure 5:28 XRD results- C5.3 Sealed-672 days.....	5-35
Figure 5:29 XRD results- C5.3 Sealed 28 days, 672 days after applying heavy liquid treatment .....	5-36
Figure 5:30 XRD results- C5.3 Soaked acid (immature) -672 days(20-25mm).....	5-37
Figure 5:31XRD results- C5.3 Soaked acid (immature) -672 days (0-5mm).....	5-38
Figure 5:32XRD results- C5.3 Soaked acid (immature) -672 days (0-5mm), (20-25mm)-after heavy liquid treatment.....	5-39
Figure 5:33 XRD results- L3.8 Sealed.....	5-40
Figure 5:34 XRD results-L3.8 Soaked.....	5-41
Figure 5:35 XRD results- L3.8 after applying heavy liquid treatment.....	5-42
Figure 6:1 General model for Localized strength distribution at a given soaking period.....	6-7
Figure 6:2 Relationship between $D_L$ and soaking period of cement treated soil.....	6-7
Figure 6:3 Relationship between $D_U$ and soaking period for Cement treated soil.....	6-8
Figure 6:4 Relationship between $D_U$ and soaking period for Lime treated soil.....	6-8
Figure 6:5 Factors influencing deterioration rate coefficient (a) Cement treated soil (b) Lime treated soil.....	6-9
Figure 6:6 Relationship of $S_L$ with soaking period of cement treated soil.....	6-9
Figure 6:7 Relationship between $S_U$ and soaking period for cement treated soil.....	6-10
Figure 6:8 Relationships of (a) $S_L$ (b) $S_U$ with soaking period for lime treated soil.....	6-11
Figure 6:9 Factors influencing localized strength rate (a) cement treated soil (b) Lime treated soil.....	6-12
Figure 6:10 Variation of unconfined compressive strength of sealed specimens for cement treated soil.....	6-12
Figure 6:11 Variation of unconfined compressive strength of sealed specimens for lime treated soil.....	6-13
Figure 6:12 Variation of strength gaining rate.....	6-13

## List of tables

Table 2.1 Properties of the compounds of cement.....	2-2
Table 3:1 Physical and mechanical properties of Miho sand .....	3-1
Table 3:2 Chemical properties of Miho sand and binders .....	3-2
Table 3:3 Mixing proportions .....	3-3
Table 3:4 Summary of testing case and curing conditions .....	3-5
Table 3:5 Difference between standard test and this study.....	3-6
Table 3:6 Summary of EPMA analysis .....	3-8
Table 3:7 Density of hydration products .....	3-12
Table 3:8 Setting of XRD apparatus.....	3-12
Table 4:1 Summary of $q_u$ and $E_{50}$ for cement treated soil.....	4-3
Table 4:2 Summary of $q_u$ and $E_{50}$ for Lime treated soil.....	4-4
Table 6:1 Summary of constants for $S_U$ cement treated soil.....	6-4
Table 6:2 Summary of constants for $S_U$ and $S_L$ lime treated soil .....	6-4
Table 6:3 Summary of equations for 5 parameters in the model.....	6-6

# 1 Introduction

## 1.1 Background

In Japan, excavations for infrastructure development such as buildings, subways generate large quantities of surplus soils (construction generated soil). According to the Japanese Ministry of Land, Infrastructure Transport and Tourism (MLIT), it was reported 140 million cubic meters of surplus soils in 2012 all over the country. This excessive generation of surplus soils caused by several problems as;

- Difficult to find reclamation sites for dumping these soils especially around large cities like Tokyo and Osaka.
- Limited capacities in reclamation sites
- Traffic congestion due to transportation for far yards
- Additional cost for disposing of large quantities of surplus soils

To overcome such circumstance, MLIT adopted a plan called ‘Construction Recycling Promotion Plan’ by setting a goal for re-utilization of surplus soil for public works projects either at the generating site or at different places. Figure 1:1 shows the flow of surplus soil generations and utilization in 2012 (Katsumi, 2015). In that year 26 million cubic meters of new soil materials from natural resources such as mountains or riverbeds were utilized. If it is possible to reutilize more surplus soils it can reduce the utilization of natural resources also.

Generally, surplus soils utilize as backfill or embankment material in earthworks. According to the survey of construction by-product which was conducted by MLIT in 2012, about 90 % of the whole soils employed in earthworks have been occupied by surplus soils as shown in Figure 1:2. In order to evaluate engineering properties of surplus soils, a standard classification system was introduced by MLIT in 1997 as shown in Figure 1:3 and surplus soils has classified into five types based on the soil type, cone index, water content, and fine content. Most (Shimazu, 2002) of the excavated soils categorized as Type 1 and Type 2 are basically re-usable without any stabilizing process while the materials with high water content and fine grain particles which are categorized in Type 3, 4 and muddy require some type of special installation or stabilization techniques due to less strength and trafficability.

---

## 1.2 Significance of the study

Generally, the engineering properties of those low-quality surplus soils are improved using chemical stabilization with cement or lime and frequently used as fill materials of road embankments. The durability and stability of those embankments are affected by the change in the long-term mechanical properties of the improved soil. Generally, practitioners tend to use low binder contents to improve a large volume of low-quality surplus soil by considering cost-effectiveness and the feasibility of the ongoing project. The minimum contents of binder recommended for cement and lime treatment are  $50 \text{ kg/m}^3$  and  $30 \text{ kg/m}^3$  respectively according to the manuals published by Japan cement association and Japan lime association. In such a case, the embankments constructed with improved soils with low binder contents are susceptible to penetration of rainwater or groundwater due to high permeability.

In general, it is well known that the strength of the improved soils increases with the curing period under controlled laboratory conditions, due to the chemical reactions between soil and binders. However, according to the site investigation conducted on a high embankment (cement-treated) in Japan, unconfined compressive strength at a certain depth below the groundwater level was hardly increased from the strength nine years ago as shown in Figure 1:4 (b) and (c) (Miyashita & Inoue, 2018). One of the possible reasons for this behavior is a negative effect from clay minerals such as allophane or amorphous contents in surplus soils on the chemical stabilization. Several studies have been conducted on the effect of those minerals and their effects on the cement and lime stabilization (Ei-kon, 1998; Kett, Ingham, & Evans, 2010; Kobashi, 1967). The other possible reason is the negative effect on the strength due to soaking under groundwater. The literature on the effect of soaking on the strength of surplus soils improved with low binder contents can be considered as zero. Most of the previous studies were conducted on the treated soil soaked under seawater in deep mixing method where larger binder contents were used (Hara, Suetsugu, & Hayashi, 2012; Hara, Suetsugu, Hayashi, & Matsuda, 2014; Kitazume, Nakamura, Terashi, & Ohishi, 2003; Ngoc, Turner, Huang, & Kelly, 2016; Takahashi, Morikawa, Fujii, & Kitazume, 2017; Yang, Yan, Liu, & Zhang, 2016) as summarized in chapter 2. Therefore, it was important to study the long-term behavior of the improved surplus soils under groundwater to increase the awareness of the possible mechanism that would undergo.

### 1.3 Objective and Scope

As discussed earlier, the aim of this study was to understand the long-term behavior of improved surplus soils with low binder content under groundwater by;

1. To evaluate the influential factors on the progression of deterioration.

In this study, actual surplus soil called Miho sand was used. This material was classified as mud in surplus soil classification and it contained low amorphous contents whose effect on the chemical stabilization could be neglected. Unconfined compression test and needle penetration test were conducted on improved Miho sand with cement / lime with low binder contents under sealed and soaked conditions. Effect of binder content, binder type, the acidity of soaking water and the maturity before soaking were studied to understand the possible factors influenced on the deterioration caused by soaking.

2. To evaluate the mechanism of deterioration in the aspect of chemical behavior.

In order to identify the possible mechanism on the deterioration caused by soaking of the improved surplus soils in the aspect of chemical behavior, several chemical tests were conducted to evaluate calcium ion distribution and for the mineral identification.

3. To propose a prediction methodology on long term tendency of deterioration.

It is important to know the possible deterioration of improved soils with low binder contents in long term, at the early stages of the design to decide the application by considering their life span and the possible strength reduction due to soaking. A methodology was developed to predict strength distribution along with the specimen after a given soaking period based on five parameters (i.e. upper bound deterioration depth, lower bound deterioration depth, upper bound localized strength ratio, lower bound strength ratio and  $q_u$  of the sealed specimen at the given time).

### 1.4 Methodology

As explained in Figure 1:5, a series of mechanical and chemical tests were conducted on the improved surplus soils with cement and lime treatment periodically up to 2 years under sealed and soaked conditions to evaluate the long term behavior of those improved soil under groundwater. Those results were used to understand the mechanism of deterioration and to establish a prediction methodology.



## 1.5 Structure of the dissertation

<b>Chapter 1</b>	<b>Introduction</b> The background regarding the reutilization of surplus soils, the significance of the study, objectives and the methodology was presented.
<b>Chapter 2</b>	<b>Literature review</b> A brief review of the previous studies on the long-term behavior of improved cement and lime treated soils were conducted.
<b>Chapter 3</b>	<b>Material, apparatus and testing procedures</b> The test material, apparatus, and measurement system mainly used in this study were presented.
<b>Chapter 4</b>	<b>Influential factors on the progression of deterioration</b> The factors influenced the progression of deterioration of improved surplus soils were evaluated based on unconfined compression and needle penetration test results.
<b>Chapter 5</b>	<b>Mechanism of deterioration of improved surplus soils</b> Mechanism of deterioration of improved soils in the aspect of chemical behavior was explained.
<b>Chapter 6</b>	<b>Prediction methodology for long term durability of improved surplus soils with low binder contents</b> An empirical model was developed to predict strength distribution.
<b>Chapter 7</b>	<b>Conclusions and recommendations</b> Conclusions of the current study and recommendations for the further studies were presented

<b>Annex A</b>	<b>Material data</b> Datasheet for cement and quick lime and the laboratory testing results on physical properties of improved soil are presented.
----------------	---

<b>Annex B</b>	<b>Unconfined compression test results</b> Summary of physical properties, stress-strain curves and failure pattern are presented.
<b>Annex C</b>	<b>Needle penetration test results (Method 1)</b> The original measurements obtained are summarized.
<b>Annex D</b>	<b>Summary of original data from XRF analysis</b> Oxides percentages measured in each curing period are presented.

<b>Appendix 1</b>	<b>Unconfined compressive strength under the sealed-unsaturated condition</b>
<b>Appendix 2</b>	<b>Needle penetration test results- Method 2</b>

## 1.6 Reference

- Ei-kon, S. 1998. Statistical correlation between allophane content and index properties for volcanic cohesive soil. *Soils and Foundations*, 38(4): 85–93.
- Hara H., Suetsugu D., & Hayashi S. 2012. Calcium Leaching Mechanism of Lime Treated Soil Immersed in Seawater. *Journal of the Society of Materials Science, Japan*, 61(1): 11–14.
- Hara H., Suetsugu D., Hayashi S., & Matsuda H. 2014. Deterioration Progress of Cement-Treated Ariake Clay under Seawater. *Journal of the Society of Materials Science, Japan*, 63(1): 49–54.
- Katsumi, T. 2015. Soil excavation and reclamation in civil engineering: Environmental aspects. *Soil Science and Plant Nutrition*, 61(sup1): 22–29.
- Kett, I. J., Ingham, J., & Evans, J. 2010. Identifying an effective binder for the stabilization of allophanic soils. *International Journal of Pavement Engineering*, 11(3): 223–236.
- Kitazume, M., Nakamura, T., Terashi, M., & Ohishi, K. 2003. *Laboratory Tests on Long-Term Strength of Cement Treated Soil*, 586–597. Presented at the Grouting and ground treatment.

- Kobashi, T. 1967. *Reaction of calcium hydroxide with allophane-Kaolinite clay minerals*, 3(1–2): 11–36.
- Miyashita, Y., & Inoue, G. 2018. *Long term mechanical property of cement treated loam used in road embankment*, 1151–1159. Presented at the Conference of Deep Foundations and Ground Improvement, Rome.
- Ngoc, P. V., Turner, B., Huang, J., & Kelly, R. 2016. *Experimental Study on the Durability of Soil-Cement Columns in Coastal Areas*, 6.
- Shimazu, A. 2002. Use of excavated excess soils in earthworks. *International Seminar on the Appropriate Use of Natural Materials in Road*.
- Takahashi, H., Morikawa, Y., Fujii, N., & Kitazume, M. 2017. Thirty-seven-year investigation of quicklime-treated soil produced by deep mixing method. *Proceedings of the Institution of Civil Engineers - Ground Improvement*, 1–13.
- Yang, J., Yan, N., Liu, Q., & Zhang, Y. 2016. Laboratory test on long-term deterioration of cement soil in seawater environment. *Transactions of Tianjin University*, 22(2): 132–138.

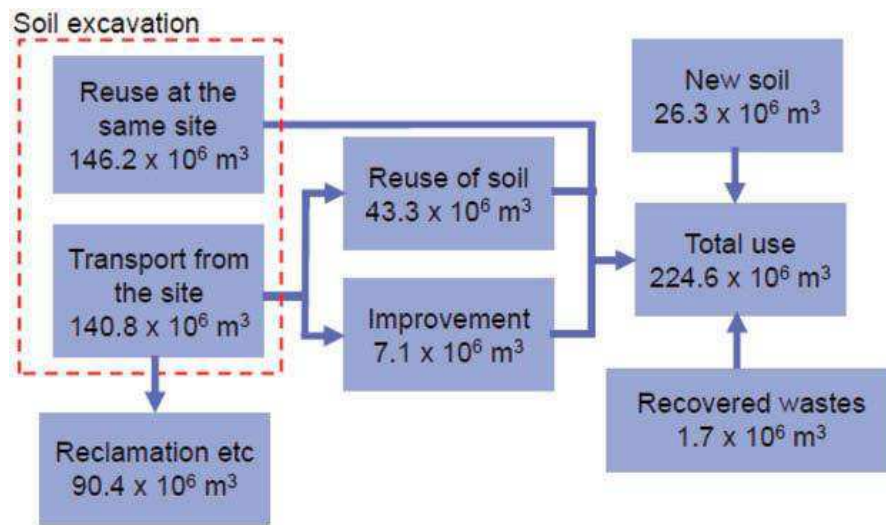
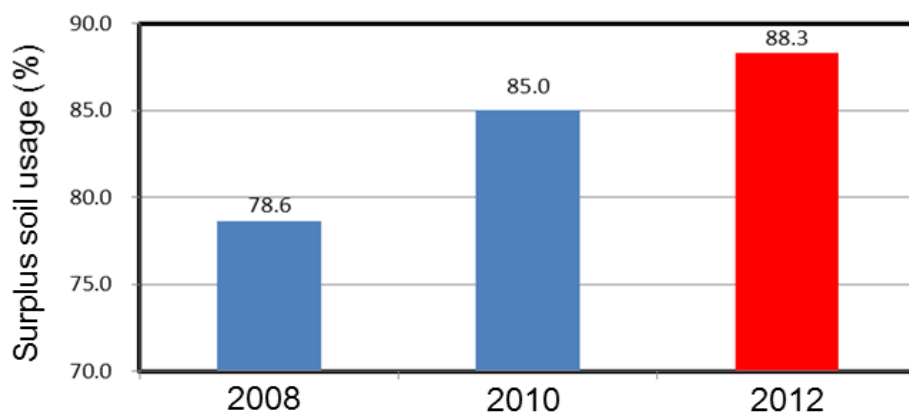


Figure 1:1 Flow of surplus soil generation and utilization in 2012 (Katsumi, 2015)



Surplus soil utilization rate (actual value) according to “Construction recycling promotion plan”, Ministry of Land, Infrastructure, Transportation and Tourism (MLIT), Japan

Figure 1:2 Utilization of surplus soils in earthworks

Class of Excess soil	Sub-division	Cone Index qc	Unified soil classification		Water content (natural gr.)
				Soil equiv.	
1 <sup>st</sup> excess soil (sand, gravel & so)	1 <sup>st</sup>		{G}	Gravel	—
			{S}	Sand	—
	1 <sup>st</sup> improved			(improved soil)	—
2 <sup>nd</sup> excess soil (sandy soil, gravelly soil & so)	2a	800KN /m2 or more	{GF}	Gravelly soil	—
	2b		{SF}	Sandy soil (Fc : 15-25%)	—
	2c			Sandy soil (Fc : 25-50%)	30% less
	2 <sup>nd</sup> improved			(improved soil)	—
3 <sup>rd</sup> excess soil (clayey soil & so applicable to normal works)	3a	400KN /m2 or more	{SF}	Sandy soil (Fc : 25-50%)	30-50%
	3b		{M},{C}	Silt, Clayey soil	40% less
	3 <sup>rd</sup> improved		{V}	Volcanic clayey (improved soil)	—
4 <sup>th</sup> excess soil (clayey soil & so except 3 <sup>rd</sup> one above)	4a	200KN /m2 or more	{SF}	Sandy soil (Fc : 25-50%)	—
	4b		{M},{C}	Silt, Clayey soil	40-80%
			{V}	Volcanic clayey	—
	4 <sup>th</sup> improved		{O}	Organic soil (improved soil)	40-80%
Muddy soil (dredged soil of qc less than 200KN/m2)	Muddy a	200kN /m2 less	{SF}	Sandy soil (Fc : 25-50%)	—
	Muddy b		{M},{C}	Silt, Clayey soil	80% less
			{V}	Volcanic clayey	—
	Muddy c		{O}	Organic soil	80% less
		{Pt}	Highly Organic	—	

qc : cone penetration resistance( 3.24cm<sup>2</sup> & 30° cone) on compacted sample in the compaction mold(φ 100mm, 127mm height, in 3 layers, 25 blows on each layer of 30cm falling height of 25N rammer)

Fc : fine grain content less than 74 μ

Figure 1:3 Japanese standard classification for surplus soils (Shimazu, 2002)

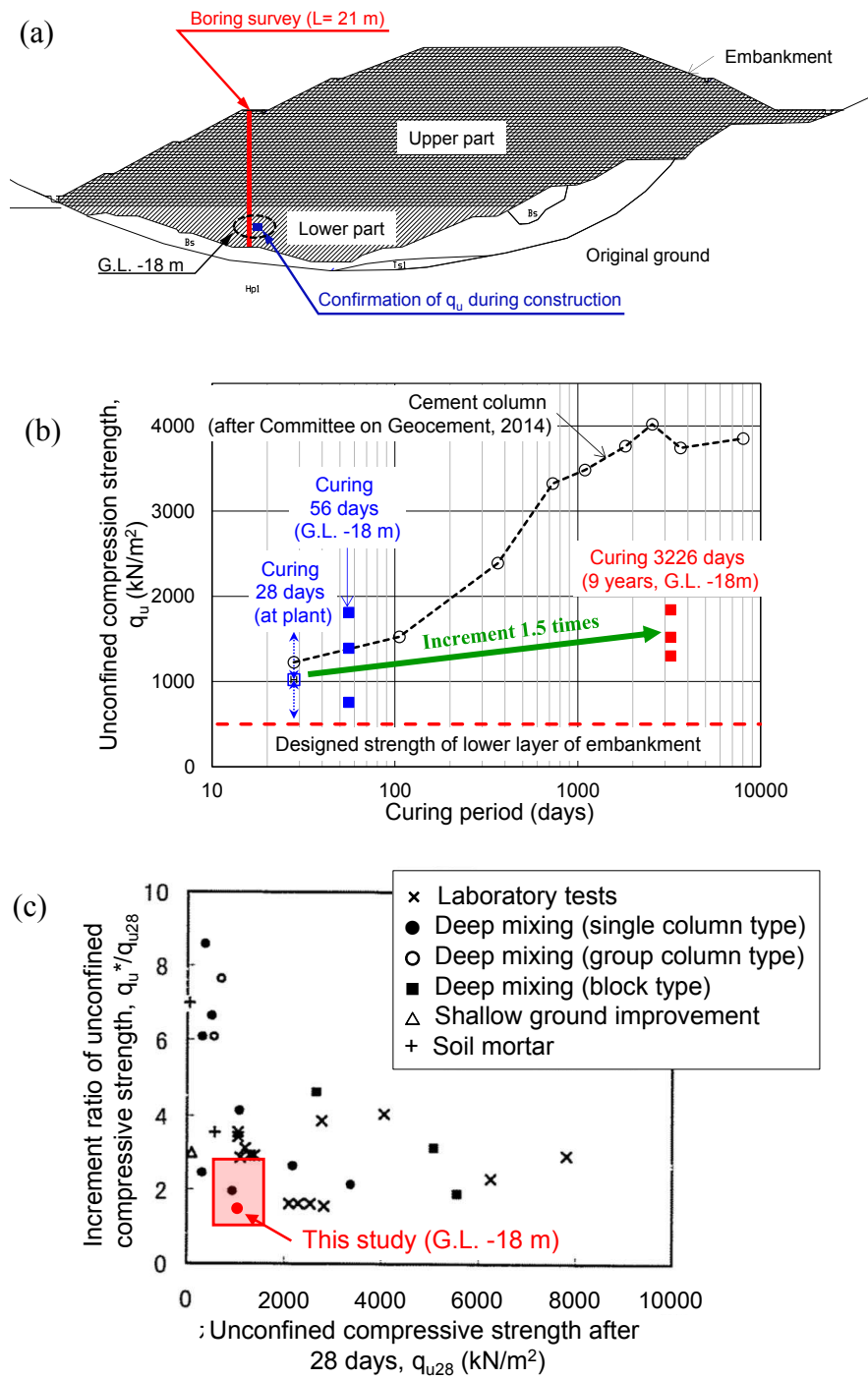


Figure 1:4 Strength gained under-groundwater after 9 years of an embankment constructed with surplus soils (Miyashita & Inoue, 2018)

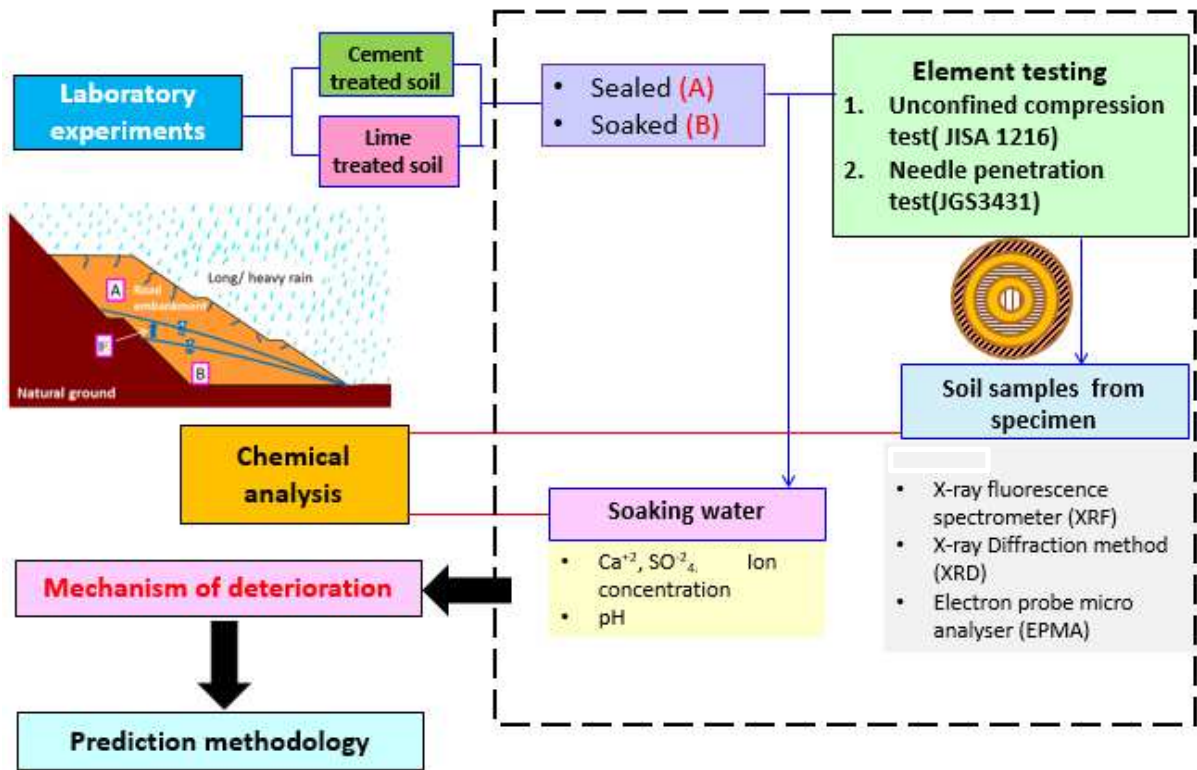


Figure 1:5 Methodology

---

## 2 Literature review

### 2.1 Cement Stabilization

Soil cement stabilization has been existence for a long time and it was first developed in the 1970s in Sweden and Japan. The engineering properties of soils such as strength, compressibility, durability can be improved by adding cement to the soil. Cement can be applied to stabilize any type of soil, except those with organic content greater than 2% or having a pH lower than 5.3 (D.T. Bergado, 1996). This stabilization technique is widely used as a deep mixing method and a shallow mixing method.

#### 2.1.1 Chemical reaction and treatment mechanism

There are four mechanisms of cement soil stabilization. They are hydration, cation exchange, carbonation and pozzolanic reactions (D.T. Bergado, 1996). Among them hydration is the most important mechanism which improves the engineering properties of soils such as enhancing strength, reducing permeability and swelling or squeezing characteristics. Cation exchange is mostly dominant in moist cohesive materials. When the soils mix with the cement, electrical charges on the soil particles are altered by resulting flocculation or aggregation of soil the particles. Carbonation is the process where additional cementitious materials are generated by using carbon dioxide from the air and the pozzolanic reactions also generated additional hydration products by reacting with free lime, alumina or silica in soil.

##### 2.1.1.1 Hydration of pure cement compounds

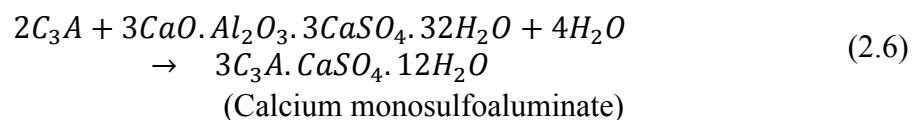
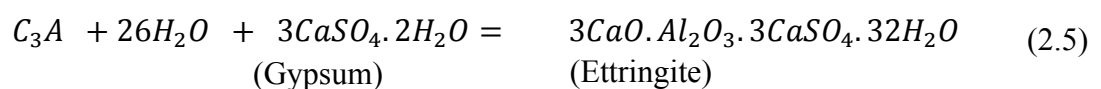
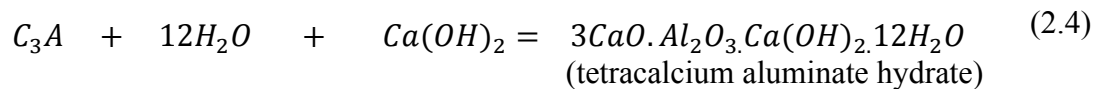
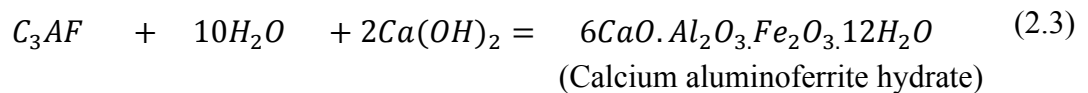
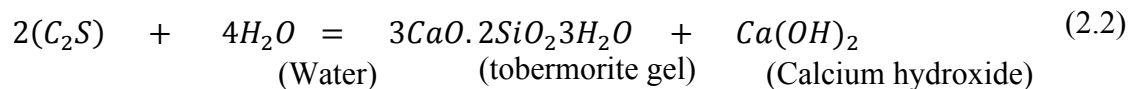
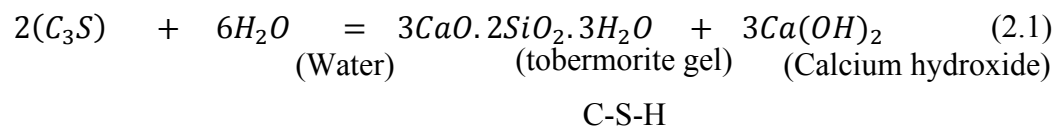
Tricalcium silicate, Dicalcium silicate, Tricalcium aluminate, and Tetra calcium aluminafetire are the four major constituents of pure cement. They are the main strength production compounds. Properties of these compounds are summarized in Table 2.1.

The development of compressive strength of pure cement compounds with the curing time is shown in Figure 2:1. When these compounds are mixed with water, the chemical reactions as stated in equations (2.1), (2.2), (2.3), (2.4), (2.5), (2.6) are occurred (D.T. Bergado, 1996). The principal hydration product is calcium silicate hydrate (tobermorite gel) which is known as C-S-H and it generated by the reaction of  $C_3S$  and  $C_2S$  with water as shown in equations (2.1) and (2.2). This has a very high surface area. Calcium sulfoaluminate hydrate which is commonly known as “ettringite” (equation (2.5)) is a stable hydration product.



Table 2.1 Properties of the compounds of cement

Main compounds in pure cement			Properties
Tricalcium silicate	3CaO.SiO <sub>2</sub>	C <sub>3</sub> S	Hydrates and hardens rapidly Responsible for initial set and early strength
Dicalcium silicate	2CaO.SiO <sub>2</sub>	C <sub>2</sub> S	Hydrates and hardens slowly Contributes to later age strength(beyond 7 days)
Tricalcium aluminate	3CaO.Al <sub>2</sub> O <sub>3</sub>	C <sub>3</sub> A	Liberate a large amount of heat during the first few days Contributes slightly to early strength development
Tetra calcium aluminoferrite	4CaO.Al <sub>2</sub> O <sub>3</sub> .Fe <sub>2</sub> O <sub>3</sub>	C <sub>4</sub> AF	Hydrates rapidly but contributes little to the strength



The microstructures of these resulting compounds are shown in Figure 2:2 (Stutzman, 2001). The resulting calcium hydroxide at solid phase is massive, hexagonal crystals about the size of 40 microns. Ettringite is a needle-like structure and the early product C-S-H like sheets. The late product of C-S-H was as in the form of a mesh so-called “honeycomb”. Figure 2:3 (Kimberly Kurtis) explains the production amount of different hydration products with the time and the changes occur in porosity.

All of the above reactions are exothermic, which means that heat is released as the reaction is progress. The rate of heat evolution is proportional to the rate of the chemical reactions (Sydney Mindess, 2003) and it can be used to map the progress of hydration. There are five stages of the reaction as initial dissolution of solids period, induction period, acceleration period, deceleration period and steady-state period as shown in Figure 2:4 (Sydney Mindess, 2003).

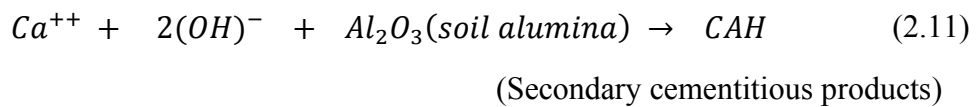
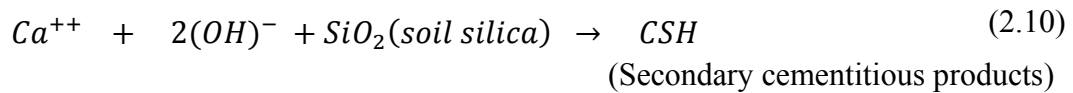
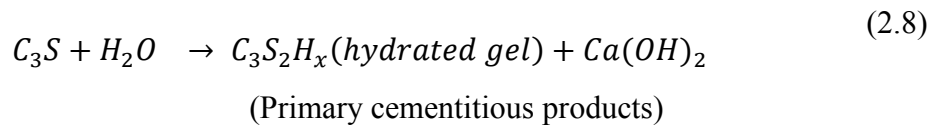
There is a thermodynamic equilibrium between the solid phase and the aqueous phase in the process of cement hydration through the dissolution of clinker phases as shown in Figure 2:5. Several studies (Damidot, Lothenbach, Herfort, & Glasser, 2011; Matschei, 2007; Matschei, Lothenbach, & Glasser, 2007; Moses & Perumal, n.d.; Rothstein, Thomas, Christensen, & Jennings, 2002; Vollpracht, Lothenbach, Snellings, & Haufe, 2016; Yamada, 2015) had been conducted on the composition of aqueous phase in the cement paste and their level of saturation as it can be used to infer information about the solid phases. Figure 2:6 shows the pH and ionic strength variation of two types of cement pastes, ordinary Portland cement (OPC) and white Portland cement (WPC) as a function of hydration time (Rothstein et al., 2002). Figure 2:7 explains the behavior of the Saturation Index (SI) relationship of Portlandite, Gypsum, Ettringite, and Monosulphae as a function of hydration time.

$$SI = \frac{IAP}{K_{sp}} \quad (2.7)$$

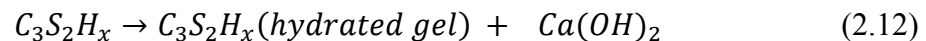
Here SI- Saturation Index, IAP- Ion activity product,  $K_{sp}$ - Solubility product. The form of equation (2.7) dictates that  $SI = 0$  indicates saturation,  $SI > 0$  indicates supersaturation, and  $SI < 0$  indicates undersaturation.

### 2.1.1.2 Reactions occur between the cement, water, and soil

When the cement is mixed with soil, the pore water of the soil is caused to start the hydration of the cement rapidly. The amount of water required for complete hydration of cement is about 40% of the weight of cement, and when the water-to-cement ratio is less than 40%, the cement that does not undergo hydration remains. As indicated in equation (2.8), the primary cementitious products, hydrated calcium silicates, hydrated calcium aluminates, and hydrated lime are created. Then the secondary cementitious products due to the pozzolanic reaction may occur by the reaction of hydrous silica and alumina with the calcium ions (equations (2.9),(2.10),(2.11)) (D.T. Bergado, 1996).



When  $pH < 12.6$ , then the following reaction occurs (D.T. Bergado, 1996)



When pH drops during the pozzolanic reaction it tends to form  $C_3S_2H_x$  into C-S-H as shown in equation (2.12). Additional formation of CSH is beneficial but if it is formed at the expense of the formation of  $C_3S_2H_x$ , it is not a benefit in terms of strength.

### 2.1.2 Effect of Cement treatment on the geotechnical properties of soil

The increase in strength of cement-treated soil is generally expressed by a model as shown in Figure 2:9 (Katoh, 2018). The calcium component contained in cement causes ion exchange on the surface of the supplied earth particles to cause flocculation, thereby improving the physical properties of the soil in the short term. In addition, cement hydration and pozzolanic reactions increase strength in the medium to long term. The phenomenon that strength increases with curing time have been confirmed by many researchers as indicated earlier and the strength also increases as the amount of cement added increases.

The geotechnical properties of soil-cement mixtures are varied with the properties of individual compounds as shown in Figure 2:8 (D.T. Bergado, 1996). The physical and mechanical

---

properties of cement treated soils have been extensively studied by several researcher by considering types of soils[ (Xiao & Lee, 2008) ,(Sarkar, Islam, Alamgir, & Rokonuzzaman, 2012), (Teja, Suresh, & Uday, 2015), (Azadegan, Jafari, & Li, 2012), (Sunkara Yashwanth, 2015),(Mu'Azuz, 2007) , (Sarkar et al., 2012), (Sunkara Yashwanth, 2015), (Mu'Azuz, 2007), (Szymkiewicz, Guimond-Barrett, Le Kouby, Reiffsteck, & Fanelli, 2013) ] and cement content [(Habeeb Adedeji Quadri, Olabambo Adeyinka Adeyemi, & Bunshiya G. Bobzom, 2013), (Farouk & Shahien, 2013) , (Azadegan et al., 2012), (Boobathiraja, Balamurugan, Dhansheer, & Adhikari, 2014), (Oyediran & Kalejaiye, 2011), (Yoon & Abu-Farsakh, 2009)] curing conditions [(Kido, Nishimoto, Hayashi, & Hashimoto, 2009), (Shihata & Baghdadi, 2001), (Reza Jolous Jamshidi, 2014)] and curing period [(Xiao & Lee, 2008) , (Lalana Kongsukprasert, Fumio Tatsuoka, & Hirofumi Takahashi, 2007) , (Sasanian & Newson, 2014)].

## 2.2 Lime Stabilization

Lime stabilization technique has a long history and was used in Greece, Rome, ancient China, and India. However, 1920 s it was started to use lime stabilization for road construction in the United States, and many laboratory/ field experiments were conducted by the end of the 1930s, and its effectiveness was recognized.

There are several forms of lime such as quicklime (CaO), hydrated lime ( Ca[OH]<sub>2</sub>), or lime slurry (National lime association, 2004). Each type of lime used in the different applications in accordance with the purpose (Katoh, 2018). Quicklime is manufactured by burning at a temperature of 900 ° C or higher, and it is mainly used for the ground improvement of 0 to 5 mm fine and about 5 to 30 mm granular material. Since quicklime uses water in the soil as hydration water for the reaction and evaporates a large amount of water in the soil by an exothermic reaction, it is particularly suitable for the improvement of soil with a high-water content. This was the reason for using quicklime in this study for enhancing engineering properties.

### 2.2.1 Chemical reactions and their effect on geotechnical properties

When quick lime is added to soil with high water content three actions begin to occur immediately (National lime association, 2004).

1. Drying

Reduce water from the reaction and enhanced workability. It can say 1/3 of quick lime is reacted by the formation of hydrated lime.

---

## 2. Modification

After initial mixing, the calcium ions from hydrated lime migrate to the surface of the clay particles and replace monovalent charge and displace water and other ions as shown in Figure 2:10. This cation exchange action enhanced flocculation and agglomeration by restructuring the particles as shown in Figure 2:11 and reduce plasticity index dramatically

## 3. Stabilization

When an adequate amount of lime is added the pH of soil increase quickly and enhance the solubility of the soluble silica and Alumina from soil particles (Cuisinier, 2010) as shown in Figure 2:12. Those released Alumina and Silica react with calcium from the lime to form calcium-silicate-hydrates (CSH) and calcium-aluminate-hydrates (CAH). This reaction takes a long time and it is highly dependent the curing conditions such as temperature and pH. (Asma Muhmed, 2013; Cuisinier, 2010; Khattab, Al-Mukhtar, & Fleureau, 2007; National lime association, 2004; Taha Jawad, Raihan Taha, Hameed Majeed, & A. Khan, 2014).

The increase in strength of quick lime treated soil with time can be generally expressed by a model as shown in Figure 2:13 (Kato, 2018). According to that flocculation by cation exchange contributes to short-term strength development and pozzolanic reaction contributes to long-term strength development. In order to find out the reason for taking long time duration for pozzolanic reaction (Rajasekaran & Rao, 1997) conducted special column test examined the relationship between strength expression and time as a factor from distance from the lime. As a result, it was revealed that the permeation of many calcium ions occurred from 7 to 15 days after the start of the test. This time coincides with the initiation period of the pozzolanic reaction. It was suggested that if the calcium ion moving in the soil gap is captured by humic functional groups before the pozzolanic reaction occurs, the progress of the pozzolanic reaction is inhibited.

### 2.3 Long term behavior of improved soils

Several decades have passed since the cement and lime stabilization was put into practical use, but during that time, the long-term durability of those improved soil and the deterioration phenomenon according to the soaking have not been mentioned much. Several studies have been conducted on a laboratory scale and field scale on the long-term durability of deep mixing

---

columns under seawater conditions (Hara, Suetsugu, & Hayashi, 2012; Hashimoto et al., 2018; Hino, Jia, Sueyoshi, & Harianto, 2012; Hirochika Hayashi, 2002; Kitazume, Nakamura, Terashi, & Ohishi, 2003; Yang, Yan, Liu, & Zhang, 2016). ((Hirochika Hayashi, 2002) investigated the long-term characteristics of cement-treated soil pile foundation in abridge abutment Dry Jet Mixing method in Hokkaido about 17 years after its construction. The needle penetration test was performed on the cement-treated cores collected center, the interspace between adjacent columns and untreated soils separately. It was shown that in the range of several tens of mm from the end of the column, it decreased compared to the outer peripheral part. In addition, the amount of cement in the column tended to decrease at the end, and the amount of CaO in the cement-unmixed ground around the column increased, and the elution of Ca from the column to the surrounding ground was observed.

(Saito et al.2005) conducted a sampling test from the boundary with the unimproved part to the deep part of the grid-like improved ground after 7 years of construction and the soil cement column wall after 13 years of construction and conducted an indoor test. As a result, in both samples, the decrease in pH and needle penetration was confirmed near the unmodified part. In addition, the measurement of CaO concentration was also carried out on the sample after 13 years of construction, and the decrease of CaO concentration was observed in the range of about 25 mm from the non-modified part.

Nakamura et al. (2006) investigated needle penetration test and CaO content of cement-treated soil specimens exposed (immersed) to freshwater and seawater and examined changes in mechanical and chemical characteristics. The needle penetration test showed that the distribution of the penetration resistance ratio was almost constant before the exposure, but the resistance ratio decreased with the exposure period. The degree of decrease in the intensity ratio is more pronounced when exposed to seawater than freshwater, but the results show that the sample exposed to freshwater is wider in the range where the decrease in intensity ratio is observed. The distribution of the amount of CaO in the sample shows a decrease in the amount of CaO in the range where the decrease in intensity ratio is observed. Similar to the needle penetration test results, the degree of decrease in CaO content is more pronounced when exposed to seawater than freshwater, but the results show that the sample exposed to freshwater is wider in the range where the decrease in CaO amount was observed.

Ikegami et al. (2002) conducted a field investigation on the long-term strength of cement stabilized soils at Daikoku Pier of Yokohama in Tokyo bay whose construction was started in

---

1971 and reclamation was completed in 1990. Needle penetration test and atomic absorption measurement test were conducted on bore samples after 20 years of their construction. From the results it was verified that strength reduced at the boundary surface of stabilized soil, the progress of deterioration in the past 20 years was around 30 to 50 mm in depth from the boundary. It was found that Ca leaching phenomenon from stabilized soil to the surrounding soil as the reason for the strength reduction.

(Hara et al., 2012) conducted a series of laboratory investigations on the durability of stabilized Ariake clay with lime/cement treated soil under seawater environment and observed Ca leaching as one of the main reasons for strength reduction.

(Kamon, Ying, & Katsumi, 1996) reported on the degradation phenomenon caused by acid rain. Changes in properties of cement-modified soil immersed in simulated acid rain prepared by mixing sulfuric acid and nitric acid in a ratio of 3: 1 was investigated. The results showed that when the pH of acid rain was low, the pH of the improved soil decreased with soaking time, and the uniaxial compressive strength also decreased. This phenomenon was considered as follows due to the decrease of Ca concentration in the improved soil. Ca in the treated soil was dissolved in pore water (Free-Ca), adsorbed on soil particles (Adsorbed-Ca), or absorbed as hydrate (Hydrated-Ca) There are three forms. By simulated acid rain, Free-Ca elutes first, and then ion exchange with H<sup>+</sup>, which is abundant in simulated acid rain, elutes Adsorbed-Ca. When these Ca contents elute, the hydrate breaks down and the pH and strength of the modified soil decrease.

From the observations of previous studies, it could understand Ca leaching as the main reason for the deterioration of the improved soils. In addition to that, it was found that there were only a few studies on the soaking under pure water or acidic water to simulate roads embankment behavior by showing the requirement of this study.

## **2.4 Evaluation method of deterioration**

### **2.4.1 Empirical models**

Several researchers reported empirical models to predict deterioration depth under seawater exposure.

Ikegami et al (2004) predicted deterioration depth of cement-treated soil by equation (2.13).

---

$$\log(D) = \log(D_0) + \frac{1}{2}(\log(t) - \log(t_0)) \quad (2.13)$$

Where  $D_0$  is the deterioration depth at  $t_0$  time,  $A$  is deterioration depth at  $t_0=1$  year

(Kitazume et al., 2003) and several researchers found deterioration of death can be written as in equation (2.14).

$$D = \alpha X t^\beta \quad (2.14)$$

Where  $t$  is elapsed time (year),  $D$  is deterioration depth at time  $t$  (mm),  $\alpha$  and  $\beta$  are constants. Figure 2:14 (Jilai, 2013) shows the summary of the  $\alpha$ ,  $\beta$  values which were obtained by previous researchers.



---

## 2.5 Reference

- Asma Muhmed, A. M. 2013. Effect of Lime Stabilisation on the Strength and Microstructure of Clay. *IOSR Journal of Mechanical and Civil Engineering*, 6(3): 87–94.
- Azadegan, O., Jafari, S. H., & Li, J. 2012. Compaction characteristics and mechanical properties of lime/cement treated granular soils. *Electron. J. Geotech. Eng*, 17: 2275–2284.
- Boobathiraja, S., Balamurugan, P., Dhansheer, M., & Adhikari, A. 2014. Study on strength of peat soil stabilised with cement and other pozzolanic materials. *Int J Civ Eng Res*, 5(4): 431–438.
- Cuisinier, O. 2010. *Short and long term performance of lime and cement stabilised soils*, 36.
- Damidot, D., Lothenbach, B., Herfort, D., & Glasser, F. P. 2011. Thermodynamics and cement science. *Cement and Concrete Research*, 41(7): 679–695.
- Dr. Kimberly Kurtis. n.d. *Portland cement hydration*. School of Civil engineering, Georgia Institute of Technology.
- D.T. Bergado. 1996. *Soft ground improvement in lowland and other environments*. American Society of Civil Engineers press.
- Farouk, A., & Shahien, M. M. 2013. Ground improvement using soil–cement columns: Experimental investigation. *Alexandria Engineering Journal*, 52(4): 733–740.
- Habeeb Adedeji Quadri, Olabambo Adeyinka Adeyemi, & Bunshiya G. Bobzom. 2013. Impact of Compaction Delay on the Engineering Properties of cement treated soil. *IOSR Journal of Mechanical and Civil Engineering*, 4(6): 9–15.
- Hara H., Suetsugu D., & Hayashi S. 2012. Calcium Leaching Mechanism of Lime Treated Soil Immersed in Seawater. *Journal of the Society of Materials Science, Japan*, 61(1): 11–14.
- Hashimoto, H., Yamanashi, T., Hayashi, H., Kawaguchi, T., Kawajiri, S., et al. 2018. Long-Term Strength Characteristics of the Cement Treated Soil after 30 Years. *Journal of the Society of Materials Science, Japan*, 67(1): 47–52.
- HINO, T., JIA, R., Sueyoshi, S., & Harianto, T. 2012. *Effect of environment change on the strength of cement/ lime treated clays*, 13.
- Hirochika Hayashi. 2002. *Field observation of longterm strength of cemenet treated soil*, 598–609.
- Jilai, M. 2013, September 24. *Evaluation on Long Term Durability of Cement Stabilized Soils under Sea Water Environment*. <https://doi.org/10.15017/1398340>.

- 
- Kamon, M., Ying, C., & Katsumi, T. 1996. Effect of acid rain on lime and cement stabilized soils. *Soils and Foundations*, 36(4): 91–99.
- Katoh, M. 2018. Mechanisms of stabilization in soil amended with lime or cement and physicochemical analysis of its reaction compounds. *Cement and Concrete Research*, 5(855): 7–11.
- Khatab, S. A., Al-Mukhtar, M., & Fleureau, J.-M. 2007. Long-Term Stability Characteristics of a Lime-Treated Plastic Soil. *Journal of Materials in Civil Engineering*, 19(4): 358–366.
- Kido, Y., Nishimoto, S., Hayashi, H., & Hashimoto, H. 2009. Effects of curing temperatures on the strength of cement-treated peat. *Proceedings of International Symposium on Deep Mixing and Admixture Stabilization*.  
<http://thesis.ceri.go.jp/center/doc/thesis/jiban/00110730001.pdf>.
- Kitazume, M., Nakamura, T., Terashi, M., & Ohishi, K. 2003. *Laboratory Tests on Long-Term Strength of Cement Treated Soil*, 586–597. Presented at the Grouting and ground treatment.
- Lalana Kongsukprasert, Fumio Tatsuoka, & Hirofumi Takahashi. 2007. Effect of curing period and stress condition. *Soils and Foundations, Japanese Geotechnical Society*, 47(3): 577–596.
- Matschei, T. 2007. *Thermodynamics of Cement Hydration*, 222.
- Matschei, T., Lothenbach, B., & Glasser, F. P. 2007. Thermodynamic properties of Portland cement hydrates in the system CaO–Al<sub>2</sub>O<sub>3</sub>–SiO<sub>2</sub>–CaSO<sub>4</sub>–CaCO<sub>3</sub>–H<sub>2</sub>O. *Cement and Concrete Research*, 37(10): 1379–1410.
- Moses, P. E., & Perumal, D. S. B. n.d. *Hydration of Cement and its Mechanisms*, 15.
- Mu’Azu, M. A. 2007. Influence of compactive effort on Bagasse ash with cement treated lateritic soil. *Leonardo Electronic Journal of Practices and Technologies*, 10(1): 79–92.
- National lime association. 2004. *Lime\_treated\_soil\_construction\_manual*. no. Bulletin 326, The Veeratile Chemical.
- Oyediran, I. A., & Kalejaiye, M. 2011. Effect of increasing cement content on strength and compaction parameters of some lateritic soils from Southwestern Nigeria. *Electronic Journal of Geotechnical Engineering*, 16: 1501–1514.
- Rajasekaran, G., & Rao, S. N. 1997. lime stabilization technique for the improvement of marine clay. *Soils and Foundations*, 37(2): 97–104.
-

- 
- Reza Jolous Jamshidi. 2014. *Evaluation of cement-treated soils subjected to cycles of freezing and thawing*. Doctoral Thesis, Dalhousie University, Halifax, Nova Scotia. <https://dalspace.library.dal.ca/handle/10222/54065>.
- Rothstein, D., Thomas, J. J., Christensen, B. J., & Jennings, H. M. 2002. Solubility behavior of Ca-, S-, Al-, and Si-bearing solid phases in Portland cement pore solutions as a function of hydration time. *Cement and Concrete Research*, 32(10): 1663–1671.
- Sarkar, G., Islam, M. R., Alamgir, M., & Rokonuzzaman, M. 2012. Study on the geotechnical properties of cement based composite fine-grained soil. *International Journal of Advanced Structures and Geotechnical Engineering ISSN*, 2319–5347.
- Sasanian, S., & Newson, T. A. 2014. Basic parameters governing the behaviour of cement-treated clays. *Soils and Foundations*, 54(2): 209–224.
- Shihata, S. A., & Baghdadi, Z. A. 2001. Long-term strength and durability of soil cement. *Journal of Materials in Civil Engineering*, 13(3): 161–165.
- Smith, T., Eng, P., Barnes, C. L., & Zupko, S. 2014. *The Use of Engineered Soils in Canada*, 19.
- Stutzman, P. E. 2001. Scanning electron microscopy in concrete petrography. *National Institute of Standards and Technology*, 2. <http://fire.nist.gov/bfrlpubs/build01/PDF/b01086.pdf>.
- Sunkara Yashwanth. 2015. Experimental studies on laterite soil stabilized with cement and aggregate. *International Journal of Research in Engineering and Technology*, 4(8): 187–192.
- Sydney Mindess. 2003. *Concrete* (Second). Pearson Education, Inc.
- Szymkiewicz, F., Guimond-Barrett, A., Le Kouby, A., Reiffsteck, P., & Fanelli, S. 2013. Strength and aging of cement treated low plastic soils. *Int. J. of GEOMATE*, 4(1): 490–494.
- Taha Jawad, I., Raihan Taha, M., Hameed Majeed, Z., & A. Khan, T. 2014. Soil Stabilization Using Lime: Advantages, Disadvantages and Proposing a Potential Alternative. *Research Journal of Applied Sciences, Engineering and Technology*, 8(4): 510–520.
- Teja, P. R. K., Suresh, K., & Uday, K. V. 2015. Effect of Curing Time on Behaviour and Engineering Properties of Cement Treated Soils. *International Journal of Innovative Research in Science, Engineering and Technology*, 4(6): 4649–4657.
- Vollpracht, A., Lothenbach, B., Snellings, R., & Haufe, J. 2016. The pore solution of blended cements: A review. *Materials and Structures*, 49(8): 3341–3367.
-

- 
- Xiao, H. W., & Lee, F. H. 2008. Curing time effect on behavior of cement treated marine clay. *Proceedings of World Academy of Science, Engineering and Technology (PWASET)*, 33: 2070–3740.
- Yamada, K. 2015. *Concrete performance/ deterioration modeling by using thermodynamic equilibrium codes*, 52.
- Yang, J., Yan, N., Liu, Q., & Zhang, Y. 2016. Laboratory test on long-term deterioration of cement soil in seawater environment. *Transactions of Tianjin University*, 22(2): 132–138.
- Yoon, S., & Abu-Farsakh, M. 2009. Laboratory investigation on the strength characteristics of cement-sand as base material. *KSCE Journal of Civil Engineering*, 13(1): 15–22.

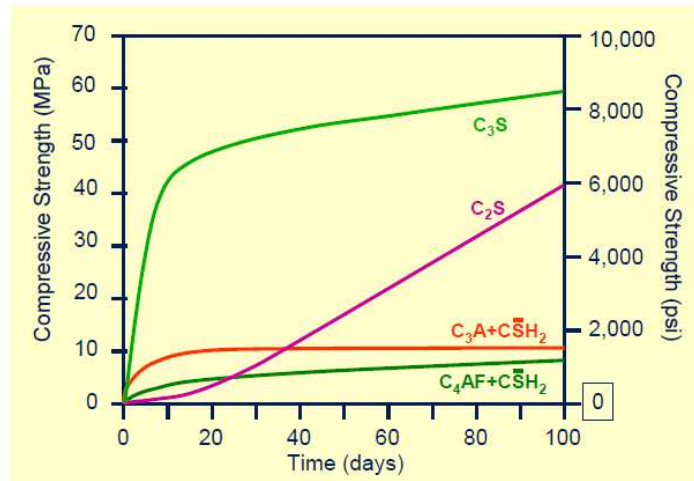


Figure 2:1 Compressive strength development in pastes of pure cement compounds

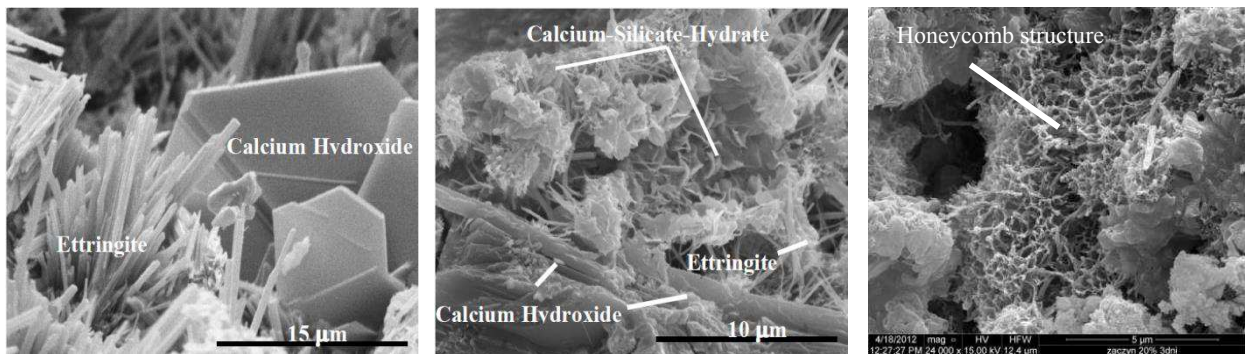


Figure 2:2 Microstructure of hydration products

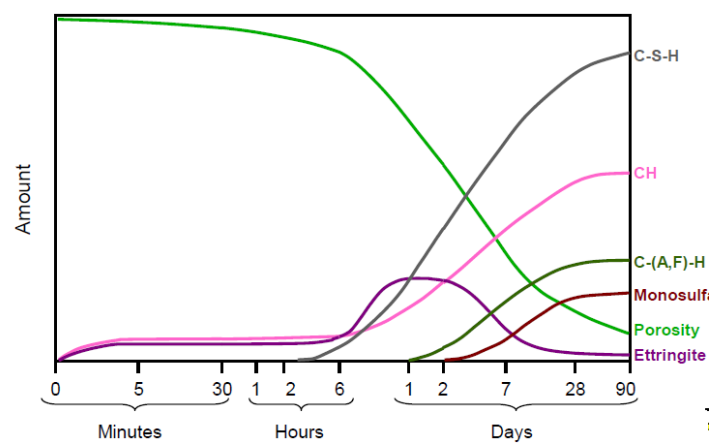


Figure 2:3 Porosity changes with time

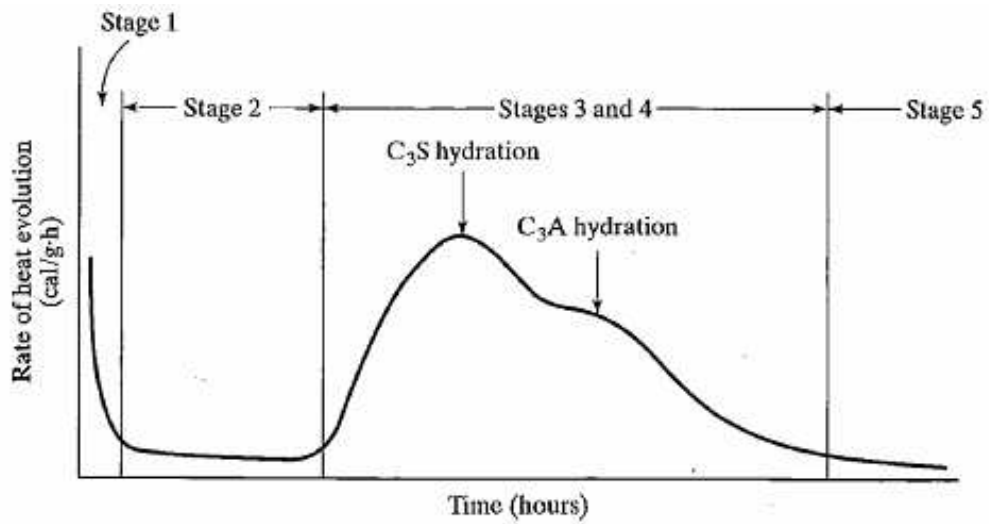


Figure 2:4 Rate of heat evolution during hydration of Portland cement

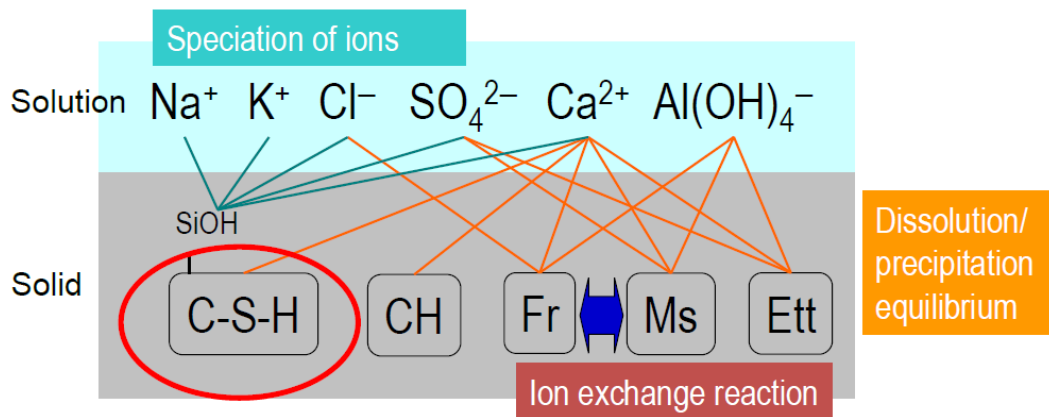


Figure 2:5 Ion equilibrium in the solid phase and pore solution (Yamada, 2015)

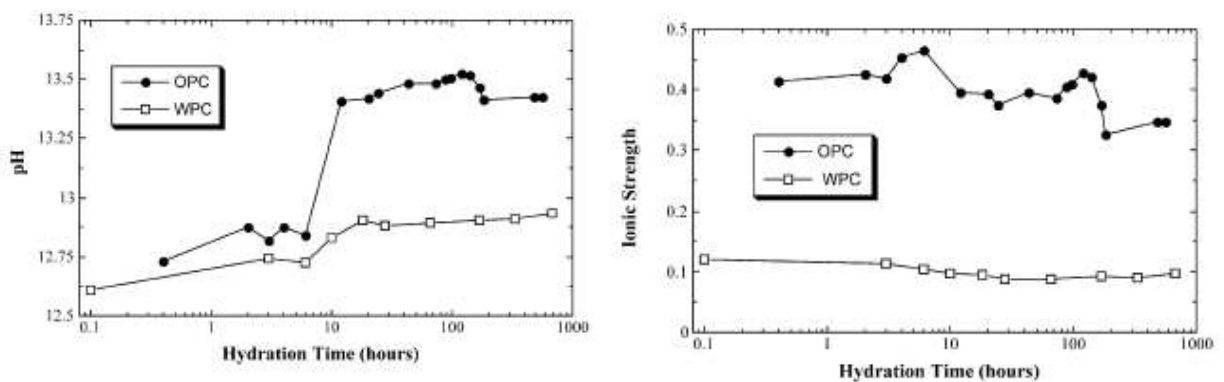


Figure 2:6 pH and ionic strength variation of cement pastes (Rothstein et al., 2002)

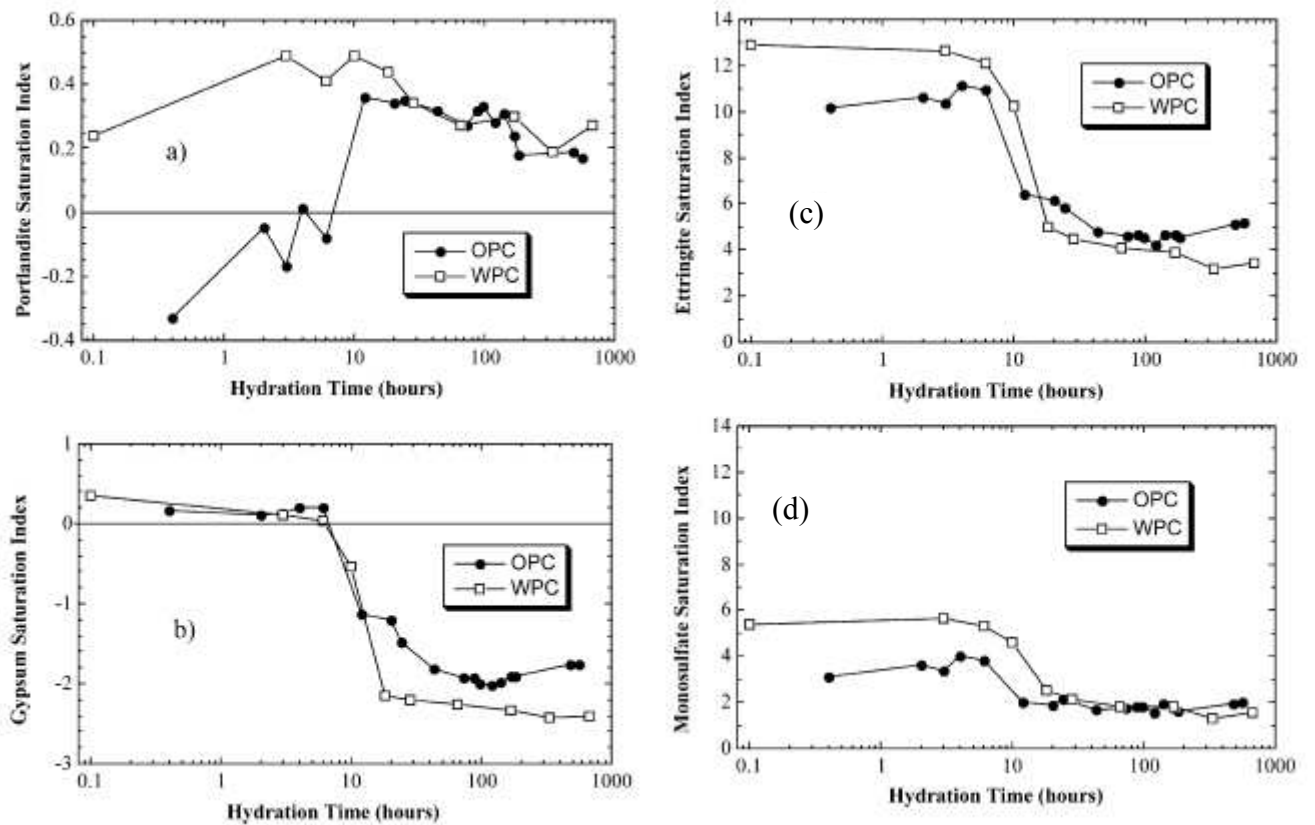


Figure 2:7 SI of (a) Portlandite (b) Gypsum (c) Ettringite (d) Monosulphate in the cement paste (Rothstein et al., 2002)

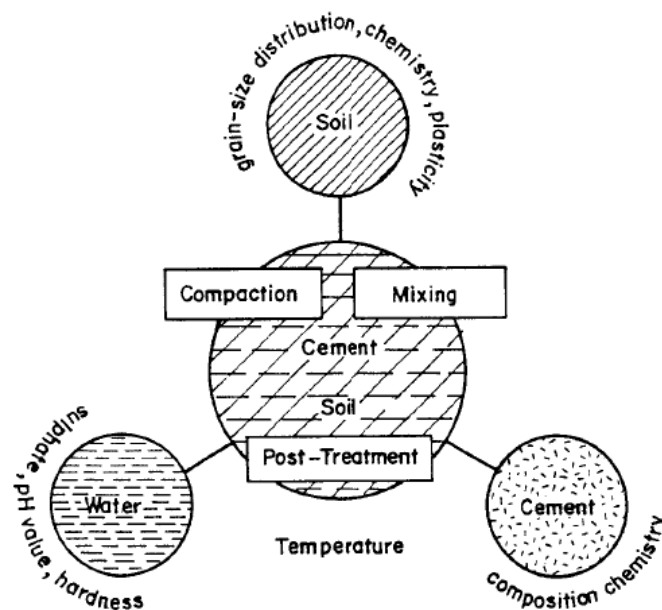


Figure 2:8 Factors affecting on the properties of cement treated soil

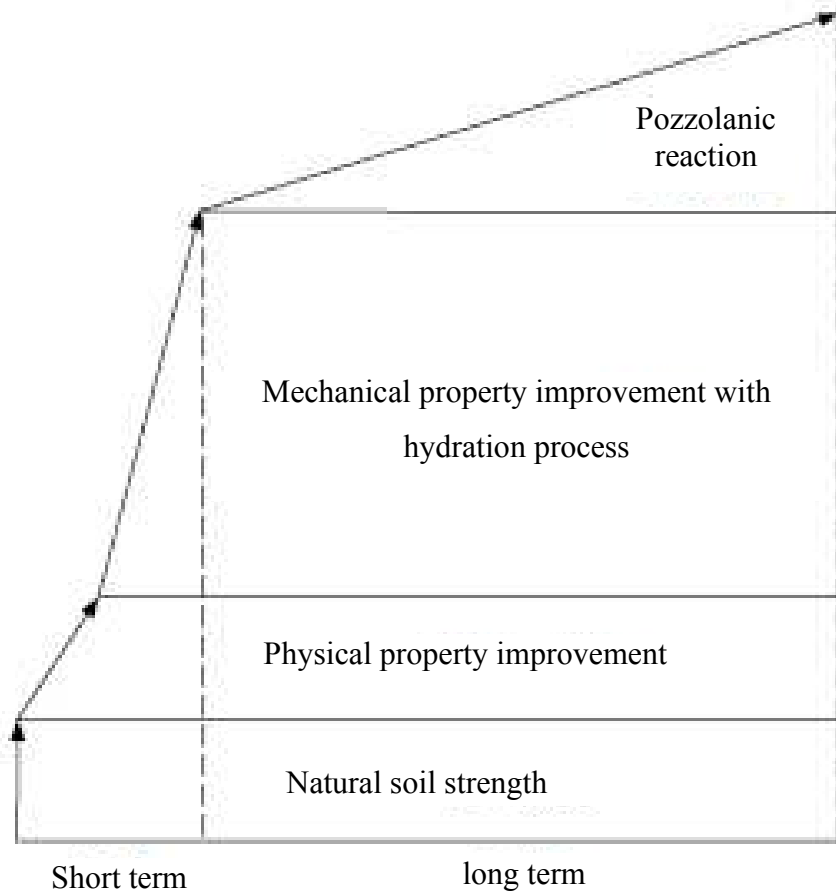


Figure 2:9 Strength increase model of cement (Katoh, 2018)

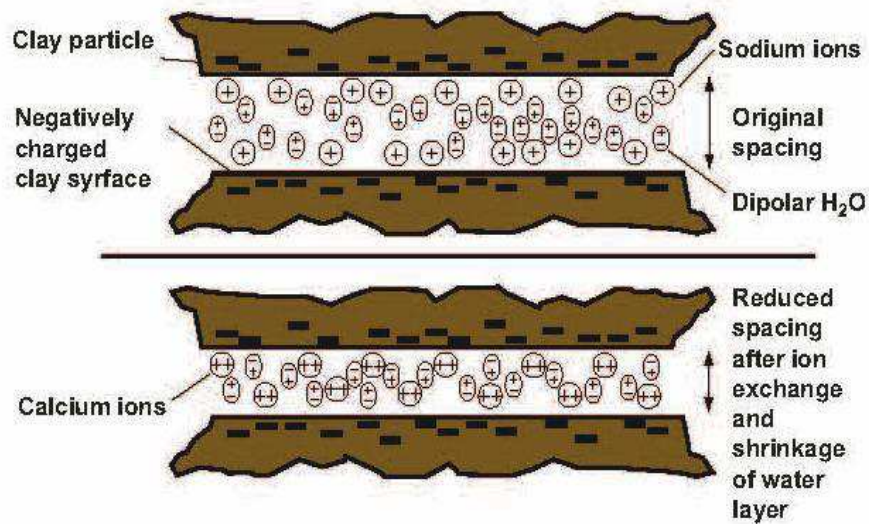


Figure 2:10 Cation exchange (Smith, Eng, Barnes, & Zupko, 2014)



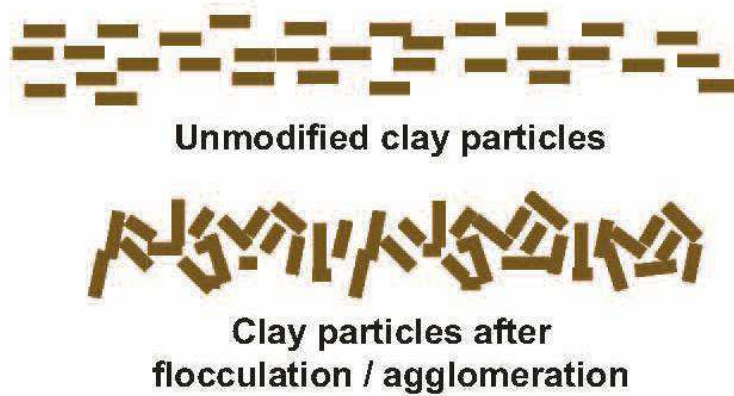


Figure 2:11 Particle restructuring -Flocculation and agglomeration (Smith et al., 2014)

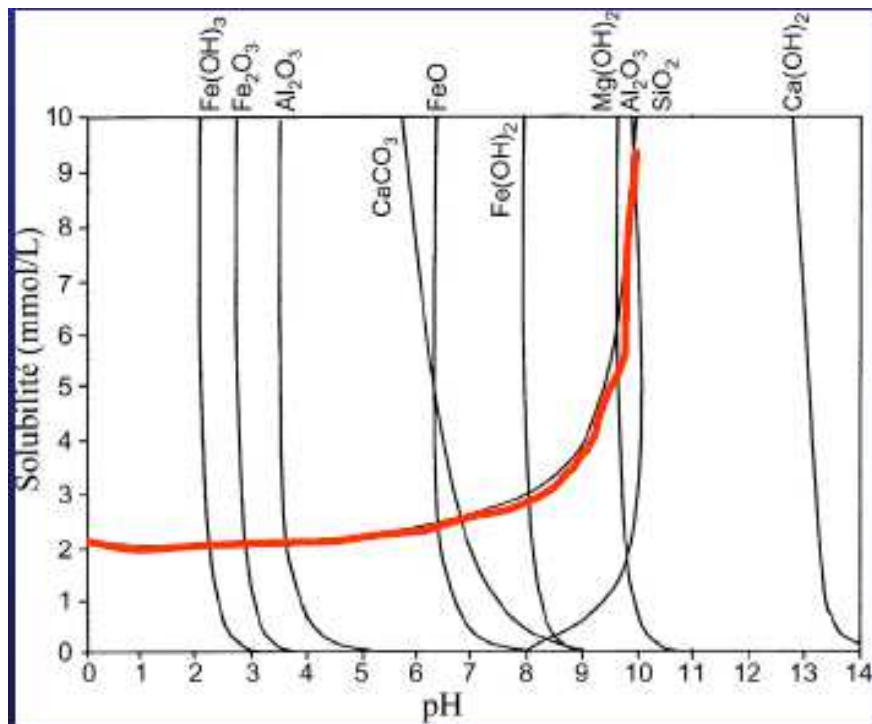


Figure 2:12 Increase of silicon and aluminum solubility in high pH environment (Cuisinier, 2010)

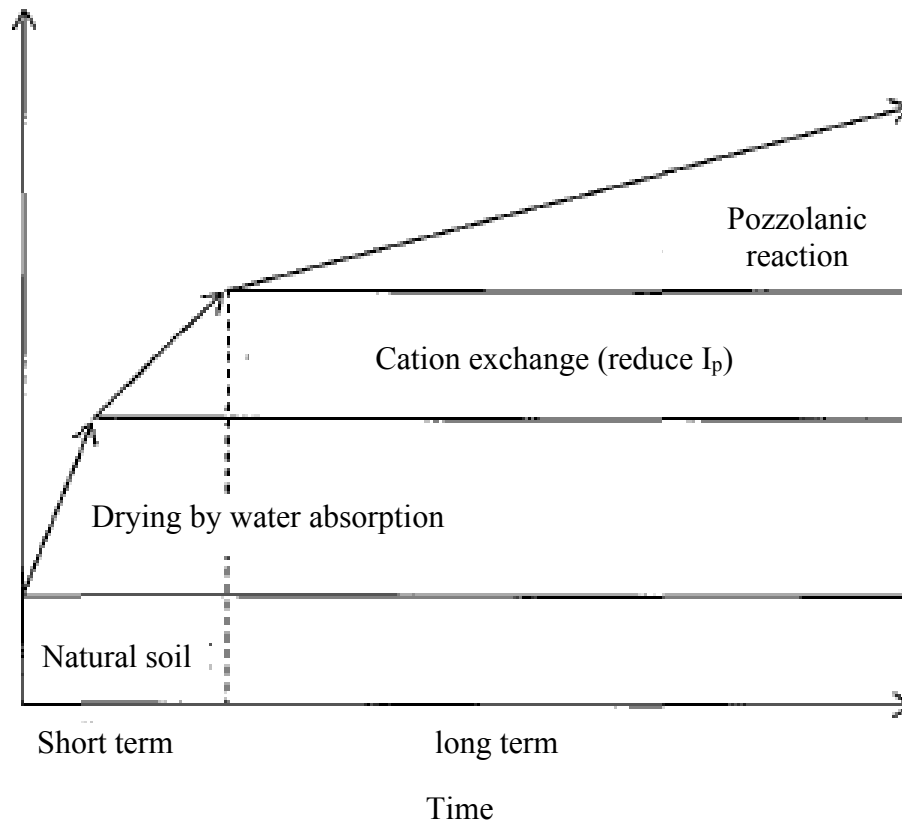


Figure 2:13 Strength change model for quick lime (Katoh, 2018)

Case	Exposure	Soil type	Binder	$q_{u28}$ (MPa)	$D = \alpha * t^\beta$	
					$\alpha$	$\beta$
This study	Tap water	Hokkaido clay	Blast-furnace B type	0.28	23.6	0.45
Terashi et al. (1983)	Sea water Soils	Kawasaki clay	Ordinary	1.5	14.8	0.49
			Portland Cement		8.0	0.38
Saito (1988)	Sea water Soils	Yokohama port clay	Ordinary Portland Cement	4.8	8.0	0.55
Kitazume et al. (2003)	Pure water	Kawasaki clay	Ordinary Portland Cement	0.5	13.1	0.51

Note: D is deterioration depth (mm), t is time (year).

Figure 2:14 Parameters on prediction methodology of deterioration depth (Jilai, 2013)

### 3 Material, Apparatus and testing procedures

#### 3.1 Introduction

The main objective of this study was to understand the long-term behavior of improved surplus soils with low binder contents under groundwater. The methodology adopted in this study is shown in Figure 3:1. In here needle penetration tests, unconfined compression tests were conducted on the specimens prepared from improved soil periodically and the chemical analysis was applied on the soil samples which were taken from different location of the specimens. In addition to that chemical analysis on the soaking water also was applied.

#### 3.2 Material properties

##### 3.2.1 Miho sand

An actual surplus soil called Miho sand from the village Miho in Ibaraki prefecture was used in this study as shown in Figure 3:2. The physical and mechanical properties of Miho sand is shown in Table 3:1. According to the surplus soil classification it was classified as Mud. The particle size distribution of Miho sand is shown in Figure 3:3. It contained fine around 47 %.

Table 3:1 Physical and mechanical properties of Miho sand

Soil classification (JGS 0051)	SF ( <i>sandy soil</i> )
Soil particle density, $\rho_s$ (g/cm <sup>3</sup> )	2.693
Optimum water content, $w_{opt}$ (%)	21.6
Maximum dry density, $\rho_{dmax}$ (g/cm <sup>3</sup> )	1.624
Natural water content, $W_N$ (%)	31
Liquid limit $W_L$	48.4
Plastic limit $W_P$	23.0
Plastic index $I_P$	25.4
Cone index, $q_c$ (kN/m <sup>2</sup> ) (with water content of 31 %)	68

In Japan, most of the low-quality soils with high fine content and water content are based on volcanic ash. It is possible to have allophane and amorphous inorganic matters in such kind of soils (Krrlclwe & Soits and Fertilizers, 1974; Parfitt, 2009). Several researchers (Kawamura, Hasaba, & Sugiura, 1971; Kett, Ingham, & Evans, 2010; Kobashi, 1967) have identified that those allophane and amorphous contents can be affected negatively on the strength when

stabilize using lime or cement. In order to understand only the effect of soaking on the strength, the negative effects appear from the mineral in soils should be minimized. The amorphous content of Miho sand was found as 10 % from the analysis conducted using Kitagawa method (Kitagawa, 1976, 1980) as shown in Figure 3:4. In this study, it was assumed that there was no negative effect on the strength from the available amorphous content. The minerals available in Miho sand was obtained by X-ray diffractometer analysis (XRD) as shown in Figure 3:5 and the quantitative amount of each ion were obtained from X-ray fluorescence spectrometer (XRF) analysis on Miho sand is shown in Table 3:2.

Table 3:2 Chemical properties of Miho sand and binders

	SiO <sub>2</sub> (wt %)	TiO <sub>2</sub> (wt %)	Al <sub>2</sub> O <sub>3</sub> (wt %)	Fe <sub>2</sub> O <sub>3</sub> (wt %)	MnO (wt %)	MgO (wt %)	CaO (wt %)	Na <sub>2</sub> O (wt %)	K <sub>2</sub> O (wt %)	P <sub>2</sub> O <sub>5</sub> (wt %)	S <sub>total</sub> (wt %)	SO <sub>3</sub> (wt %)
Miho sand	61.69	0.73	19.92	6.86	0.11	1.29	1.48	1.18	1.54	0.10	0.03	-
Cement	Not measured						56.37	Not measured			3.13	6.08
Quick lime	Not measured						94.93	Not measured			-	<0.02

### 3.2.2 Cement

The used cement type was TL-3E Sumitomo Osaka Cement which is widely used for the shallow and deep improvement of poor-quality soil. It is a hexavalent chromium soluble cement and was developed in Japan to make the effectiveness against low-quality soils greater than Ordinary Portland cement, (Annex A). XRD results and the XRF results of cement are shown in Figure 3:7 and Table 3:2 respectively.

### 3.2.3 Lime

Quick lime was used as the lime type in this study as it is a recommended stabilization type for improving trafficability of soil,(Annex A). XRD results and the XRF results of quick lime are shown in Figure 3:6 and Table 3:2 respectively.

## 3.3 Mixing proportions and specimen preparation method

Three binder contents from each type of binder were selected as shown in Table 3:3. The middle contents of lime and cement were decided by considering the 7 days unconfined compressive strength as of 100 kN/m<sup>2</sup>. These low contents of lime and cement coincided with the minimum values which were empirically recommended in the manuals published by Japan Lime Association and Japan Cement Association, respectively. The smaller and larger contents of lime and cement were simply set to be 0.5 and 1.5 times the middle contents to investigate

the effect of the binder contents. The water content of Miho sand was set to its natural water content as 31 %.

Table 3:3 Mixing proportions

Binder type	Percentage as dry weight of Miho sand (%)	
	Binder content (%)	Water (%)
Cement	1.7	31
	<b>3.5</b>	31
	5.3	31
Lime	1.2	31
	<b>2.5</b>	31
	3.8	31

One of the binders and Miho sand were mixed uniformly by a soil mixer for 5 minutes. Cylindrical specimens with 50 mm in diameter and 100 mm in height were prepared by applying static compaction as shown in Figure 3:8. The dry density of the specimens was set to 1.4 g/cm<sup>3</sup> by considering standard proctor compaction results as shown in Figure 3:9. This was confirmed by the result of large-scale model tests to investigate the characteristics of compaction using actual construction machines.

### 3.4 Curing method

All specimens were cured under two different curing conditions as shown in Figure 3:10 (a) and (b). In case A which is called hereafter as sealed, specimens were wrapped with plastic sheets to avoid moisture transportation and cured inside a plastic container while maintaining temperature and humidity in a constant value. Saturation was applied by applying vacuum pressure under pure water for three sealed specimens, one day prior to the testing date. The reasons for applying saturation for the sealed specimens was to maintain the same degree of saturation of the soaked specimens. Author conducted a series of testing for the same types of specimens under unsaturated condition as explained in Appendix 1 and it was found higher strength under unsaturated conditions than in saturated conditions due to the difference in degree of saturation which may be due to the suction stress as a confinement (Chae, Kim, Park, & Kato, 2010; Lu, Godt, & Wu, 2010).

To evaluate the effect of soaking (case B) under groundwater on the long-term behavior of the specimens another three sets of specimens were prepared. First sets of specimens cured under

pure water with a pH of 7 after three days of their preparation (immature). Second sets of specimens were soaked under artificially made acidic water with a pH of 4.5 in immature condition as shown in Figure 3:10 (b). Third sets of specimens were prepared and cured under sealed conditions up to 6 months (mature) and then soaked under acidic water and illustrated here as case B<sup>1</sup>. Case B was designed to see the effect of soaking on long term behavior of embankment material if it exposes in immature state while case B<sup>1</sup> was designed to simulate the possible deterioration of improved soil after gaining strength fully, due to the increase of groundwater level or water infiltration through cracks or other water paths in the embankment as systematically shown in Figure 3:10 (c). In all the cases the volume of the specimen to soaking water was maintained as 1:5.

The pH of artificially made acidic water was set as 4.5 by considering the pH of actual rainwater of Japan in the past few decades as shown in Figure 3:11. In here acidic water was prepared by mixing pure water with sulfuric acid (H<sub>2</sub>SO<sub>4</sub>), nitric acid (HNO<sub>3</sub>) and hydrochloric acid (HCl) in a proportion of 5:2:3. In all soaked cases, the soaking water was exchanged once a week in the initial 28 days. Then the duration was increased to 2 weeks until 168 days, while it was increased again to 4 weeks from 168 days to 672 days. The setting up of tap lines for soaking water exchange is shown in Figure 3:12. In addition to that, constant temperature within the range of 17-23 degrees of Celsius was maintained in all the cases. Types and contents of the binders, conditions of curing and specimens when tested, and types of water for soaked curing were organized in Table 3:4 with indicating their notation abbreviated in this thesis.

### **3.5 Unconfined compression test**

#### **3.5.1 Apparatus**

The testing apparatus which was used to conduct the unconfined compression test is shown in Figure 3:13. In here small size, strain-controlled triaxial apparatus was used. In this apparatus, the strain was controlled automatically by computer, whenever the input values were given through software called Visual show Basic. According to the Japanese Geotechnical Standard-Method for the unconfined compression test of soils (JGS 0511- 2009), the strain rate of the loading system should be 1% per minute. Since the sample height was 100mm, the motor speed was set for 1mm/min rate.

### 3.5.2 Devices for measuring stress

The axial load was measured by a load cell which was fixed inside the triaxial cell, which gives true results regardless of the piston friction. The load cells adopted in this study were electronic –resistant strain - gauge type transducers. The main body was made from a block of phosphor-bronze as shown in Figure 3:14. Four electronic resistant strain gauges were set as two at the compression side and two at the tension side as forming a Whitestone Bridge. Therefore, a voltage difference can be detected whenever any axial load was changed in the loading piston.

Table 3:4 Summary of the testing case and curing conditions

Binders	Binder contents	Curing conditions		Types of soaking water	Notations abbreviated
		Sealed	-		
Cement	1.7 %	Sealed	-	-	C1.7 Seal
		Soaked	immature	Acid	C1.7 Soak -Acid (immature)
	3.5 %	Sealed	-	-	C3.5 Seal
		Soaked	immature	Pure	C3.5 Soak -Pure (immature)
			immature	Acid	C3.5 Soak -Acid (immature)
	5.3 %	mature	Acid	C3.5 Soak-Acid (mature)	
		Sealed	-	-	C5.3 Seal
	Soaked	immature	Acid	C5.3 Soak -Acid (immature)	
	Quick lime	1.2 %	Sealed	-	-
Soaked			immature	Acid	L1.2 Soak -Acid (immature)
2.5 %		Sealed	-	-	L2.5 Seal
		Soaked	immature	Pure	L2.5 Soak -Pure (immature)
			immature	Acid	L2.5 Soak -Acid (immature)
mature		Acid	L2.5 Soak-Acid (mature)		
3.8 %		Sealed	-	-	L3.8 Seal
		Soaked	immature	Acid	L3.8 Soak -Acid (immature)

In this study, two load cells with a capacity of 200 kg (2 kN) and 1000 kg (10 kN) were used. The load cells were calibrated manually by loading and unloading metallic discs of known weight on an aluminum disc screwed to the top of the loading piston to vary within 5V of digital output. Calibration curves for load cell 2 kN and 10 kN are shown in Figure 3:15 (a) and (b) respectively.

### 3.5.3 Device for measuring strain

An External Displacement Transducer having a capacity of 30 mm displacement was used to measure the axial strain of the specimen. As shown in Figure 3:16 (a) it was externally fixed as it is touching a rigid horizontal plate connected to the loading piston. This was a conventional type transducer which worked in a linear proportional manner between displacement and voltage. The EDT was calibrated by measuring the output voltage by adding and removing blocks with known standard heights. Calibration curve for EDT is shown in Figure 3:16 (b).

### 3.5.4 Testing procedure

Unconfined compression tests were conducted on both case A and case B specimens after 7, 28, 168, 336 and 672 days of their preparation. In the cases of the specimens cured under case B<sup>1</sup> the tests were conducted after 175, 196, 336 and 504 days of their preparation. In all the cases three specimens from each curing types were tested. The compressive stress and the deformation of each specimen were measured and recorded. In addition to that, the failure mode also recorded. Finally, a soil sample from each specimen was collected for checking the moisture content.

## 3.6 Needle penetration test

In order to find out localized strengths and the progression of deterioration, needle penetration test was conducted. Several researchers (Hashimoto et al., 2018; Ngoc, Turner, Huang, & Kelly, 2016; Takahashi, Morikawa, Fujii, & Kitazume, 2017) stated needle penetration test as an effective testing method for evaluating the deterioration of improved soils. In addition to that needle penetration test was identified as a proper index test for estimating unconfined compressive strength within 0.1 -100 MPa as shown in Figure 3:17 (Ulusay and Erguler 2012). In this study, needle penetration tests were conducted under two methods and they were slightly different from the JGS 3431 standard as summarized in Table 3:5.

Table 3:5 Difference between standard test and this study

	JGS 3431 standard	This study	
		Method-1	Method-2
Needle diameter (mm)	0.84	0.84	0.84
Needle length (mm)	10	30	15
Penetration rate (mm/minute)	20±5	11	11



### **3.6.1 Apparatus**

The same small, strain-controlled triaxial apparatus which was used for unconfined compression test was used for conducting needle penetration test as shown in Figure 3:18. In this setup, penetration resistance was measured by using 2 kN load cell and a high accuracy electric balance. Penetration depth was measured by external displacement transducer which was introduced in section 3.5.3.

### **3.6.2 Testing procedure**

#### **3.6.2.1 Method 1**

Needle penetration tests were conducted from three directions at the middle height of the specimens up to 20 mm depth as illustrated in Figure 3:19. The tests were conducted periodically after 7, 28, 168, 336 and 672 days of their preparation under both case A and B. In the cases of the specimens cured under case B<sup>1</sup> the tests were conducted after 175, 196, 336 and 504 days of their preparation.

#### **3.6.2.2 Method 2**

In order to understand whether there was a negative effect on the measured penetration resistance in method 1 due to the long length of the needle, method 2 was conducted following standard needle penetration test only after the curing of 672 days as illustrated in Figure 3:20 (a). In here first, the needle was penetrated 10 mm depth only from one side at three or four different heights of the specimen as shown in Figure 3:20 (b). After that 5mm depth of the surface layer was trimmed off and another set of measurements were obtained in next 10 mm depth. This procedure was followed to get measurements at depths of 0-10, 5-15, 10-20, 15-25 and 20-30 mm from the exposed surface. The obtained results were summarized in appendix 2.

## **3.7 Electron probe microanalysis (EPMA)**

### **3.7.1 Apparatus**

JXA-8230 electron probe microanalyzer from JEOL company was used as in Figure 3:21 (b). The configuration of the apparatus is shown in Figure 3:22 (Mori & Yamada, 2007). In here an electron beam was applied to the surface of the specimen under vacuum and then the characteristic X-ray generated by irradiation, corresponding to each chemical composition of the sample was detected by detectors. By analyzing the intensity and the wavelength of the X-rays, the elements present in the specimen surface could be identified and quantified.

Importance and the limitation of the application of Electron probe microanalysis on ion transportation or phase changes in geology, improved soil or concrete were explained by several researchers (Batanova, Sobolev, & Magnin, 2018; Elakneswaran, Iwasa, Nawa, Sato, & Kurumisawa, 2010; Lanari, Vho, Bovay, Airaghi, & Centrella, 2019; Lerouge et al., 2017; McGee, 2001; Mori & Yamada, 2007; Mori, Yamada, Hosokawa, & Yamamoto, 2006; Yoshida, Matsunami, Nagayama, & Sakai, 2010; Zhao, Zhang, & Essene, 2015). The main purpose of using EPMA analysis on this study was to identify the calcium distribution of the sealed and soaked specimens.

### 3.7.2 Specimen preparation

After conducting needle penetration test under method 1, the specimen was broken into two parts from the middle height. Then one of those parts was dried under 40-degree oven (Scrivener, Snellings, & Lothenbach, 2015) around 14 days until the pore water evaporate. Then a cross-section was sliced near to the middle height of the specimen and reinforced it by the intrusion of an epoxy resin. In order to prevent loss of water-soluble minerals (Mori & Yamada, 2007), the surface was polished using kerosene until gaining a smooth surface. Finally, the specimen was dried under vacuum and applied a carbon coating as shown in Figure 3:21 (a). The detailed procedure for specimen preparation is included in JSCE-G 574-2005.

### 3.7.3 Testing procedure

EPMA measurement was taken with an acceleration voltage of 50 kV, beam current of 100 nA, the unit measurement time of 10 ms/point and pixel size of 35  $\mu\text{m}$ . Ion distribution of calcium, carbon, and silica was obtained. EPMA tests were conducted only on the limited types of specimens by considering the limitation of the use of apparatus as summarized in Table 3:6.

Table 3:6 Summary of EPMA analysis

Curing type	Curing period (days)	Cement 3.5 %	Cement 5.3 %	Lime 2.5 %	Lime 3.8 %
Sealed	28	x	x	x	x
	168	o	x	x	x
	336	x	x	o	o
Soaked-acid (immature)	28	o	x	x	o
	168	o	x	x	o
	336	o	x	o	o

## **3.8 X-ray Fluorescence spectrometer analysis (XRF)**

### **3.8.1 Apparatus**

X-ray fluorescence spectrometer analysis was conducted to quantify the oxide percentage from each element in the soil specimen. As shown in Figure 3:23, JEOL JSX-3400RII Energy Dispersive X-Ray Fluorescence Spectrometer was used. In this apparatus, an X-ray beam was applied to the surface of the specimen and the energy emitted from fluorescent X-ray radiation was measured to identify the elements which were present (Brouwer, 2003). Then quantitative analysis was conducted by considering intensities of the emitted energy and the weight percentage of oxides of each element were obtained. This method had been used by several researchers (Baranowski, Rybak, & Baranowska, 2002; Kodom, Preko, & Boamah, 2012) for quantitative evaluation of elements.

### **3.8.2 Specimen preparation**

After conducting needle penetration test and the unconfined compression test on all the cases powdered soil samples from different distance from surface as 0-5 mm, 10-15 mm and 20-25 mm were collected as schematically shown in Figure 3:24 (a). Additional powdered samples were collected from the outermost (0 mm) layer of the soaked specimens as there was thin white color deposition as shown in Figure 3:24 (b). All the collected samples were dried under 40-degree oven (Scrivener et al., 2015) around 14 days until all the pore water evaporate. Dried samples were finely grounded using a mechanical grinder. Around 1.2 g was collected and compacted inside a metal ring until it becomes thin and gives uniform density and thickness. It was important to maintain the same density and the thickness in each case to compare quantified results because the fluorescence depends on the thickness and the density of the material (Brouwer, 2003).

### **3.8.3 Testing procedure**

XRF measurements were taken on all the improved or natural soil specimens which were collected in all the curing periods. The analyses were conducted by applying X-ray voltage of 15 kV, X-ray current of 0.3mA and measurement times of 300 s.

## **3.9 X-ray diffractometer analysis (XRD)**

### **3.9.1 Apparatus**

X-ray powder diffractometer analysis is widely used to characterize crystalline and amorphous materials. This technique had been reported in most of the studies based on improved soils for

qualitative analysis of phase changes due to change of curing period or curing conditions (Chew, Kamruzzaman, & Lee, 2004; Elena & Lucia, 2012; Jadhav & Debnath, 2011; Kadum, Al-Azzawi, & al-Attar, 2018; Kamruzzaman, Chew, & Lee, 2009; Rahman, Siddique, & Uddin, 2010; Sharpley, 2015; Tabet, Cerato, Elwood Madden, & Jentoft, 2018; Ureña Nieto, 2014; Voglis, Kakali, & Tsivilis, 2001). In addition to that several studies were discussed on the application of this technique to quantitative analysis of minerals using Rietveld analysis ((Aranda\*, De la Torre, & Leon-Reina, 2012; Hoshino, Yamada, & Hirao, 2006; Scrivener, Füllmann, Gallucci, Walenta, & Bermejo, 2004; Scrivener et al., 2015).

As shown in Figure 3:26 Empyrean, Malvern Panalytical apparatus was used in this study. In here X-ray beam was applied to the specimen and the intensity of the peaks of the diffracted X-ray was detected by the detectors. The angle or position of the peak was determined by Bragg's law. Crystalline or amorphous structures contained in minerals have a unique three-dimensional arrangement of atoms. So, the position of the peaks and the relative intensities are identical to each mineral. This concept helped to identify unknown minerals in the sample.

### **3.9.2 Specimen preparation**

Powdered soil samples were collected from each case at every curing periods by following the same procedure as explained in section 3.8.2. Those specimens were dried under 40-degree oven up to curing period of 336 days. From analysis results, it was found that temperature affected the minerals and destroy or change hydration products. Hence the drying method of the specimen was changed by using acetone after a curing period of 672 days. In addition to that same procedure was applied to the specimens after reproducing 7 and 28 days curing. The specimens were separated into two groups. XRD analysis was applied to one set only after drying using acetone. For the second sets of specimen heavy liquid was applied to separate hydration products and the soil particles before applying XRD analysis. Because the binder contents used in this study was relatively small, the amount of generated hydration products assumed to be small.

#### **3.9.2.1 Acetone application**

The particles of the collected soils from different depths were crushed to make the diameter less than 2 mm and put them into separate beakers (capacity 100 ml) as 10 g of wet soil for each. Then 50 ml of acetone liquid was poured into the beaker and mixed them well and sealed the top of the beaker with plastic wrapping as shown in Figure 3:27. After 2 hours, used acetone was slowly removed while giving no opportunity to escape soil particles and another 50 ml of

acetone was poured again. After more 2 hours of waiting, acetone was removed and allow the soil to dry in the air around 5 minutes. After vaporized all liquid acetone, the beaker with soil was put inside a 40-degree oven around 5 minutes. After drying the soil properly, it was further crushed into small particles and put into an airtight container and sealed. The acetone application procedure was conducted inside a ventilation chamber considering safety and health issues. The procedure followed here was explained in detail in the report of the technical committee on cement chemistry C-11 (Study on the method of stopping hydration for hardened cement paste or mortar and cement hydrates) in Japan. The main purpose for the application of acetone in this study was to exchange pore water into acetone to minimize carbonation (Scrivener et al., 2015) while the samples stores before applying XRD analysis.

### 3.9.2.2 Heavy liquid application

A heavy liquid application was conducted using “Bromoform ( $\text{CHBr}_3$ )” liquid as shown in Figure 3:28 (a). The original density of the liquid was  $2.65 \text{ g/cm}^3$  and it contained 2 % of ethanol. The density of the liquid was reduced to  $2.3 \text{ g/cm}^3$  by adding more ethanol as the density of most hydration products are less than that value as summarized in Table 3:7 (Scrivener et al., 2015; Taylor, 1997).

5g of soil from each case were put into separate testing tubes and then 20 ml of heavy liquid was added and sealed. Then the tubes were put into a centrifugal separator and rotate at a speed of 4000 rpm until 15 minutes as shown in Figure 3:28 (b) and (c). After that procedure, the lighter part floating in the liquid was separated under vacuum by washing with ethanol as shown in Figure 3:29. The heavy liquid was applied again for the lighter part by repeating the above procedure to further separation of soil particles and hydration products. Finally, the separated particles were washed with acetone and let them dry in the air for several minutes.

### 3.9.3 Testing procedure

After application of acetone or heavy liquid to the improved or natural soil samples, the collected powder was further crushed to fines using agate mill as shown in Figure 3:30 (a). Then the powdered sample was leveled on a glass mold and covered it with an aluminum supporter as shown in Figure 3:30 (b) and (c) respectively. XRD patterns were obtained using  $\text{Cu K}\alpha$  ( $\lambda = 1.54178 \text{ \AA}$ ). The apparatus setup is summarized in Table 3:8.

Table 3:7 Density of hydration products

Hydration product	Chemical formula	Density (g/cm <sup>3</sup> )
Gypsum	CaSO <sub>4</sub> ·2H <sub>2</sub> O	2.31
Portlandite	Ca (OH) <sub>2</sub>	2.24
Calcite	CaCO <sub>3</sub>	2.71
Ettringite	Ca <sub>6</sub> Al <sub>2</sub> (SO <sub>4</sub> ) <sub>3</sub> (OH) <sub>12</sub> ·26H <sub>2</sub> O	1.77
Thaumasite	Ca <sub>3</sub> Si(OH) <sub>6</sub> ·12H <sub>2</sub> O	1.89
Monosulfate	Ca <sub>4</sub> [Al <sub>2</sub> (OH) <sub>12</sub> ] [(1-x) SO <sub>4</sub> .x(OH) <sub>2</sub> ]. 6H <sub>2</sub> O	2.01
Stratlingite	Ca <sub>2</sub> Al <sub>2</sub> (SiO <sub>2</sub> ) (OH) <sub>10</sub> .2.5(H <sub>2</sub> O)	1.94
Monocarbonate		2.17

Table 3:8 Setting of XRD apparatus

X-ray tube voltage (kV)	45
X-ray tube current (mA)	40
Scan range (2θ)	5-65
Scan step size	0.026261
Number of points	2284
Time per step (s)	176.715

### 3.10 Soaking water measurement

The soaking water was collected each time they were exchanged for checking pH value, Ca concentrations and sulfate concentrations. pH value was measured by a glass electrode method using a compact analyzer (Horiba LAQUA twin B-712) as shown in Figure 3:31. The concentration of Ca was obtained by ion electrode method using another compact analyzer (Horiba LAQUA twin B-715). The concentration of sulfate was quantified by ion chromatography (JIS K 0102 41.3).

---

### 3.11 Reference

- Aranda, M. A. G., De la Torre, A. G., & Leon-Reina, L. 2012. Rietveld Quantitative Phase Analysis of OPC Clinkers, Cement and Hydration Products. *Reviews in Mineralogy and Geochemistry*, 74(1): 169–209.
- Baranowski, R., Rybak, A., & Baranowska, I. 2002. *Speciation Analysis of Elements in Soil Samples by XRF*, 10.
- Batanova, V. G., Sobolev, A. V., & Magnin, V. 2018. Trace element analysis by EPMA in geosciences: Detection limit, precision and accuracy. *IOP Conference Series: Materials Science and Engineering*, 304: 012001.
- Brouwer, P. 2003. *Theory of XEF: Getting acquainted with the principles*. Almelo: PANalytical BV.
- Chae, J., Kim, B., Park, S., & Kato, S. 2010. Effect of suction on unconfined compressive strength in partly saturated soils. *KSCE Journal of Civil Engineering*, 14(3): 281–290.
- Chew, S. H., Kamruzzaman, A. H. M., & Lee, F. H. 2004. Physicochemical and Engineering Behavior of Cement Treated Clays. *Journal of Geotechnical and Geoenvironmental Engineering*, 130(7): 696–706.
- Dipova, N. 2018. Nondestructive Testing of Stabilized Soils and Soft Rocks via Needle Penetration. *Periodica Polytechnica Civil Engineering*.  
<https://doi.org/10.3311/PPci.11874>.
- Elakneswaran, Y., Iwasa, A., Nawa, T., Sato, T., & Kurumisawa, K. 2010. Ion-cement hydrate interactions govern multi-ionic transport model for cementitious materials. *Cement and Concrete Research*, 40(12): 1756–1765.
- Elena, J., & Lucia, M. D. 2012. Application of X-ray diffraction (XRD) and Scanning electron microscopy (SEM) methods to the portland cement hydration processes. *Journal of Applied Engineering Sciences*, 2(15): 35–42.
- Hashimoto, H., Yamanashi, T., Hayashi, H., Kawaguchi, T., Kawajiri, S., et al. 2018. Long-Term Strength Characteristics of the Cement Treated Soil after 30 Years. *Journal of the Society of Materials Science, Japan*, 67(1): 47–52.
- Hoshino, S., Yamada, K., & Hirao, H. 2006. XRD/Rietveld Analysis of the Hydration and Strength Development of Slag and Limestone Blended Cement. *Journal of Advanced Concrete Technology*, 4(3): 357–367.
- Jadhav, R., & Debnath, N. C. 2011. Computation of X-ray powder diffractograms of cement components and its application to phase analysis and hydration performance of OPC cement. *Bulletin of Materials Science*, 34(5): 1137–1150.

- 
- Kadum, N., Al-Azzawi, Z., & al-Attar, T. 2018. XRD analysis for hydration products of different lime-pozzolan systems. (T. S. Al-Attar, M. A. Al-Neami, & W. S. AbdulSahib, Eds.) *MATEC Web of Conferences*, 162: 02007.
- Kamruzzaman, A. H., Chew, S. H., & Lee, F. H. 2009. Structuration and Destructuration Behavior of Cement-Treated Singapore Marine Clay. *Journal of Geotechnical and Geoenvironmental Engineering*, 135(4): 573–589.
- Kawamura, M., Hasaba, S., & Sugiura, S. 1971. A function of free lime and characteristics of cement hydration in compacted clay-cement mixtures. *Proceedings of the Japan Society of Civil Engineers*, 1971(191): 117–131.
- Kett, I. J., Ingham, J., & Evans, J. 2010. Identifying an effective binder for the stabilisation of allophanic soils. *International Journal of Pavement Engineering*, 11(3): 223–236.
- Kitagawa, Y. 1976. Determination of allophane and amorphous inorganic matter in clay fraction of soils: I. Allophane and allophane-halloysite mixture. *Soil Science and Plant Nutrition*, 22(2): 137–147.
- Kitagawa, Y. 1980. Rapid Determination of Allophane and Amorphous Inorganic Materials in Soils. *Japan Agricultural Research Quarterly*, 14(1): 15–19.
- Kobashi, T. 1967. *Reaction of calcium hydroxide with allophane-Kaolinite clay minerals*, 3(1–2): 11–36.
- Kodom, K., Preko, K., & Boamah, D. 2012. X-ray Fluorescence (XRF) Analysis of Soil Heavy Metal Pollution from an Industrial Area in Kumasi, Ghana. *Soil and Sediment Contamination: An International Journal*, 21(8): 1006–1021.
- Krrrlclwe, Y., & SoitsandFertilizers, D. 1974. Dehydratioonf Allophaneand Its StructuralFormula. *American Mineralogist*, 59: 1094–1974.
- Lanari, P., Vho, A., Bovay, T., Airaghi, L., & Centrella, S. 2019. Quantitative compositional mapping of mineral phases by electron probe micro-analyser. *Geological Society, London, Special Publications*, 478(1): 39–63.
- Lerouge, C., Gaboreau, S., Grangeon, S., Claret, F., Warmont, F., et al. 2017. In situ interactions between Opalinus Clay and Low Alkali Concrete. *Physics and Chemistry of the Earth, Parts A/B/C*, 99: 3–21.
- Lu, N., Godt, J. W., & Wu, D. T. 2010. A closed-form equation for effective stress in unsaturated soil: Effective stress in unsaturated soil. *Water Resources Research*, 46(5). <https://doi.org/10.1029/2009WR008646>.
- McGee, J. et al. 2001. Application of Electron Probe Microanalysis to the Study of Geological and Planetary Materials. *Microscopy and Microanalysis*, 7: 200–210.
-



- Mori, D., & Yamada, K. 2007. A Review of Recent Applications of EPMA to Evaluate the Durability of Concrete. *Journal of Advanced Concrete Technology*, 5(3): 285–298.
- Mori, D., Yamada, K., Hosokawa, Y., & Yamamoto, M. 2006. Applications of Electron Probe Microanalyzer for Measurement of Cl Concentration Profile in Concrete. *Journal of Advanced Concrete Technology*, 4(3): 369–383.
- Ngoc, P. V., Turner, B., Huang, J., & Kelly, R. 2016. *Experimental Study on the Durability of Soil-Cement Columns in Coastal Areas*, 6.
- Parfitt, R. L. 2009. Allophane and imogolite: Role in soil biogeochemical processes. *Clay Minerals*, 44(01): 135–155.
- Rahman, Md. M., Siddique, A., & Uddin, Md. K. 2010. Microstructure and chemical properties of cement treated soft bangladesh clays. *Soils and Foundations*, 50(1): 1–7.
- Scrivener, K. L., Füllmann, T., Gallucci, E., Walenta, G., & Bermejo, E. 2004. Quantitative study of Portland cement hydration by X-ray diffraction/Rietveld analysis and independent methods. *Cement and Concrete Research*, 34(9): 1541–1547.
- Scrivener, K., Snellings, R., & Lothenbach, B. (Eds.). 2015. *A Practical Guide to Microstructural Analysis of Cementitious Materials*. CRC Press. <https://doi.org/10.1201/b19074>.
- Sharpley, I. 2015. *The Effect of Hydration on the Microstructural Properties of Individual Phases of Ordinary Portland Cement*, 62.
- Tabet, W. E., Cerato, A. B., Elwood Madden, A. S., & Jentoft, R. E. 2018. Characterization of Hydration Products' Formation and Strength Development in Cement-Stabilized Kaolinite Using TG and XRD. *Journal of Materials in Civil Engineering*, 30(10): 04018261.
- Takahashi, H., Morikawa, Y., Fujii, N., & Kitazume, M. 2017. Thirty-seven-year investigation of quicklime-treated soil produced by deep mixing method. *Proceedings of the Institution of Civil Engineers - Ground Improvement*, 1–13.
- Taylor, H. F. W. 1997. *Cement chemistry* (2nd ed). London: T. Telford.
- Ulusay, R., & Erguler, Z. A. 2012. Needle penetration test: Evaluation of its performance and possible uses in predicting strength of weak and soft rocks. *Engineering Geology*, 149–150: 47–56.
- Ureña Nieto, C. G. 2014. *A study on the use of non-conventional additives for stabilisation of expansive soils*. Editorial de la Universidad de Granada, Granada.
- Voglis, N. A., Kakali, G. T., & Tsvilis, S. G. 2001. Identification of Composite Cement Hydration Products by Means of X-Ray Diffraction. *Mikrochimica Acta*, 136: 181–183.
-

Yoshida, N., Matsunami, Y., Nagayama, M., & Sakai, E. 2010. Salt Weathering in Residential Concrete Foundations Exposed to Sulfate-bearing Ground. *Journal of Advanced Concrete Technology*, 8(2): 121–134.

Zhao, D., Zhang, Y., & Essene, E. J. 2015. Electron probe microanalysis and microscopy: Principles and applications in characterization of mineral inclusions in chromite from diamond deposit. *Ore Geology Reviews*, 65: 733–748.

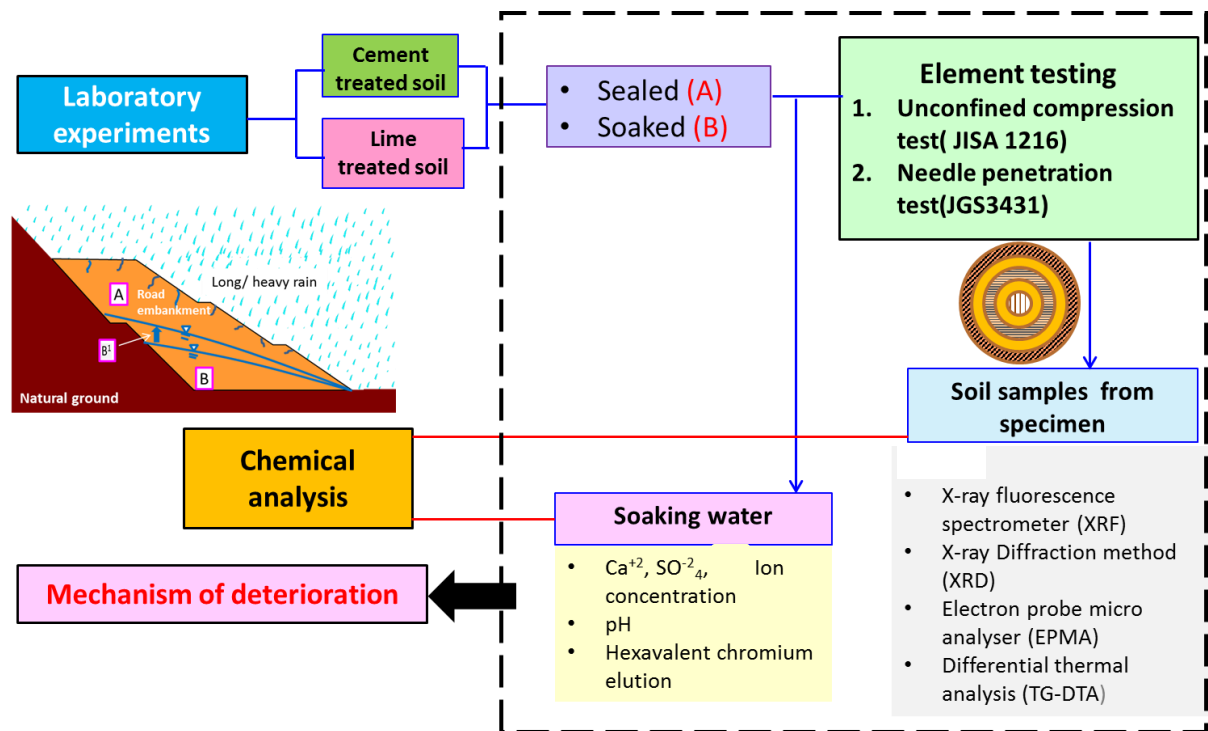


Figure 3:1 Methodology

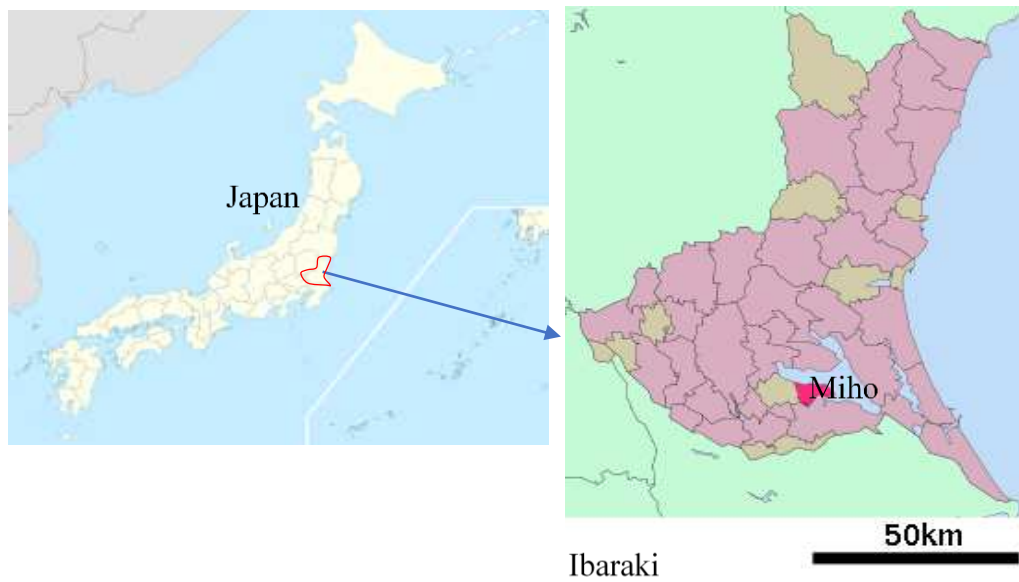


Figure 3:2 Location where Miho sand was taken

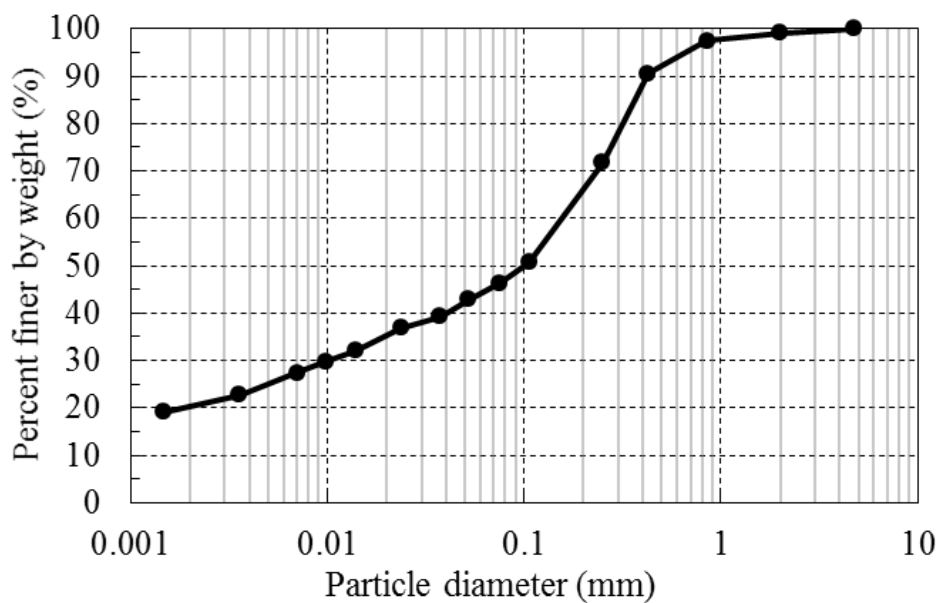


Figure 3:3 Particle size distribution of Miho sand

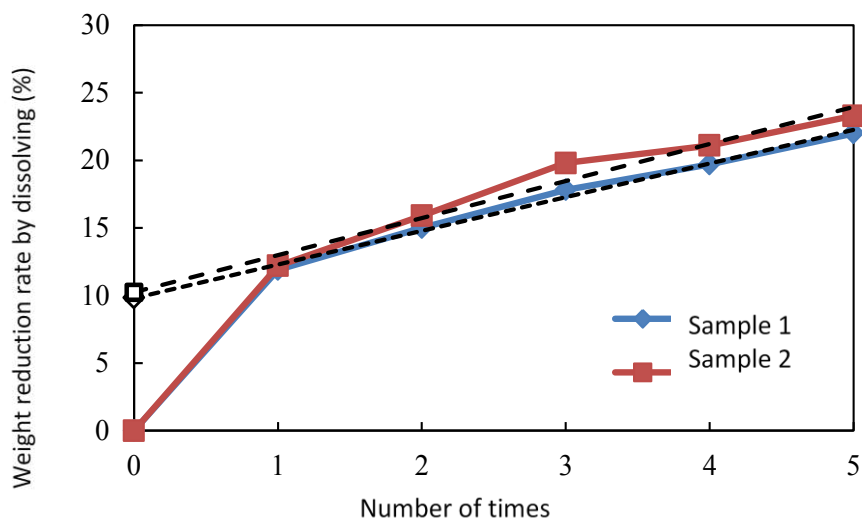


Figure 3:4 Amorphous content in Miho sand

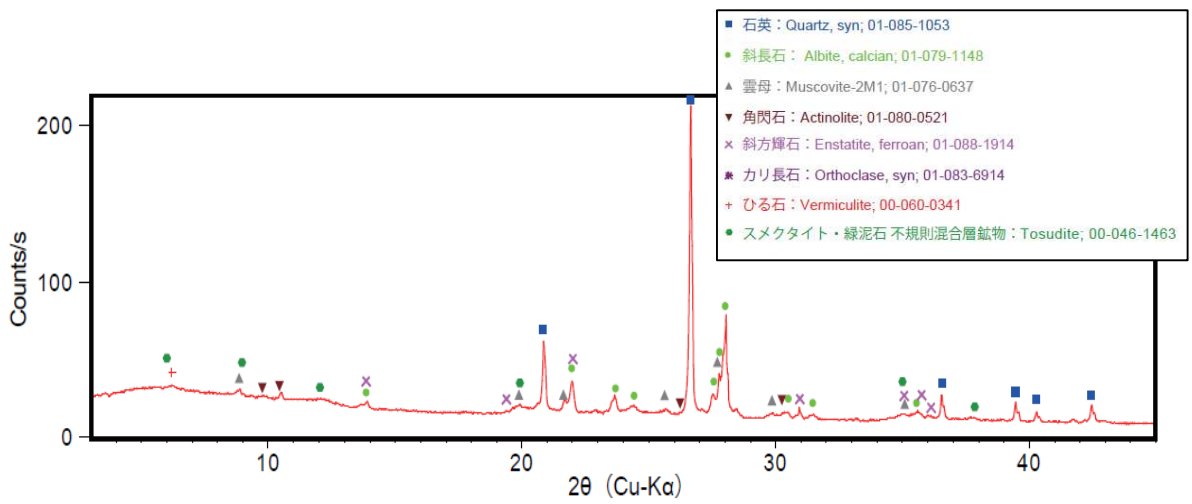


Figure 3:5 Minerals identified by XRD analysis- Miho sand

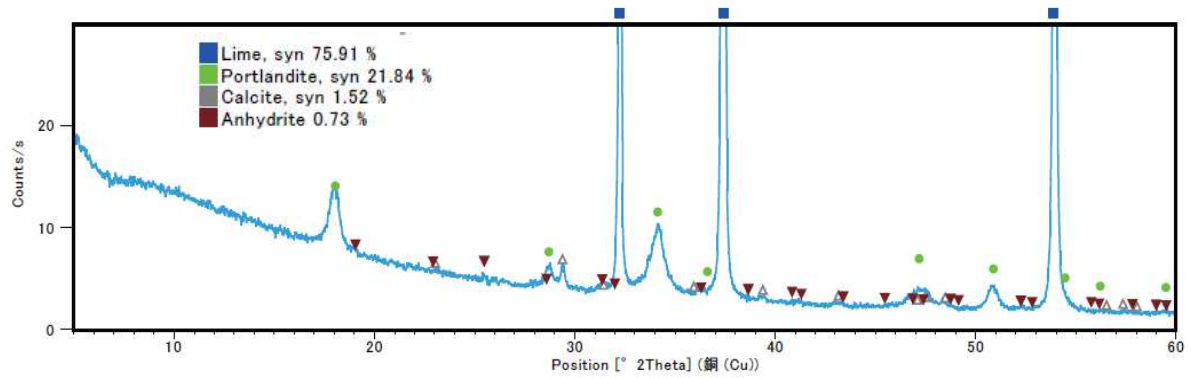


Figure 3:6 Minerals identified by XRD-Quick lime

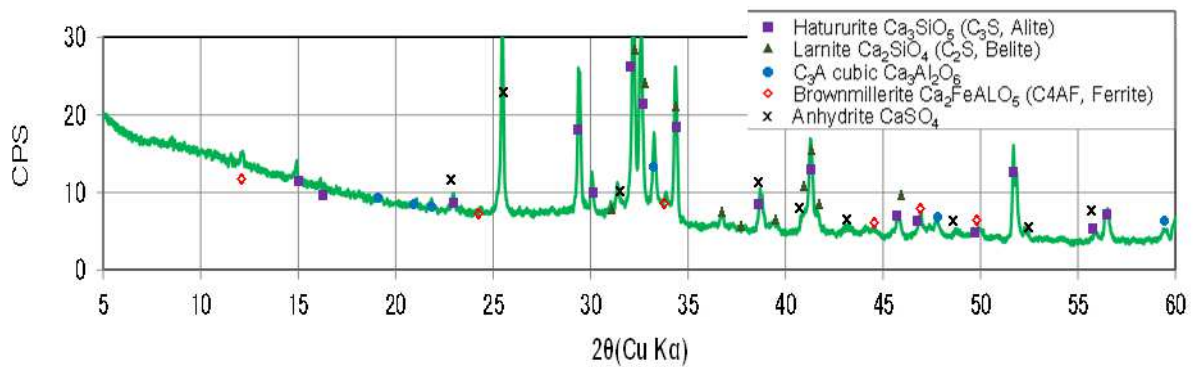


Figure 3:7 Minerals identified by XRD - Cement

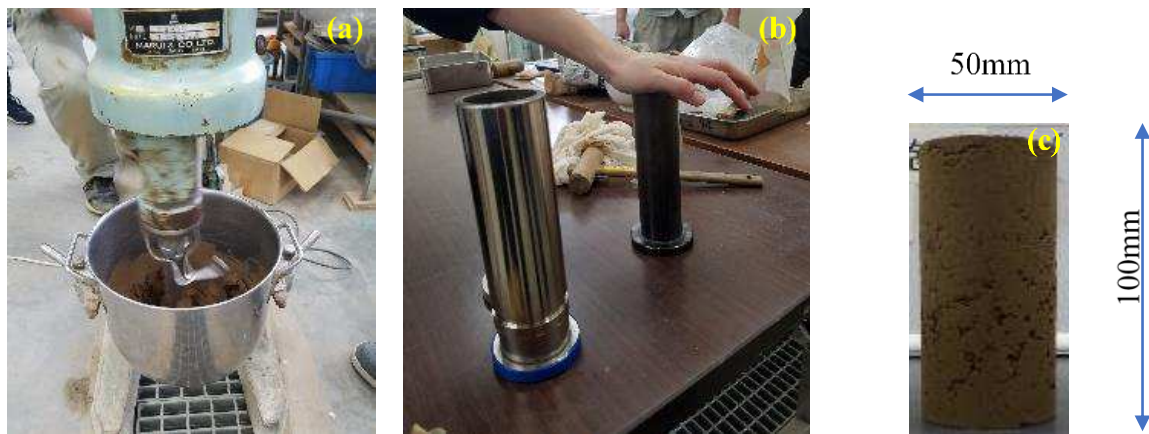


Figure 3:8 Specimen preparation method (a) Mixture (b) Standard mold (c) Dimensions of specimen

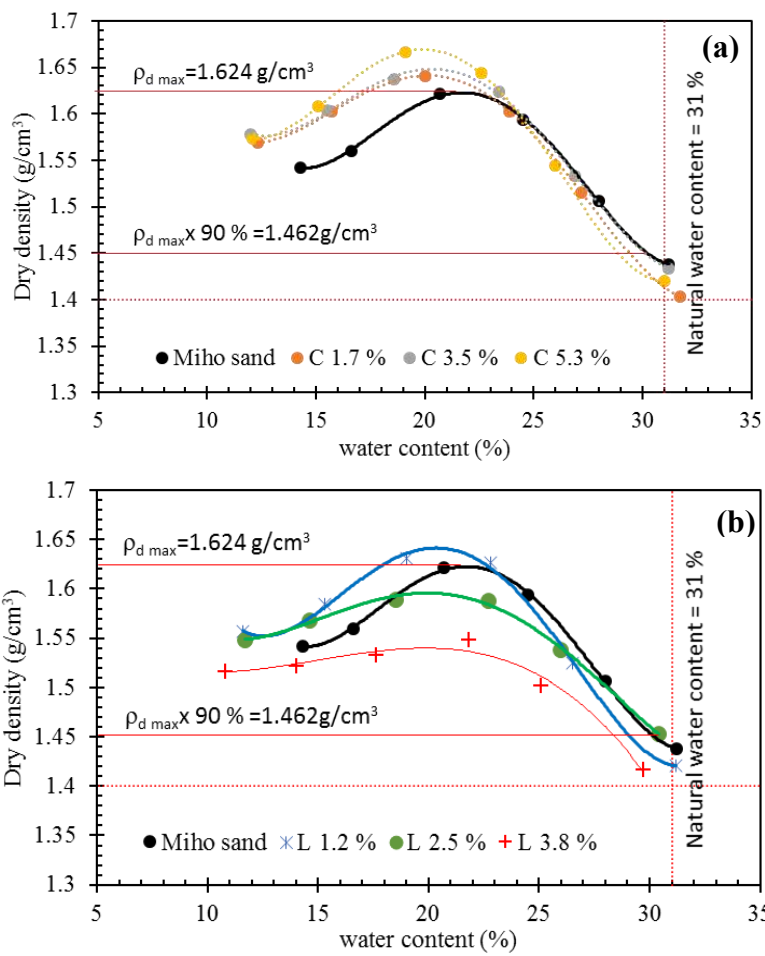


Figure 3:9 Standard proctor compaction curve (a) cement-treated soil (b) Lime treated soil

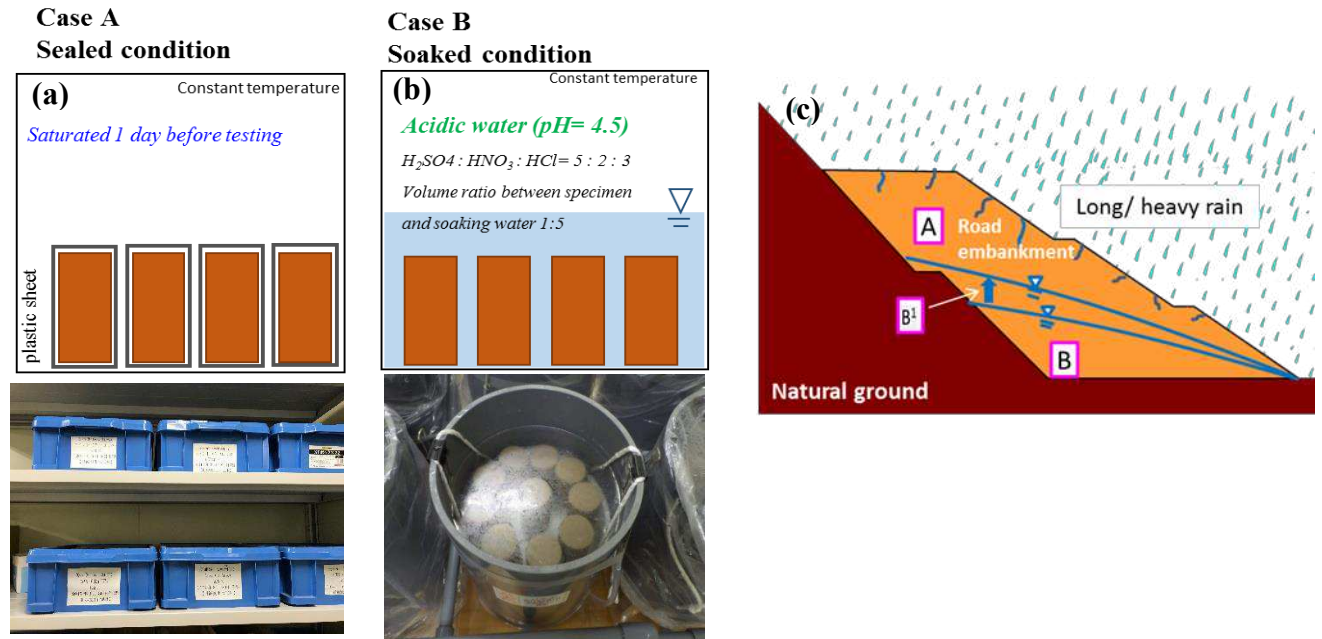
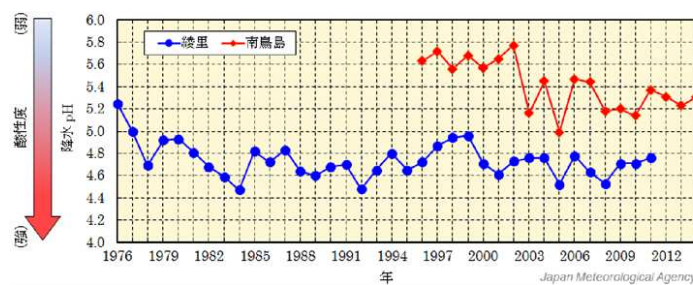


Figure 3:10 Curing conditions (a) Sealed condition (b) Soaked condition (c) Systematic figure of a road embankment which simulate each curing conditions



Change of acidity of precipitation (Japan Meteorological Agency)

Figure 3:11 Change of acidity of precipitation



Figure 3:12 Setting up of tap lines for changing soaking water



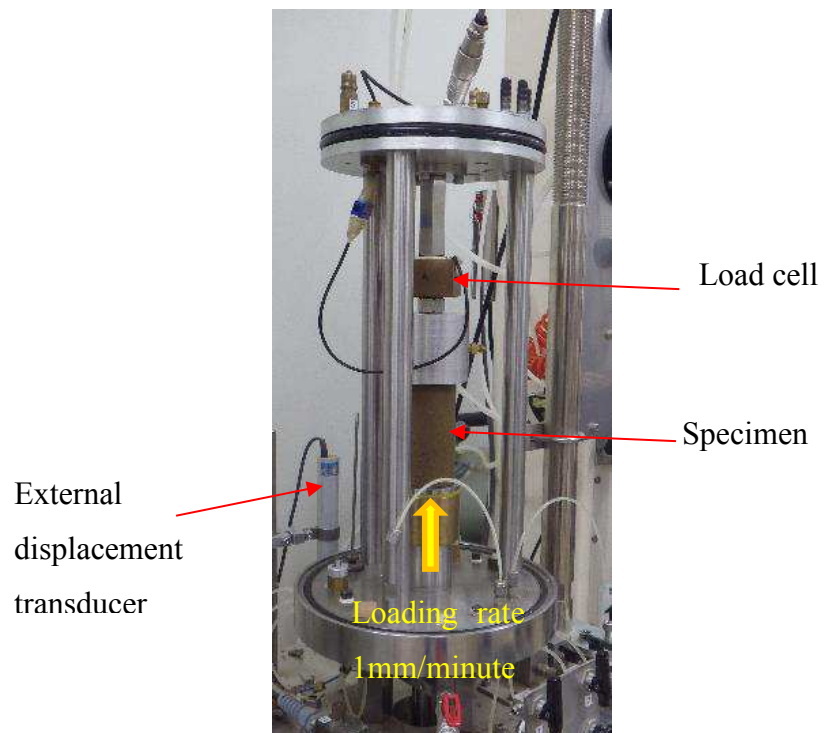


Figure 3:13 Unconfined compression test apparatus



Figure 3:14 Load cell



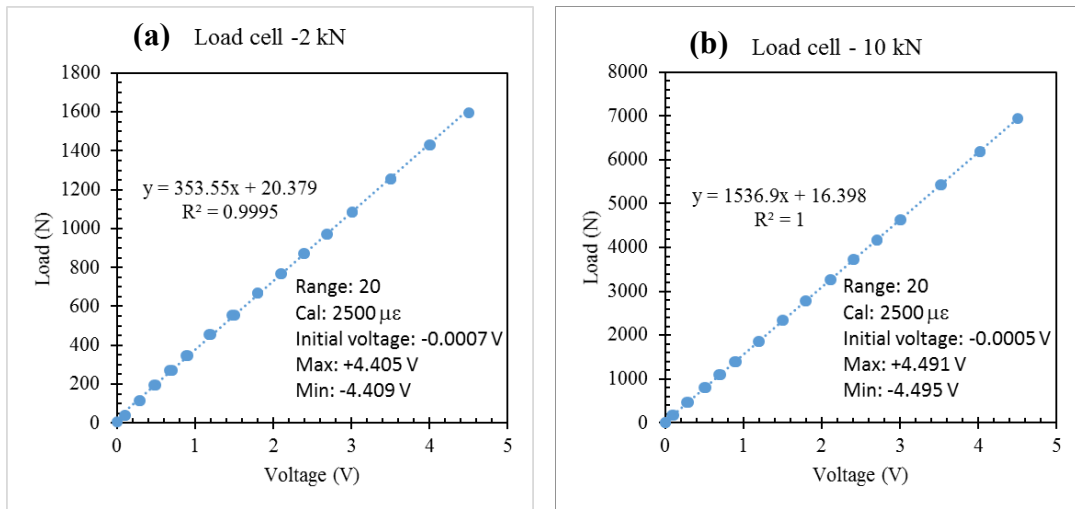


Figure 3:15 Calibration curves for load cell (a) 2 kN (b) 10 kN

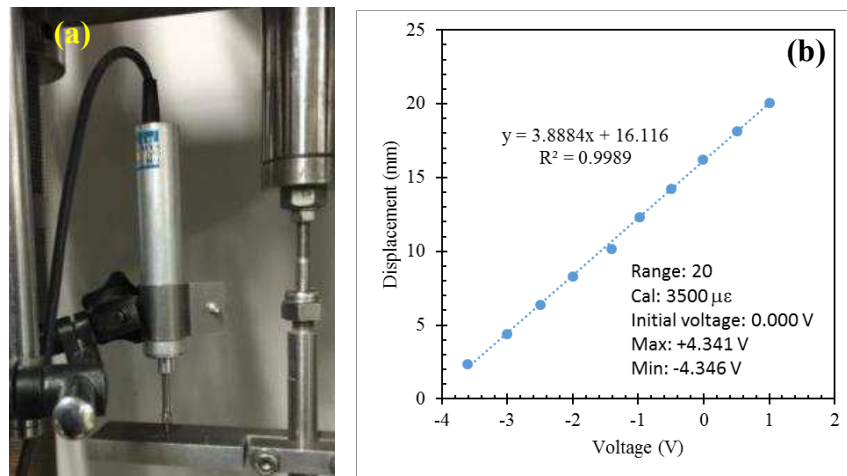


Figure 3:16 (a) External Displacement Transducer (EDT) (b) Calibration curve of EDT

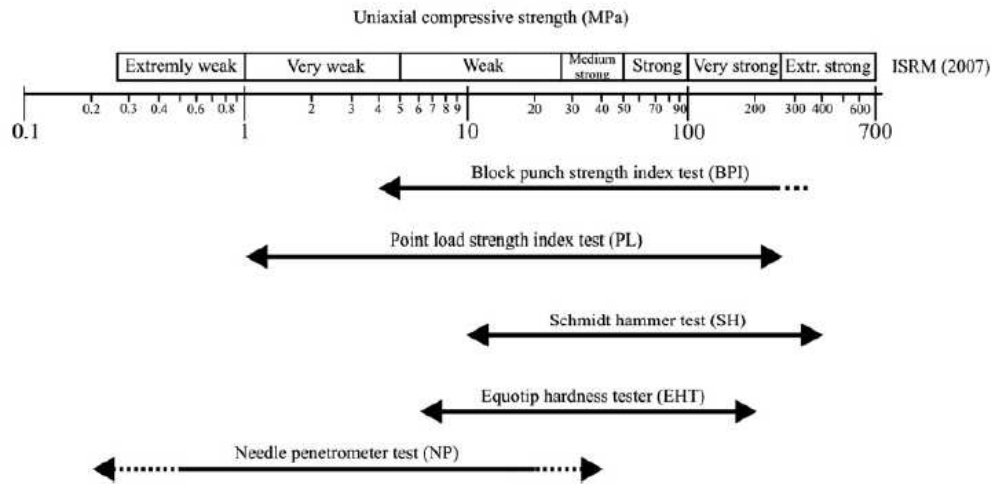


Figure 3:17 Range of applicability of Needle penetration test

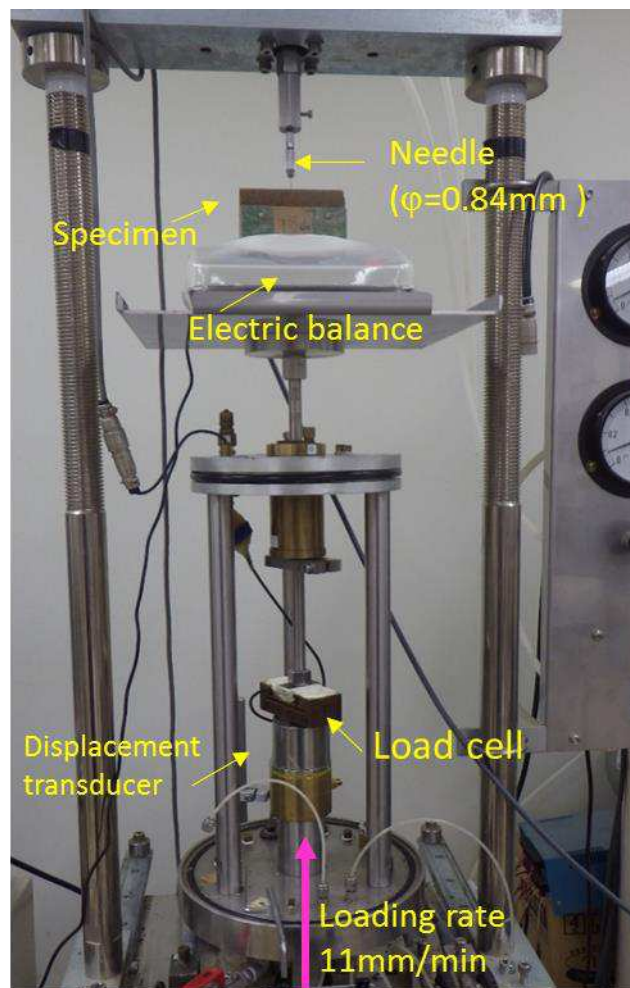


Figure 3:18 Needle penetration test apparatus setup

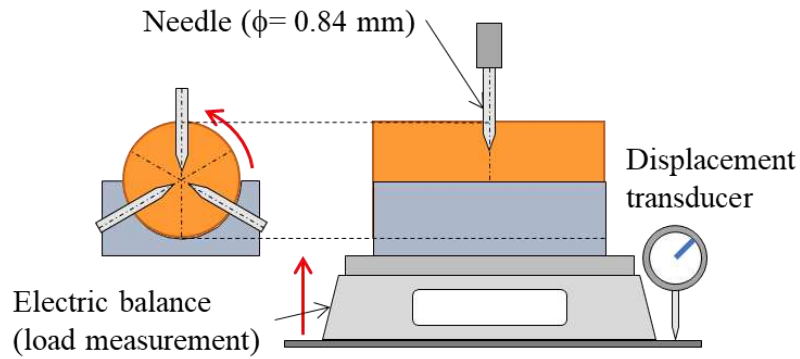


Figure 3:19 Needle penetration test- method 1

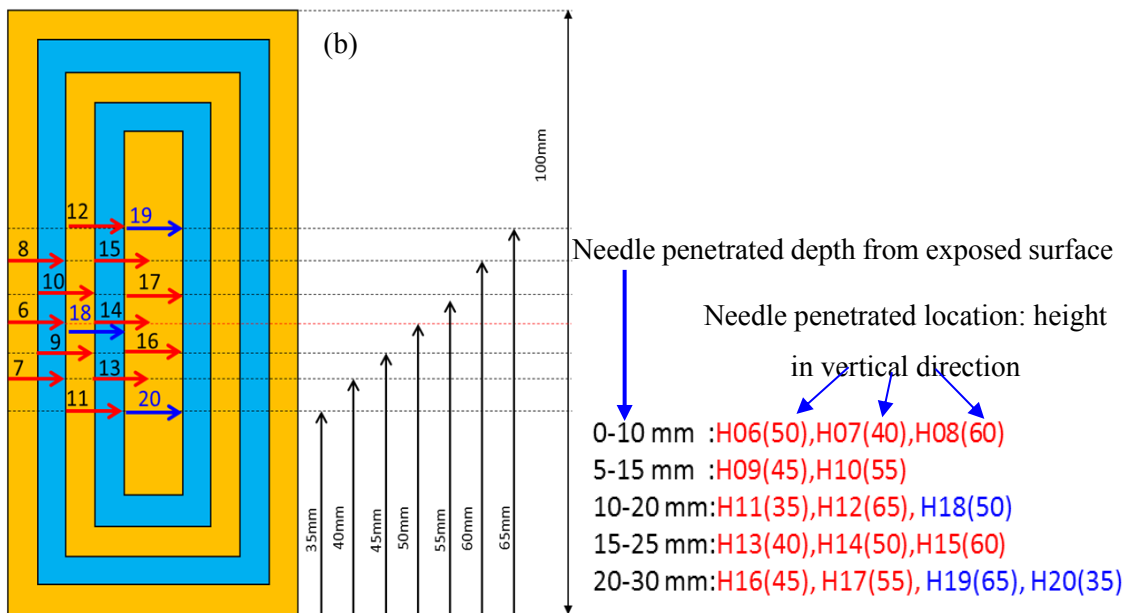
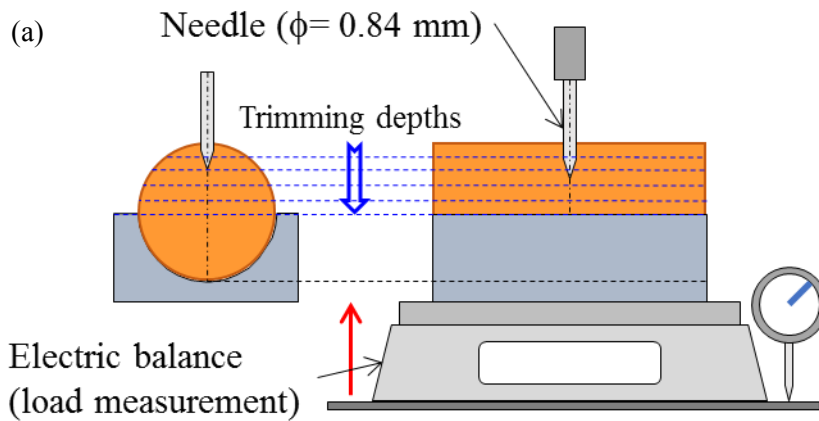


Figure 3:20 (a) Needle penetration test -method 2 (b) Illustration of needle penetrated depth and the location





Figure 3:23 XRF apparatus

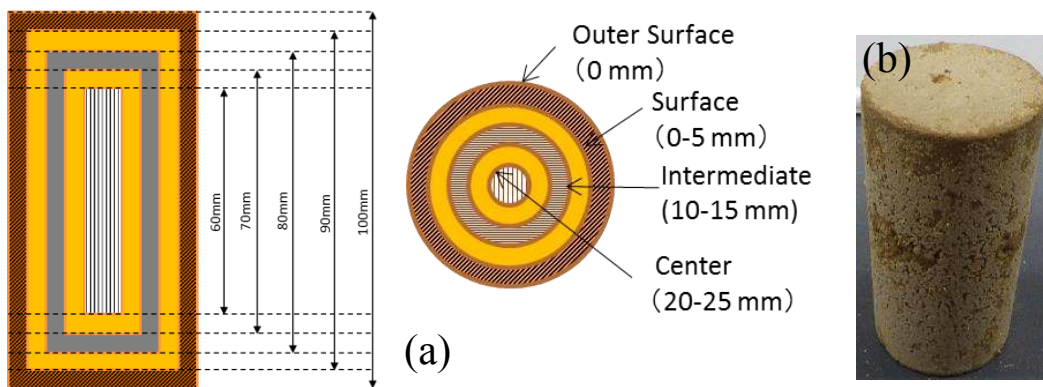


Figure 3:24 (a) Powdered sample collected location (b) Whitish deposition at the outermost layer



Figure 3:25 Compacted soil specimen for XRF analysis



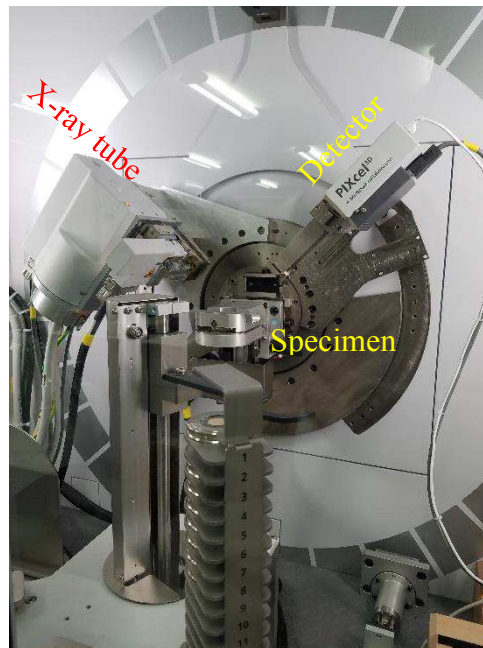


Figure 3:26 XRD apparatus



Figure 3:27 Acetone application

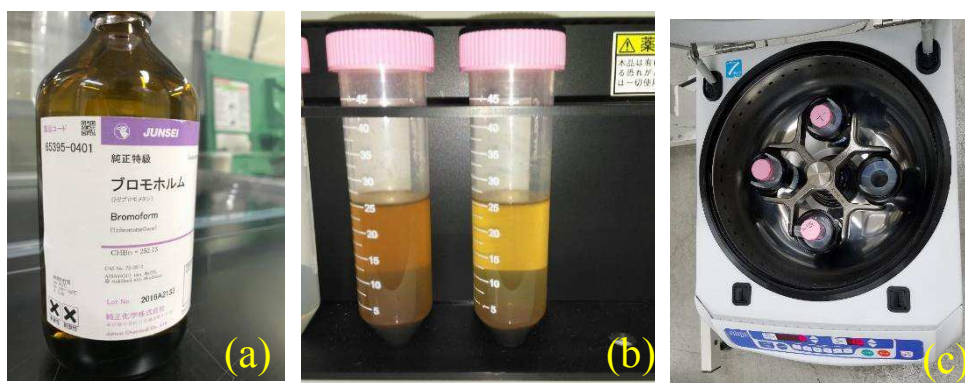


Figure 3:28 (a) Heavy liquid (b) mixing proportion (c) separation using centrifugal rotation

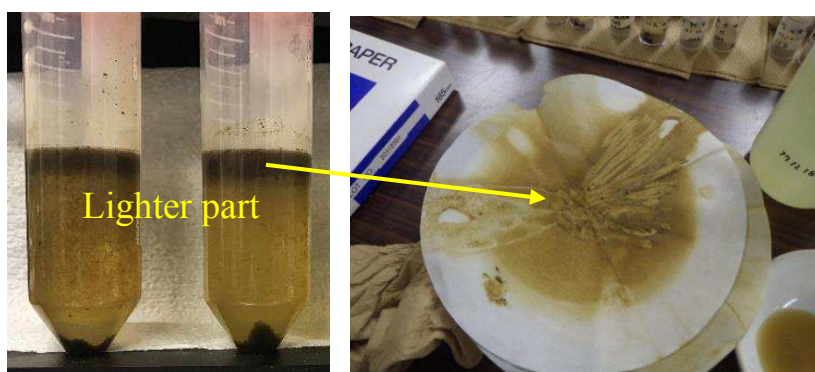


Figure 3:29 After separation of lighter particles by heavy liquid method



Figure 3:30 (a) Agate mill (b) leveling of the specimen (c) prepared specimen for XRD analysis

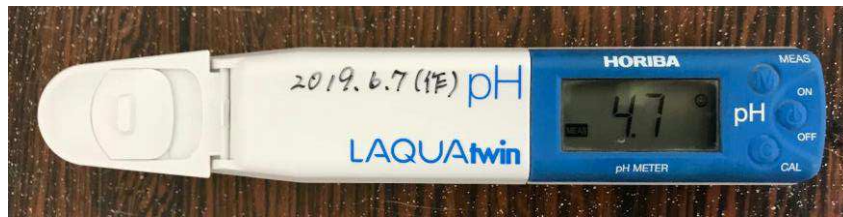


Figure 3:31 apparatus for measuring pH of soaking water



---

## 4 Influential factors on the progression of deterioration

### 4.1 Introduction

The long-term behavior of embankment which was constructed using improved surplus soils with low binder contents is affected by the change of the long-term mechanical properties of the improved soils by subjecting to different environmental exposure conditions. This chapter was prepared to discuss the stages of deterioration against soaking period by using unconfined compression test results (Hashimoto et al., 2018; Kitazume, Nakamura, Terashi, & Ohishi, 2003; Takahashi, Morikawa, Fujii, & Kitazume, 2017). Then the needle penetration test results (Ngoc, Turner, Huang, & Kelly, 2016; Takahashi et al., 2017; Yang, Yan, Liu, & Zhang, 2016) were used to explain the spatial variation of the localized strengths and their relationship with the soaking period.

### 4.2 Unconfined compression test results

#### 4.2.1 Stress-strain relationship

As explained in section 3.5.4 and Table 3:4, at a given curing period unconfined compression tests were conducted for three specimens after curing under each condition. Typical stress-strain relationships obtained after curing for 672 days under sealed and soaked conditions for improved Miho sand with a cement content of 3.5 % and lime content of 2.5 % are shown in Figure 4:1 (a) and (b) respectively. In both treatments, the highest unconfined compressive strength ( $q_u$ ) was obtained in sealed curing condition. In lime treated soil slight reduction in  $q_u$  was obtained in all soaked cases. However, in cement treated soils a clear reduction in  $q_u$  was obtained in soaked specimens. In both lime and cement treatment, there was no clear difference in their stress-strain relationships of the specimens under pure and acidic water. In order to find out the changes in the stiffness due to soaking deformation modulus,  $E_{50}$  was evaluated following the method shown in Figure 4:2. The obtained average values of  $q_u$  and  $E_{50}$  values for the three samples in each case are summarized in Table 4:1 and Table 4:2 for cement treated soil and lime treated soil respectively. The physical properties and mechanical properties of all specimens tested in unconfined compression test are summarized in Annex B.

#### 4.2.2 Relationship between the curing period and $q_u$ , $E_{50}$ in sealed and soaked conditions

Relationships between  $q_u$  values with curing period for cement treated soils and lime treated soils which were cured under sealed condition are shown Figure 4:3 and Figure 4:4 respectively.

In both treatment higher  $q_u$  values were obtained when increasing the binder content. In addition, to that, the  $q_u$  values were gradually increased with curing time except for the smallest binder contents by showing a logarithmic relationship with time. Similar observation done in previous studies.

Relationships between  $q_u$  values and  $E_{50}$  with curing period for cement treated soils which were cured under sealed and soaked condition are shown in Figure 4:5 and Figure 4:6 respectively. Under the soaked immature condition, lower strengths than those of sealed specimens were obtained after 7 days in C1.7, 28 days in C3.5, and 168 days in C5.3. That is, the effect of the soaked curing in the immature conditions appeared as the decrease in the strengths earlier when the content of the cement was smaller. When increase the soaking period up to 672 days further reduction in the unconfined compressive strengths were obtained under soaked immature case for all cement contents. In addition to that, there was no clear difference in  $q_u$  values under soaking of pure and acidic water. In cement 3.5, when soaking start after the specimens become matured also a clear reduction in the strength due to soaking was observed. However, it was observed from the difference that the effect of soaking on the strength depends on the gained strength before soaking in cement treatment. Deformation modulus of cement treated soils generally followed the same trend as  $q_u$  even though there was scattering in the data may be because of the effect of bedding error on the failure mechanism.

In the lime treated soils,  $q_u$  values of soaked immature specimens were almost the same as those of sealed specimens in the early curing period, as shown in Figure 4:7. Strengths of those specimens became slightly lower than those of sealed specimens after 28 days in L1.2 and 168 days in L2.5. In the largest lime content, L3.8, the strength of soaked specimens after 336 days decreased from 168 days. In other words, a clear difference was observed from the strengths of the sealed specimens after 336 days in L3.8. There was no clear difference between the strengths of soaked specimens soaked in an immature state and mature state after 672 days, irrespective of the different durations for sealed and soaked curing. The variation of deformation modulus with curing period for lime treated soil is shown Figure 4:8. In here also generally followed the same trend as  $q_u$  except for 168 days sealed specimen in L3.8 content.

The relationship between deformation modulus,  $E_{50}$  and  $q_u$  are shown in Figure 4:9 (a) and (b) for cement treated soil and lime treated soil respectively for sealed and soaked specimens. In both cases, a linear relationship was observed as stated in previous studies (Takahashi et al. 2017) also.

Table 4:1 Summary of  $q_u$  and  $E_{50}$  for cement treated soil

Content (%)	Curing period		Curing type			$q_u$ (kPa)	$E_{50}$ (Mpa)	
	weeks	days						
1.7	1	7	Sealed	–	Sat	44.19	4.99	
			Soaked	immature	Acid	21.92	2.30	
	4	28	Sealed	–	Sat	44.44	3.69	
			Soaked	immature	Acid	26.67	3.66	
	24	168	Sealed	–	Sat	45.93	3.78	
			Soaked	immature	Acid	26.80	3.60	
	48	336	Sealed	–	Sat	44.32	5.37	
			Soaked	immature	Acid	29.24	4.24	
	96	672	Sealed	–	Sat	47.11	4.09	
			Soaked	immature	Acid	27.81	3.82	
	3.5	1	7	Sealed	–	Sat	89.78	18.05
				Soaked	immature	Pure	69.21	18.57
Acid						68.38	15.92	
4		28	Sealed	–	Sat	254.96	70.36	
			Soaked	immature	Pure	138.82	21.94	
					Acid	142.88	29.67	
24		168	Sealed	–	Sat	337.39	95.75	
			Soaked	immature	Pure	170.31	26.24	
					Acid	166.12	32.06	
25		175	Soaked	mature	Acid	326.57	67.34	
28		196	Soaked	mature	Acid	357.64	81.11	
48		336	Sealed	–	Sat	385.79	79.00	
			Soaked	immature	Pure	174.82	24.52	
					Acid	165.03	23.48	
96		672	Soaked	immature	Acid	307.28	65.60	
					Sealed	–	Sat	347.62
			Soaked	mature	Pure	101.87	16.25	
Acid		119.87			16.00			
Soaked		mature	Acid	192.37	30.55			
5.3		1	7	Sealed	–	Sat	596.82	131.86
				Soaked	immature	Acid	600.76	170.25
		4	28	Sealed	–	Sat	952.19	186.09
				Soaked	immature	Acid	894.34	224.84
		24	168	Sealed	–	Sat	1488.10	397.80
	Soaked			immature	Acid	906.46	235.78	
	48	336	Sealed	–	Sat	1485.47	401.56	
			Soaked	immature	Acid	964.77	178.11	
	96	672	Sealed	–	Sat	1334.55	285.75	
			Soaked	immature	Acid	851.51	138.32	

Table 4:2 Summary of  $q_u$  and  $E_{50}$  for Lime treated soil

Content (%)	Curing period		Curing type			$q_u$ (kPa)	$E_{50}$ (Mpa)	
	weeks	days						
1.2	1	7	Sealed	–	Sat	28.39	4.27	
			Soaked	immature	Acid	26.65	2.41	
	4	28	Sealed	–	Sat	28.14	3.08	
			Soaked	immature	Acid	24.40	2.51	
	24	168	Sealed	–	Sat	31.53	6.15	
			Soaked	immature	Acid	23.06	2.19	
	48	336	Sealed	–	Sat	35.39	5.99	
			Soaked	immature	Acid	26.88	3.92	
	96	672	Sealed	–	Sat	42.55	6.80	
			Soaked	immature	Acid	24.09	1.96	
	2.5	1	7	Sealed	–	Sat	76.88	22.04
				Soaked	immature	Pure	84.30	15.51
Acid						99.43	26.41	
4		28	Sealed	–	Sat	88.19	24.02	
			Soaked	immature	Pure	119.99	43.44	
					Acid	96.12	24.20	
24		168	Sealed	–	Sat	109.83	24.65	
			Soaked	immature	Pure	97.43	23.66	
					Acid	89.25	14.51	
25		175	Soaked	mature	Acid	113.88	25.09	
28		196	Soaked	mature	Acid	103.53	17.83	
48		336	Sealed	–	Sat	196.84	34.26	
			Soaked	immature	Pure	99.90	22.48	
					Acid	105.87	22.96	
96		672	Soaked	immature	mature	Acid	116.04	31.62
					Sealed	–	Sat	128.93
			Soaked	mature	Pure	89.42	19.72	
Acid		96.36			17.41			
Soaked	mature	Acid	98.05	17.76				
3.8	1	7	Sealed	–	Sat	124.87	19.16	
			Soaked	immature	Acid	194.31	56.98	
	4	28	Sealed	–	Sat	404.92	130.94	
			Soaked	immature	Acid	367.97	108.58	
	24	168	Sealed	–	Sat	414.04	66.21	
			Soaked	immature	Acid	430.69	115.48	
	48	336	Sealed	–	Sat	558.69	121.04	
			Soaked	immature	Acid	377.63	83.27	
	96	672	Sealed	–	Sat	549.18	110.52	
			Soaked	immature	Acid	352.39	81.57	

---

## 4.3 Progression of deterioration

### 4.3.1 Definition of deterioration and its stages

The literal meaning of the word “deterioration” is the process of becoming progressively worse. In previous studies based on deep mixing method (Hara, Suetsugu, Hayashi, & Matsuda, 2014; Kitazume et al., 2003), this word was mostly used to explain the strength reduction from a gained strength. In this study, the effect on long term strength was studied when soaking start in an immature state that means before fully strength was gained. From unconfined compressive strength values explained in section 4.2.2, it was observed that in most of the early stages the strength of soaked specimens did not reach to the strength of sealed specimens due to the difference in curing conditions. To explain those scenarios clearly, in this study, the word “deterioration” was referred to the strength reduction of the soaked specimen with respect to the sealed specimen at a given curing period.

In order to discuss the deterioration, strength ratio was defined as the ratio of the  $q_u$  value in each soaked condition to the averaged  $q_u$  value in sealed condition at a given curing period. The obtained strength ratios were plotted against the soaking period. In the case of immature specimens soaking period was three days less than from total curing period and in the case of mature specimens that value was 168 days. The obtained relationship between the soaking period and the strength ratio for cement 3.5 soaked acid (immature) is shown in Figure 4:10. The three data shown in a given curing period were the strength ratios obtained for each soaked specimen. A line was drawn linking the average value of those data. The line shown as strength ratio of 1 represents the average strength of sealed specimen at the given curing time. A clear reduction in the strength ratio was obtained after soaking of 25 days. From that relationship progression of deterioration could be explained as two stages as follows;

1. Primary deterioration – up to 25 days of soaking
2. Secondary deterioration – from 25 days to 672 days of soaking

As these two stages observed in cement treated soil with the content of 3.5 % after soaking in an immature state, further discussion was done on the influential factors on the appearance of those two stages.

---

### 4.3.2 Influence of soaking water type

In order to find out the influence of soaking water type on appearing of primary and secondary deterioration stages in cement treated soils in an immature state, the strength ratios obtained for C3.5-soaked acid and C3.5- soaked pure were plotted together in the same graph against soaking period as shown in Figure 4:11. The deterioration in acid water followed the same trend with pure water while showing no effect from the initial pH value of soaking water. This behavior was different from the behavior which was observed in previous studies. (Ghobadi, Abdilor, & Babazadeh, 2014; Kamon, Ying, & Katsumi, 1996).

From soaking water analysis, it was observed that the pH of soaking water in both cases also followed the same trend even though the pH value of soaking water changed into different value in each time they exchanged as shown in Figure 4:12. This means in short period of time the pH of both types of water increased and the effect of acidity did not affect on the deterioration. In addition to that, it was understood that the concentration of acids was very low in soaking water preparation even though it maintained a pH of 4.5. Several researchers (Hino, Jia, Sueyoshi, & Harianto, 2012; Nakarai, Ishida, & Maekawa, 2006) had stated that effect of acidity may appear not only because of pH value but also due to the high concentrations of  $\text{SO}_4^{2-}$  or  $\text{Cl}^-$  ions. From soaking water analysis, it was found the concentration of  $\text{SO}_4^{2-}$  ions in acid water as small as 0.51mg/l. This might be the reason for the same trend of deterioration when soaking in both pure and acid water. However, in pure water soaking primary deterioration was clearly appeared.

### 4.3.3 Influence of binder content

The relationship between the soaking period and strength ratio for C1.7, C3.5 and C5.3 under soaked- the acid (immature) case is shown in Figure 4:13. In all three cement contents, primary deterioration clearly appeared. In C5.3 condition the primary deterioration was smaller than the primary deterioration obtained in C 3.5. In the case of C1.7, the strength ratio after 25 days of soaking was larger than the strength ratio of C3.5. These results show that there is optimum cement content for the primary deterioration. However, in C1.7 it was difficult to evaluate the strength ratio accurately as there was a difference in the degree of saturation in sealed specimens and soaked specimens as summarized in Annex B. By considering that fact it could be concluded that the primary deterioration became smaller when increasing cement content from 3.5 % to 5.3 %.

---

#### 4.3.4 Influence of gained strength before soaking

In an actual embankment, the groundwater level can fluctuate, and deterioration can appear in a part where fully strength gained. Figure 4:14 shows the relationship between the soaking period and the strength ratio for the case where soaking was applied in immature and mature case of C 3.5. It was found that there was no appearance of primary deterioration when curing the specimens under the sealed condition for 168 days before start soaking and strength ratio gradually decreases when increase soaking period.

#### 4.3.5 Influence of binder type

Figure 4:15 shows the relationship between strength ratio and soaking period for C 3.5 and L2.5 for soaked immature cases. The 7<sup>th</sup> day strength of both binder type was set to as 100 kPa in sealed condition as described in section 3.3. From the results, it could be observed a clear reduction in strength ratio after 25 days as primary deterioration in cement treated soil while there was no primary deterioration in lime treated soil.

In lime treated soil also strength ratio was calculated for each case described in section 3.3 and the obtained relationships for each case are shown in Figure 4:16, Figure 4:18 and Figure 4:19 to discuss the influence of soaking water type, lime content and gained strength before soaking respectively on progression of deterioration. From all the cases no primary deterioration was observed. In addition to that in lime treated soil also no effect from soaking water type on the deterioration was observed as a variation of pH in both soaking water followed the same trend as in Figure 4:17.

#### 4.3.6 Summary of influential factors on the progression of deterioration

From the discussion stated in the above sections, it was found that primary deterioration appeared in cement treated soil when the specimens exposed to water only in an immature state. In all cases in lime treated soil and soaked mature case in cement treated soil did not show primary deterioration. A similar trend was followed by deformation modulus ratio as shown in Figure 4:20 in both lime and cement treated soil even though there were some scattering in data.

---

#### 4.4 Needle Penetration test results

Needle penetration test was conducted on cement and lime treated surplus soils in order to find out the localized strength distribution and the deterioration depth in a given soaking period. In this section, the results obtained from method 1 for horizontal measurement was summarized for the conclusions. The three measurements obtained in each case and the physical properties of each specimen were summarized in Annex C. As it was difficult to evaluate accurately the reasons for the deterioration in lower binder contents due to slight changes in physical properties needle penetration test results on lower binder contents were not discussed in detail. But all measured data were stated in Annex B.

The relationships between needle penetration resistance (NPR) and the penetration length under sealed and soaked (immature) conditions of cement treated soil were summarized according to the curing period and curing conditions for C3.5 as shown in Figure 4:21 respectively. The penetration resistance stated here was the average value of three measurements and the variation of the three measurements at each 1 mm depth was shown in the figure by horizontal lines. Under the sealed condition, the maximum values of NPR became large when increasing the curing period from 7 to 672 days. Under soaked (immature) case NPR in both specimens of soaked acid and pure always less than NPR of sealed specimens irrespective to depth. Similar observations obtained C5.3 content also as shown in Figure 4:23. In addition to that, no clear effect of acidity appears in the needle penetration test results. NPR of soaked conditions was increased while increasing curing period from 7 to 168 days and 336 days for C3.5 and C5.3 respectively. After increasing curing period to 672 days NPR becomes smaller in all depths. Especially, a very small NPR was observed at a depth less than 10 mm.

The obtained relationship between NPR and the penetration length for C3.5 soaked (mature) case is shown in Figure 4:22. A clear appearance of lower NPR compared to sealed specimens throughout the depth were obtained after soaking of 504 days. This means maturity before soaking is affected on the NPR.

The relationships between needle penetration resistance (NPR) and the penetration length under sealed and soaked (immature) conditions of lime treated soil were summarized according to the curing period for L2.5 (immature), L2.5 (mature) and L3.8 (immature) as shown in Figure 4:24 , Figure 4:25 and Figure 4:26 respectively. In most of the case, NPR of soaked specimens was slightly changed from NPR of sealed specimens.



#### 4.4.1 Evaluation method for localized strength

In a needle penetration test, the resistance obtained at a particular depth is the accumulated resistance along with the penetrated depth and the initial tip resistance as described in detail by (Dipova, 2018). In order to find out the exact resistance at a particular depth, the needle penetration resistance rate (NPRR) at that location should be considered as shown in Figure 4:27. In order to find out the localized strength along with the depth of soaked specimens, a relationship between NPRR and the unconfined compressive strength was obtained for lime and cement treated soil as shown in Figure 4:28 by following recommended relationship by previous researchers (Ulusay & Erguler, 2012) as shown in Figure 4:29. The obtained nonlinear relationships from this study were plotted among the above recommendations as shown in Figure 4:30. As the low unconfined compressive strengths due to low binder contents, the curves obtained from this study shown a lower trend. By using that relationship, the distribution of unconfined compressive strength along the depth of soaked specimens was estimated based on NPRR at each 1mm depth. For these evaluations, the NPRR was evaluated in each 1 mm depth by considering data from 30 measuring points. A typical estimated UCS distribution along with depth for the soaked specimen is shown in Figure 4:31. By using that relationship localized strength ratio at a given curing period for a given type of soaked specimens was evaluated as;

$$\text{Localized strength ratio} = \frac{\text{Estimated UCS from NPRR}_{(soaked)}}{\text{Experimental UCS}_{(sealed)}}$$

#### 4.4.2 Localized strength ratio distribution along with the depth

The obtained localized strength ratio distribution along the penetrated depth for cement treated soil C3.5 soaked -acid (immature), C3.5 soaked- pure (immature), C5.3 soaked (immature) and C3.5 soaked (mature) cases are shown in Figure 4:32, Figure 4:33, Figure 4:34 and Figure 4:35 respectively. In all immature cases, localized strength ratio (LSR) was less than 1.0 irrespective to the depth and the soaking periods. When considering the LSR distribution up to 25 days of soaking it could identify two deterioration mechanisms as

- (a) Internal deterioration (throughout the specimen)
- (b) Deterioration driven from the surface (near the exposed surface)

---

When increasing the soaking period LSR changed as explained in section 4.4.4. This observation was different from the previous studies (Takahashi et al. 2017; Kitazume et al. 2003; Ngoc et al. 2016; Hara et al. 2014) in deep mixing cement with larger cement contents under soaking of seawater. In those studies, reduction in strengths was found only near the surface but not at the core area. Therefore, comparing with the larger cement contents, soil improved with low binder contents can suffer a larger reduction in strength under soaking in the immature state which might need more attention in large scale structures such as road embankments.

In mature case appearance of  $LSR < 1$  was observed from the exposed surface after soaking of 168 days and it progressed throughout the specimen after soaking of 504 days due to deterioration driven from surface. No internal deterioration was observed at 25 days of soaking.

The obtained localized strength ratio distribution along the penetrated depth for lime treated soil L2.5 soaked -acid (immature), L2.5 soaked- pure (immature), L2.5 soaked (immature) and L3.8 soaked (mature) cases are shown in Figure 4:36, Figure 4:37, Figure 4:38 and Figure 4:39 respectively. In L2.5 both soaked immature and mature cases appearance of  $LSR < 1$  was observed from the exposed surface after soaking of 168 days and it progressed throughout the specimen after. In the case of L3.8, a clear appearance of  $LSR < 1$  was observed after curing of 28 days in different wording after 25 days of soaking. In all the lime cases deterioration mechanism was due to the deterioration driven from the surface.

#### 4.4.3 Definition of parameters to describe localized strength distribution

From the above strength distributions, it could observe two deterioration depths as upper bound deterioration depth ( $D_U$ ) and the lower bound deterioration depth ( $D_L$ ). When increasing the soaking period these deterioration depths increased while changing localized strength ratios (LSR) in relevant depths, hereafter called as upper bound LSR ( $S_U$ ) and lower bound LSR ( $S_L$ ) as shown in Figure 4:40.

To confirm this identified model was reasonable to explain the distribution of localized strength at a given time, the UCS estimated from NPRR and the UCS obtained from experiments for soaked specimens were plotted against each other for all the cases of cement and lime separately as shown Figure 4:41 (a) and (b) respectively. In the case of cement treated soil, it agreed by 86% and in lime treated soil that value was 69 %. In most of the cases C3.5 and L2.5 shown 1:1 fitting. However, L3.8 results did not agree fully to model.

---

#### 4.4.4 Variation of deterioration depths ( $D_U$ and $D_L$ ), localized strength ratios ( $S_U$ and $S_L$ ) with soaking period

Figure 4:42 (a) and (b) shows the relationships of deterioration depths and the strength ratios with the soaking period for C3.5-Soak acid (immature) case. Both  $D_U$  and  $D_L$  gradually increased with the soaking period. The lower bound localized strength ratio ( $S_L$ ) gradually decreased with the soaking period. However, the upper bound localized strength ratio ( $S_U$ ) showed a complex behavior with three phases.

Phase I - up to 25 days – Internal deterioration

Phase II - from 25 days to 333 days– Recovery from internal deterioration

Phase III - after 333 days – Deterioration driven from the surface

Similar behavior observed in C3.5 soak pure (immature) also as shown in Figure 4:43. In this case, phase II appeared between the soaking period of 25-168 days. However, from those graphs, it could understand primary deterioration appeared basically due to internal deterioration. Secondary deterioration appeared as a combined mechanism due to recovery from internal deterioration and deterioration driven from the surface in accordance with the soaking period.

In the case of C5.3 upper bound localized strength ratio ( $S_U$ ) showed only two phases where gradual reduction up to 25 days (internal deterioration) and gradual increment up to 672 days (recovery form internal deterioration) as shown in Figure 4:44(b). In here also primary deterioration could be explained from the internal deterioration. Both upper bound and lower bound deterioration depths increased gradually when increasing the soaking period.

In C3.5 soak acid (mature) specimens, up to 672 days, lower bound deterioration depths were zero, while upper bound deterioration depths increased with the soaking period as shown in Figure 4:45(a). Both upper bound and lower bound localized strength ratios gradually decreased with the soaking period as shown in Figure 4:45 (b). Upper bound localized strength ratio started to reduce from 1 after soaking of 168 days as a result of the extension of deterioration driven from the surface to the core of the specimen. It could not observe internal deterioration in this case which caused for not appearing primary deterioration in the C3.5 soak acid (mature) specimens.

Figure 4:46, Figure 4:47, Figure 4:48 and Figure 4:49 show relationship with soaking period and deterioration depth, localized strength ratio for L2.5 soak acid (immature), L2.5 soak pure (immature), L3.8 soak acid (immature) and L2.5 soak acid (mature) respectively. In all the cases lower bound deterioration depth ( $D_L$ ) was zero up to 672 days and upper bound deterioration depth ( $D_U$ ) gradually increased with the soaking period. In addition to that, all the cases localized strength ratio for lower bound and upper bound also gradually decreased with the soaking period without any clear drop at soaking of 25 days due to internal deterioration. Therefore, there was no primary deterioration in lime treated soils. The secondary deterioration was due to deterioration driven from the exposed surface.

#### 4.5 Summary and conclusion

1. By plotting strength ratio obtained from unconfined compression test against soaking period, it was observed  $SR < 1$  in all cases in both cement and lime treated soil by proving soaking caused for deterioration.
2. In cement treated soil progression of deterioration observed as two stages as primary deterioration up to soaking of 25 days and secondary deterioration from 25 days to 672 days of soaking when improved soil exposed to groundwater in an immature state. The appearance of primary deterioration depended on cement content and the initial strength (maturity) before exposing to water. Secondary deterioration appeared in all cases of cement treated soils.
3. In lime treated soil progression of deterioration was appeared as one stage, secondary deterioration.
4. From needle penetration test results, deterioration along the depth of the specimen was identified due to two mechanisms
  - (a) Internal deterioration
  - (b) Deterioration driven from the exposed surface
5. Progression of deterioration along the distance of the specimen at a given time could explain by four parameters as lower bound deterioration depth  $D_L$ , lower bound localized strength ratio  $S_L$ , upper bound deterioration depth  $D_U$  and upper bound localized strength ratio  $S_U$ .
6. In cement treated immature case both  $D_L$ , and  $D_U$  gradually increased with soaking period showing a logarithmic relationship with time. In cement treated the mature case and all cases in lime treated soil,  $D_L=0$ , and  $D_U$  gradually increased with soaking period showing a logarithmic relationship with time.

7. In all cases of cement treated soil and lime treated soil lower bound localized strength ratio ( $S_L$ ) gradually decreased with the soaking period due to deterioration driven from the surface.
8. In cement treated immature case upper bound localized strength ratio ( $S_U$ ) showed three phases (I) internal deterioration (II) Recovery from internal deterioration (III) deterioration driven from the surface. Appearance time and appearance of phase II and III depended on soaking water type and cement content.
9. In cement treated soil, the mature case and all cases of lime treated soil, upper bound localized strength ratio ( $S_U$ ) gradually decreased with the soaking period due to deterioration driven from the surface.
10. In cement treated immature case primary deterioration could be explained from internal deterioration. Secondary deterioration was due to the combined effect of recovery from internal deterioration and the deterioration driven from the surface.
11. In cement treated mature case and lime treated soils secondary deterioration was due to the deterioration driven from the surface.

---

## 4.6 Reference

- Dipova, N. 2018. Nondestructive Testing of Stabilized Soils and Soft Rocks via Needle Penetration. *Periodica Polytechnica Civil Engineering*, 62(2): 539–544.
- Ghobadi, M. H., Abdilor, Y., & Babazadeh, R. 2014. Stabilization of clay soils using lime and effect of pH variations on shear strength parameters. *Bulletin of Engineering Geology and the Environment*, 73(2): 611–619.
- Hara H., Suetsugu D., Hayashi S., & Matsuda H. 2014. Deterioration Progress of Cement-Treated Ariake Clay under Seawater. *Journal of the Society of Materials Science, Japan*, 63(1): 49–54.
- Hashimoto, H., Yamanashi, T., Hayashi, H., Kawaguchi, T., Kawajiri, S., et al. 2018. Long-Term Strength Characteristics of the Cement Treated Soil after 30 Years. *Journal of the Society of Materials Science, Japan*, 67(1): 47–52.
- Hino, T., Jia, R., Sueyoshi, S., & Harianto, T. 2012. *Effect of environment change on the strength of cement/ lime treated clays*, 6(2):153-165.
- Kamon, M., Ying, C., & Katsumi, T. 1996. Effect of Acid Rain on Lime and Cement Stabilized Soils. *Soils and Foundations*, 36(4): 91–99.
- Kitazume, M., Nakamura, T., Terashi, M., & Ohishi, K. 2003. *Laboratory Tests on Long-Term Strength of Cement Treated Soil*, 586–597. Presented at the Grouting and ground treatment.
- Nakarai, K., Ishida, T., & Maekawa, K. 2006. Modeling of Calcium Leaching from Cement Hydrates Coupled with Micro-Pore Formation. *Journal of Advanced Concrete Technology*, 4(3): 395–407.
- Ngoc, P. V., Turner, B., Huang, J., & Kelly, R. 2016. *Experimental Study on the Durability of Soil-Cement Columns in Coastal Areas*, 6.
- Takahashi, H., Morikawa, Y., Fujii, N., & Kitazume, M. 2017. Thirty-seven-year investigation of quicklime-treated soil produced by deep mixing method. *Proceedings of the Institution of Civil Engineers - Ground Improvement*, 1–13.
- Ulusay, R., & Erguler, Z. A. 2012. Needle penetration test: Evaluation of its performance and possible uses in predicting strength of weak and soft rocks. *Engineering Geology*, 149–150: 47–56.
- Yang, J., Yan, N., Liu, Q., & Zhang, Y. 2016. Laboratory test on long-term deterioration of cement soil in seawater environment. *Transactions of Tianjin University*, 22(2): 132–138.



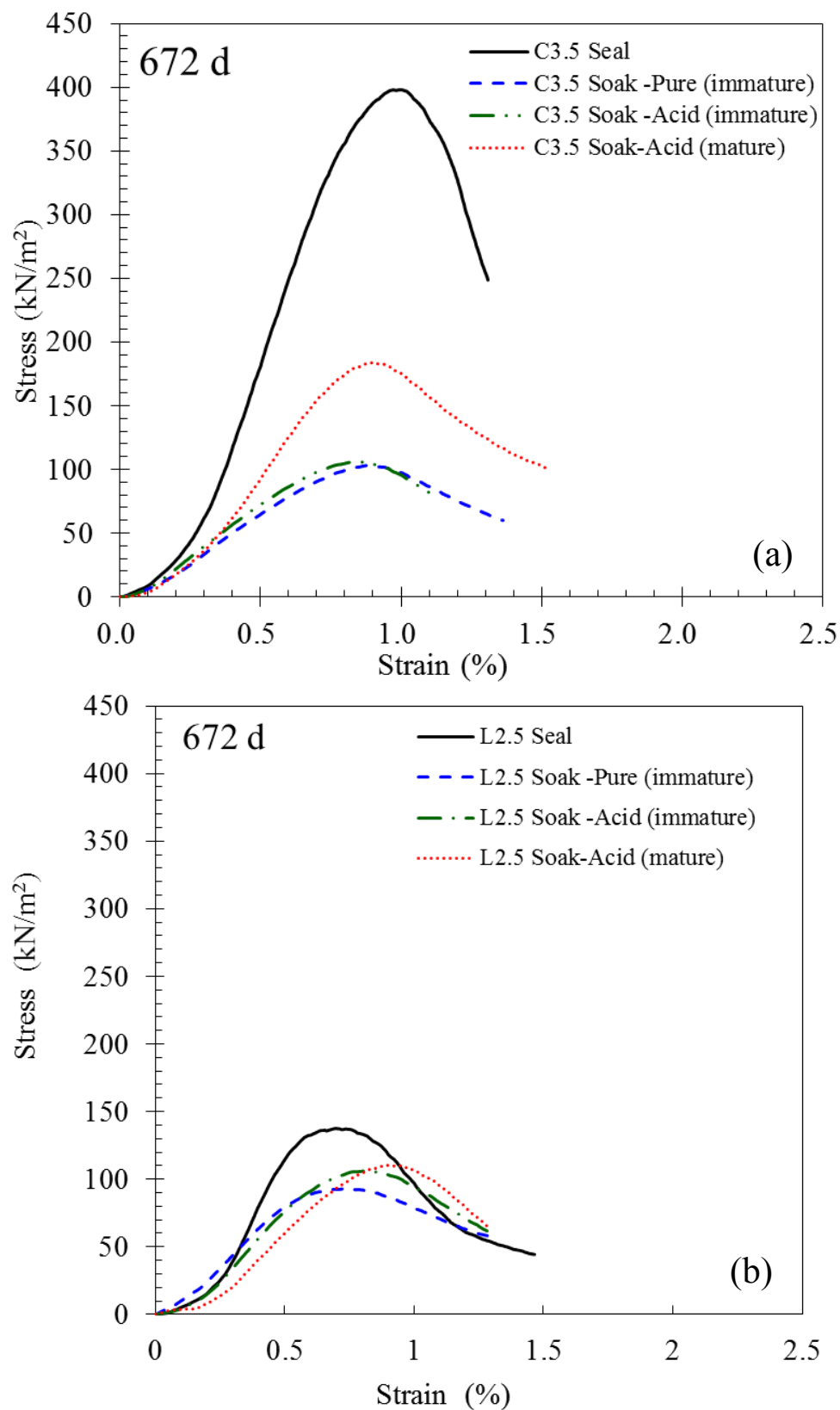


Figure 4:1 Stress strain relationship after curing of 672 days (a) cement 3.5 % (b) Lime 2.5 %



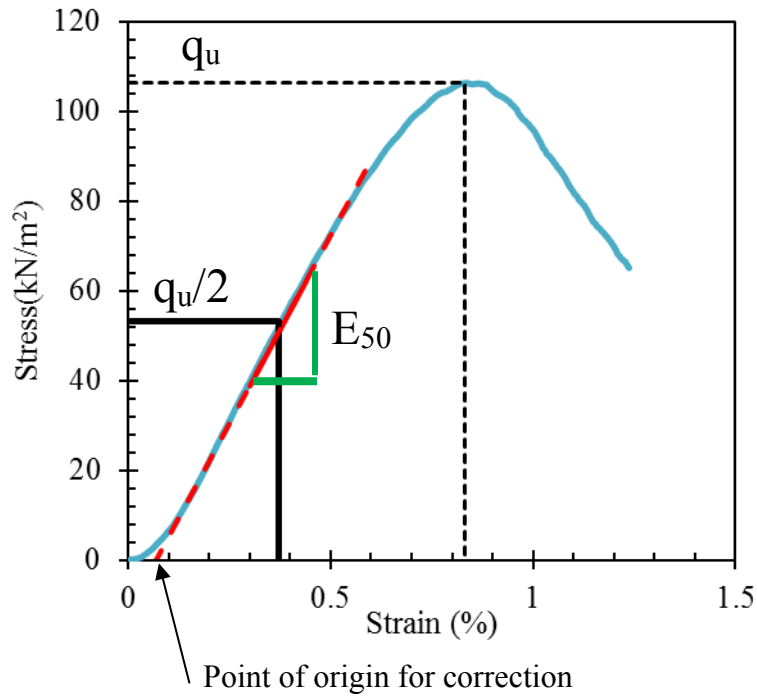


Figure 4:2 Calculation method for deformation modulus,  $E_{50}$

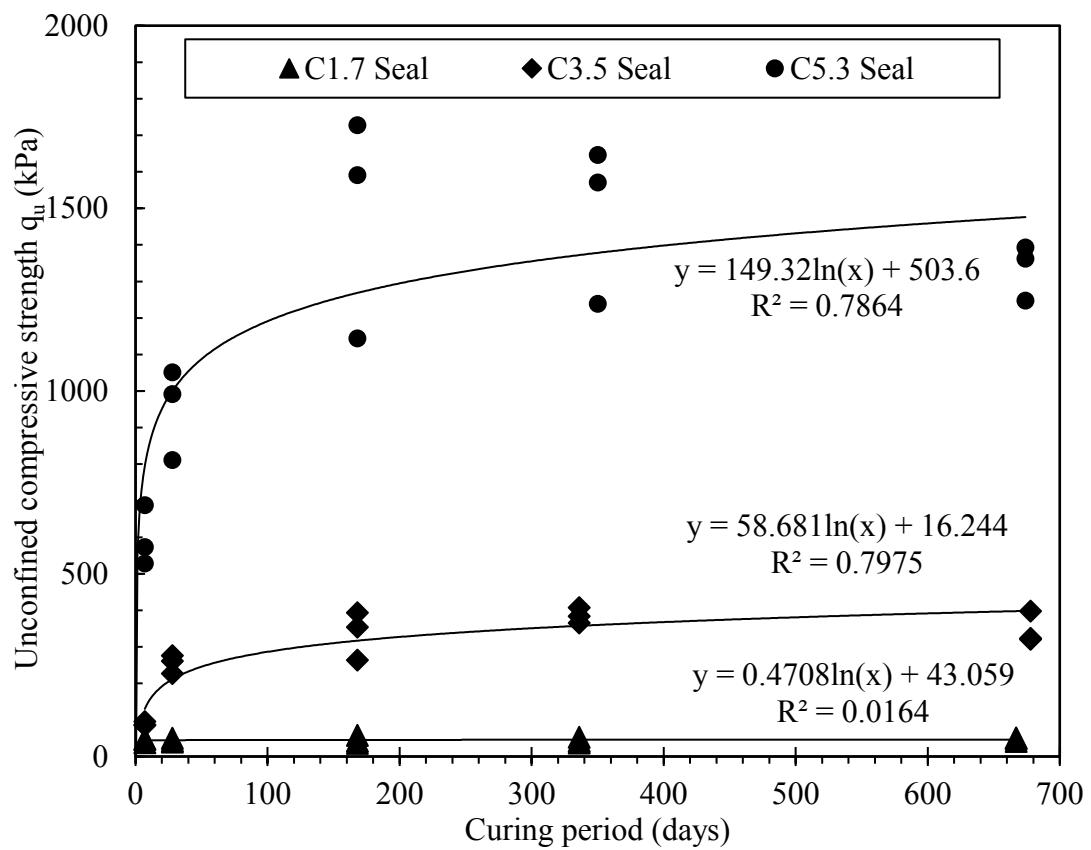


Figure 4:3 relationship between  $q_u$  and curing period of cement treated soil -sealed condition

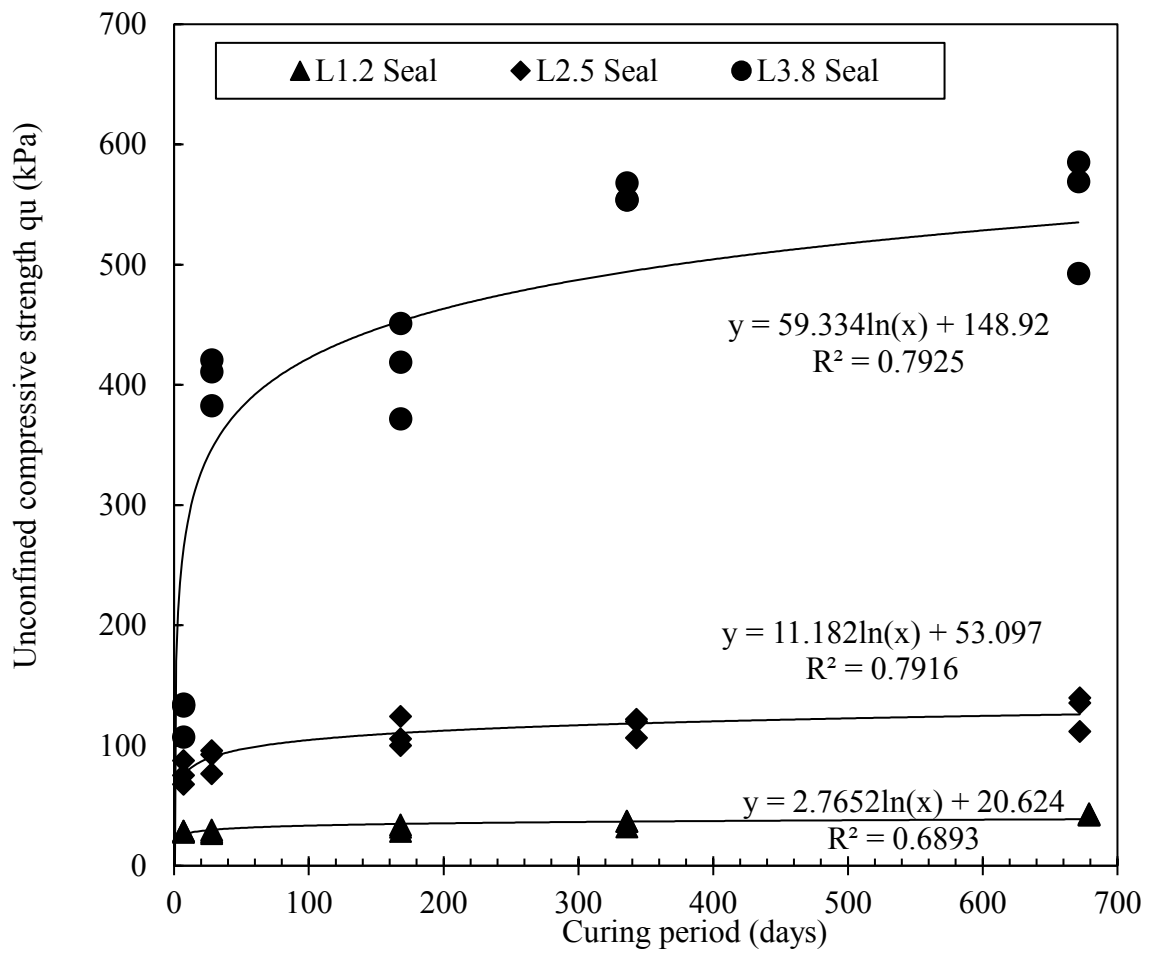


Figure 4:4 Relationship between qu and curing period for lime treated soil- sealed condition

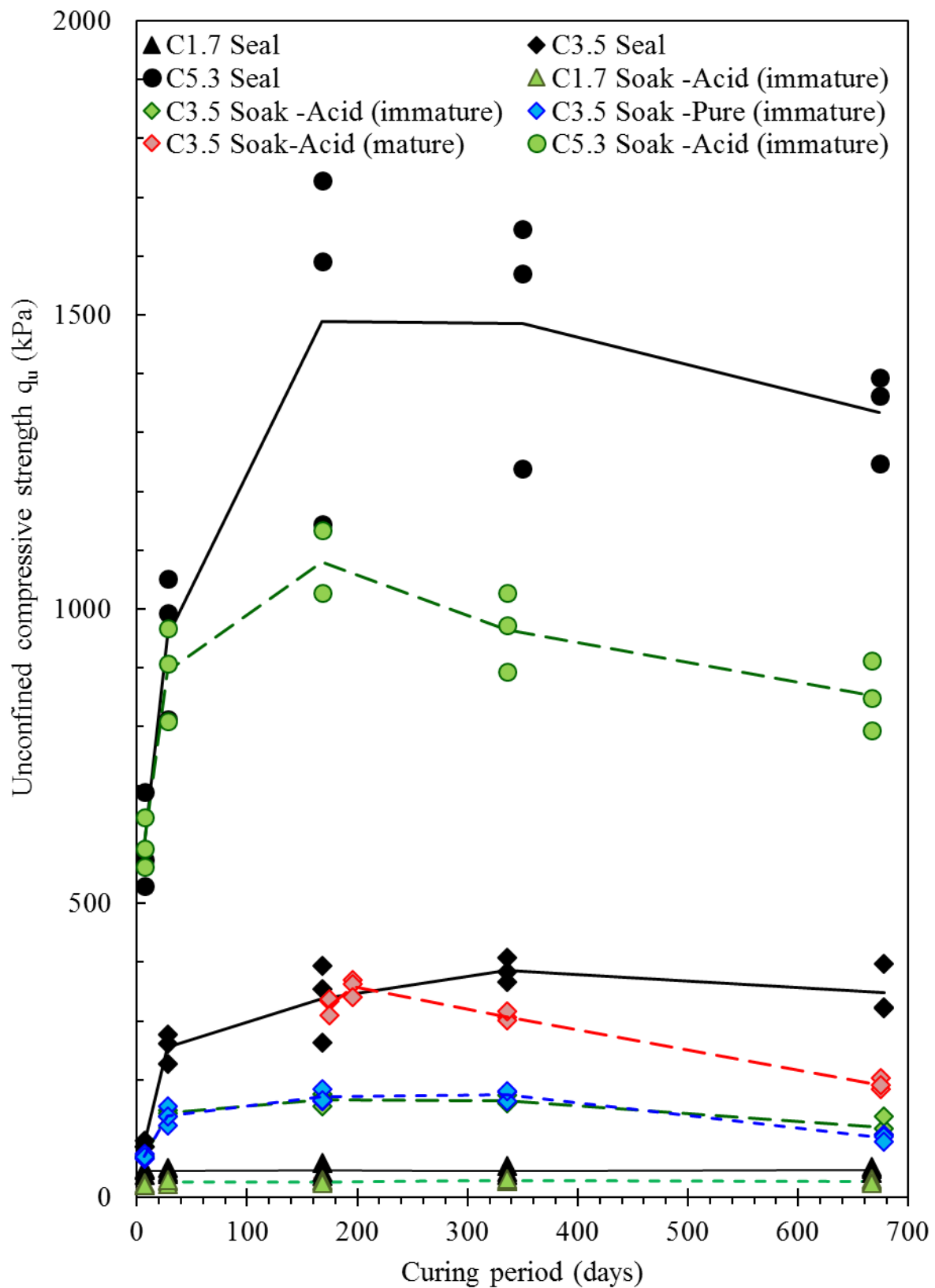


Figure 4:5 Relationship between unconfined compressive strength and curing period of cement treated soil

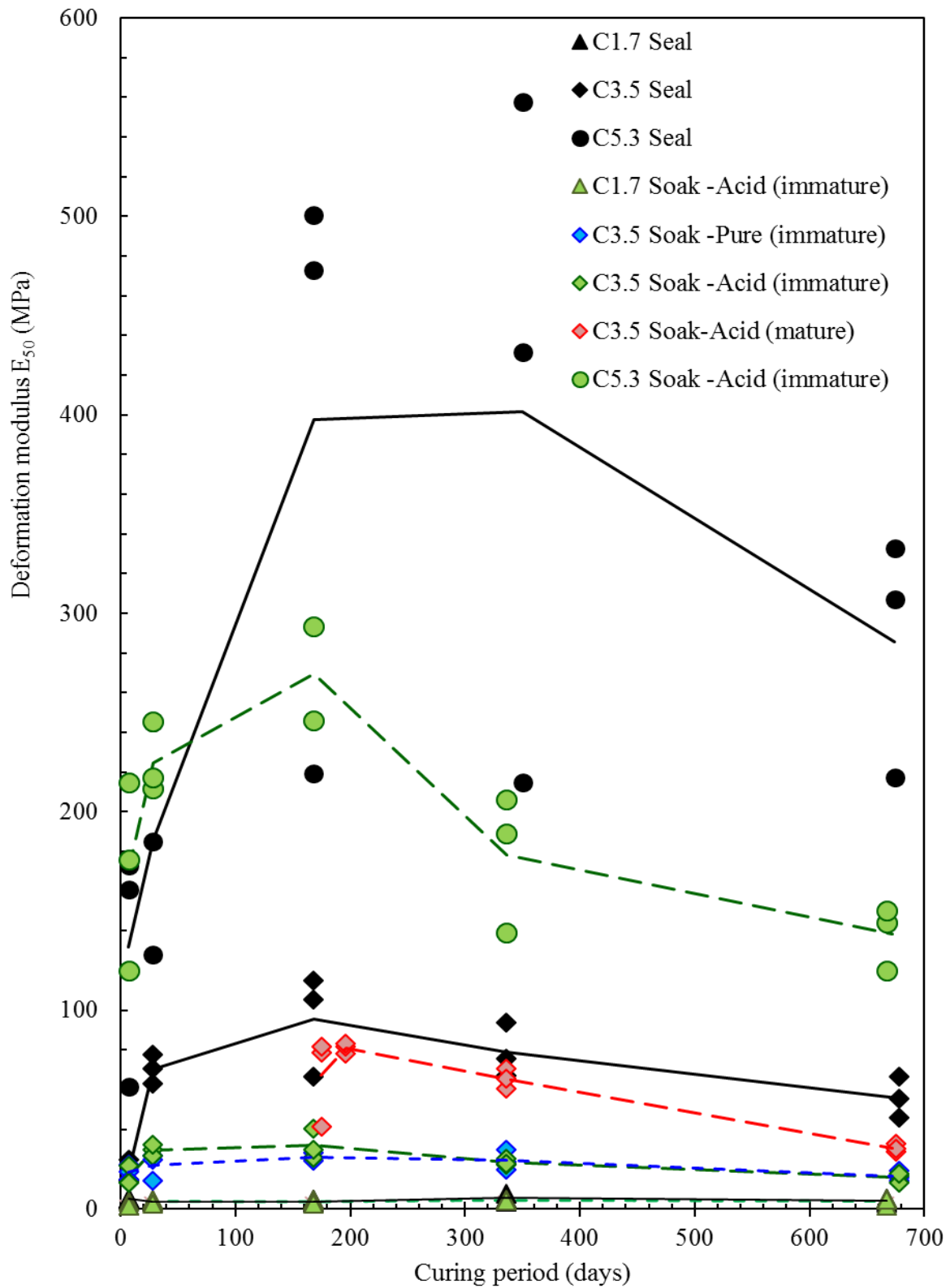


Figure 4:6 Relationship between deformation modulus and curing time of cement treated soil

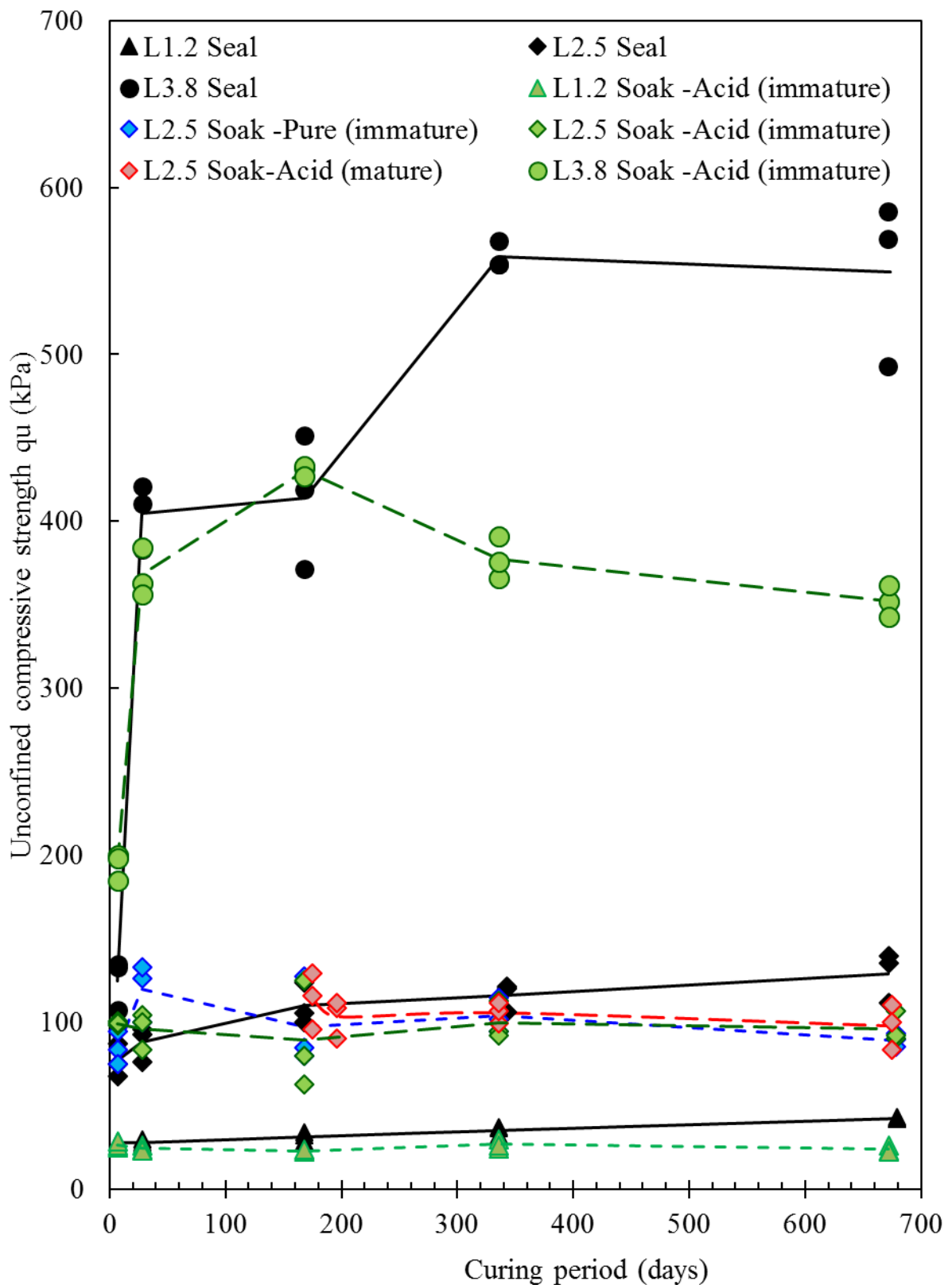


Figure 4:7 Relationship between unconfined compressive strength and curing period of lime treated soils

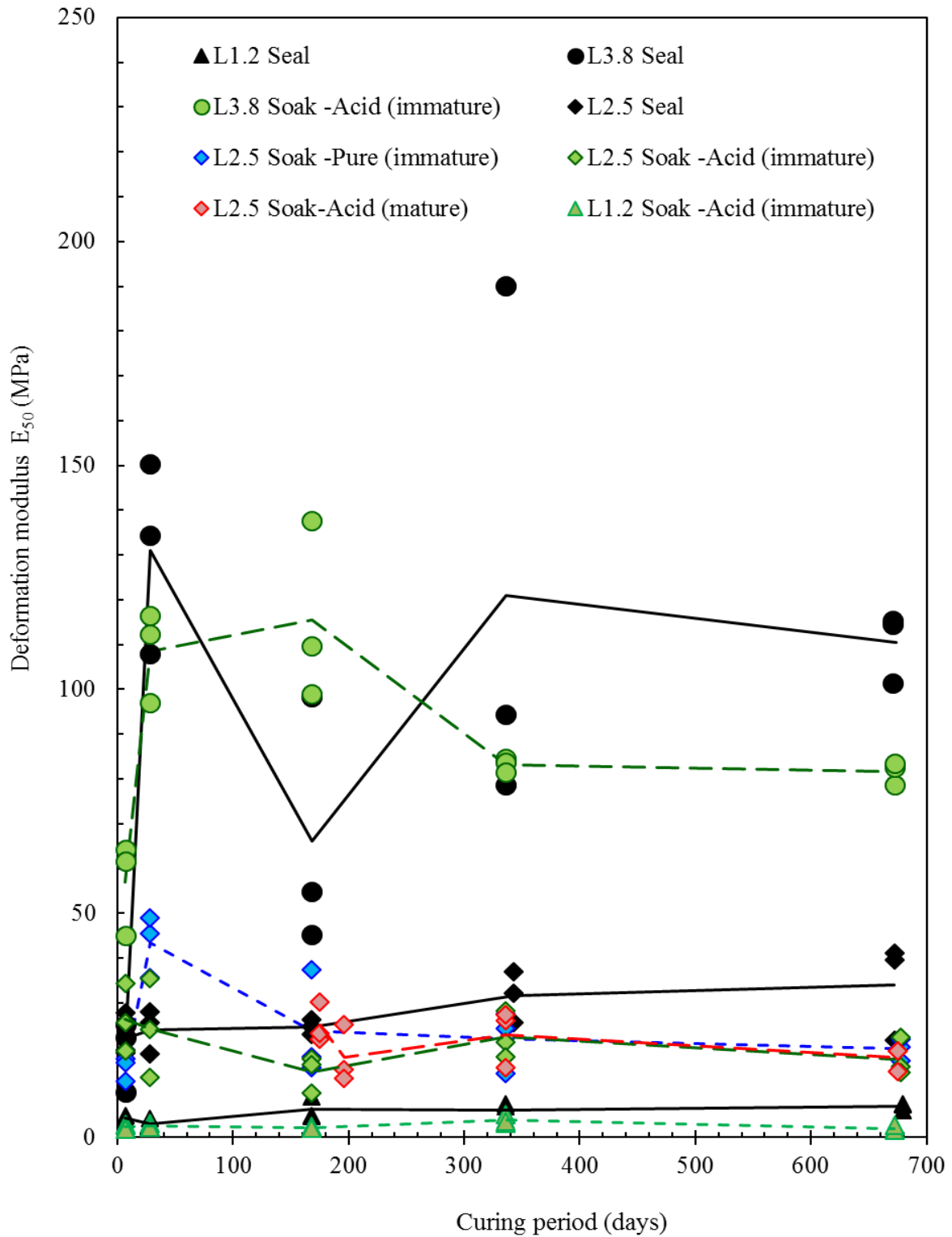


Figure 4:8 Relationship between deformation modulus and curing period of lime treated soil

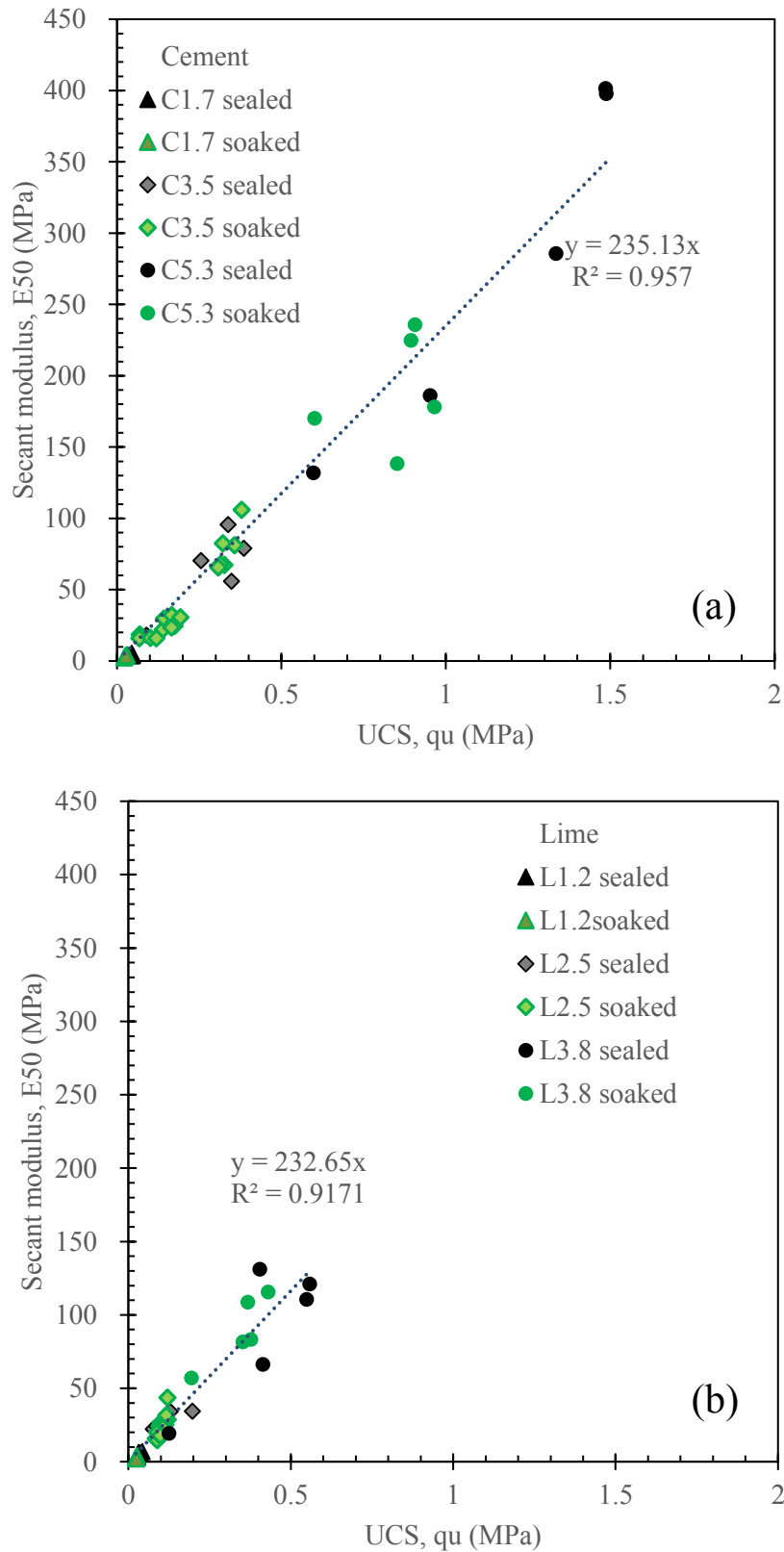


Figure 4:9 Relationship between unconfined compressive strength and deformation modulus (a) cement treated soil (b) lime treated soil

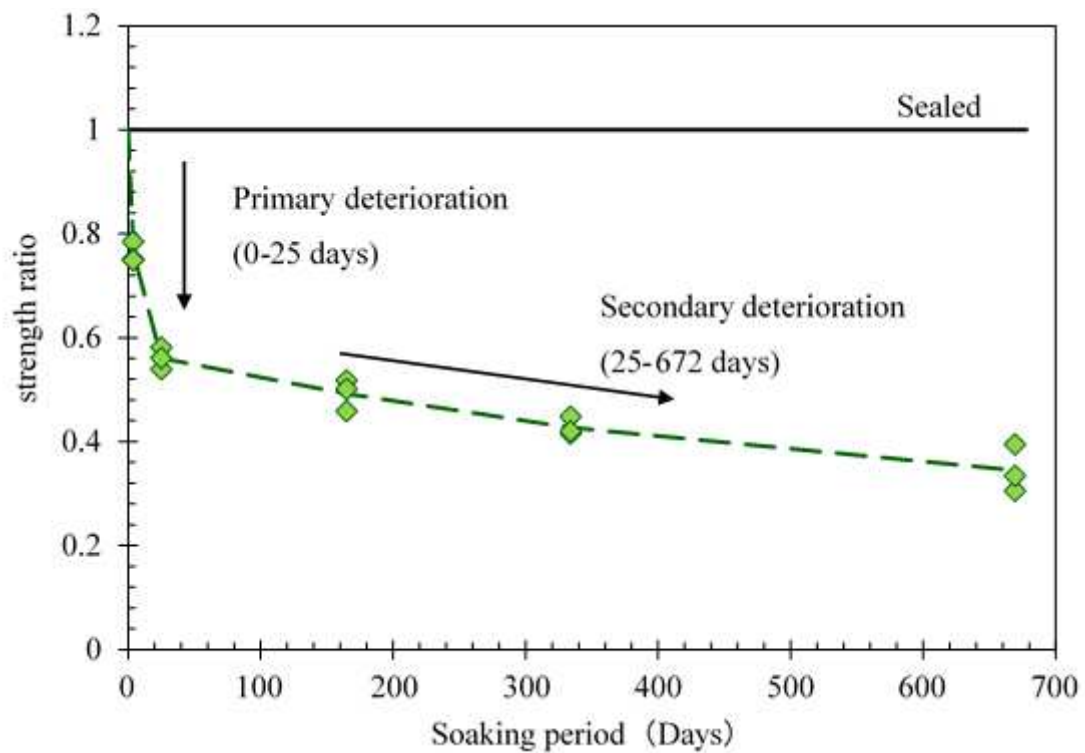


Figure 4:10 Stages in deterioration of soaked C3.5 acid (immature)

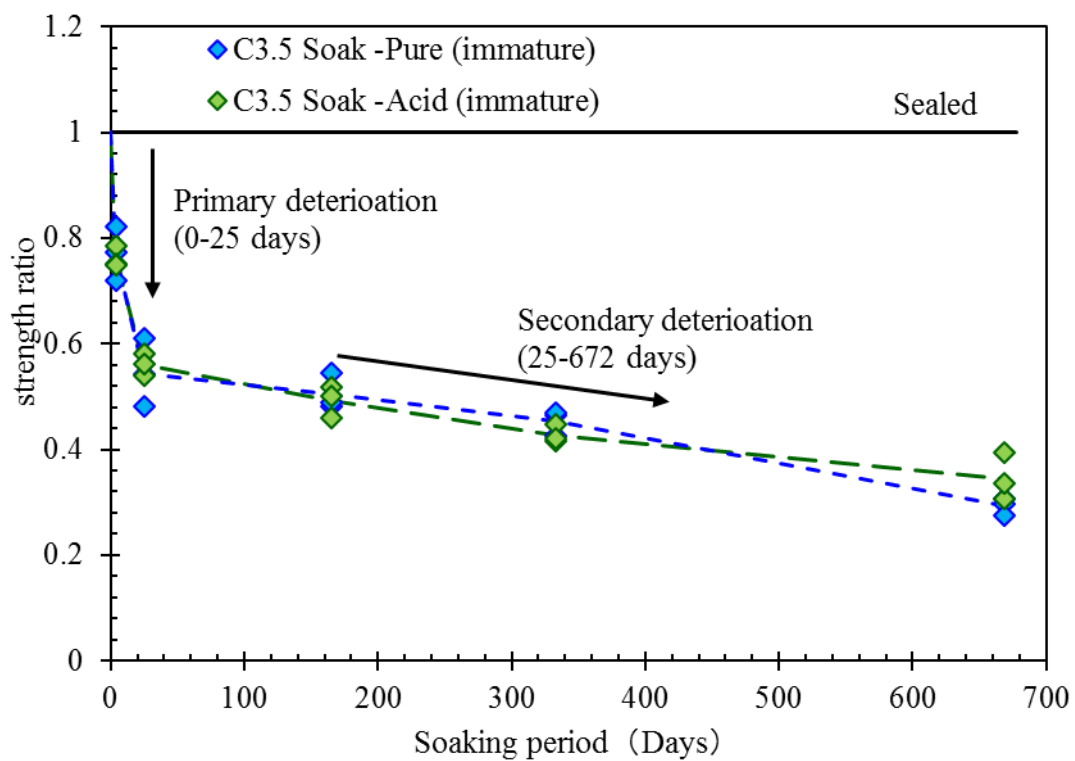


Figure 4:11 Influence of soaking water type - C3.5 soaked (immature)



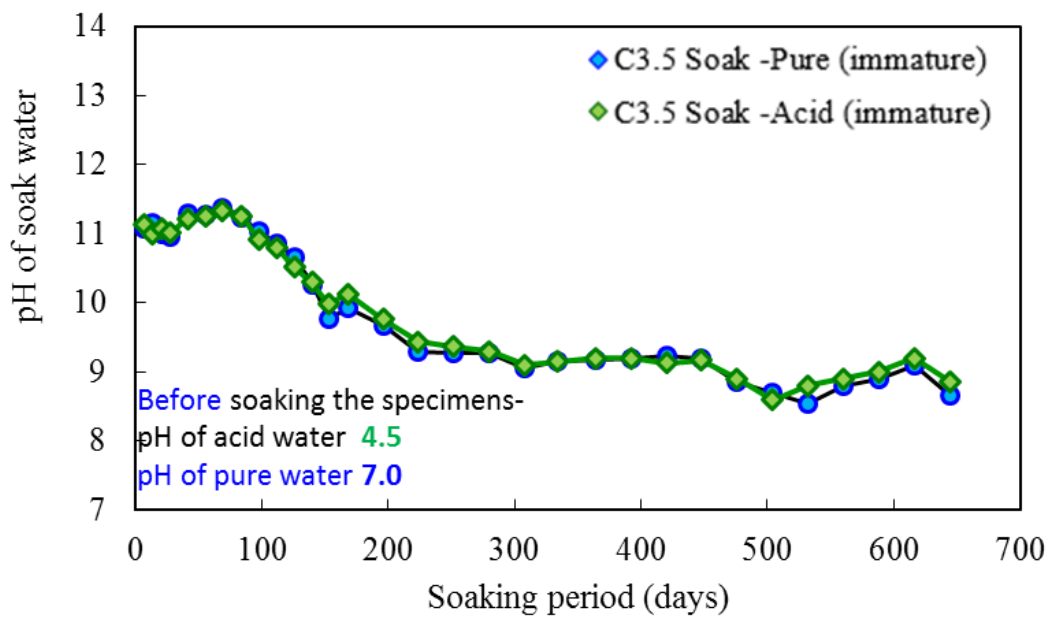


Figure 4:12 Variation of pH with soaking period- C3.5 soaked (immature)

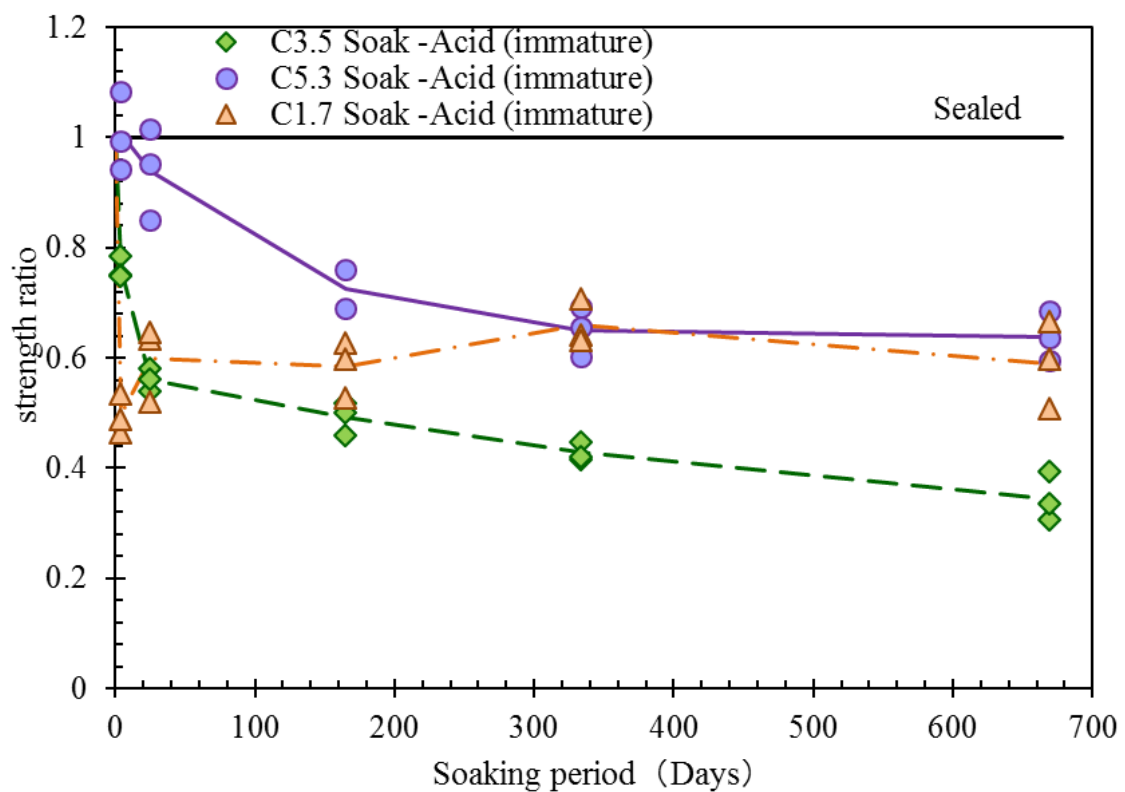


Figure 4:13 Influence of cement content- soaked (immature)

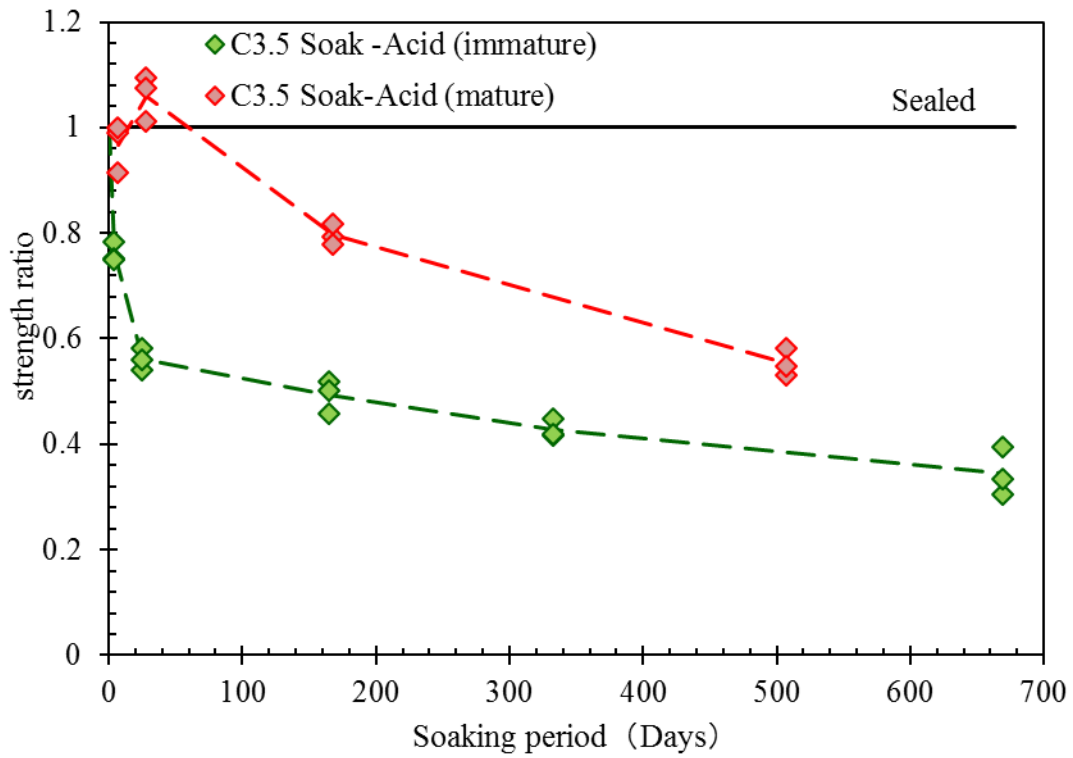


Figure 4:14 Influence of maturity before soaking -C3.5

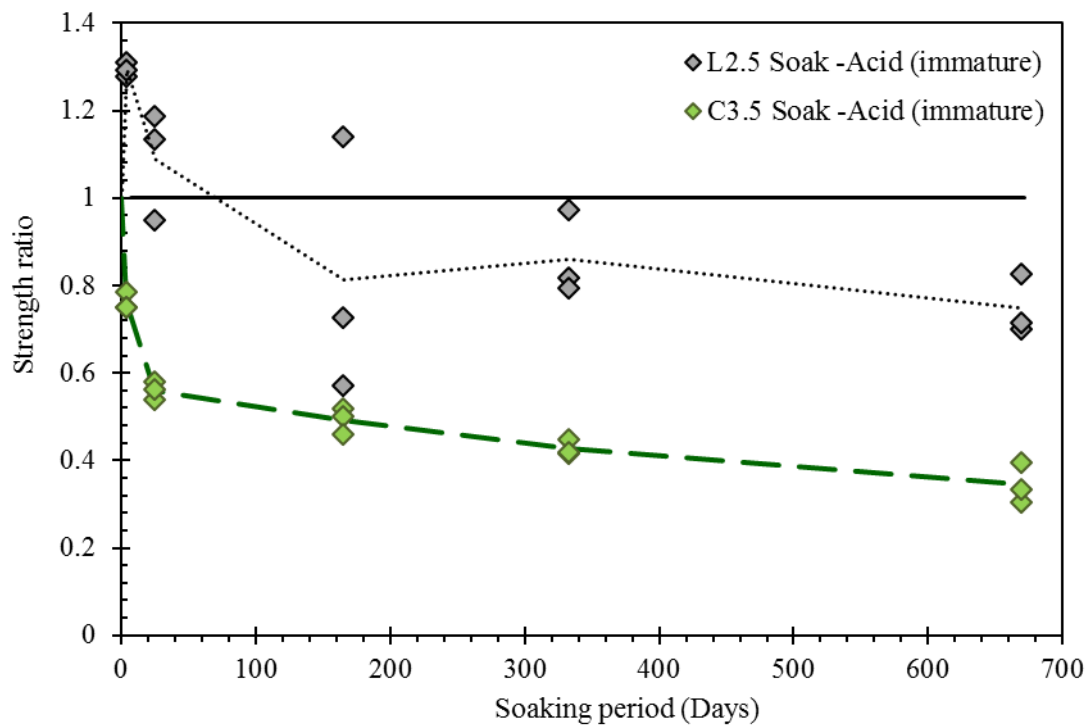


Figure 4:15 Influence of binder type soaked (immature)

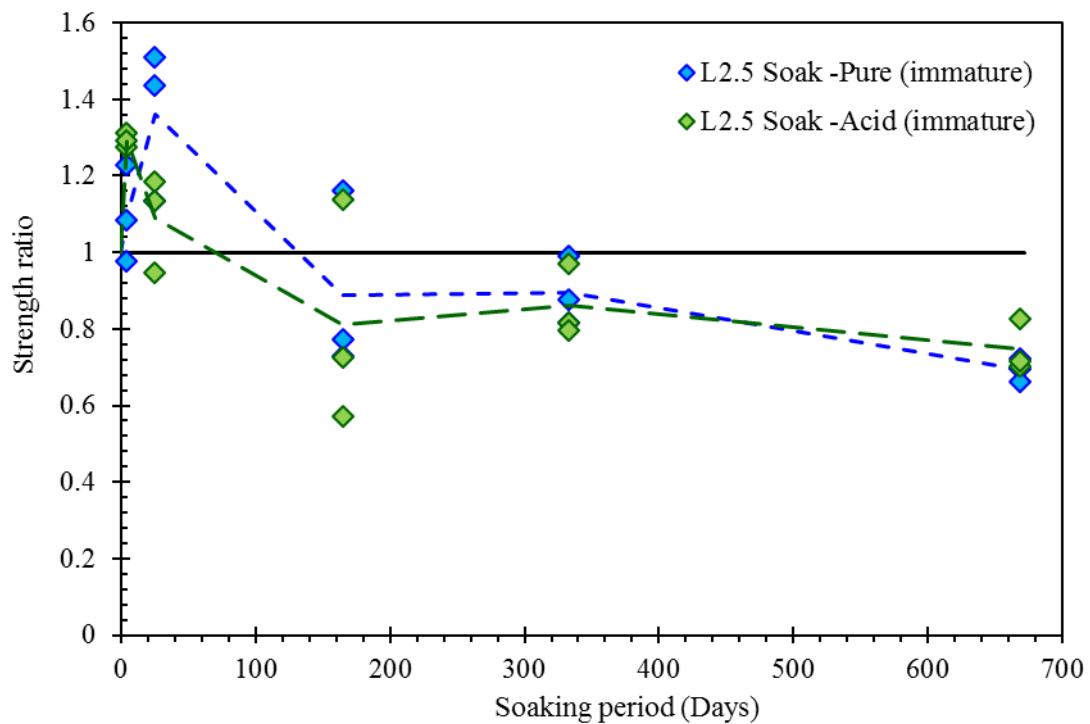


Figure 4:16 Influence of soaking water type -L2.5 soaked (immature)

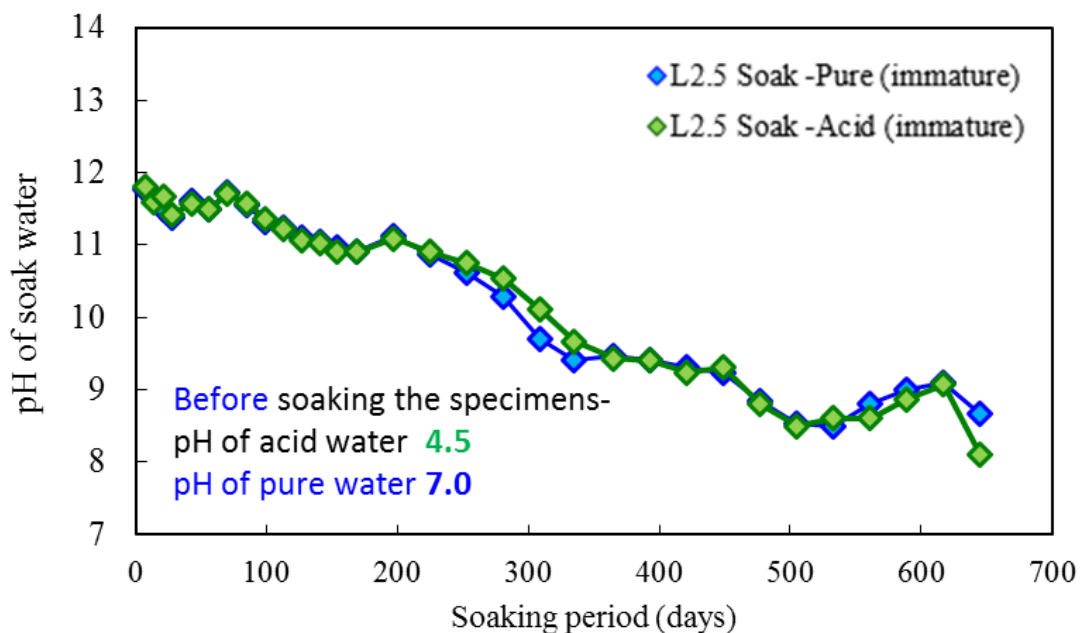


Figure 4:17 Variation of pH with soaking period- L2.5 (immature)

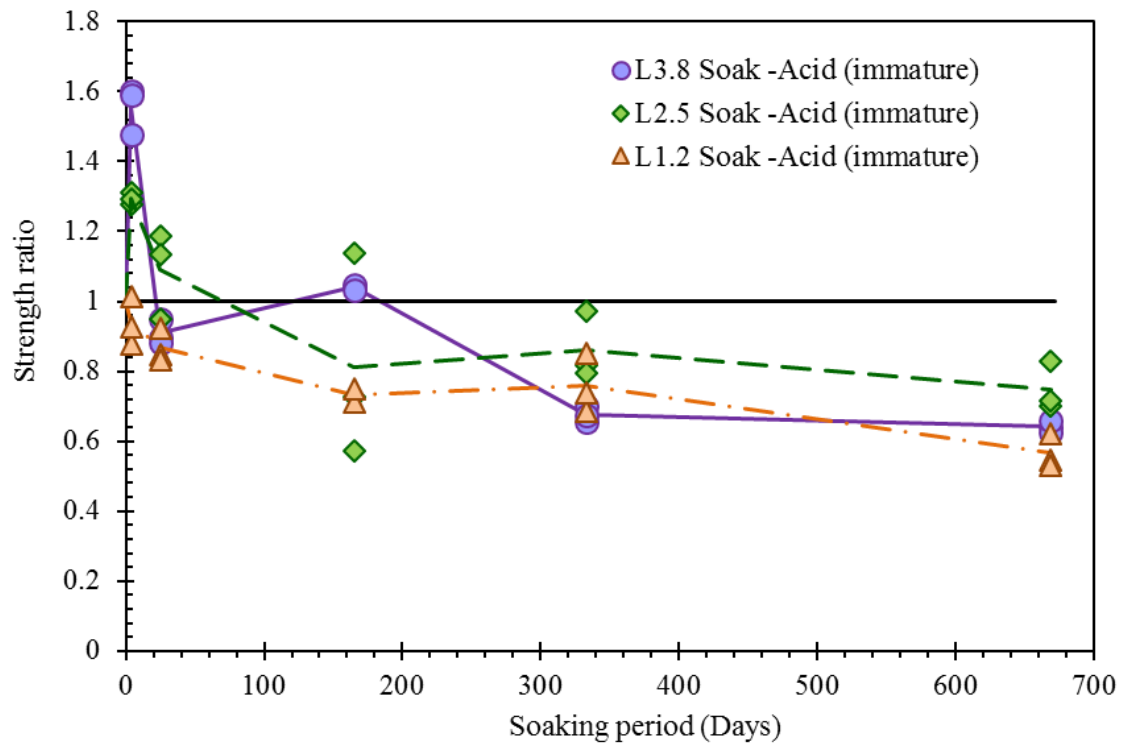


Figure 4:18 Influence of lime content- soaked (immature)

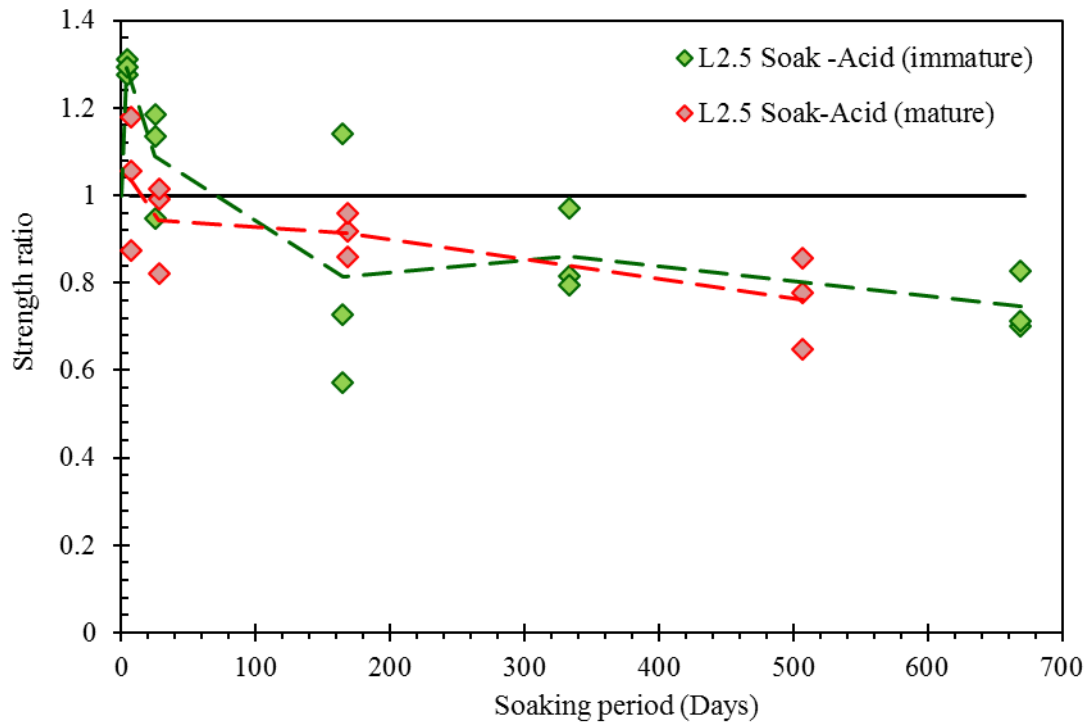


Figure 4:19 Influence of maturity before soaking -L2.5 acid

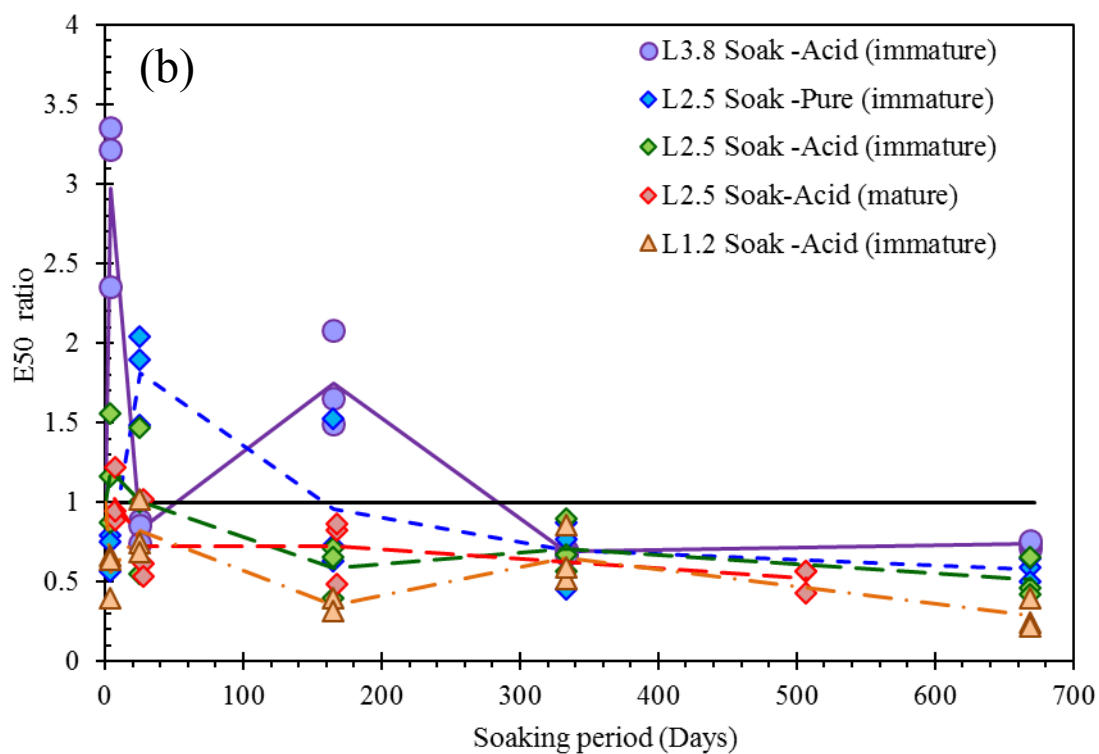
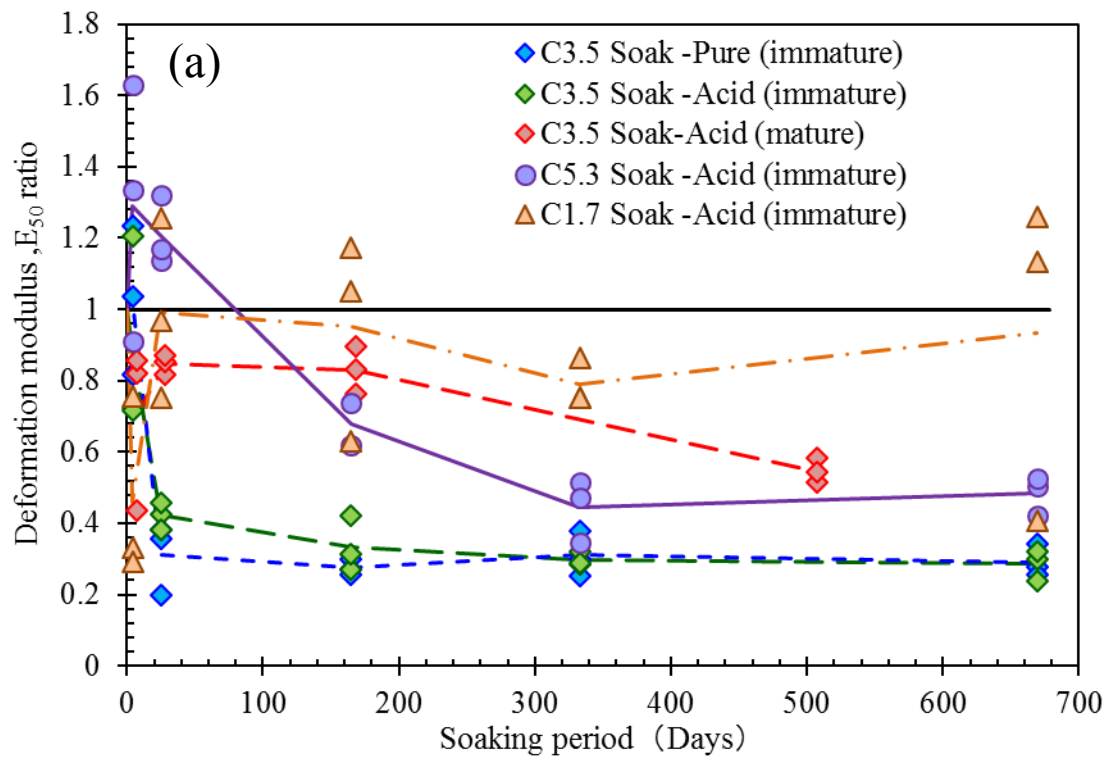


Figure 4:20 Relationship between E50 ratio and soaking period (a) cement treated soil (b) Lime treated soil

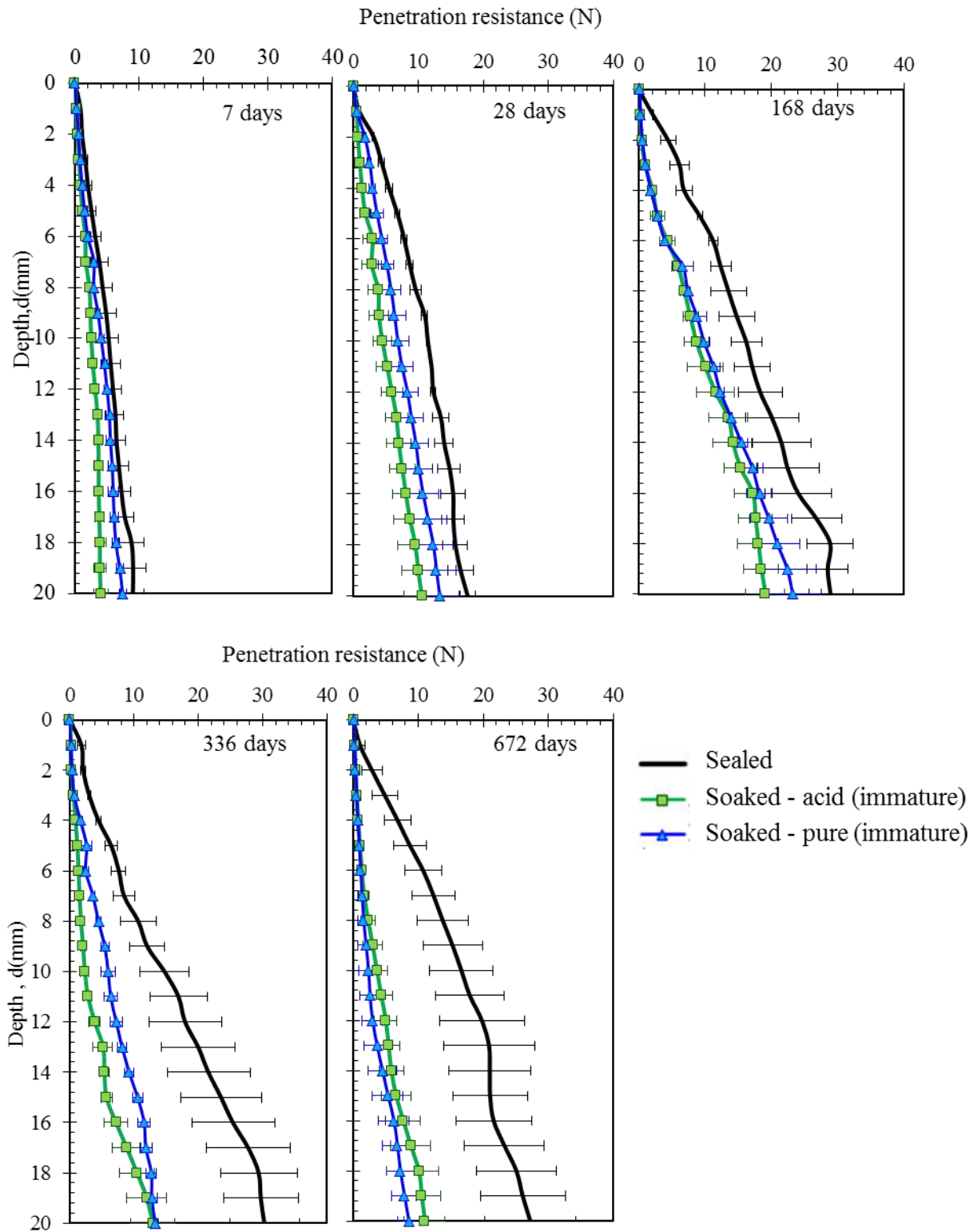


Figure 4:21 Needle penetration test results- C3.5 sealed and soaked (immature)

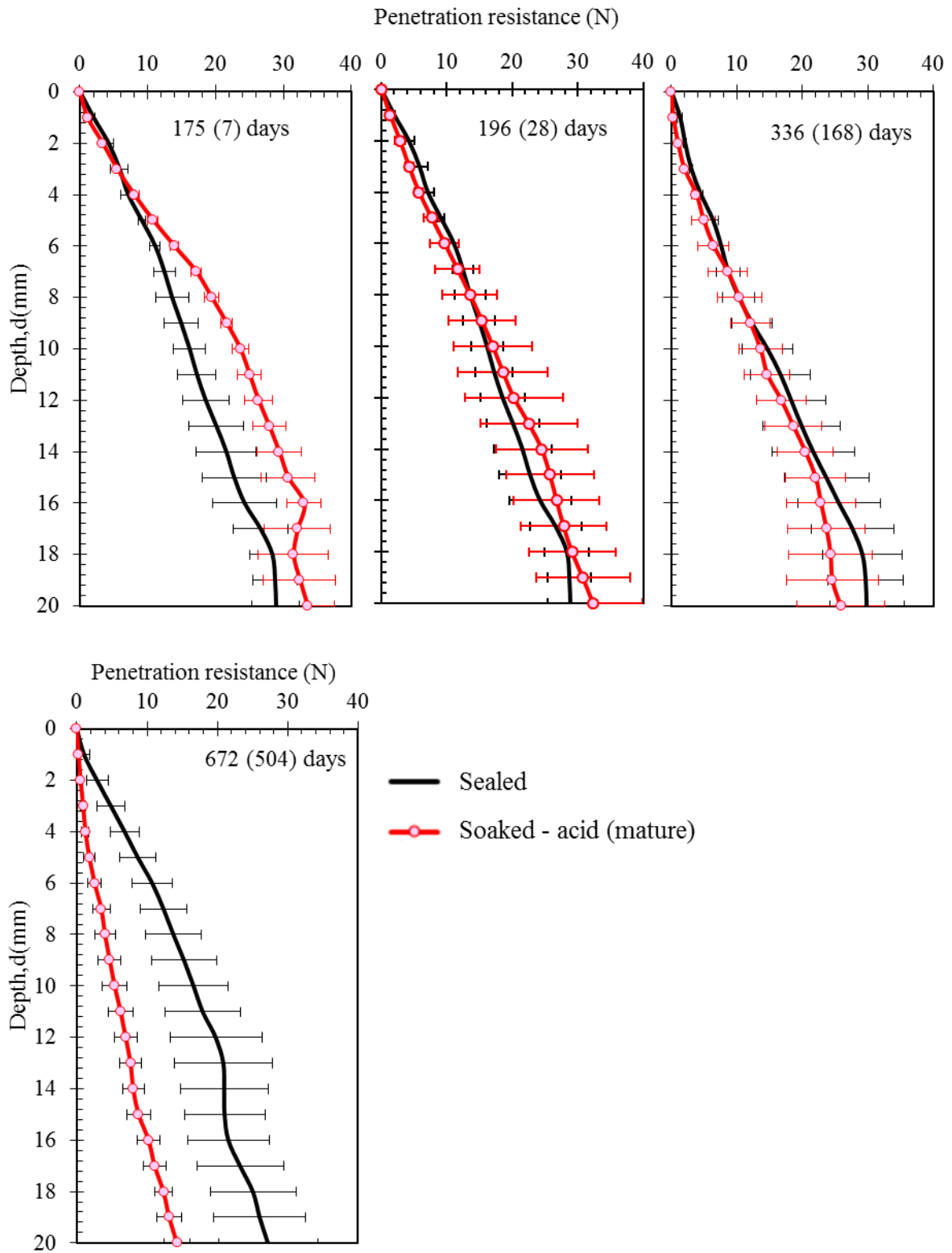


Figure 4:22 Needle penetration test results- C3.5 sealed and soaked (mature)

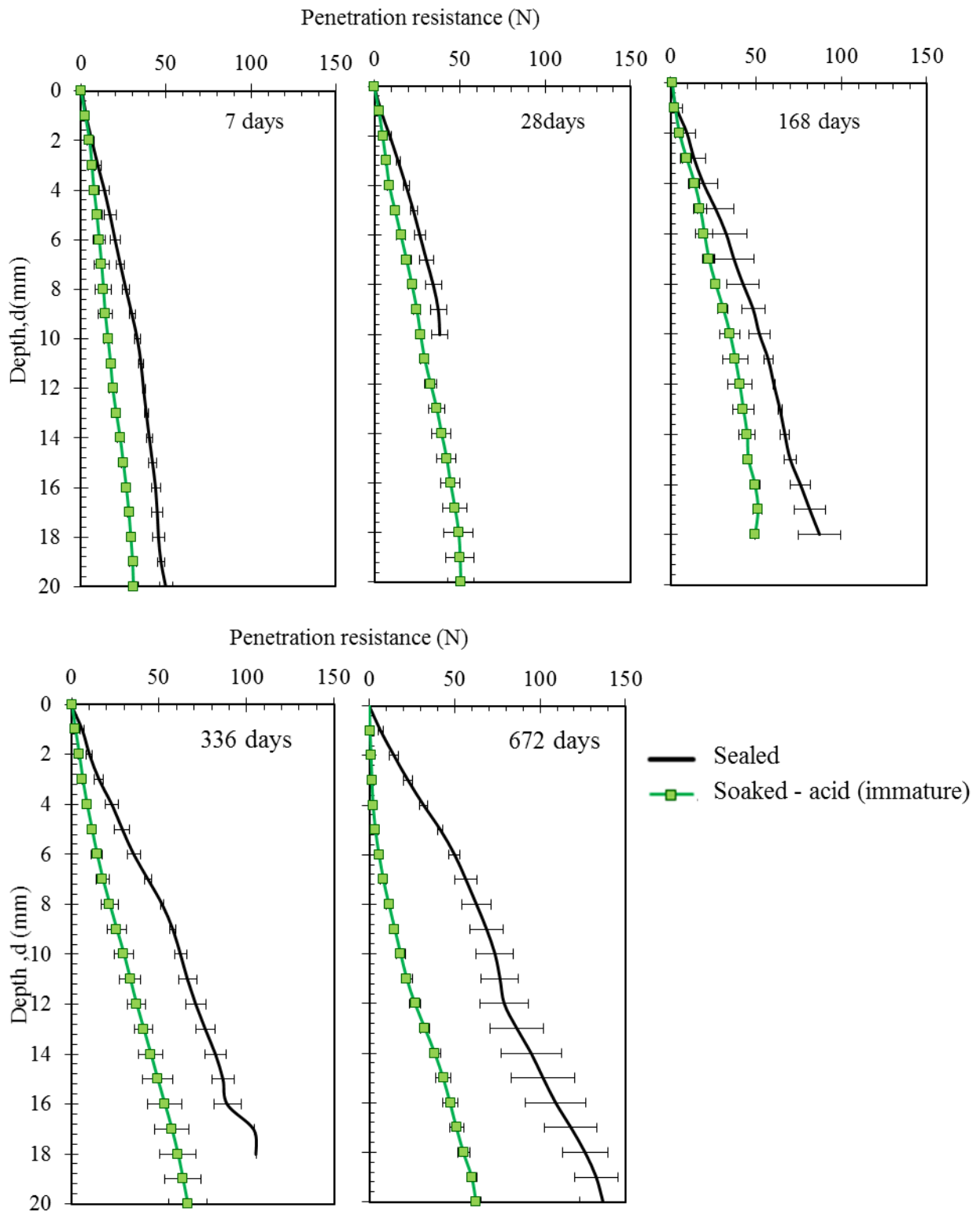


Figure 4:23 Needle penetration test results C5.3 sealed and soaked (immature)



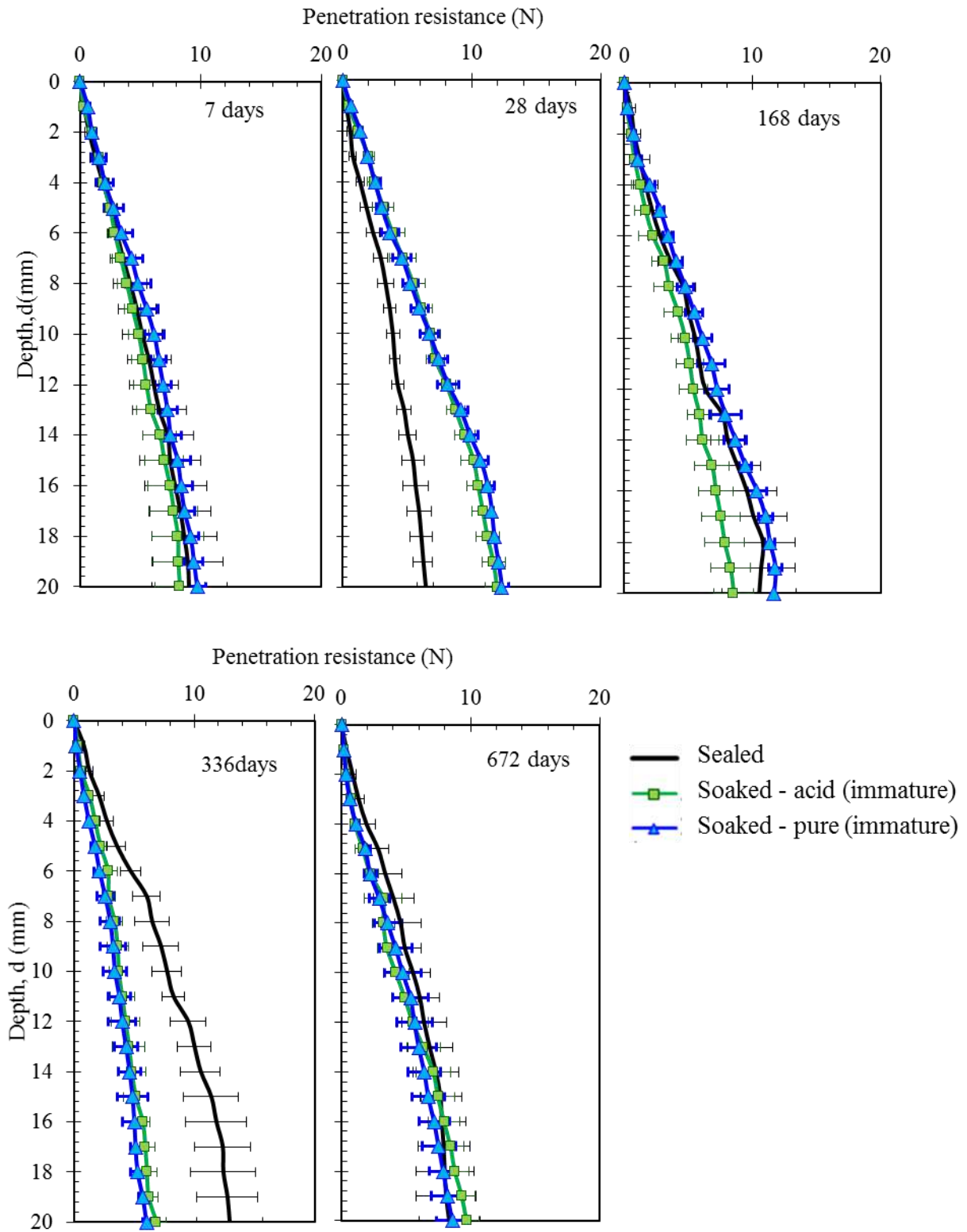


Figure 4:24 Needle penetration test results - L2.5 sealed and soaked (immature)

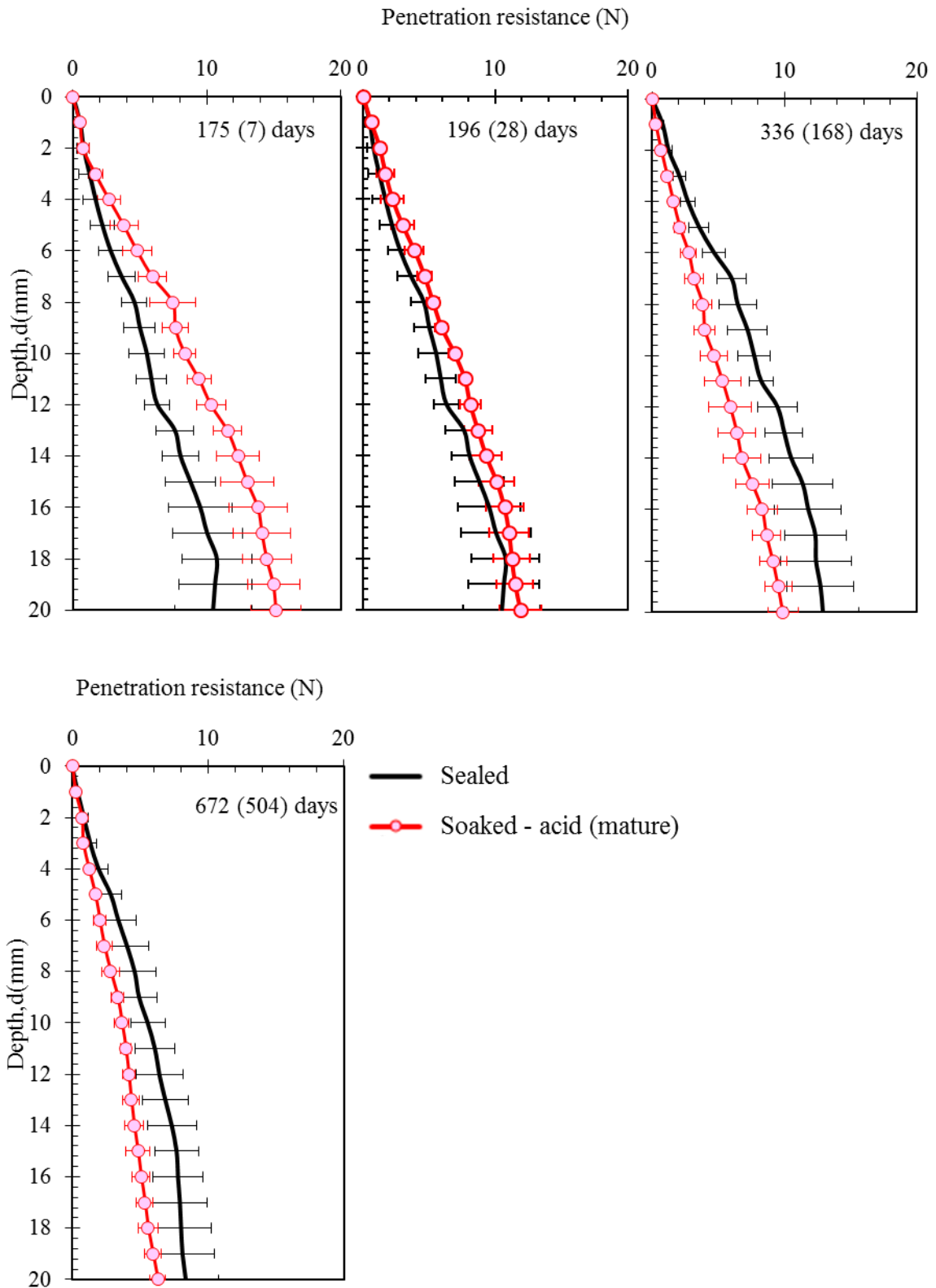


Figure 4:25 Needle penetration test results- L2.5 sealed and soaked (matured)

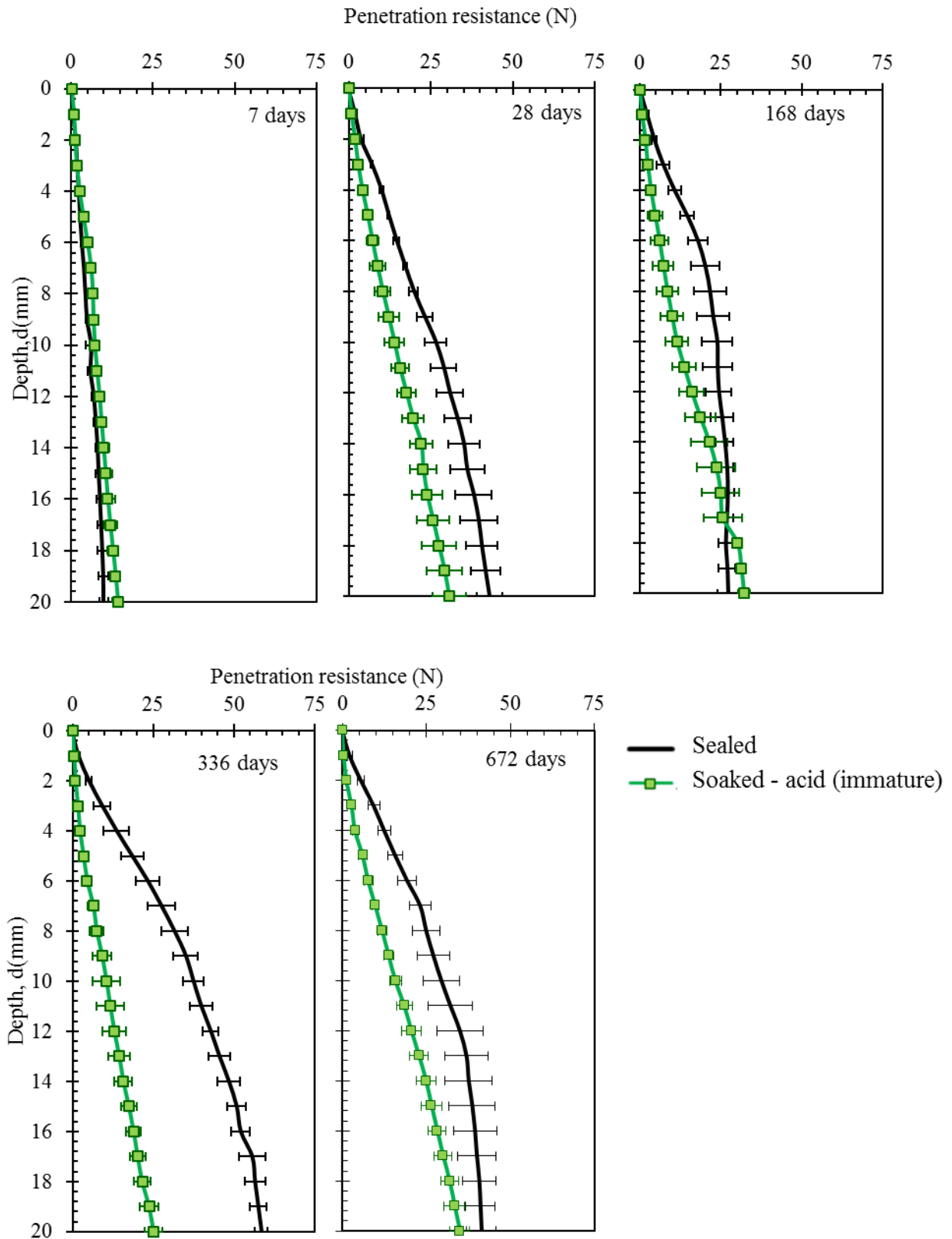


Figure 4:26 Needle penetration test results- L3.8 sealed and soaked (immature)

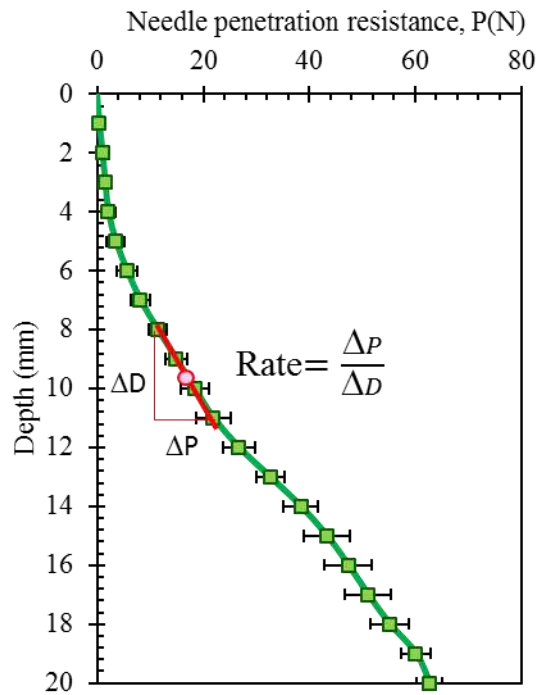


Figure 4:27 Evaluation method of needle penetration resistance rate

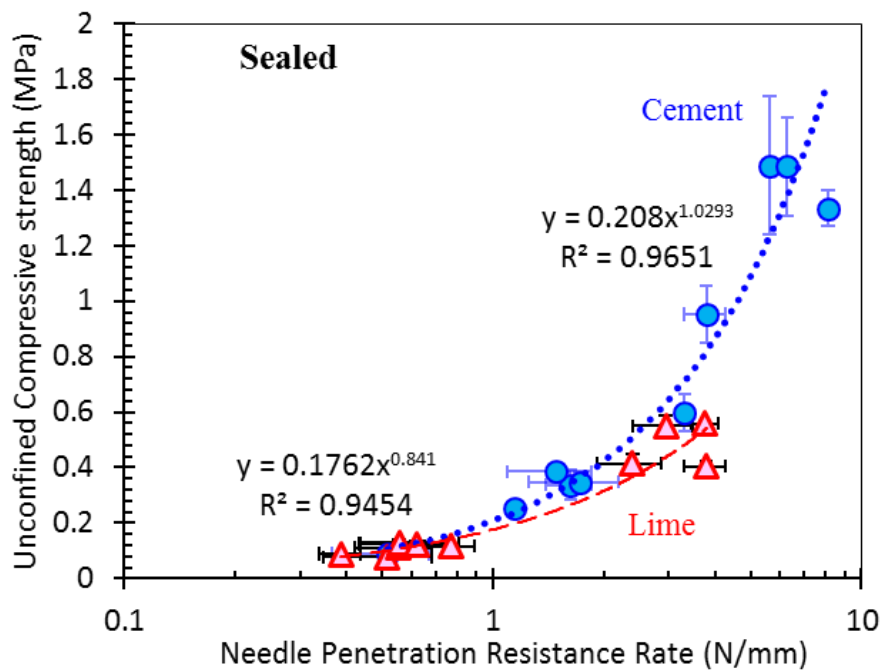


Figure 4:28 Relationship between needle penetration resistance ratio and unconfined compressive strength of sealed specimens

Investigator(s) and/or company	Relationship	Units	
		UCS	NPR
Erguler and Ulusay (2007, 2009)	$UCS = 0.51NPR^{0.8575}$ ( $r = 0.87$ )	MPa	N/mm
Maruto Co. Ltd. (2006) <sup>a</sup>	$\log UCS = 0.978 \log NPR + 2.621$ ( $r = 0.914$ )	kN/m <sup>2</sup>	N/mm
Okada et al. (1985)	$\log UCS = 0.978 \log NPR + 1.599$ ( $r = 0.914$ )	kgf/cm <sup>2</sup>	kgf/mm
Takahashi et al. (1998)	$UCS = 1.5395NPR^{0.9896}$ ( $r = 0.90$ )	MPa	N/mm
Naoto et al. (2004)	$UCS = 27.3NPR + 132$ ( $r = 0.834$ ) (for sandstone)	kN/m <sup>2</sup>	N/cm
	$UCS = 41.8NPR - 4$ ( $r = 0.899$ ) (for Ariaka clay)	kN/m <sup>2</sup>	N/cm
Yamaguchi et al. (1997)	$\log UCS = 0.982 \log NPR - 0.209$ ( $r = 0.872$ )	kgf/cm <sup>2</sup>	kgf/cm

r: coefficient of correlation.

Figure 4:29 Relationship of UCS and NPRR recommended by previous researchers (Ulusay & Erguler, 2012)

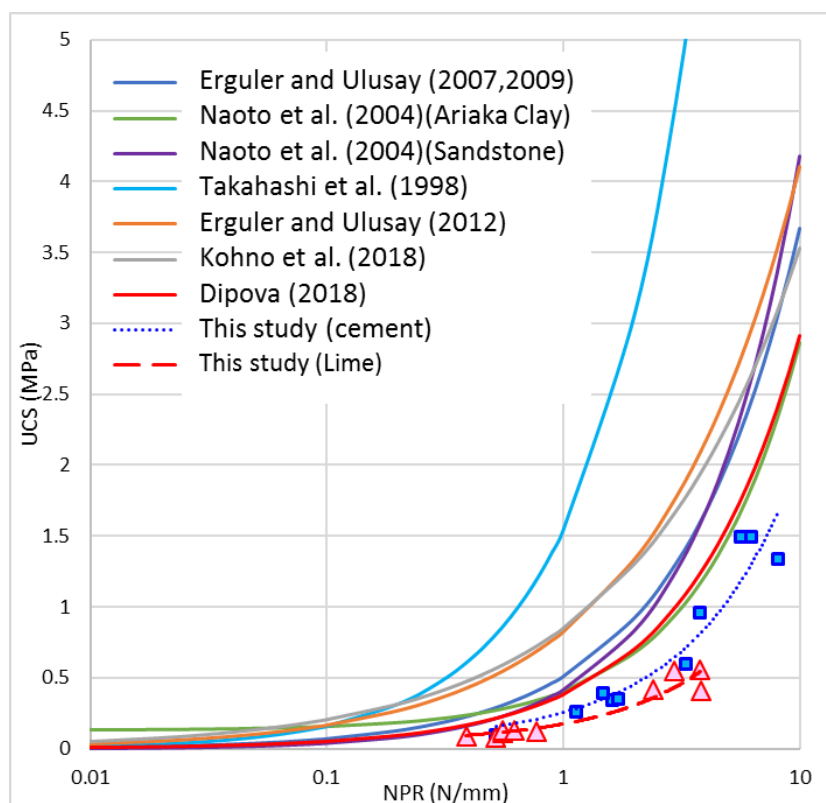


Figure 4:30 Comparison of existing empirical models and the results obtained in this study to predict UCS from NPR

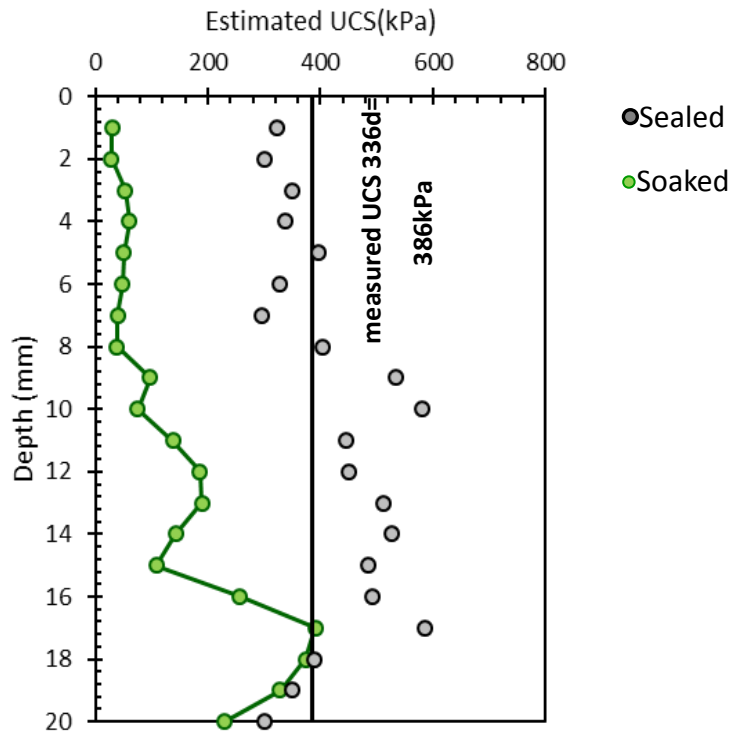


Figure 4:31 Estimated UCS for sealed and soaked specimens based on the relationship between NPRR and UCS

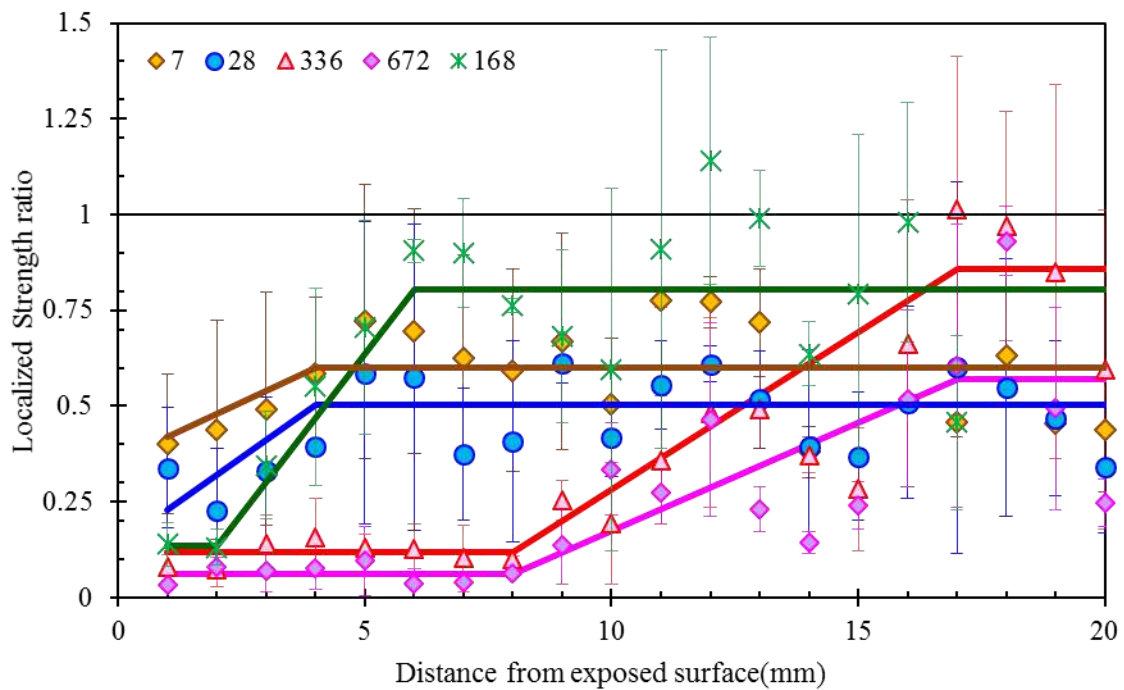


Figure 4:32 Relationship between localized strength ratio and the distance from exposed surface- C3.5 acid (immature)

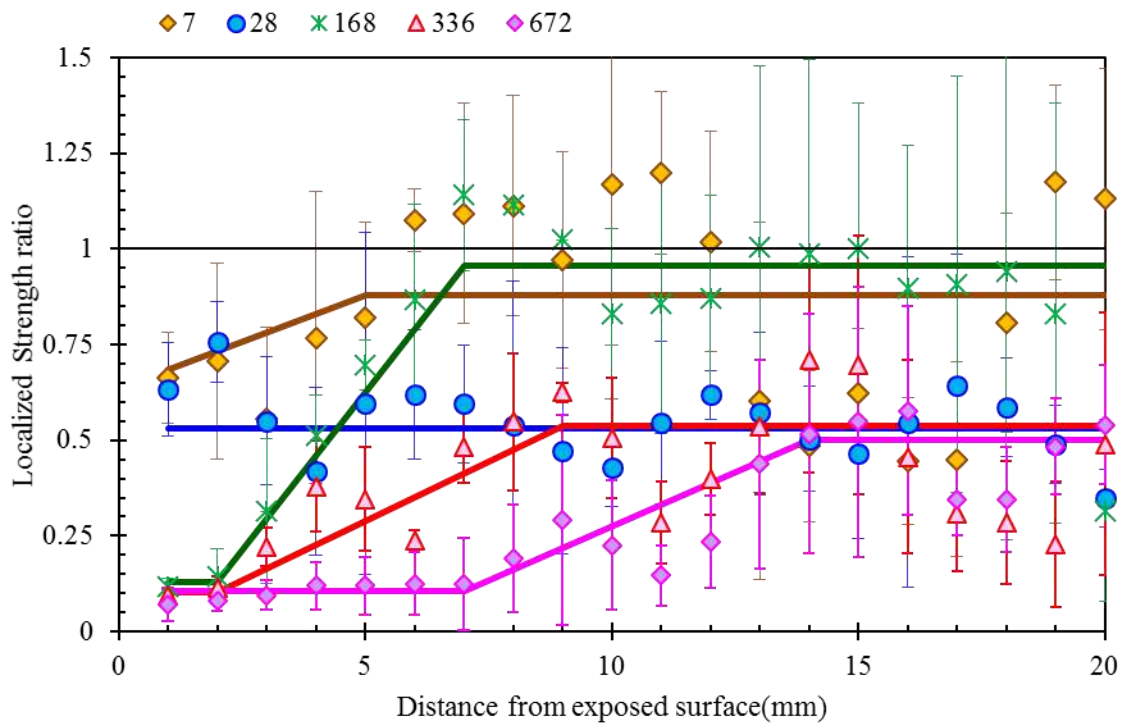


Figure 4:33 Relationship between localized strength ratio and the distance from exposed surface- C3.5 pure (immature)

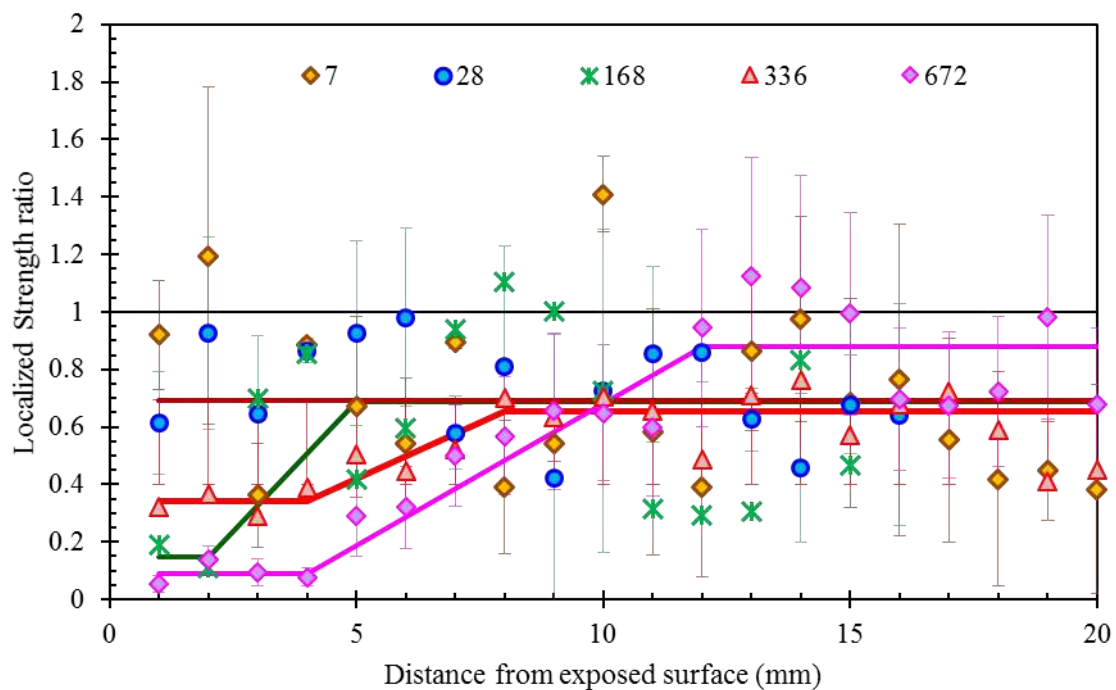


Figure 4:34 Relationship between localized strength ratio and the distance from exposed surface -C5.3 acid (immature)

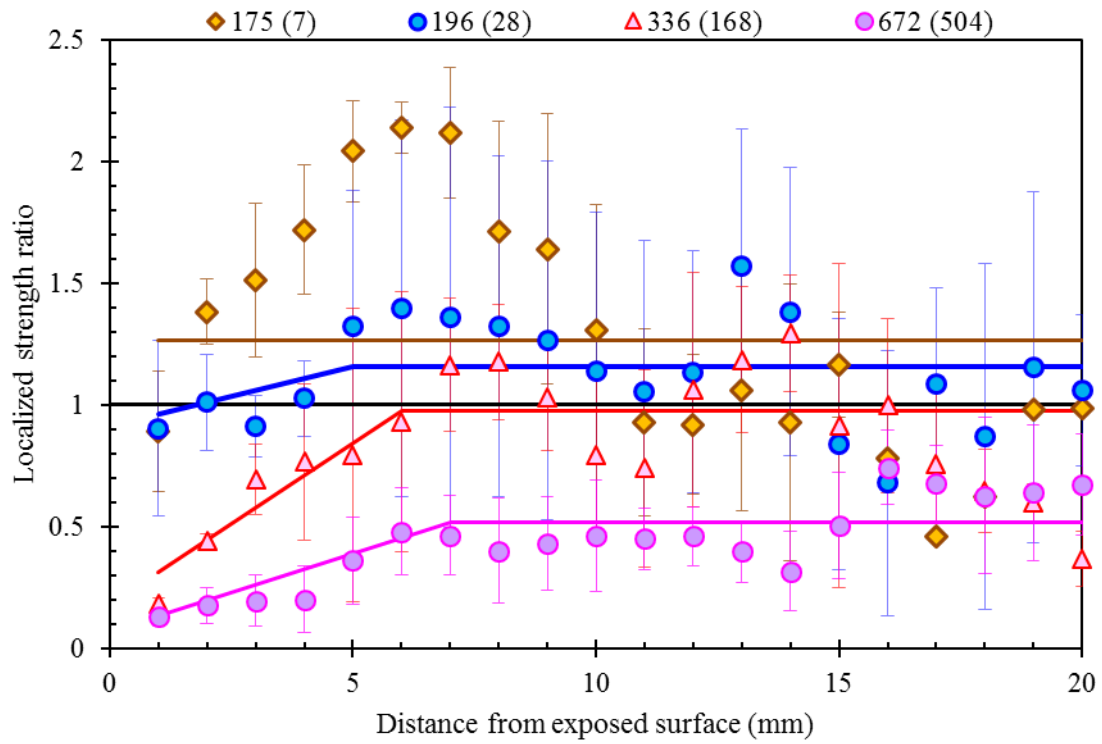


Figure 4:35 Relationship between localized strength ratio and the distance from exposed surface- C3.5 acid (mature)

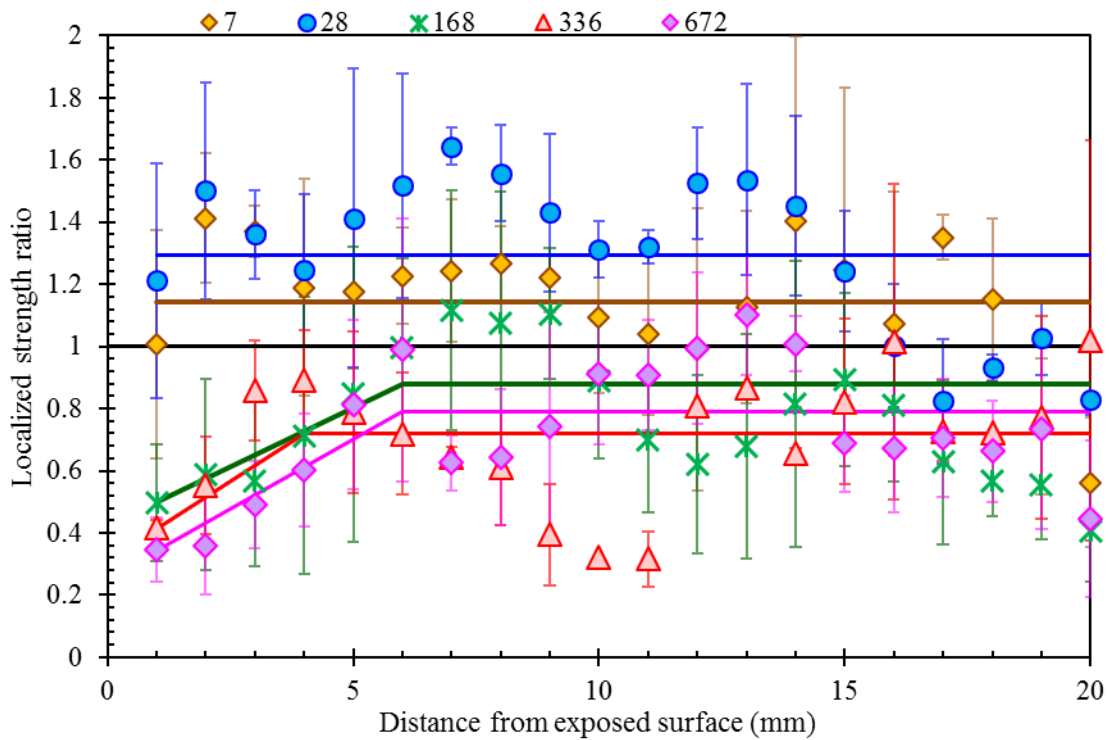


Figure 4:36 Relationship between localized strength ratio and the distance from exposed surface- L2.5 acid (immature)



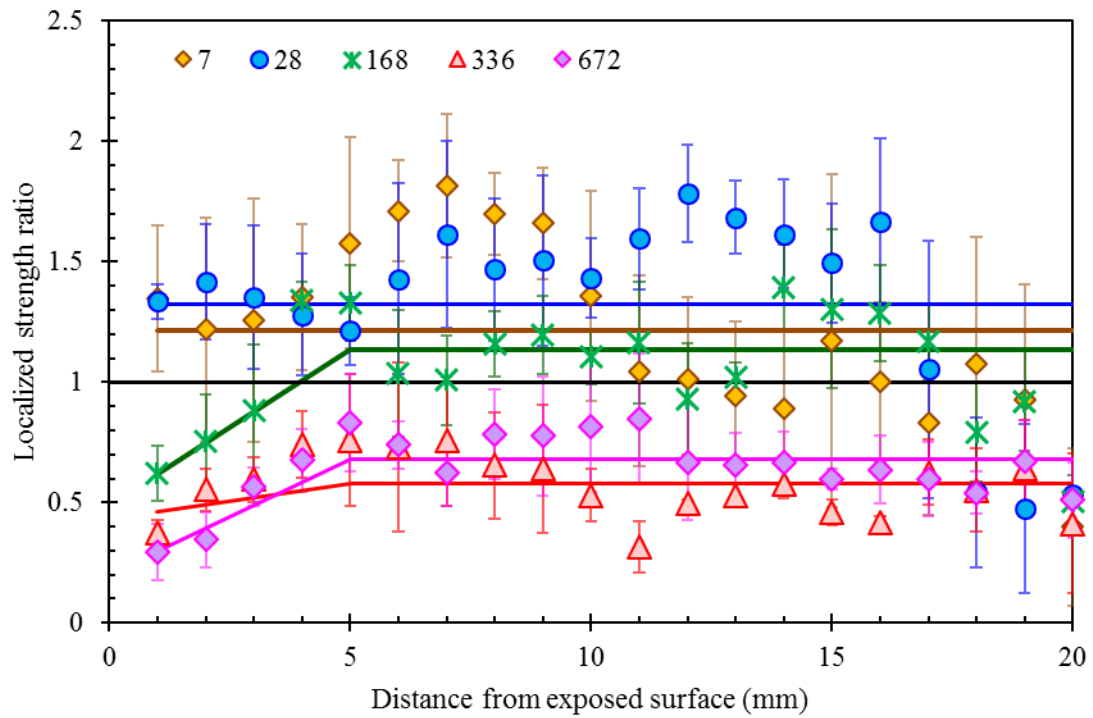


Figure 4:37 Relationship between localized strength ratio and the distance from exposed surface- L2.5 pure (immature)

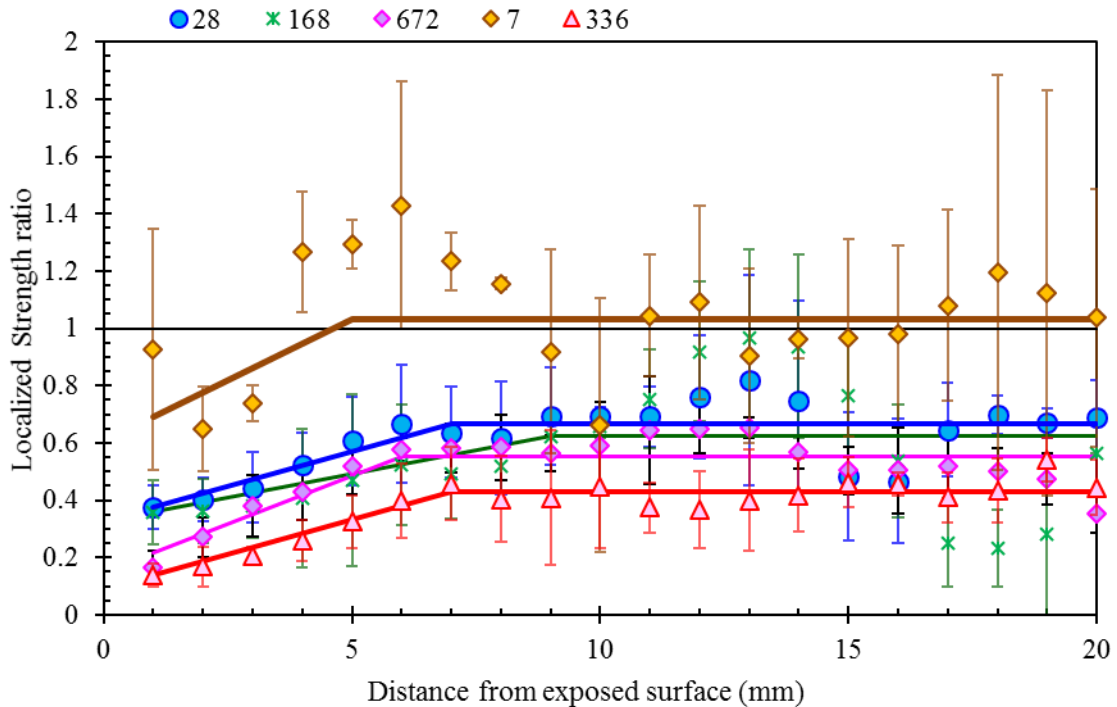


Figure 4:38 Relationship between localized strength ratio and the distance from exposed surface- L3.8 acid (immature)

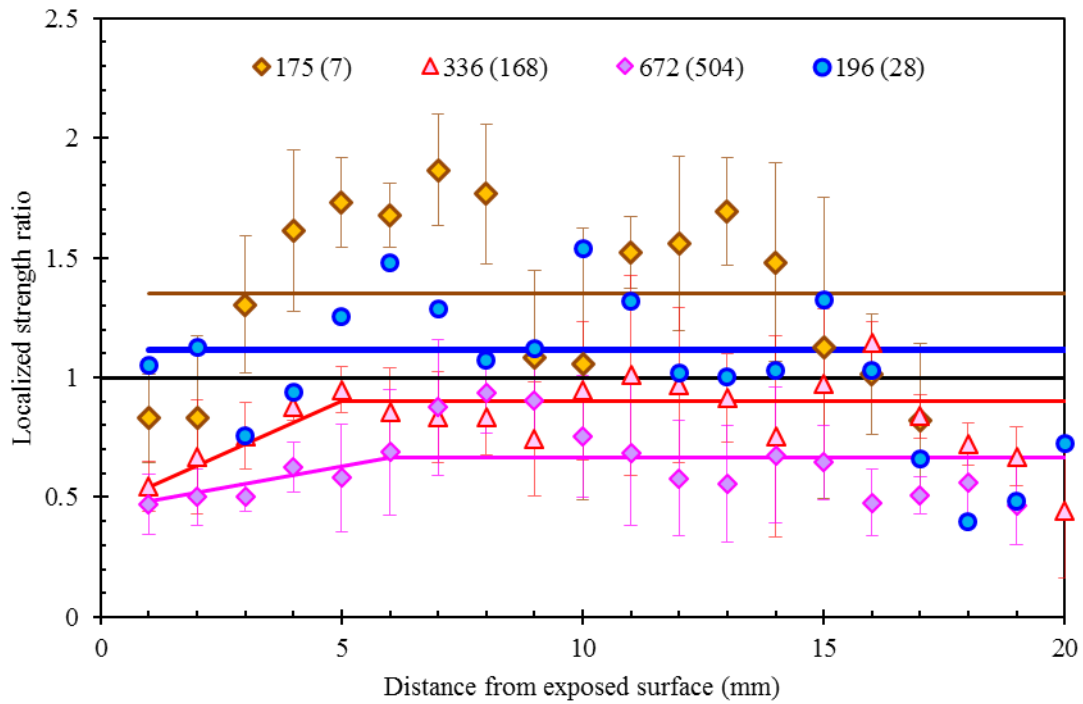


Figure 4:39 Relationship between localized strength ratio and the distance from exposed surface -L2.5 acid (mature)

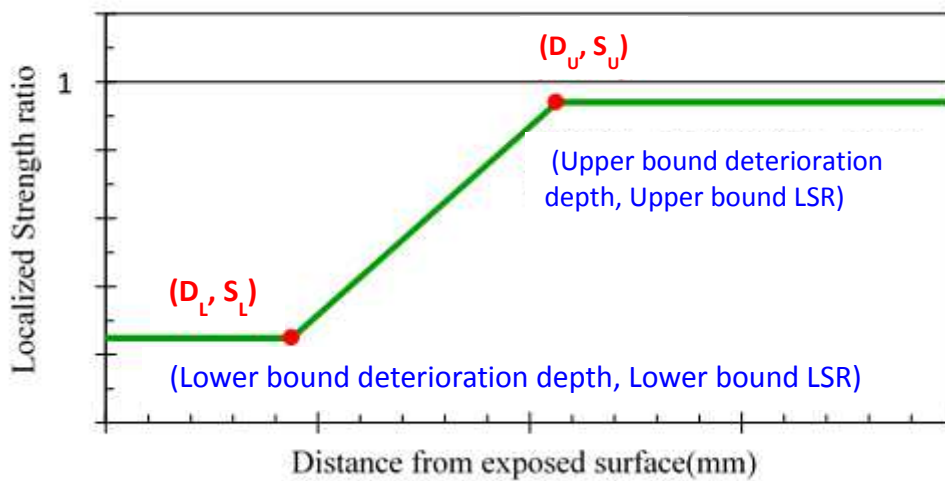


Figure 4:40 General distribution of localized strength ratio at a given soaking period

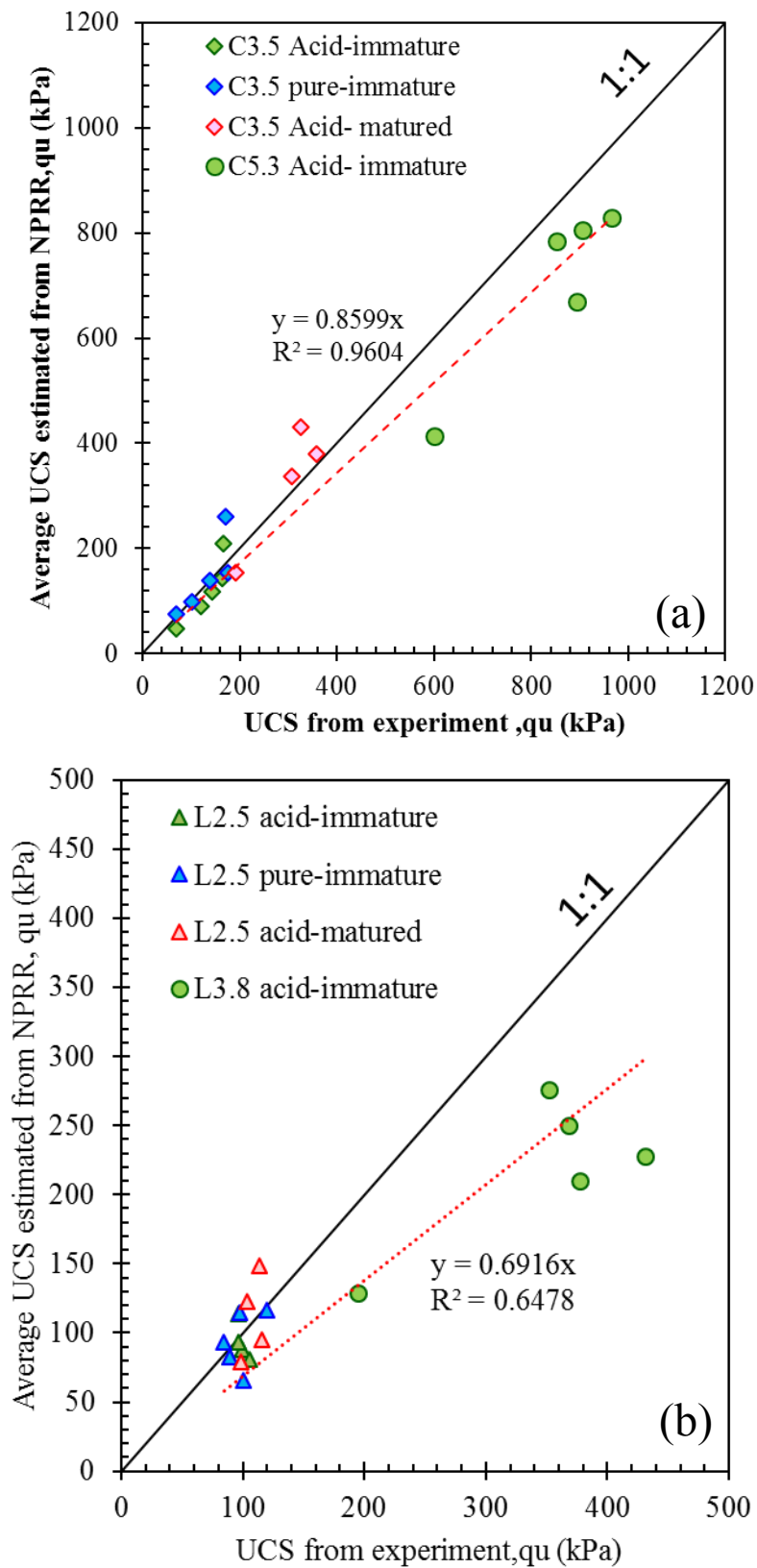


Figure 4:41 Relationship between estimated UCS and experimental UCS for soaked specimens (a) cement treated soil (b) Lime treated soil

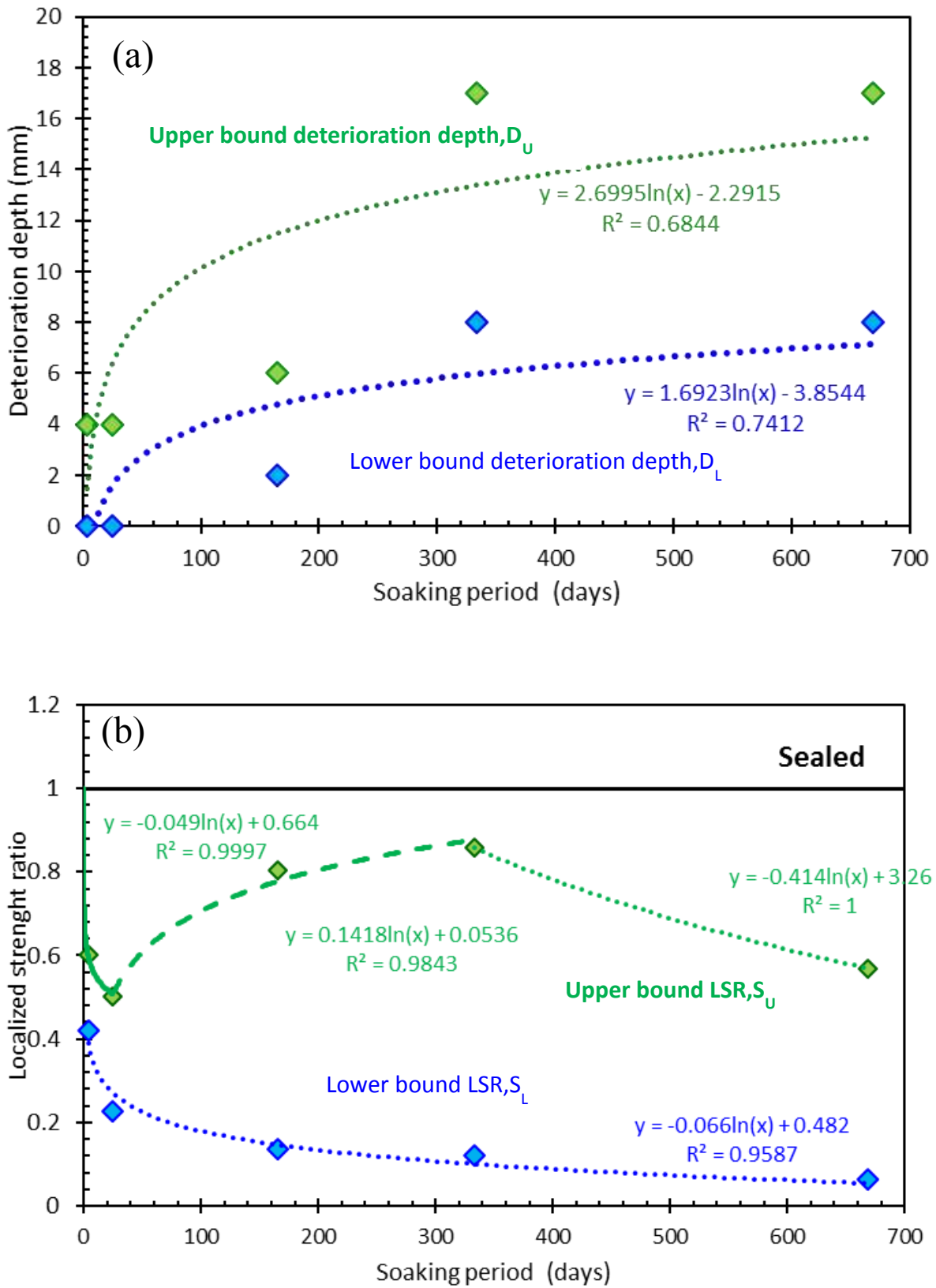


Figure 4:42 C3.5Soak-acid (immature) (a) variation of deterioration depth (b) variation of localized strength ratio

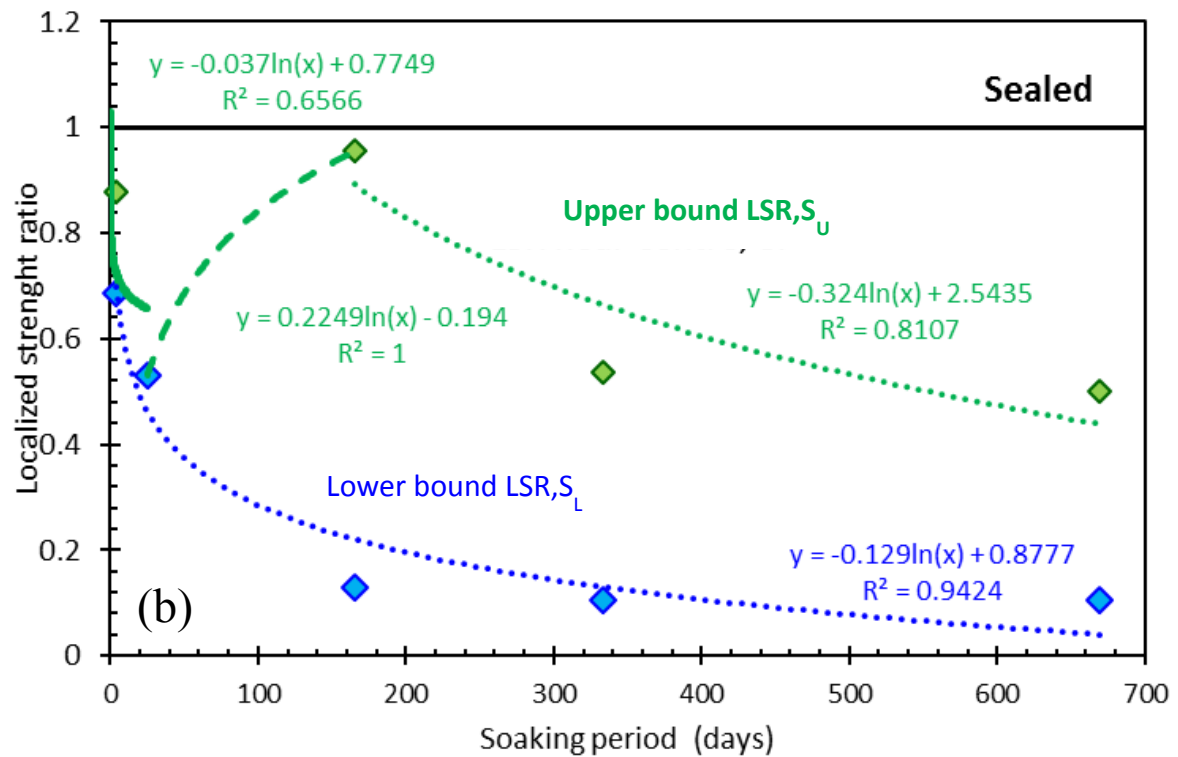
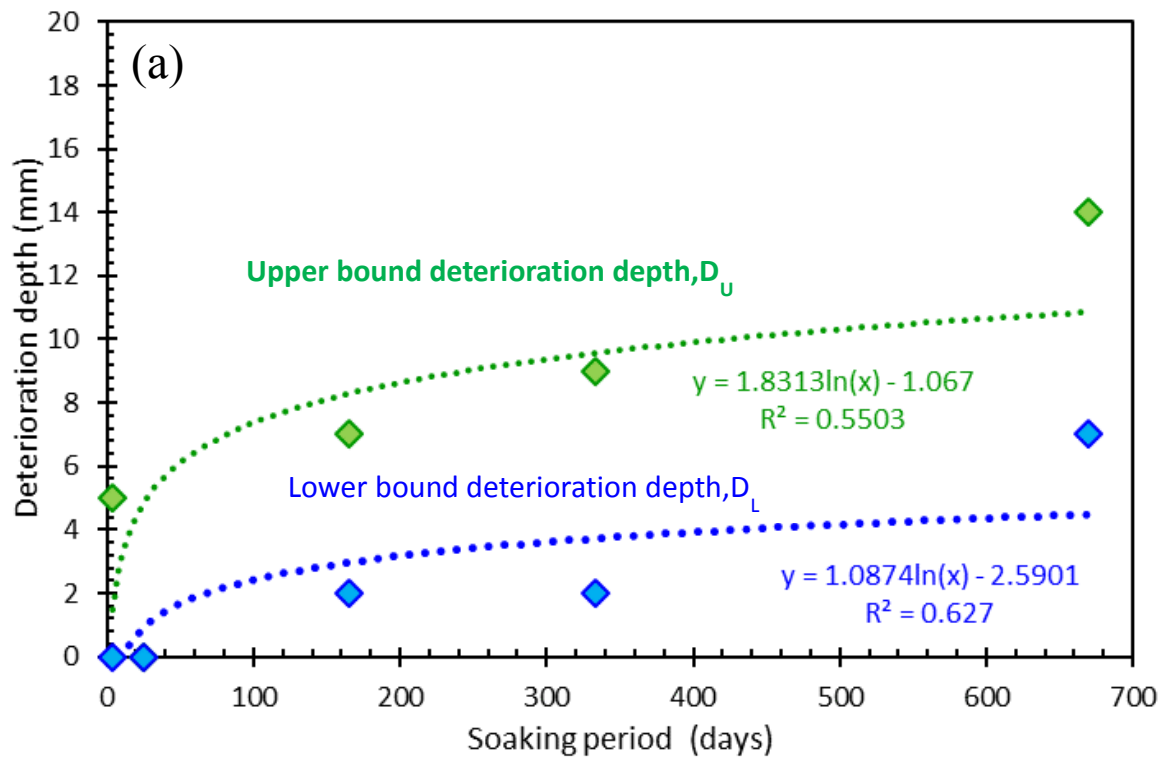


Figure 4:43 C3.5-Soak Pure (immature) (a) variation of deterioration depth (b) variation of localized strength ratio

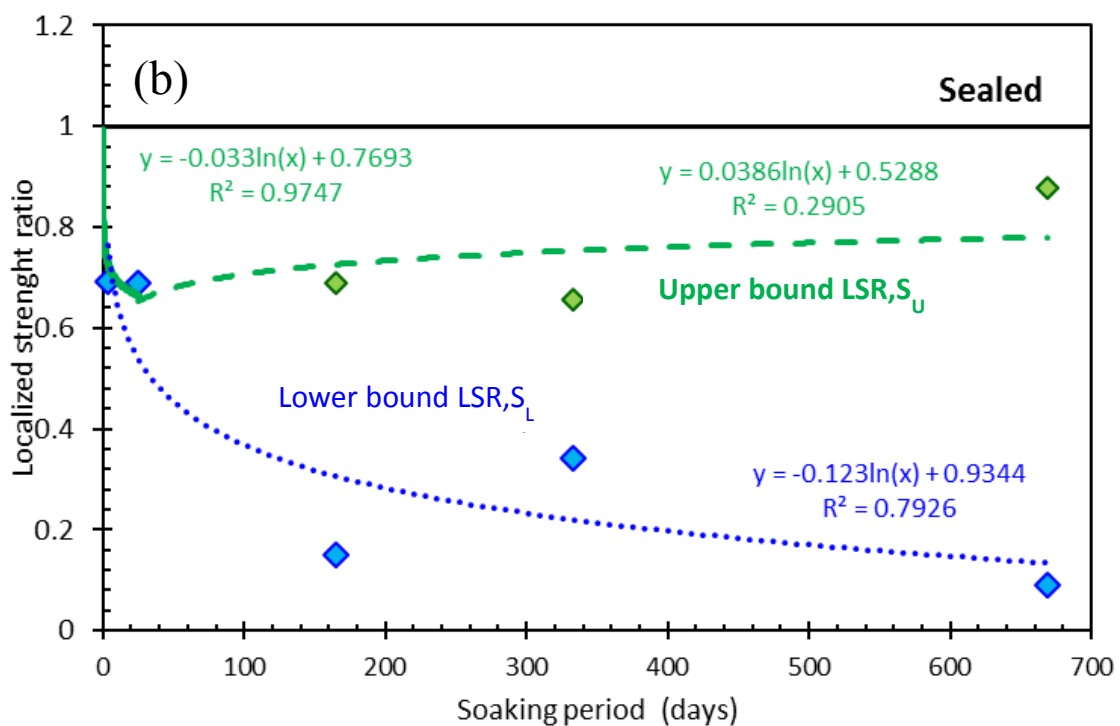
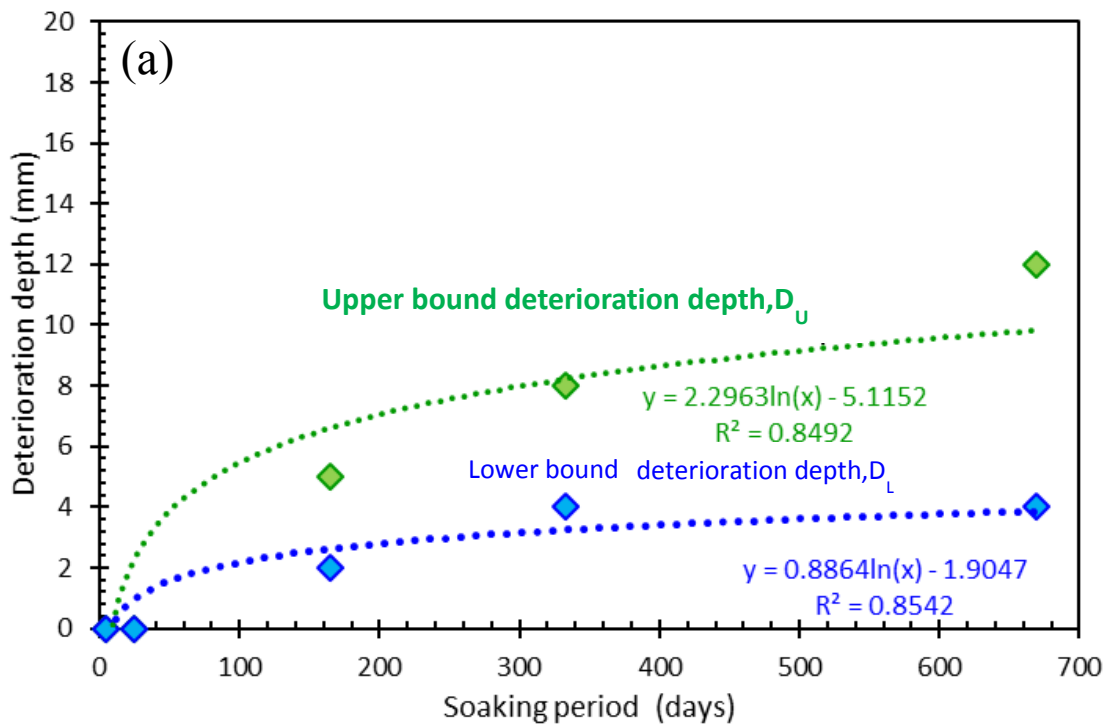


Figure 4:44 C5.3-Soaked (immature) (a) Variation of deterioration depth (b) Variation of localized strength ratio

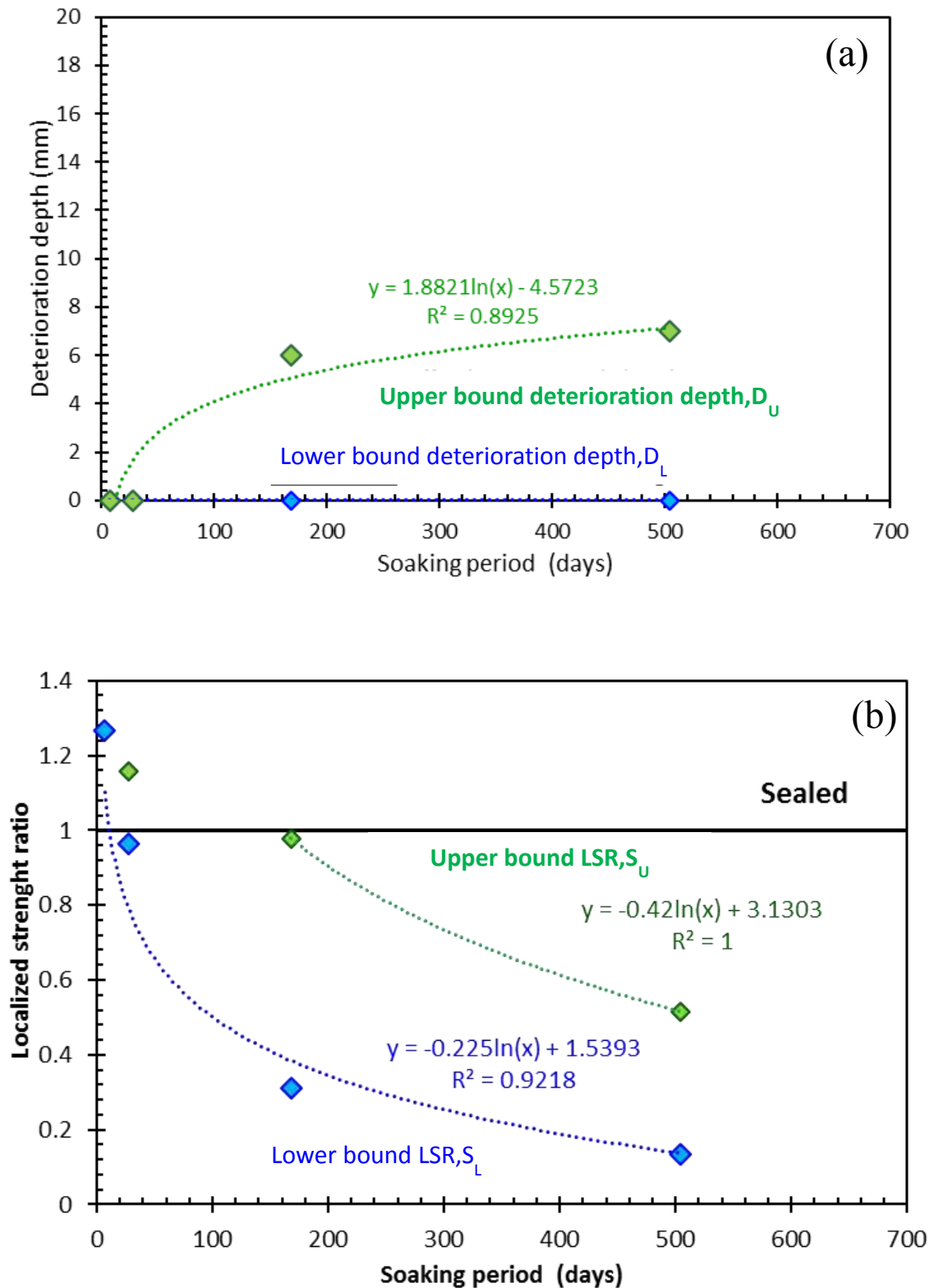


Figure 4:45 C3.5-Soak acid (mature) (a) Variation of deterioration depth (b) Variation of localized strength ratio

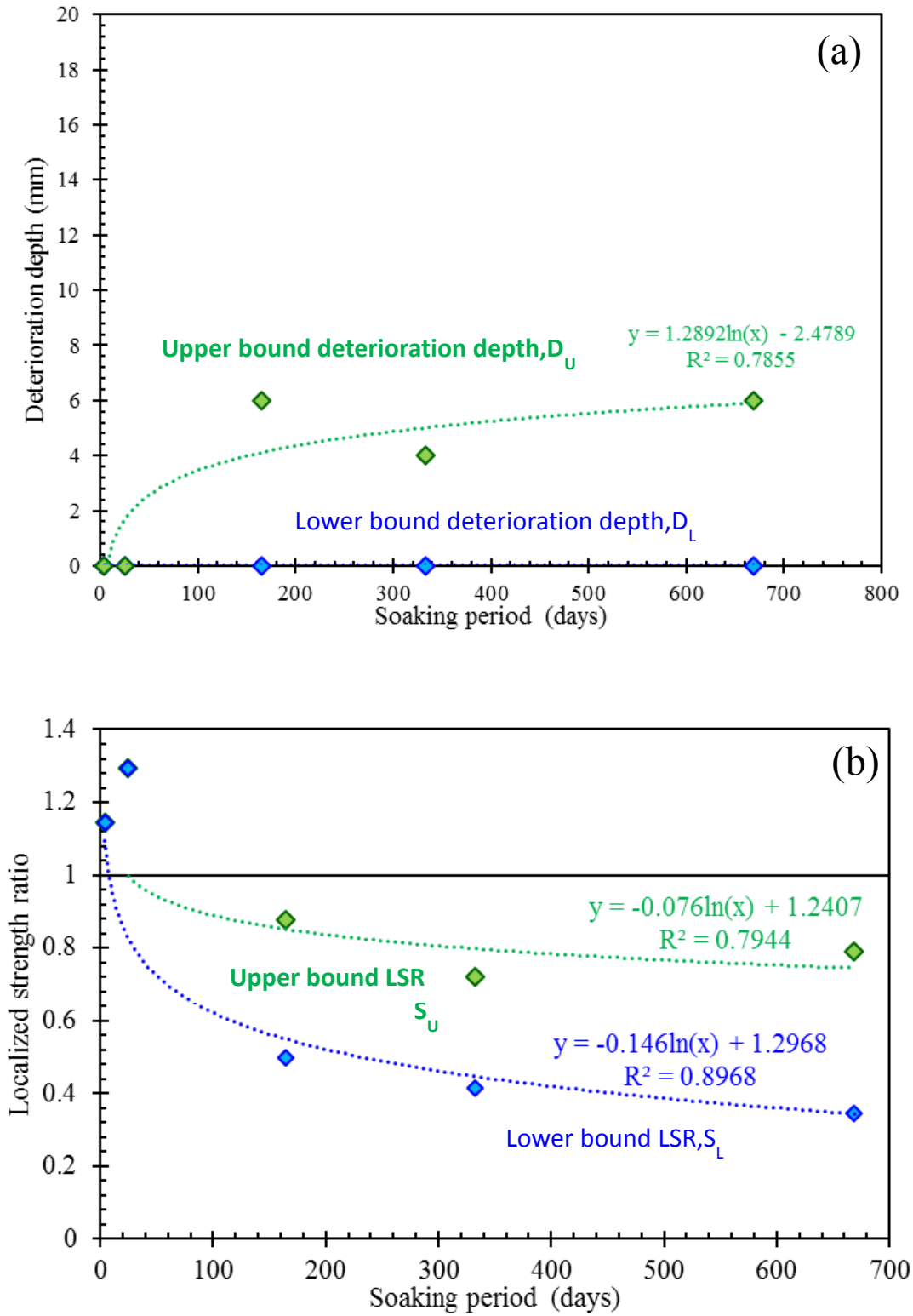


Figure 4:46 L2.5 Soak acid (immature) (a) deterioration depth (b) localized strength ratio



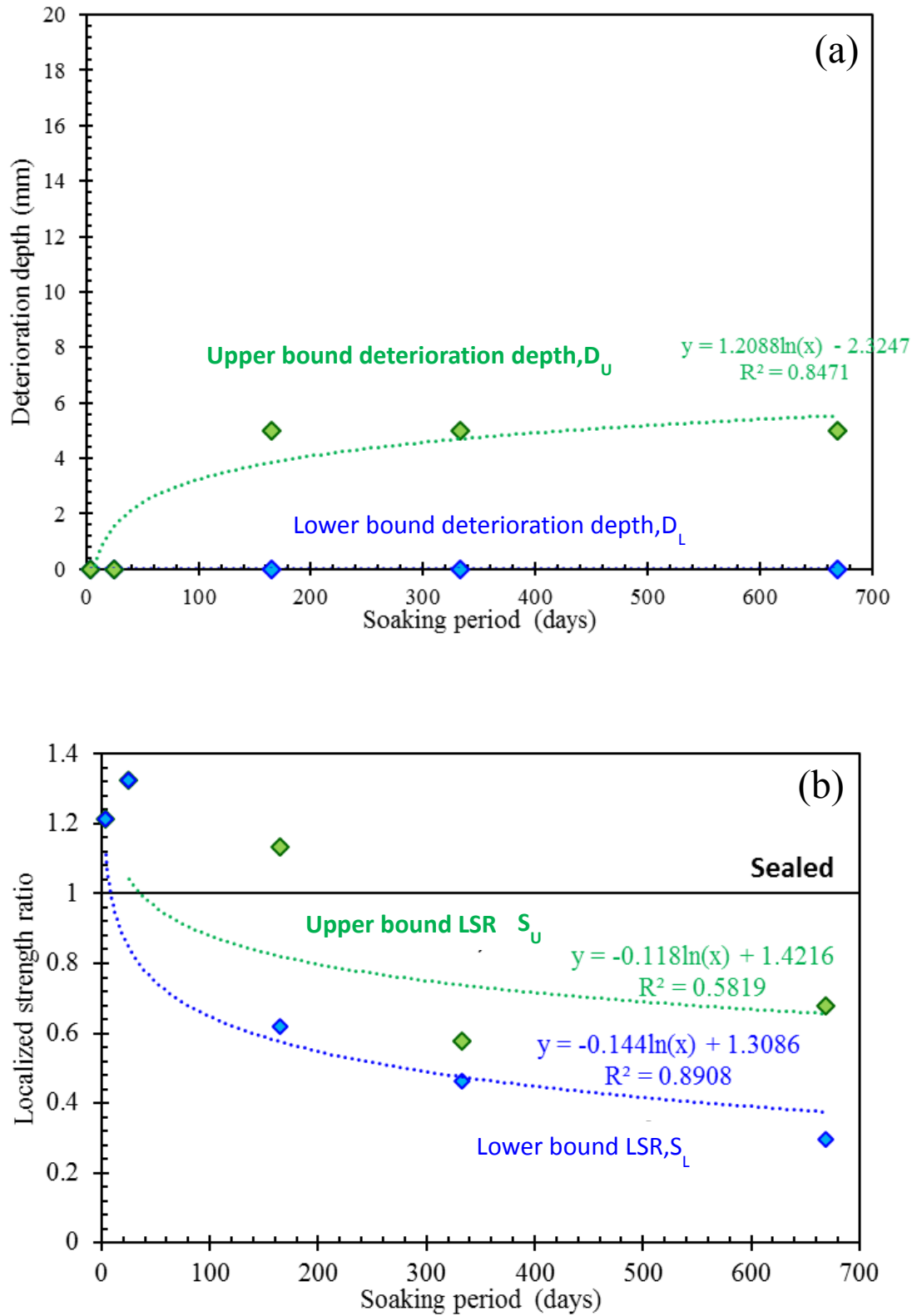


Figure 4:47 L2.5 Soak Pure (immature) (a) Deterioration depth (b) localized strength ratio

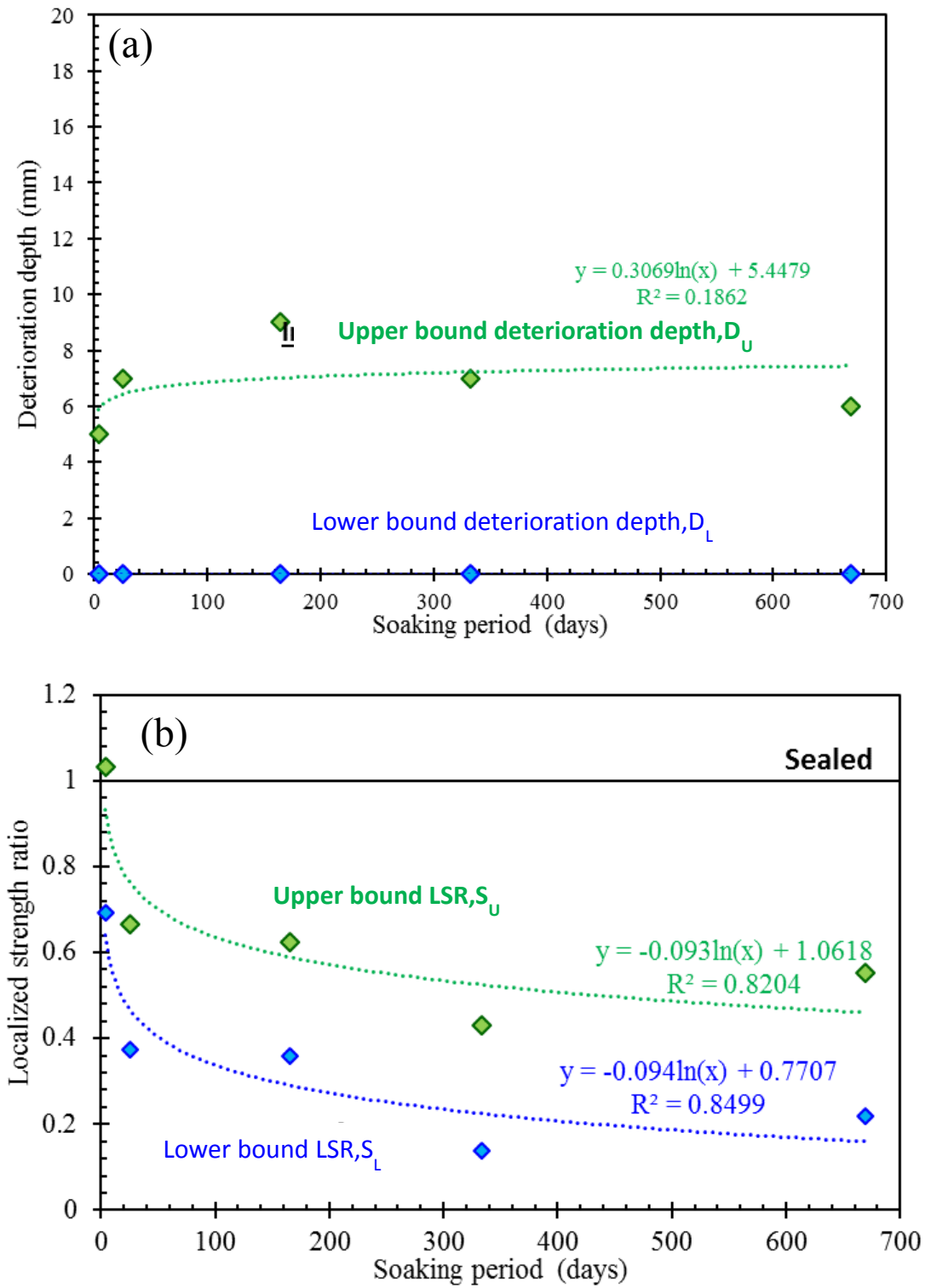


Figure 4:48 L3.8 Soak acid (immature) (a) deterioration depth (b) Localized strength ratio

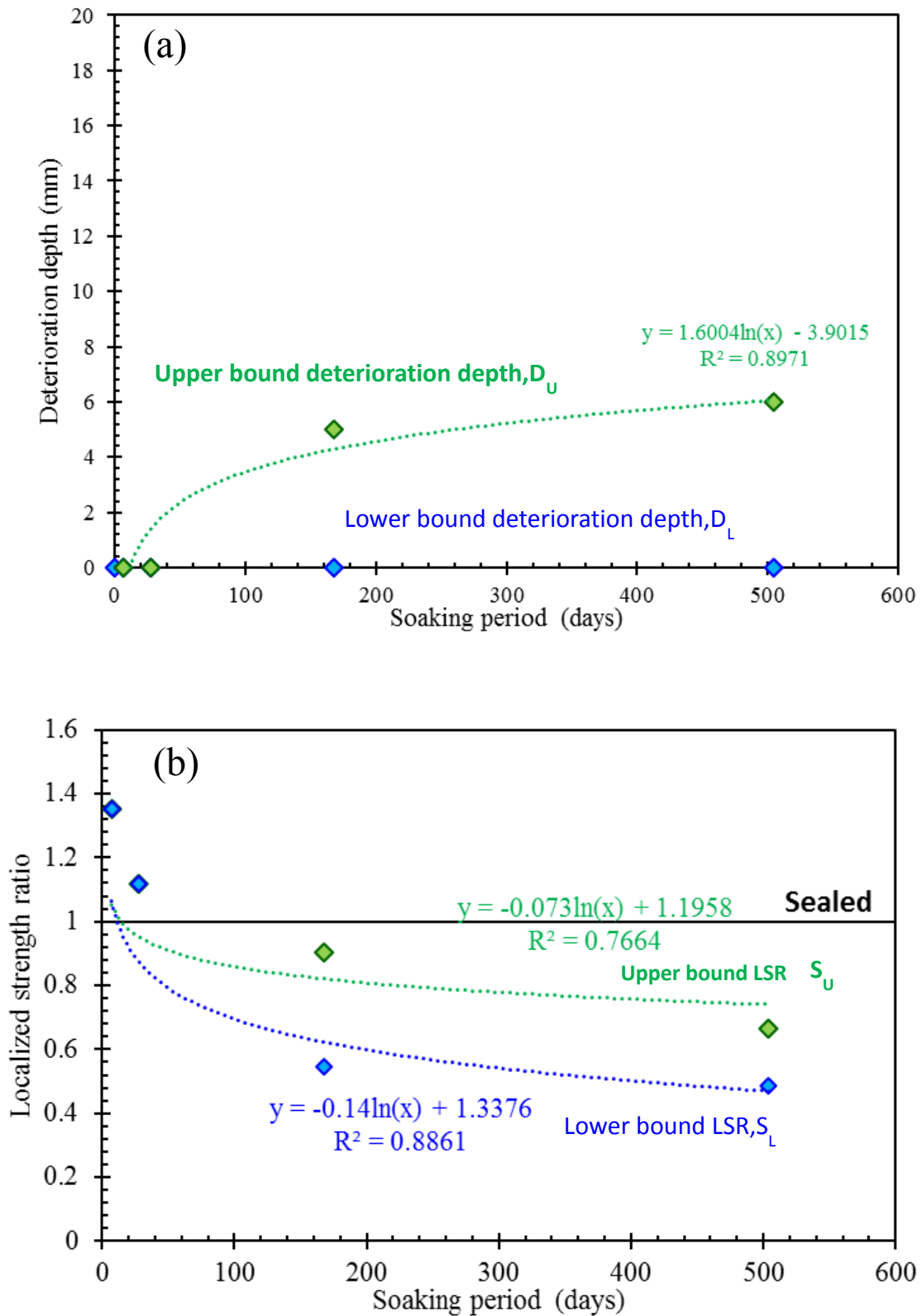


Figure 4:49 L2.5- Soak acid (immature) (a) deterioration depths (b) Localized strength ratios

## 5 Mechanism of deterioration

### 5.1 Introduction

This chapter explains the mechanism of deterioration of improved surplus soils with low binder content under groundwater from chemical aspects. From localized strength distribution analysis, it was identified two possible actions for the deterioration of those improved soils as internal deterioration and deterioration driven from the surface. In previous studies (Hashimoto et al., 2018; Ikegami, Ichiba, Ohishi, & Terashi, 2005; Kitazume, Nakamura, Terashi, & Ohishi, 2003; Ngoc, Turner, Huang, & Kelly, 2016; Takahashi, Morikawa, Fujii, & Kitazume, 2018; Yang, Yan, Liu, & Zhang, 2016) it was identified calcium leaching as one of the reason for long term deterioration of columns made by deep cement mixing under seawater .

In order to find out the reason for the deterioration in chemical aspects Calcium (Ca) ion in soaking water and soil sample was measured. The obtained relationships between localized strength distribution and Ca ion distribution measured by EPMA and XRF analysis were summarized in this chapter. In addition to that, the results obtained from XRD analysis also was summarized.

### 5.2 Soaking water analysis results

Figure 5:1, Figure 5:2 and Figure 5:3 indicate the changes in pH value, accumulated amounts of Ca and sulfate which were measured from the collected water of both lime and cement treated soil specimens after soaking over the curing period. The amounts of accumulated Ca and sulfate was the leached amounts from a single specimen.

It should be noted that the pH of pure water and acid water was set to 7 and 4.5 before starting soaking and each time they were exchanged. However, after soaking the specimens, in all cases of both cement and lime treated soils pH values soaking water was increased alkaline conditions. This was an indication of moving hydroxyl ions form specimens to soaking water. In early stages of soaking the highest pH value was observed in the largest lime content, L3.8, while the pH values of other cases were varied in response to the types and the contents of the binders. In all the cases pH values were gradually decreased when increasing the curing period and reached around a pH of 9.

In both cases of leaching of Ca ions and Sulphate ions leaching rates were large at initial stages of soaking while those were gradually decreased in all the cases. In the case of lime treatment cured under immature state, the cumulative amount of leached Ca ion was larger when larger the lime content. It was assumed that the amount of sulfate leached from lime treated soil was due to the leaching from the component of Miho sand. It should be noted here that the original amount of sulfate in the acidic water was calculated as 0.51 mg/L and can be neglected when compared to the values measured in Figure 5:3. In the case of cement treated soil cured under immature condition, the amount of Ca leached was almost the same in C5.3 and C3.5, while smaller accumulation was observed in C1.7. At initial stages of soaking, cumulative leached amount of sulfate was largest in C3.5 immature case.

### 5.3 Ca ion distribution in the specimen

#### 5.3.1 EPMA analysis results

Figure 5:4 shows typical ion distributions for C, Si and Ca which were obtained EPMA measurements. In order to get the Ca ion distribution along the radius of the soil specimen it was required to eliminate voids and the Ca contributed from Miho sand. In the analysis, position and the size of the voids in each specimen were identified and eliminated using the EPMA results of carbon ion distribution as carbon was the main constituent in the epoxy resin. In the calculation, it was assumed all the voids were properly filled with epoxy resin and the carbon weight % of voids were decided as 15 or 30 according to the obtained results in resin ( in this case 15). To distinguish the cement paste from the soil particles, the range for cement paste was selected as silica < 28 weight %, by considering silicon dioxide composition in Miho sand following previous studies (Mori, Yamada, Hosokawa, & Yamamoto, 2006). After choosing the pixels only with cement paste, Ca ion distribution was averaged radially from the center to the surface using a MATLAB script. In the calculation, the number of pixels only with cement paste within a 5 mm radius was counted. Then the thickness of the next hollow circle was determined through iterations by keeping the initially counted number of data as a constant. The same procedure was followed up to the edge of the specimen as shown in Figure 5:5.

Figure 5:6, Figure 5:7 and Figure 5:8 shows the obtained Ca ion distribution from EPMA analysis and the calculated Ca ion profiles along the radius of the specimens for C3.5 Soak acid (immature), L3.8 Soak acid (immature) and L2.5 Soak acid (immature) respectively. In each case, it was contained one sealed specimen several soaked specimens. By considering the

---

color distribution a clear difference could be observed in Ca ion distributions between sealed and soaked specimens, especially after soaking of 336 days.

In C3.5 case, under the sealed condition, the standard deviation of analysis results was 0.11 and 0.08 at a distance of 0-5 mm and 20-25 mm respectively due to the variation in the microstructure. By considering that fact, a clear difference in Ca contents between sealed and soaked specimens could be observed throughout the specimen after soaking of 168 and 336 days.

### 5.3.2 XRF analysis results

Figure 5:9, Figure 5:10, Figure 5:11 and Figure 5:12 shows the relationship between Ca ion weight percentage and the distance from the surface of the sealed and soaked specimens after curing for (a) 28, (b) 168, (c) 336 and (d) 672 days respectively. Figure 5:10 and Figure 5:12 were the same graphs shown in Figure 5:9 and Figure 5:11, after scaling up the vertical axis. Ca ion percentage was calculated from CaO percentage obtained by XRF analysis. It should be noted that the Ca ion percentage showed in each case represented Ca ion after eliminating Miho sand. Under the sealed condition, Ca ion percentages in all the specimens did not change with the distance. On the other hand, under soaked condition Ca ion had leached out from center to surface. A noticeable reduction was observed at the distance less than 5mm from the exposed surface in both types of specimens after 672 days. In addition to that larger Ca, ion percentages were observed at the outer surface of the soaked specimens as a thin layer of calcium carbonate was precipitated on the surface as shown in Figure 5:13. To see the variation of Ca ion content relative to sealed condition with the soaking period, Ca ratio between soaked and sealed specimens at 0-5mm, 0-15mm and 20-25mm from the surface of the specimen, were evaluated.

## 5.4 Mechanism of internal deterioration and its recovery

From the discussion in Chapter 4, it was identified internal deterioration and its recovery appeared in cement treated soil when they were exposed to groundwater in immature state as shown in Figure 5:14. In order to find out the mechanism, obtained Ca ratio for 0-5mm and 20-25mm depths were plotted against soaking period as shown in Figure 5:15, Figure 5:16, and Figure 5:17 for C3.5 soak-acid, C3.5 soak-pure and C5.3 soak acid respectively. When compare the Ca ratio and upper bound localized strength ratios of those cases, it could observe a reduction in internal deterioration while there was no reduction in the Ca ratio within the first 25 days of soaking. In addition to that, the recovery from internal deterioration appeared while

there was a slight reduction in the Ca ratio. It was identified that internal deterioration and its recovery cannot be explained well with Ca distribution.

In the case of sealed specimens, when cement particles touch water, ions from cement particles move to pore water to initiate the hydration reaction. Precipitation of hydration products starts after pore water saturates with ions as described by several researchers (Damidot, Lothenbach, Herfort, & Glasser, 2011; Matschei, 2007; Matschei, Lothenbach, & Glasser, 2007; Rothstein, Thomas, Christensen, & Jennings, 2002; Taylor, 1997). When the cement treated specimens start to soak in immature state (in this case from 4 th day from preparation), ions in pore water try to move to soak water due to concentration difference of ions between the specimen and the soaking water. This was observed from soaking water analysis for sulfate ions. When considering the soaking water analysis, it could observe higher concentrations of the leached amount of sulfate ions within the first 25 days and that was gradually decreased as shown in Figure 5:18. In addition to that continuous leaching of calcium ions also observed. This action delayed the saturation process of pore water and reduce the amount of hydration products that can produce in the system. In this study, soaking water was exchanged every week up to one month to simulate severe conditions that can appear in the initial construction period of embankments. After one month soaking water was exchanged twice a month. That made a delay to ion mobilization action from pore water to soaking water. Because of that saturation index (SI) of pore water could increase and that helped to produce the additional amount of hydration products which caused for the recovery process of internal deterioration by increasing upper boundary localized strength ratio. However, this is a hypothesis made through the observations in this study. The experimental results obtained in this study was not enough to prove that. Further analysis required with quantitative analysis with thermogravimetric analysis on the soil specimens (TG/DTA) (Scrivener, Snellings, & Lothenbach, 2015).

## 5.5 Mechanism of deterioration driven from the surface

### 5.5.1 Cement treated soil (immature) soaking

When plot the Ca ratio at 0-5mm depth and the lower bound strength ratio  $S_L$  against soaking period a tendency was observed in strength reduction while reducing the Ca distribution. Those data were replotted against each other as shown in Figure 5:19 for all immature cases. In here instead of  $S_L$ , the averaged strength ratios obtained within 0-5mm depth were plotted. In the same figures, the sudden drop of  $S_L$  due to internal deterioration was shown by dash lines. A clear tendency of strength reduction was observed due to leaching of calcium when increasing

---

the soaking period. The relationship seems to be a linear relationship. By considering this fact it concluded the deterioration driven from the surface was caused by the calcium leaching process.

In C3.5 specimens which were soaked in water in immature condition, it was observed deterioration driven from the surface at upper bound LSR after 333 days of soaking. However, this phenomena could not explain with Ca ion distribution due to the limitation of available data.

### **5.5.2 Cement treated soil (mature) soaking**

Figure 5:20 shows the relationships between Ca ratios and strength ratios for both 0-5mm and 20-25mm depths. It could observe both  $S_U$  and  $S_L$  reduced while reducing Ca ratio when increasing the soaking period. By considering that fact the averaged strength ratios within 0-5mm, 10-15mm and 20-25mm depths were plotted against Ca ratio and a binomial relationship was obtained in each other. This relationship was somehow different from the relationships observed by previous studies on deep mixing cement. In those studies, they observed a linear relationship among Ca ratio and the strength ratio. It was suggested that there is a difference in calcium leaching mechanism of improved soil with low binder contents and large binder contents which might be due to the difference in the pore structure. In improved soil with low binder contents, it was suggested the pore distribution was act as a dual model with macropores and micropores as introduced by (Nakarai, Ishida, & Maekawa, 2006) as shown in Figure 5:25. This phenomenon needs to be verified by studying pore distribution with the mercury intrusion method.

### **5.5.3 Lime treated all soaked cases**

Figure 5:21, Figure 5:22, Figure 5:23 and Figure 5:24 shows the obtained relationships between Ca ratio and strength ratios for L2.5 acid (immature), L2.5 pure (immature), L2.5 acid (immature) and L3.8acid (immature) respectively. In all the cases a clear tendency of strength reduction was observed while reducing Ca ratio. Similar to cement immature case the relationships between Ca ratio and the strength ratios had a polynomial relationship. In here also it was assumed this happened because of the dual pore distribution. As a summary, it could say that the deterioration driven from the surface in lime treated soils was due to leaching of calcium ions.



---

## 5.6 Mineral identification

X-ray diffractometer analysis (XRD) was applied on powdered samples and obtained the intensity within 2 theta angles of 0-65. However, there was no clear difference in the peaks in the range of 40-65. Because of that in this report, the angle between 0-40 was shown. The X-ray diffraction mineral patterns were identified by comparison with file standard X-ray powder diffraction patterns (International Centre for Diffraction Data (ICDD), Mineral Powder diffraction file Search Manual, 1988) of the most commonly found minerals.

As explained in Chapter 1, Miho sand did not contain much clay minerals such as montmorillonite, Kaolinite, Halloysite. It contained basically Quartz, Albite, Muscovite, Actinolite, Enstatite, Orthoclase, Vermiculite, and Tosudite. These minerals did not consider as bad clay minerals.

The cement that was used in this study was a blended cement. It was suspected that it contained some amount of slag from the constituent proportions given by the company datasheet. However, it couldn't be proven from the analysis results as the cement contents were comparably low.

Even though XRD analysis was conducted for every case, clear identification of minerals up to some extent could be done only by the results obtained for cement 5.3 % and lime 3.8 % contents. Figure 5:26, Figure 5:27 and Figure 5:28 shows the XRD patterns which were obtained for C5.3 under sealed conditions after curing of 7, 28 and 672 days respectively. In the same figures, XRD pattern which was obtained for Miho sand was shown for comparing the peaks. In all the cases ettringite peak at an angle of 9.2 and 15.9 was observed. In addition to that, calcite peak was observed at 29.4 only in specimen cured up to 672 days. This might be due to the carbonation reaction which was given as a result of poor sealing of the specimen. In all cases, no portlandite was observed. This might be due to the limitation of this technique as it cannot detect mineral when the amount is small. Figure 5:29 shows the results which were obtained after applying heavy liquid application for the sealed specimens. In the same figure, it was shown the pattern from Miho sand after and before applying heavy liquid application for the comparison of the results. However, there were no clear peaks from hydration products in all cases. It was found that the heavy liquid that we used had a pH of 3.0. This might be one of the reasons for not showing hydration products. In addition to that as the amount of hydration products are small it can be converted into other minerals or can be destroyed in the process of sample preparation. From the results of the current study, it was concluded that heavy liquid

---

method was not a good option to separate small quantity of hydration products from improved soil.

Figure 5:30 and Figure 5:31 shows the XRD patterns obtained for C5.3 Soaked-acid (immature) 672 days 20-25mm depth and 0-5mm depth respectively. In Figure 5:30, it was observed clear peaks of ettringite and a very small peak of calcite. From needle penetration test results, it was observed the localized strength ratio near the center was increased at 672 soaking period due to the recovery of internal deterioration. This appearance of ettringite might be due to that action. In the case of Figure 5:31, the peaks of ettringite were disappeared and a clear peak was observed for calcite. From needle penetration test results, it was found this depth which had lower bound strength ratio. That means calcium leaching action which resulted in the deterioration driven from the surface might be due to leaching of Ca from ettringite. So far in most of the modeling leaching of Calcium and C-S-H was only considered as it was the main mechanism in concrete structures (Nakarai et al., 2006). But from the results of this study, it seems that it required to consider leaching of ettringite also as it played a big role in cement stabilized soil. Figure 5:32 shows XRD patterns of the soaked specimens after applying heavy liquid application. As explained in the previous section that technique was not successful in this study.

Figure 5:33, Figure 5:34, and Figure 5:35 shows the XRD patterns obtained for L3.8 sealed, Soaked-acid (immature) 672 days and sealed and soaked after applying heavy liquid respectively. Under sealed condition, the known mineral which could be identified was only calcite. Those peaks did not appear in the soaked specimens. Similar to observations in the cement, it could not observe peaks for portlandite as the contents were small. In addition to that, the application of heavy liquid did not succeed in lime treated soil also.

## 5.7 Summary and conclusions

This chapter explained the mechanism of deterioration of improved surplus soils under groundwater from chemical aspects.

The analyzed results of this chapter can be summarized as follows.

1. From both XRF and EPMA analysis it was observed that Ca ions had leached out from specimen to soaking water. In addition to that in larger soaking period Ca was precipitated as  $\text{CaCO}_3$  on the surface of the specimen.

2. Internal deterioration and its recovery could not be explained with the remaining Ca ions. It was suggested that action was a result of the mobilization of ions from pore water to soaking water.
3. When cement treated specimen soak in the immature state the deterioration driven from the surface was appeared due to calcium leaching. The Ca ratio and the localized strength at 0-5 mm depth showed a linear relationship.
4. In the case of soaking cement treated soil in a mature state and all cases of lime treated soil, Ca leaching was identified as the reason for the deterioration driven from the surface. Ca ratio and the strength ratio throughout the specimen showed a polynomial relationship.
5. XRD analysis was applied to identify the mineral in improved soils. In cement treated soil it could find ettringite and Calcite peaks only. From the soaked specimens, it was found ettringite had disappeared at the surface. It was suggested that Ca leaching from ettringite also contribute to strength reduction.
6. In lime treated soil only a clear appearance of calcite could be observed as a known mineral.
7. The heavy liquid application was not successful for separating small quantities of hydration products from both cement and lime stabilized soils.

---

## 5.8 Reference

- Damidot, D., Lothenbach, B., Herfort, D., & Glasser, F. P. 2011. Thermodynamics and cement science. *Cement and Concrete Research*, 41(7): 679–695.
- Hashimoto H., Yamanashi T., Hayashi H., Kawaguchi T., Kawajiri S., et al. 2018. Long-Term Strength Characteristics of the Cement Treated Soil after 30 Years. *Journal of the Society of Materials Science, Japan*, 67(1): 47–52.
- Ikegami, M., Ichiba, T., Ohishi, K., & Terashi, M. 2005. Long-term properties of cement treated soil 20 years after construction. *Proceedings of the 16th International Conference on Soil Mechanics and Geotechnical Engineering*, 1199–1202.
- Kitazume, M., Nakamura, T., Terashi, M., & Ohishi, K. 2003. *Laboratory Tests on Long-Term Strength of Cement Treated Soil*, 586–597. Presented at the Grouting and ground treatment.
- Matschei, T. 2007. *Thermodynamics of Cement Hydration*, 222.
- Matschei, T., Lothenbach, B., & Glasser, F. P. 2007. Thermodynamic properties of Portland cement hydrates in the system CaO–Al<sub>2</sub>O<sub>3</sub>–SiO<sub>2</sub>–CaSO<sub>4</sub>–CaCO<sub>3</sub>–H<sub>2</sub>O. *Cement and Concrete Research*, 37(10): 1379–1410.
- Mori, D., Yamada, K., Hosokawa, Y., & Yamamoto, M. 2006. Applications of Electron Probe Microanalyzer for Measurement of Cl Concentration Profile in Concrete. *Journal of Advanced Concrete Technology*, 4(3): 369–383.
- Nakarai, K., Ishida, T., & Maekawa, K. 2006. Modeling of Calcium Leaching from Cement Hydrates Coupled with Micro-Pore Formation. *Journal of Advanced Concrete Technology*, 4(3): 395–407.
- Ngoc, P. V., Turner, B., Huang, J., & Kelly, R. 2016. *Experimental Study on the Durability of Soil-Cement Columns in Coastal Areas*, 6.
- Rothstein, D., Thomas, J. J., Christensen, B. J., & Jennings, H. M. 2002. Solubility behavior of Ca-, S-, Al-, and Si-bearing solid phases in Portland cement pore solutions as a function of hydration time. *Cement and Concrete Research*, 32(10): 1663–1671.
- Scrivener, K., Snellings, R., & Lothenbach, B. (Eds.). 2015. *A Practical Guide to Microstructural Analysis of Cementitious Materials*. CRC Press.  
<https://doi.org/10.1201/b19074>.
- Takahashi, H., Morikawa, Y., Fujii, N., & Kitazume, M. 2018. Thirty-seven-year investigation of quicklime-treated soil produced by deep mixing method. *Proceedings of the Institution of Civil Engineers - Ground Improvement*, 171(3): 135–147.
- Taylor, H. F. W. 1997. *Cement chemistry* (2nd ed). London: T. Telford.

Yang, J., Yan, N., Liu, Q., & Zhang, Y. 2016. Laboratory test on long-term deterioration of cement soil in seawater environment. *Transactions of Tianjin University*, 22(2): 132–138.

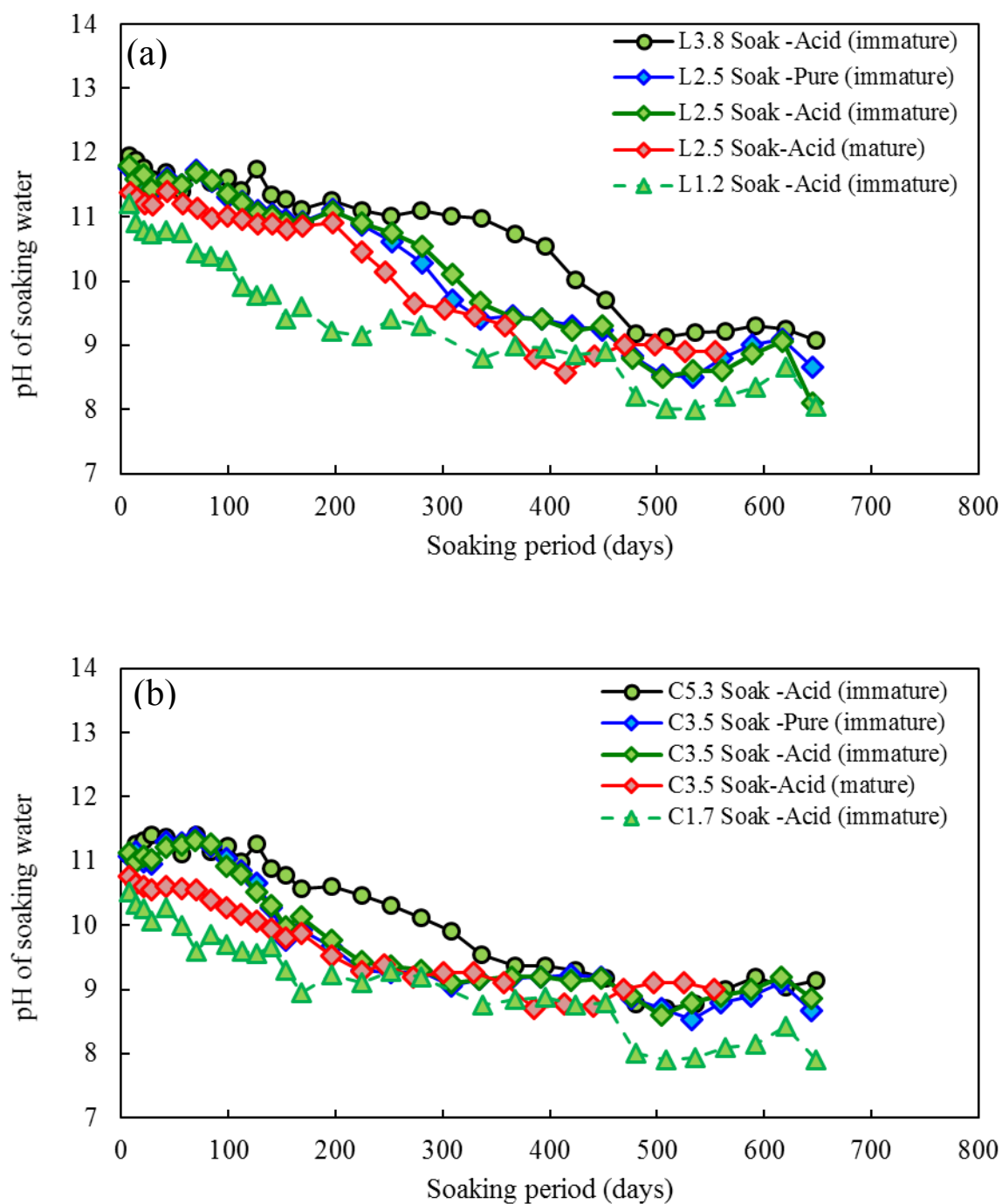


Figure 5.1 pH of soaking water (a) Lime treated soil (b) Cement treated soil

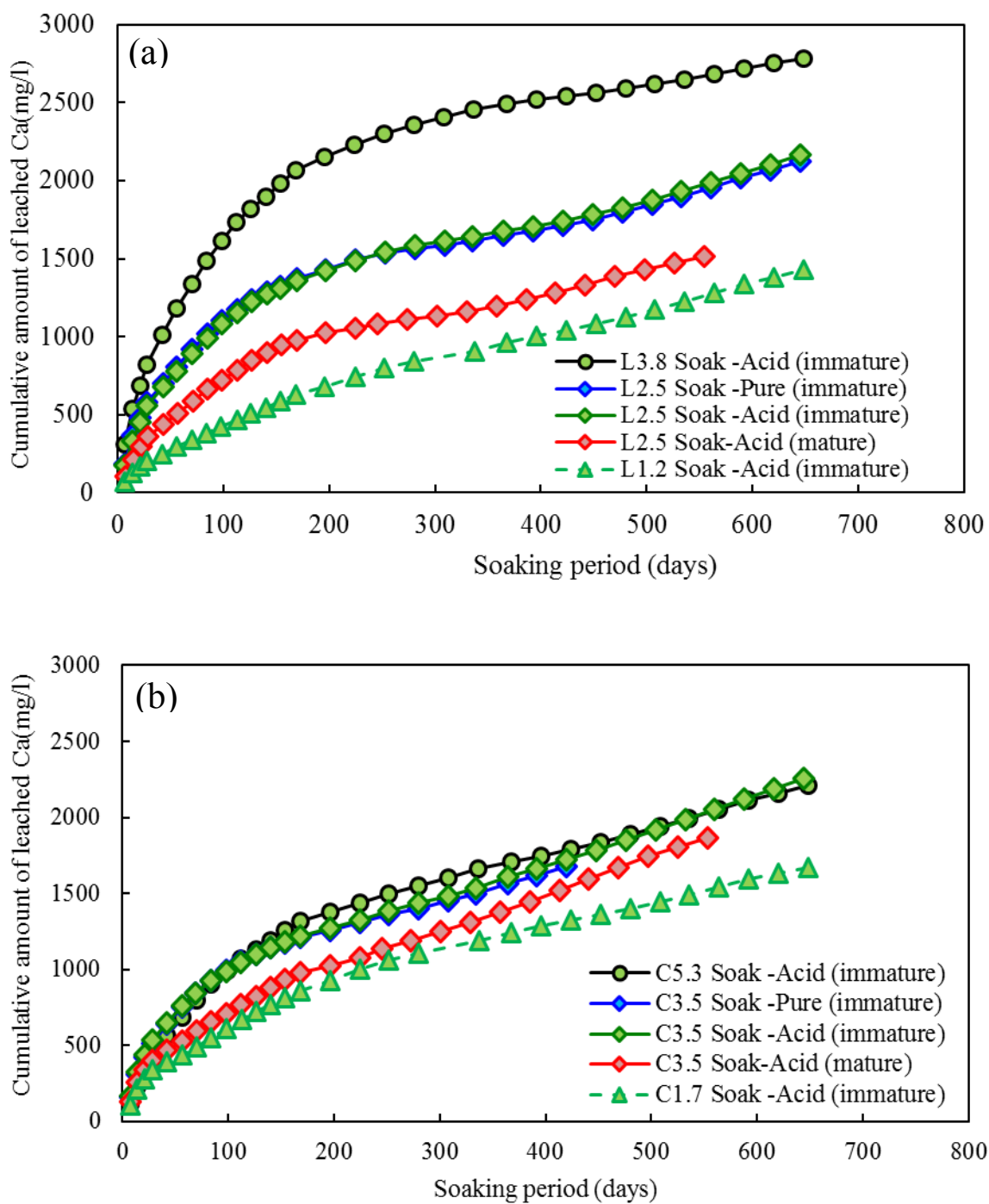


Figure 5:2 Cumulative amount of leached Ca (a) Lime treated soil (b) Cement treated soil

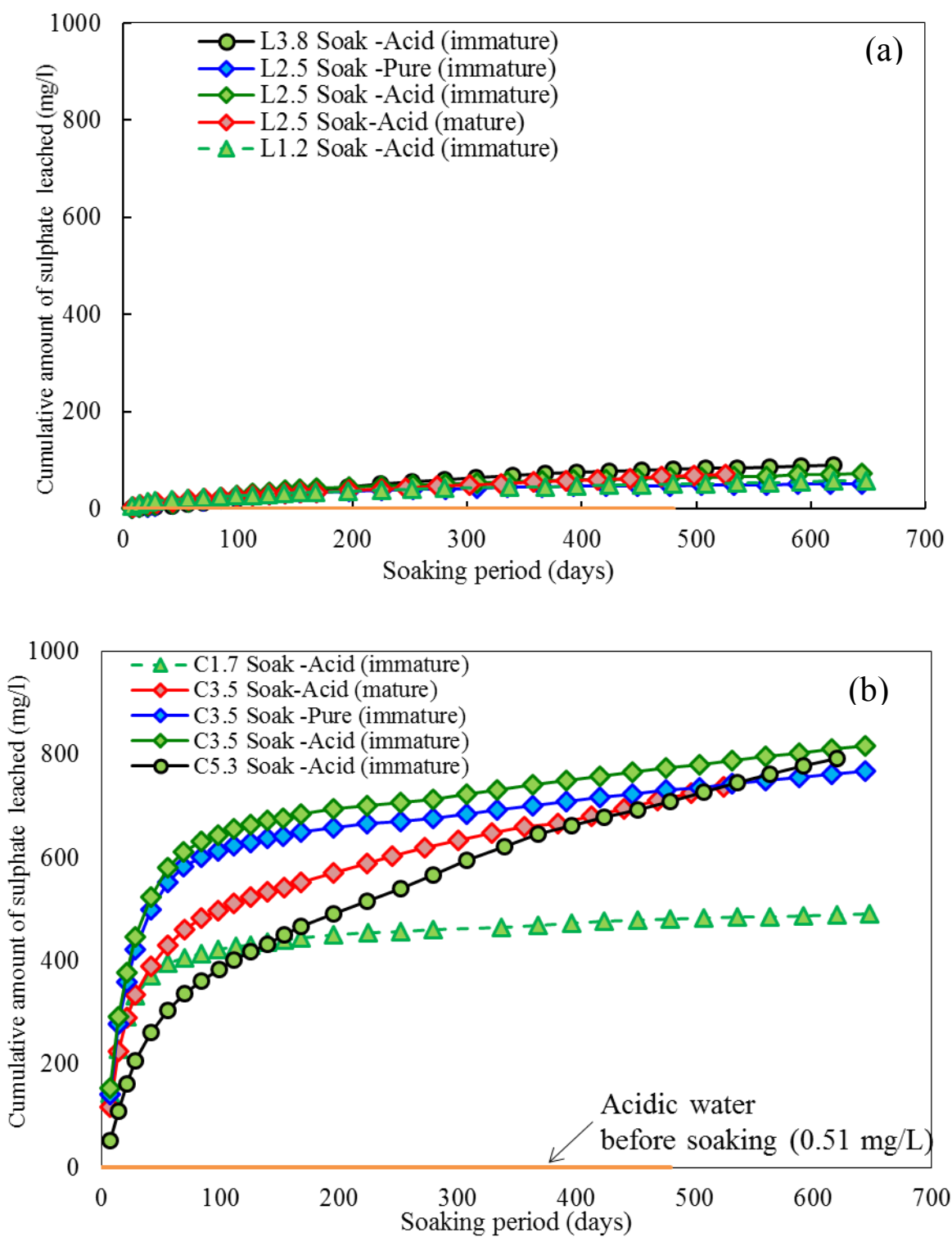


Figure 5:3 Cumulative amount of leached sulphate (a) Lime treated soil (b) Cement treated soil



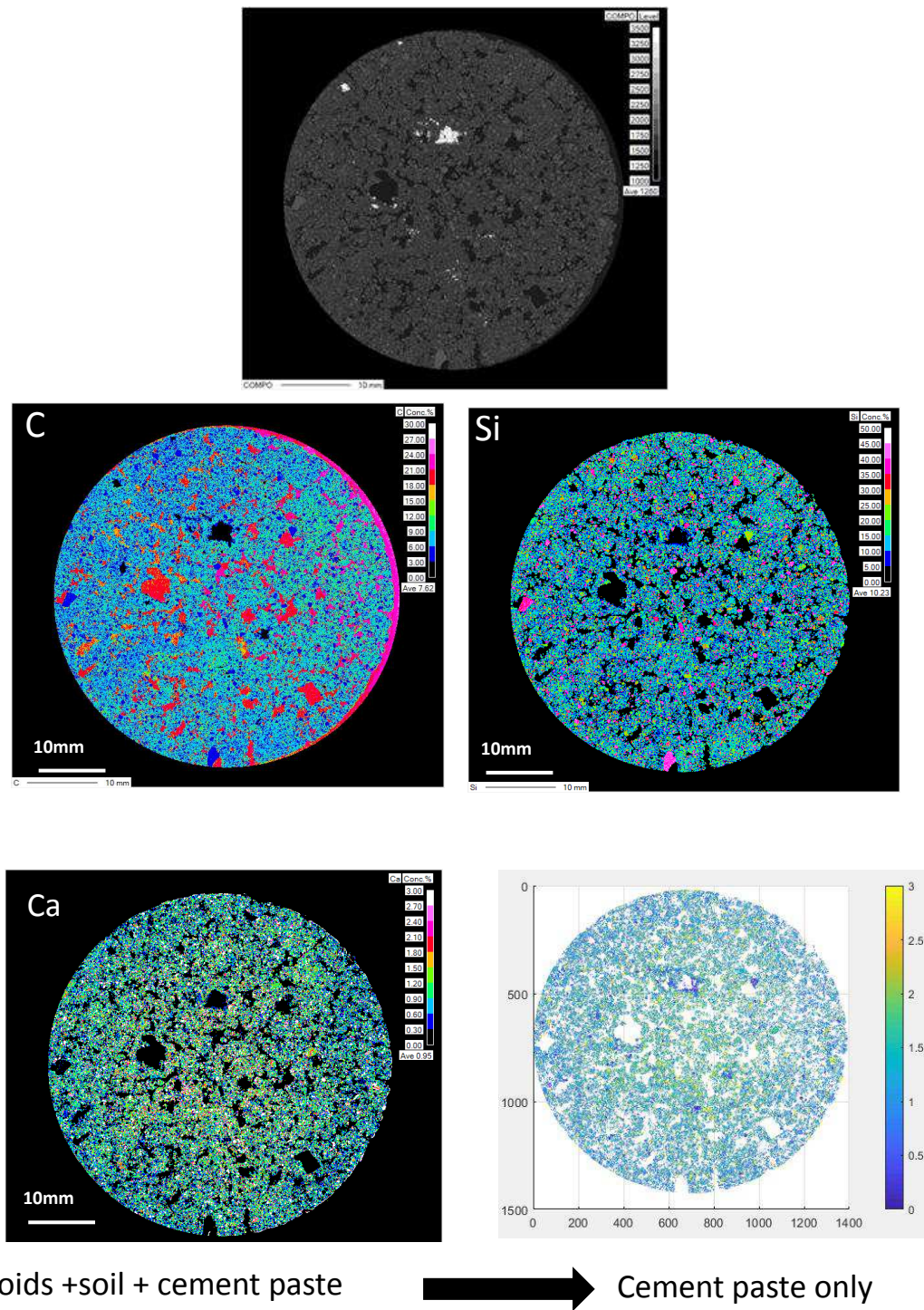


Figure 5:4 Elimination method of voids and soil particles

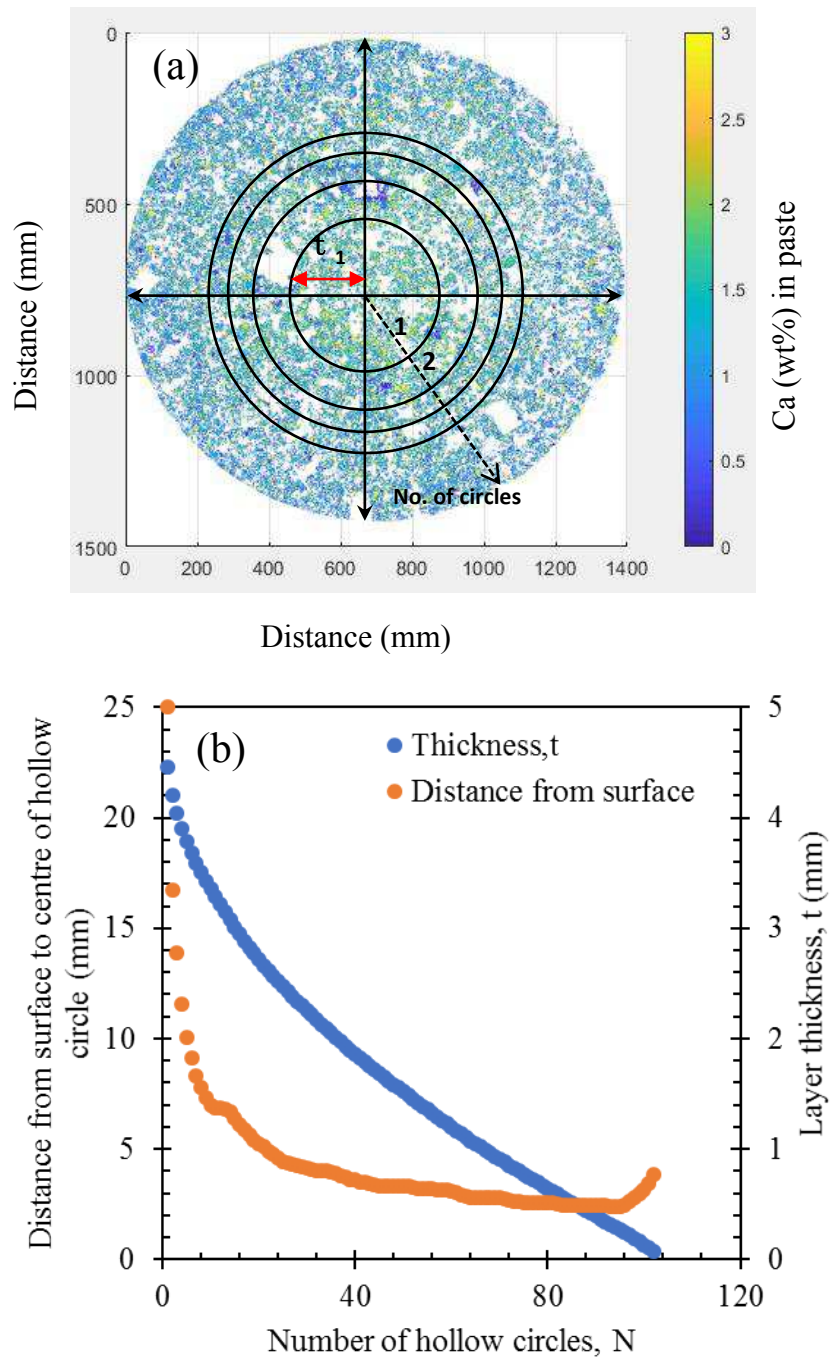


Figure 5.5 Averaging method along radius



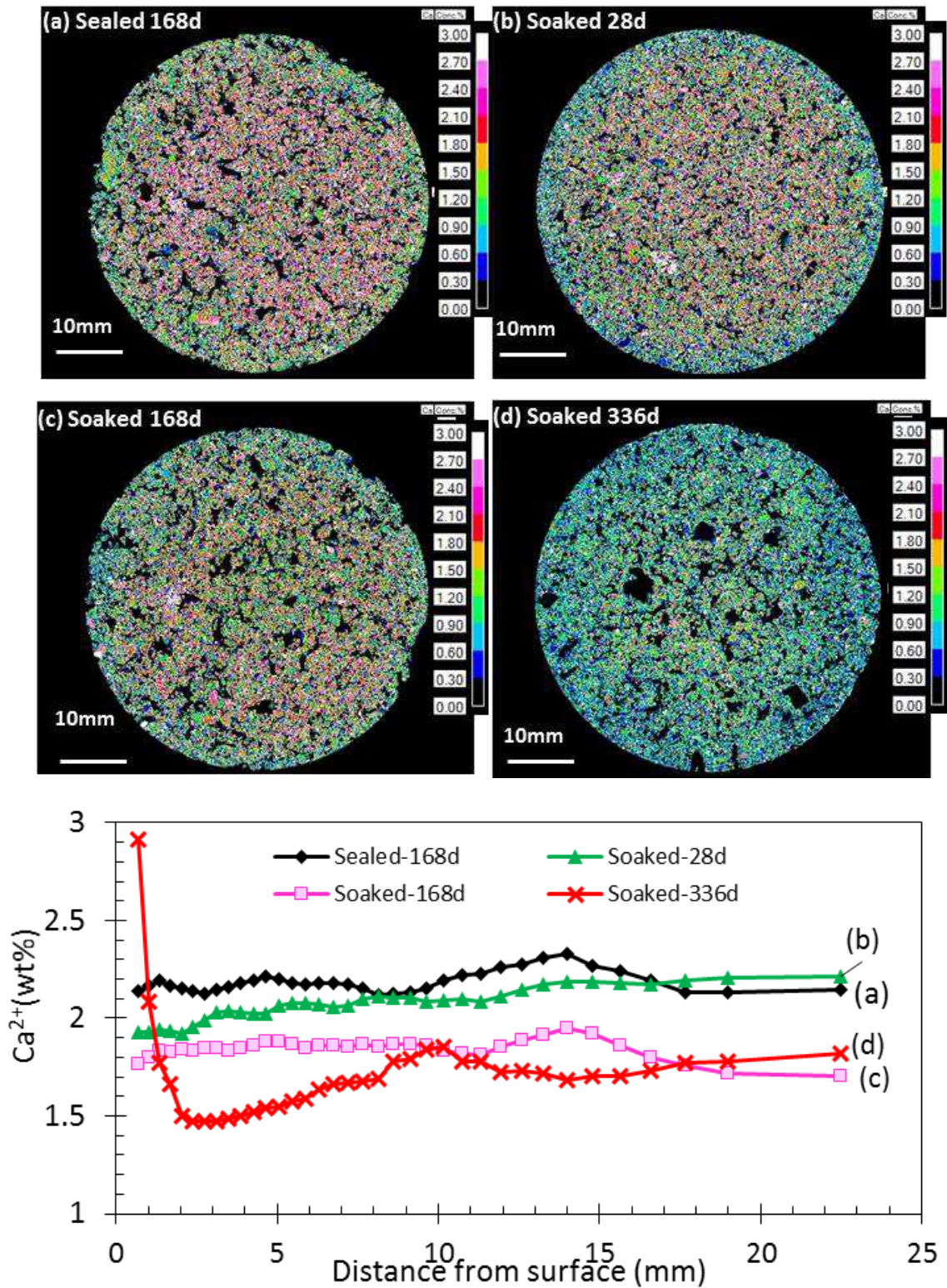


Figure 5:6 EPMA-Ca ion distribution C3.5-Acid (immature)

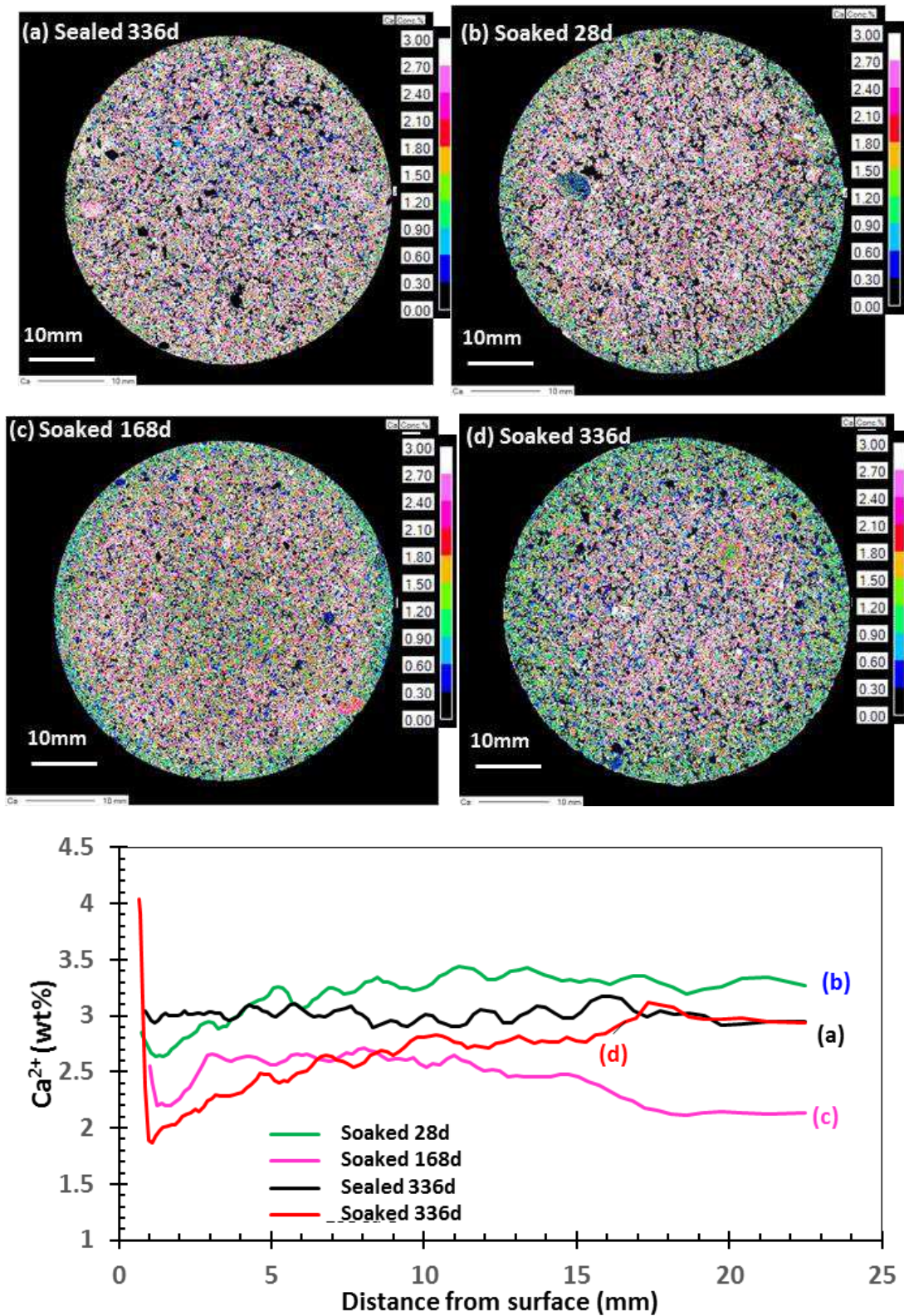


Figure 5:7 EPMA- Ca ion distribution L3.8-Acid (immature)



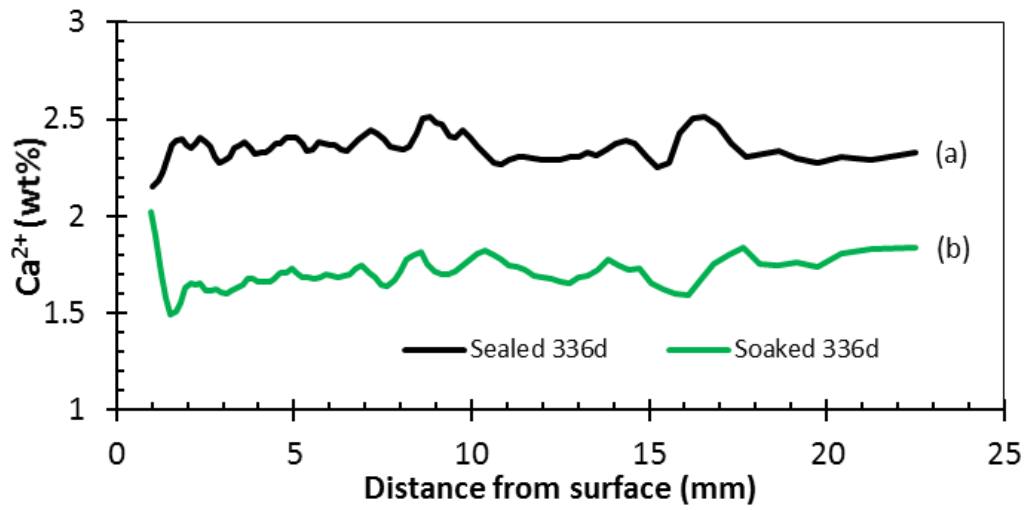
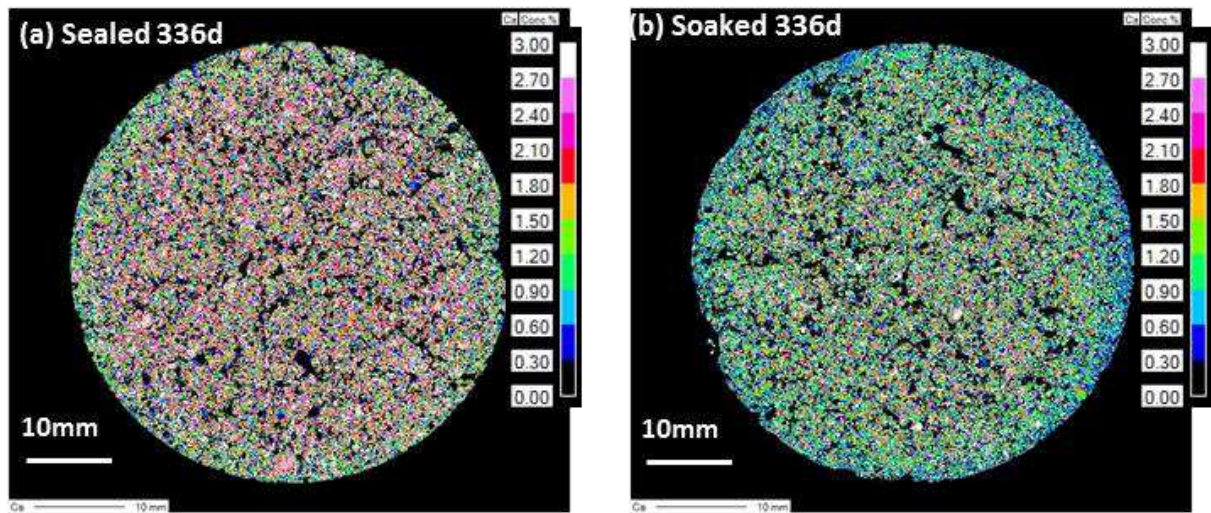


Figure 5:8 EPMA-Ca ion distribution L2.5 Soak acid (immature)

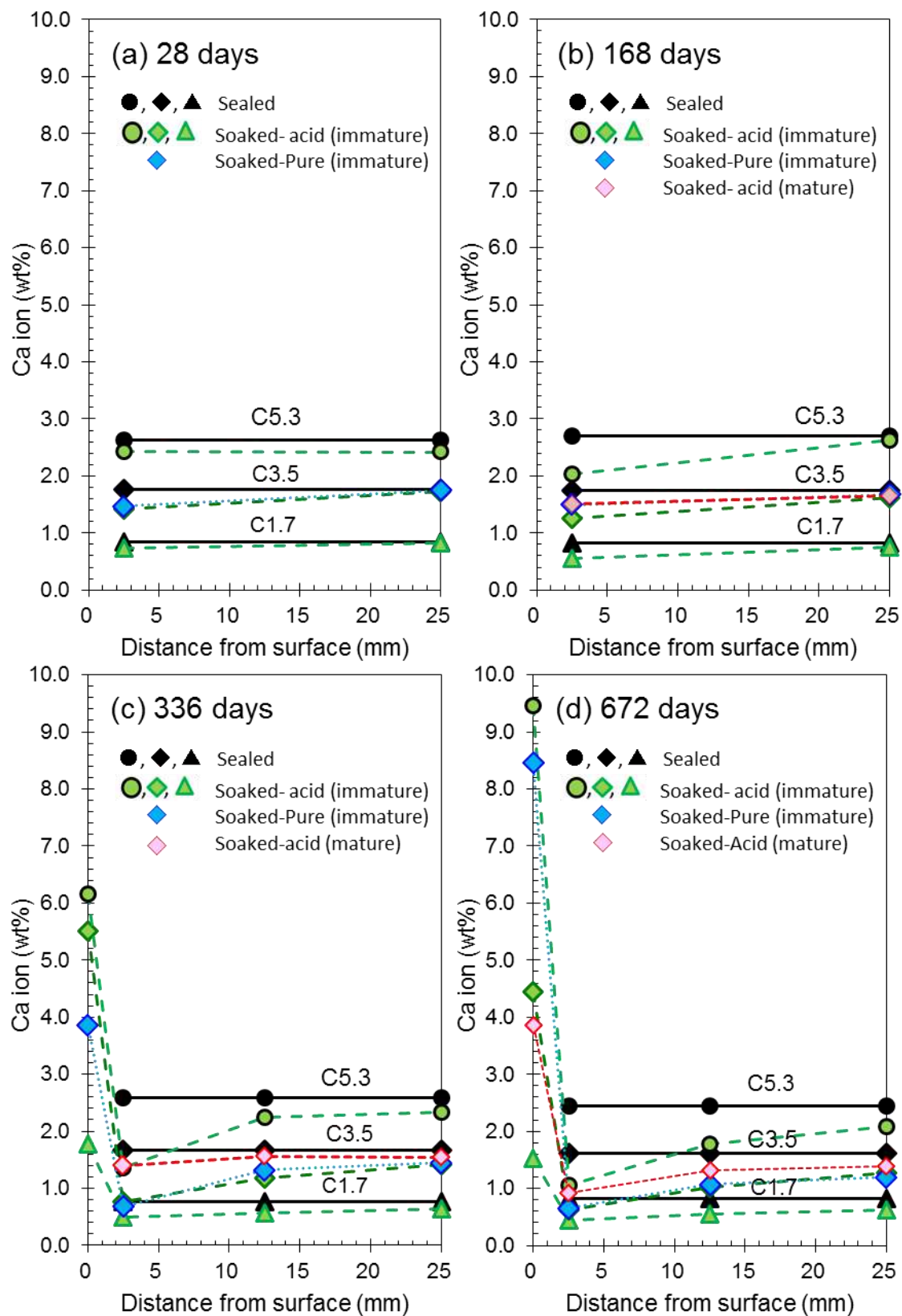


Figure 5:9 XRF-Ca ion distribution-Cement treated soil

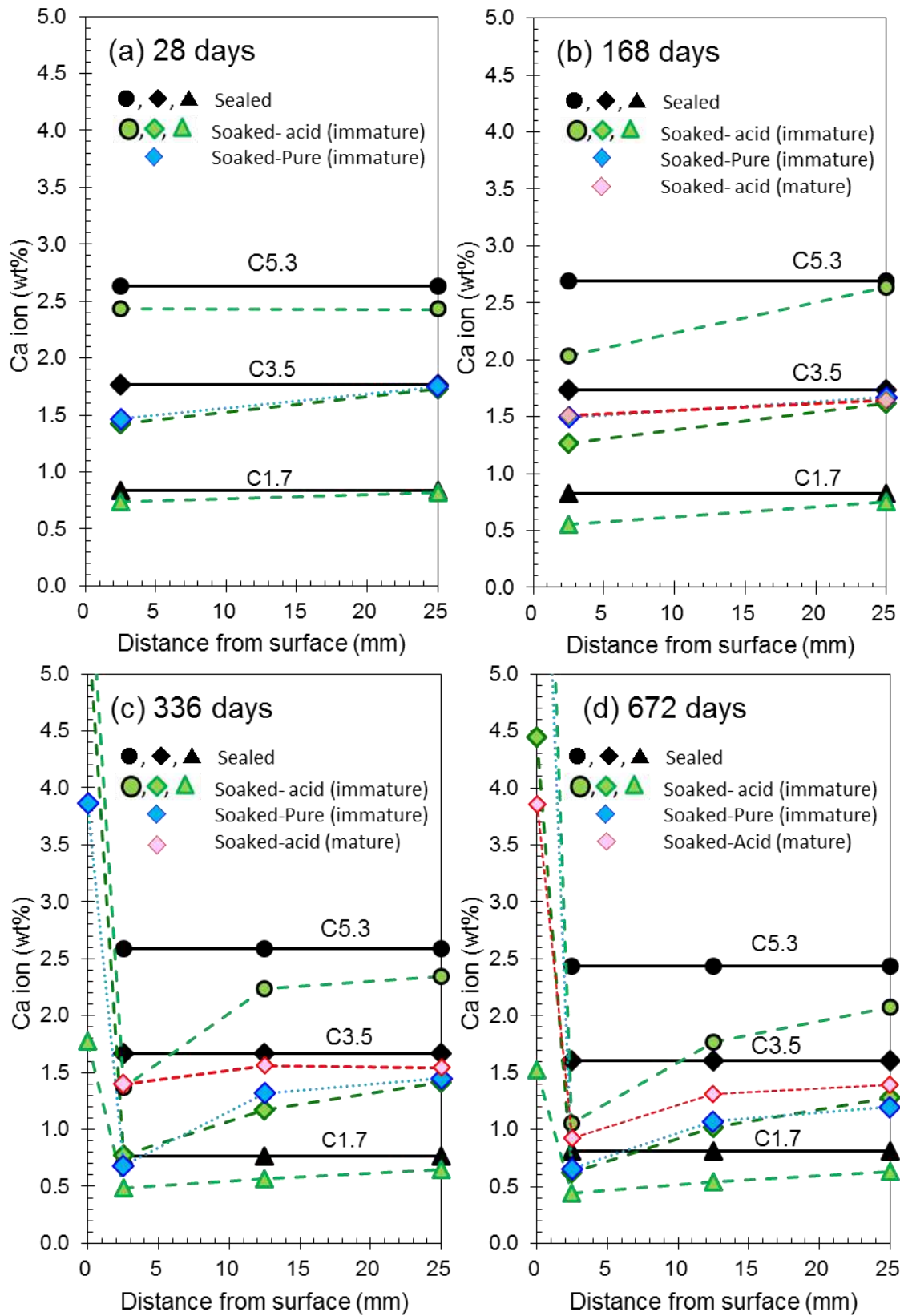


Figure 5:10 XRF-Ca ion distribution- Cement treated soil (change vertical scale)

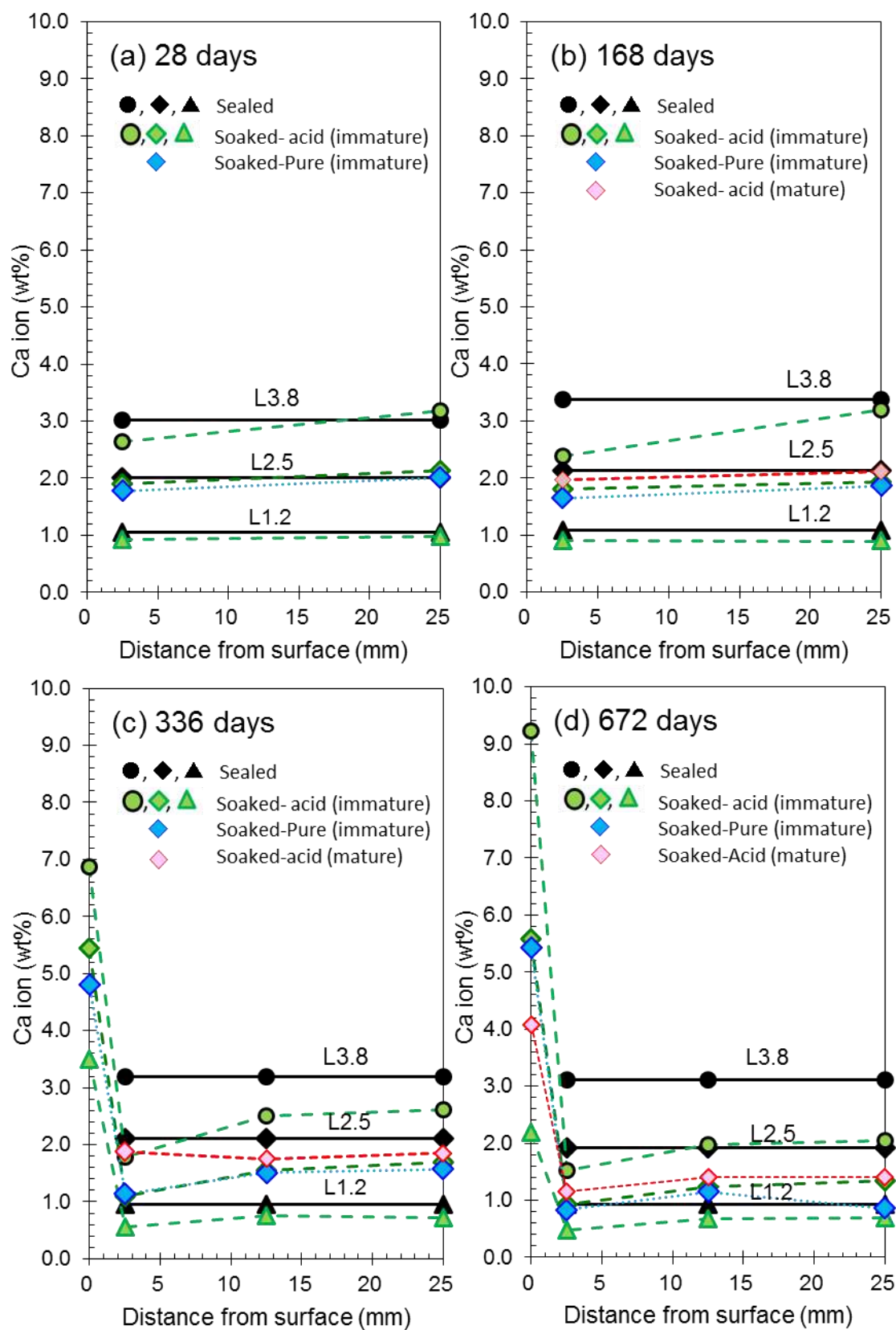


Figure 5:11 XRF-Ca ion distribution-Lime treated soil



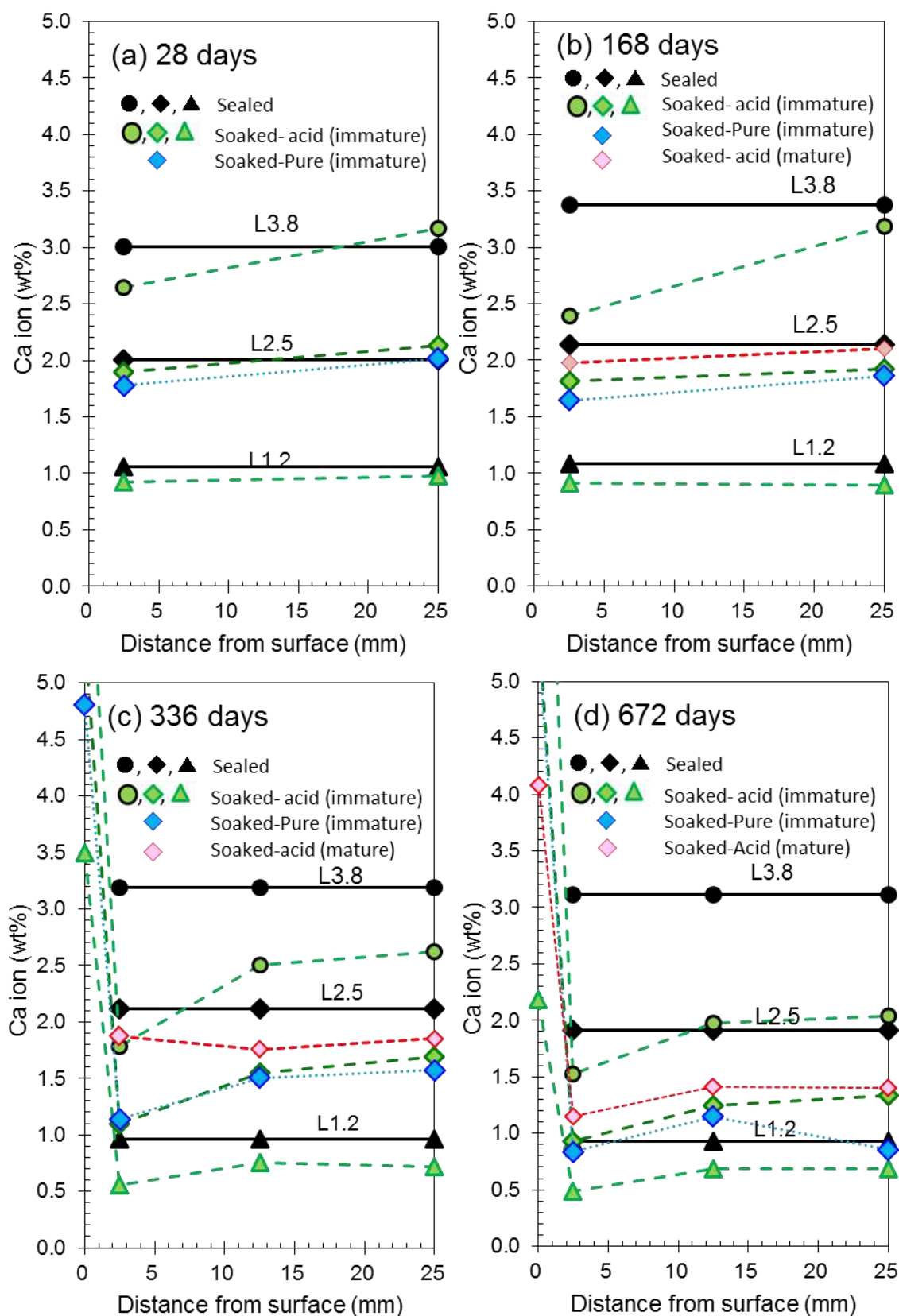


Figure 5:12 XRF-Ca ion distribution- Lime treated soil (change vertical axis)

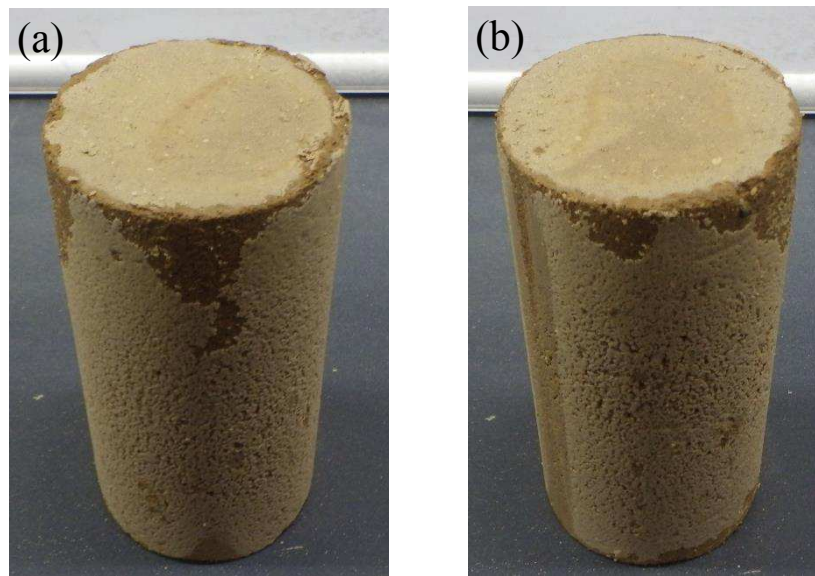


Figure 5:13 Thin  $\text{CaCO}_3$  layer precipitated after 672 days soaking of (a) C 5.3 (b) L3.8

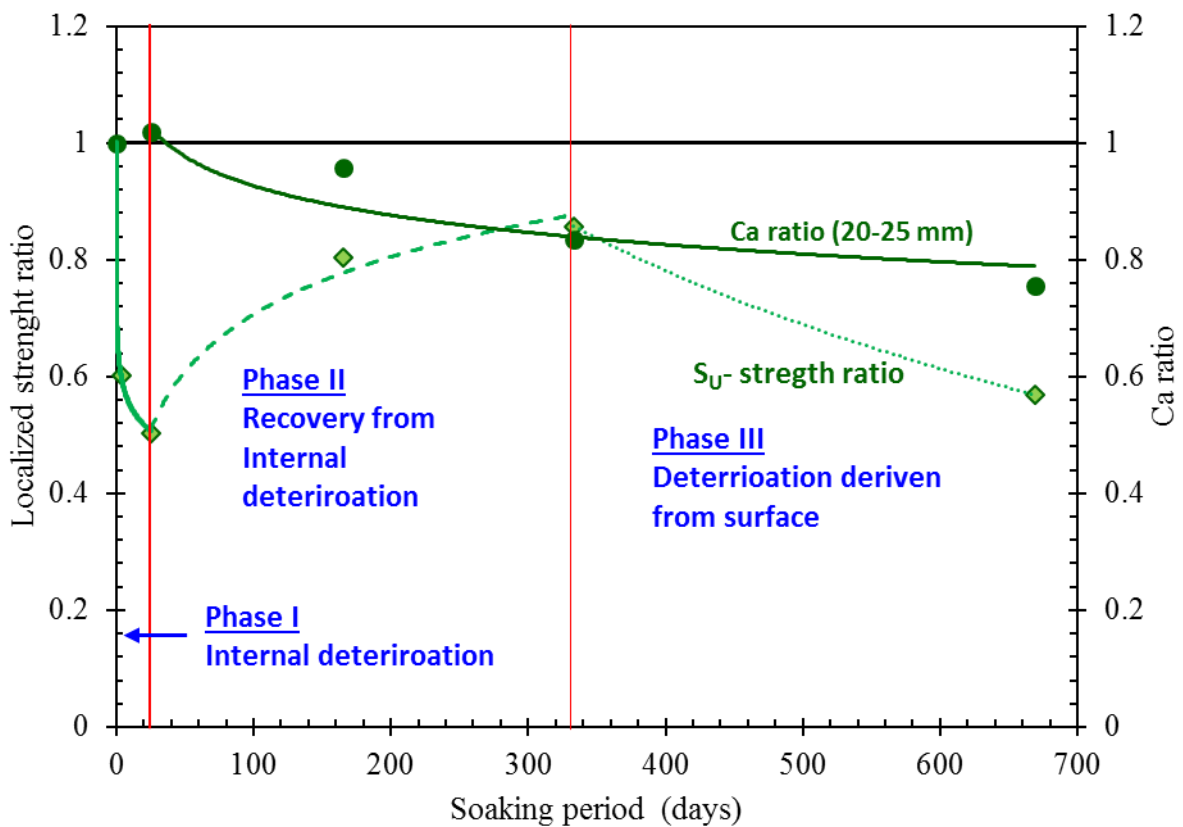


Figure 5:14 Variation of  $S_U$  of C3.5- soak acid (immature)

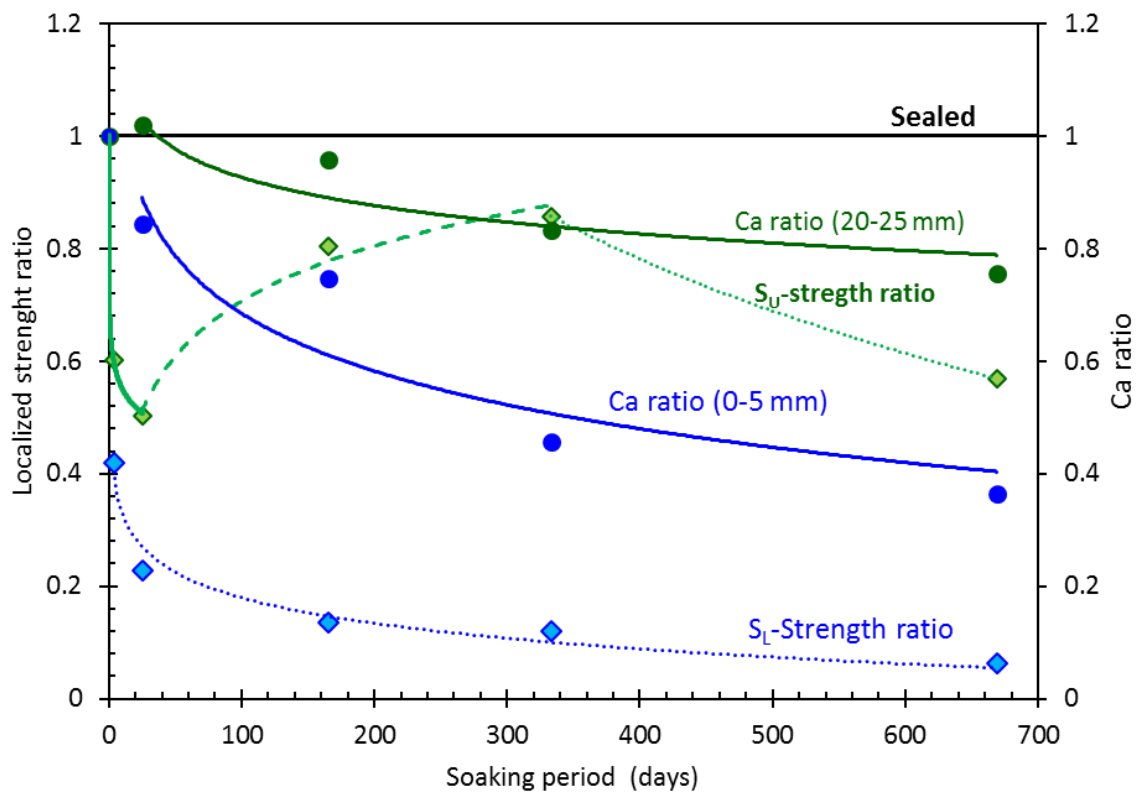


Figure 5:15 Ca ratio and Strength ratio relationship with soaking period- C3.5 acid (immature)

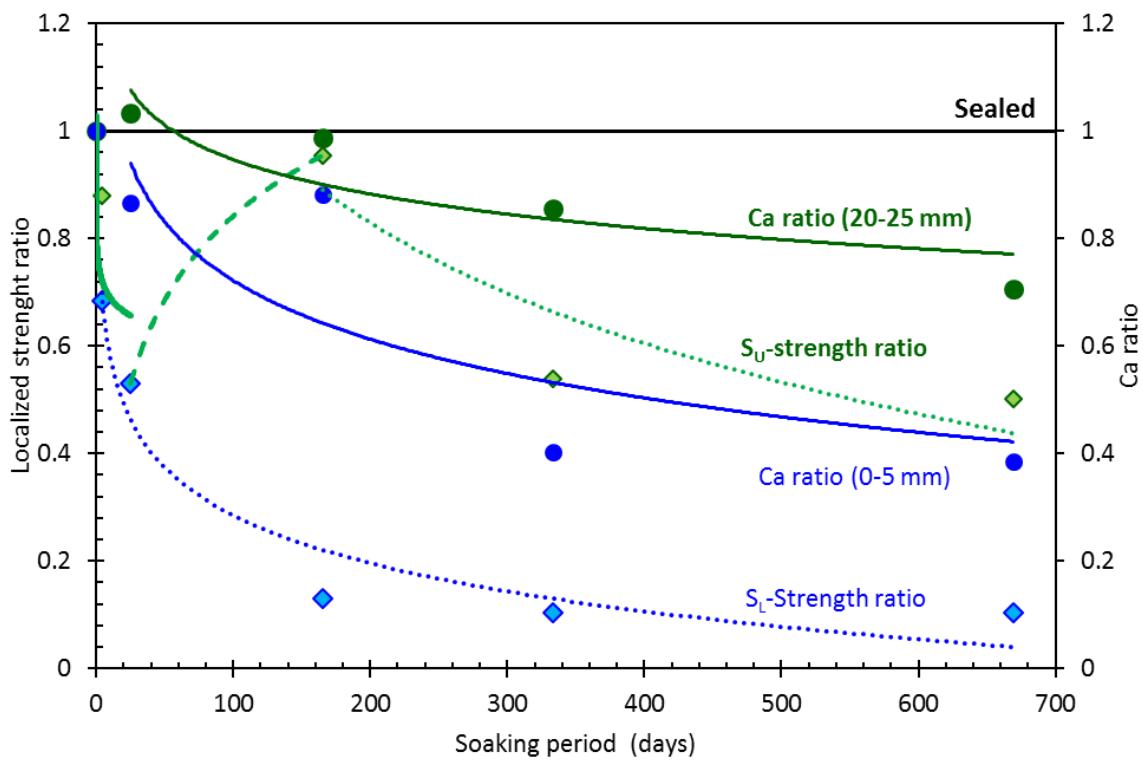


Figure 5:16 Ca ratio and Strength ratio relationship with soaking period- C3.5 Pure (immature)

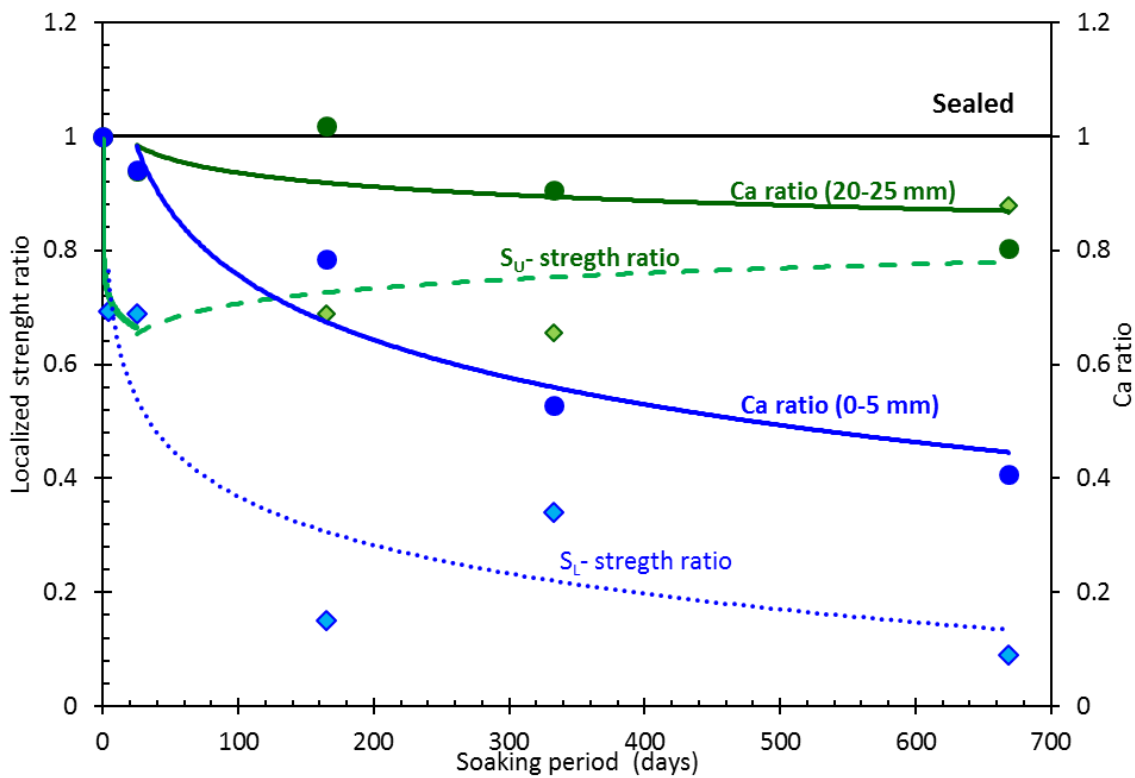


Figure 5:17 Ca ratio and Strength ratio relationship with soaking period- C5.3 Acid (immature)

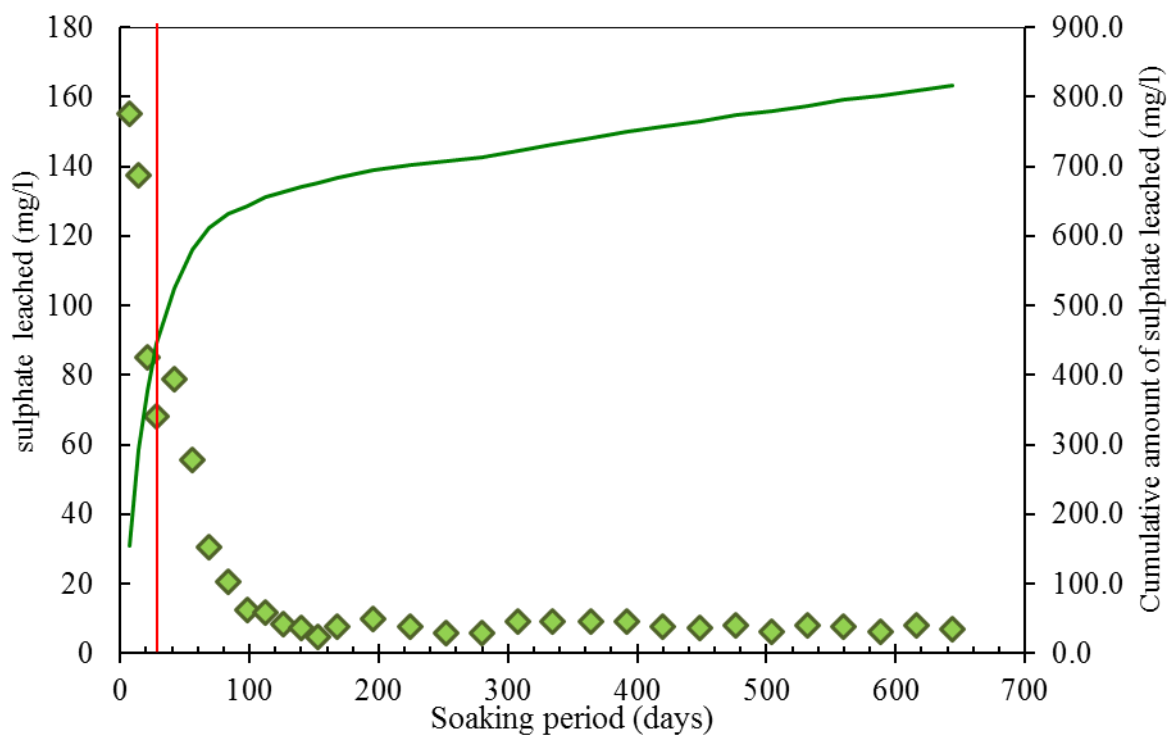


Figure 5:18 Leaching of sulphate ions with soaking period-C3.5 Soak acid (immature)

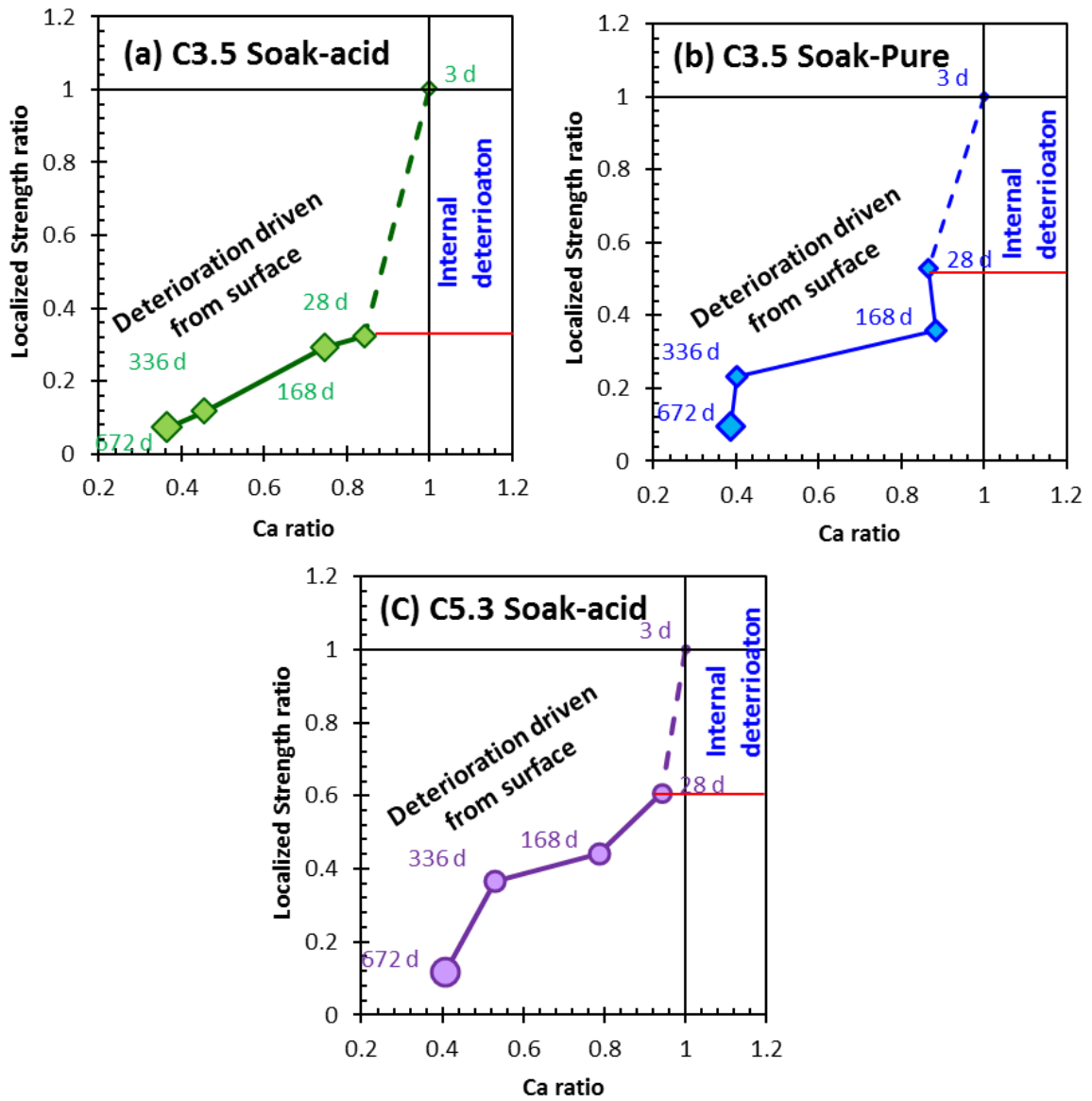


Figure 5:19 Relationship with Ca ratio and  $S_L$  at 0-5mm

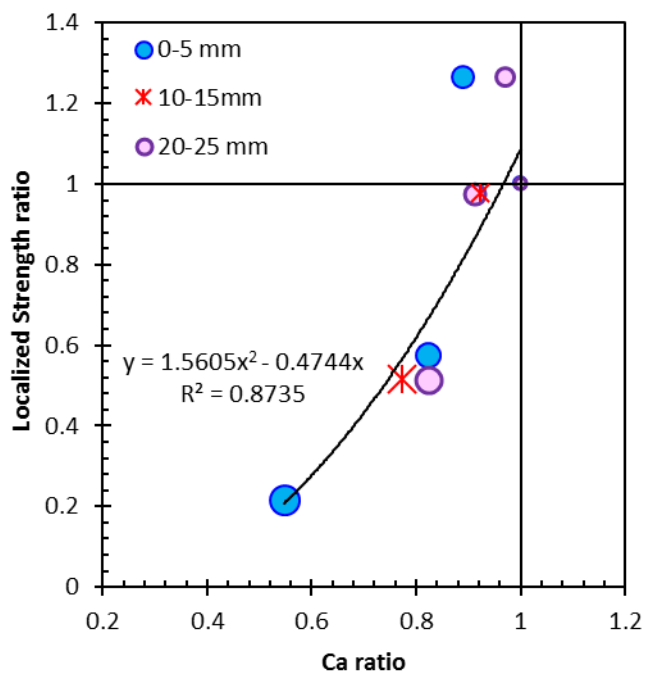
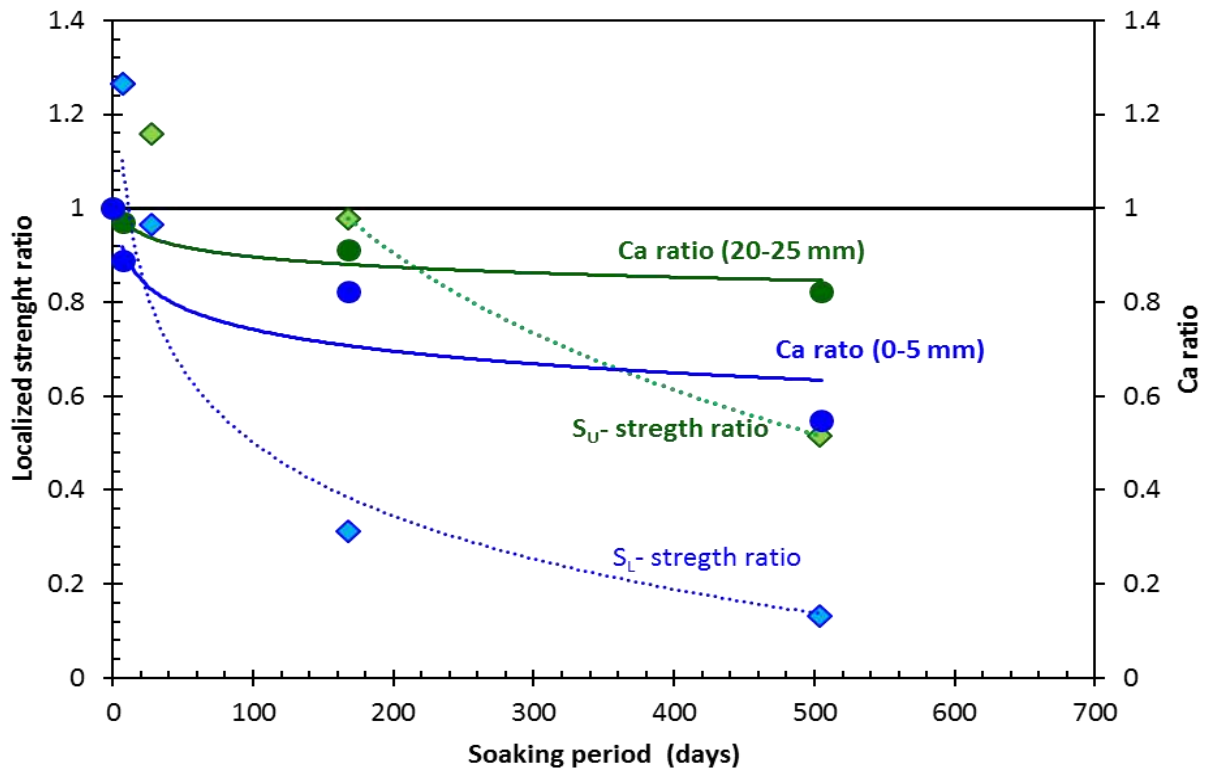


Figure 5:20 Relationship between Ca ratio and localized strength ratio- C3.5 Soaked acid (mature)

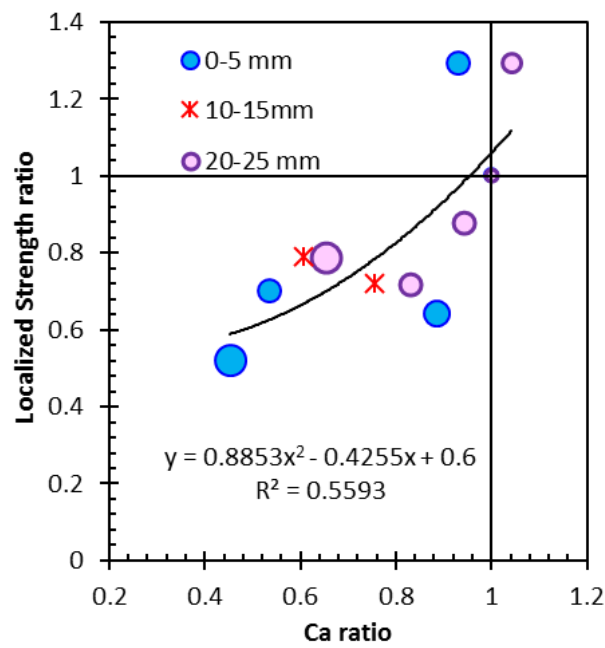
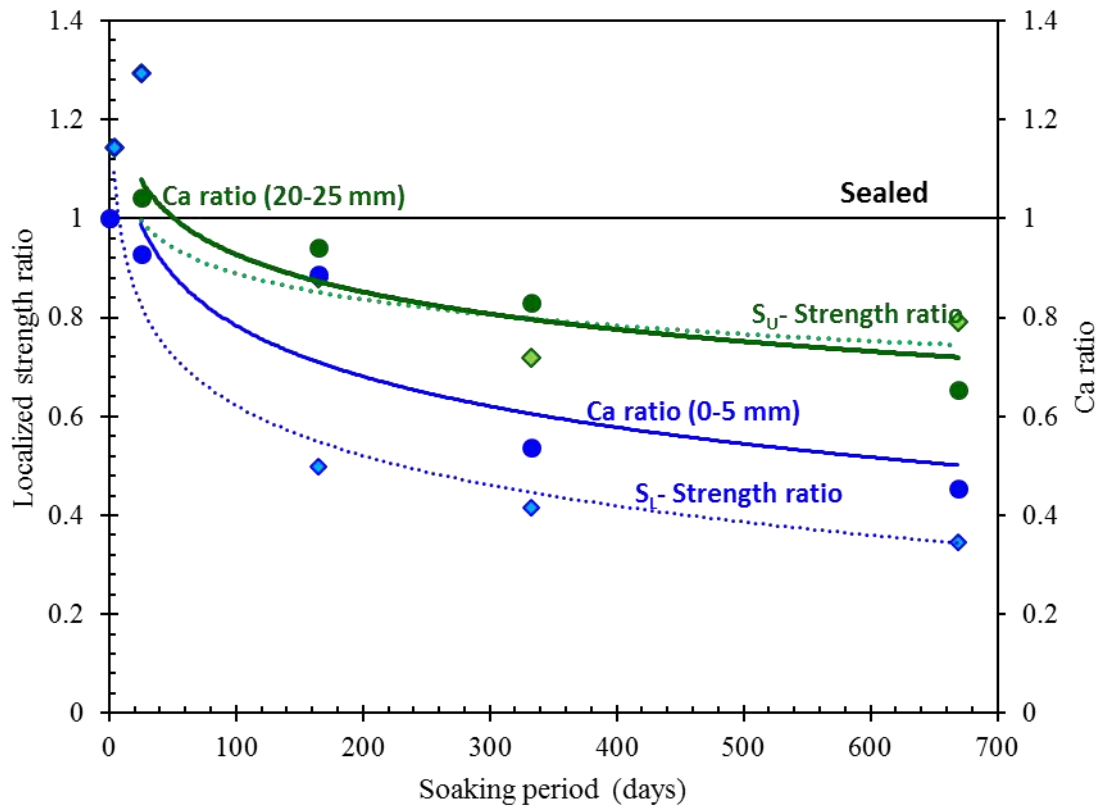


Figure 5:21 L2.5-Soaked acid (immature)

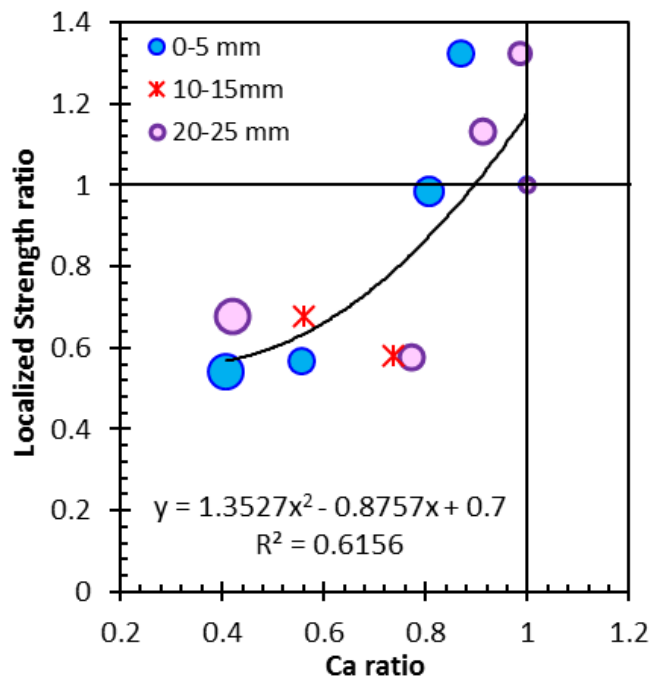
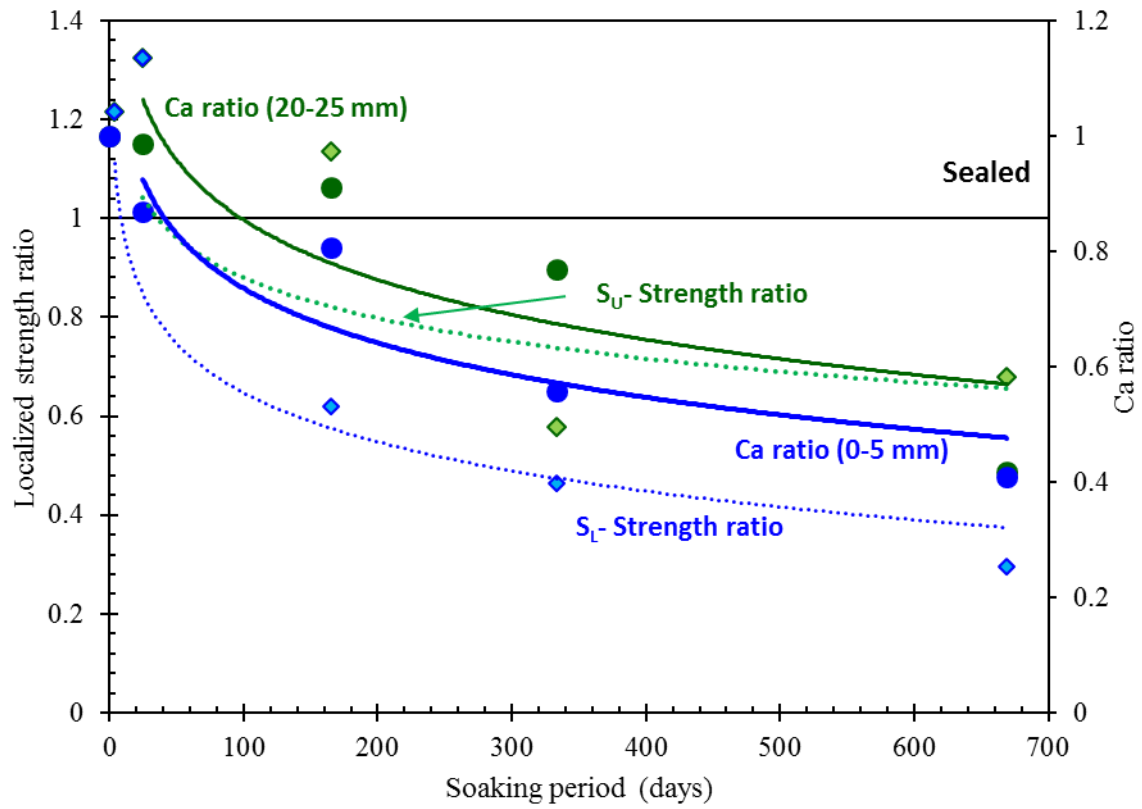


Figure 5:22 L2.5- Soaked Pure (immature)



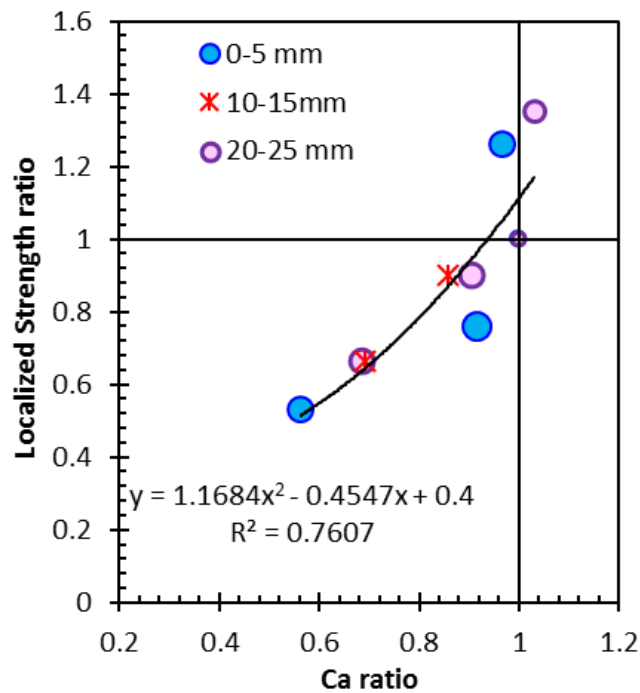
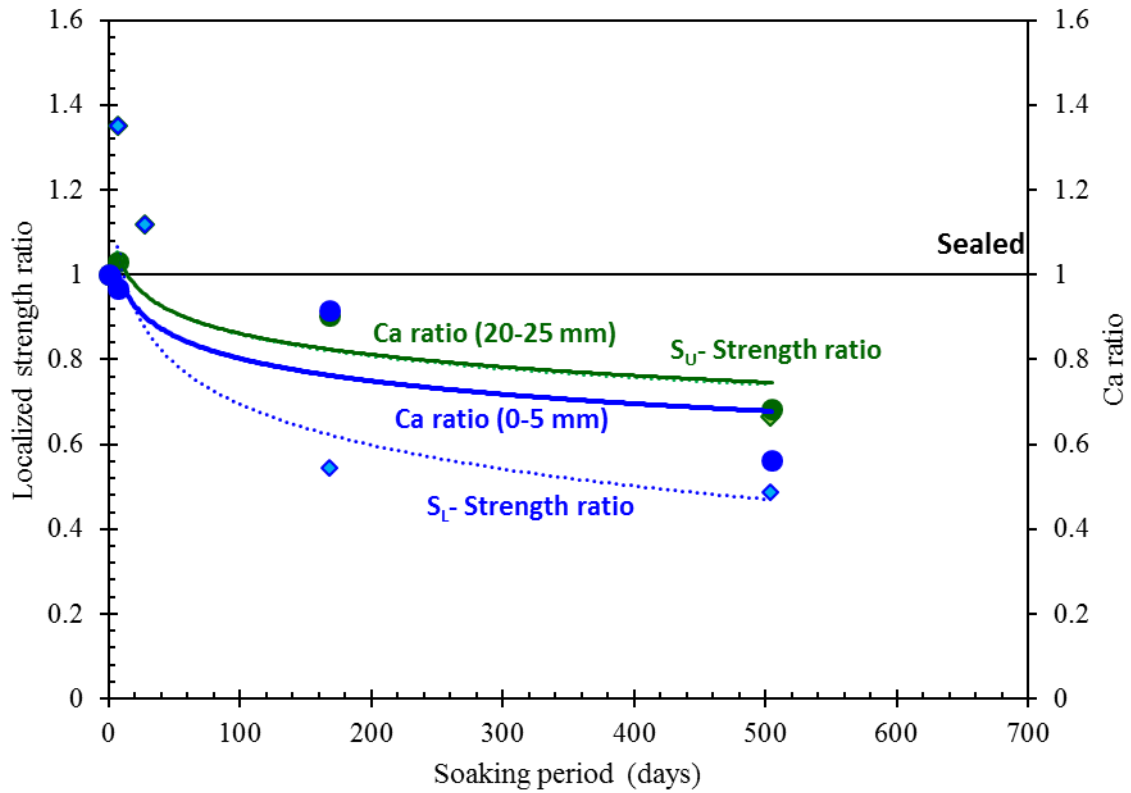


Figure 5:23 L2.5- Soaked acid (mature)

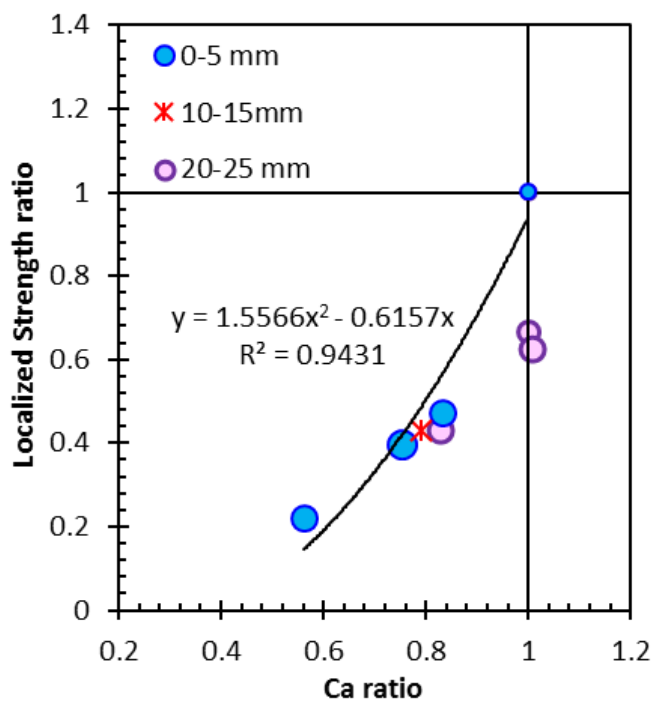
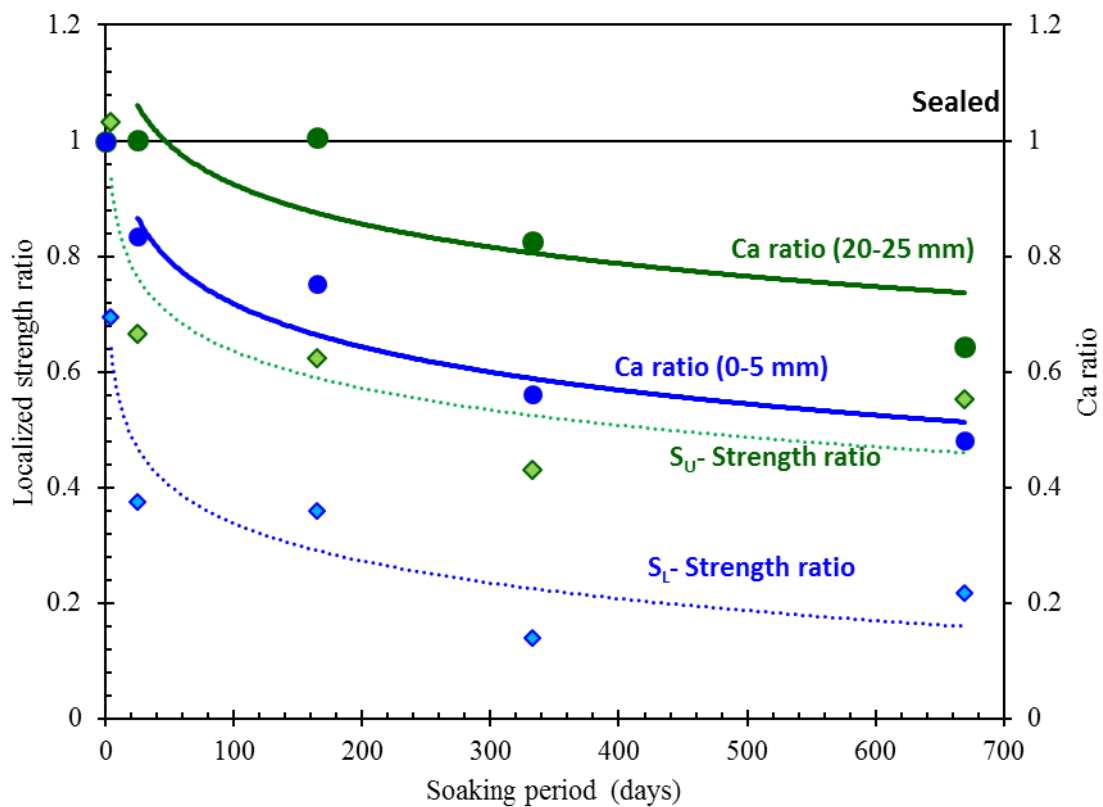


Figure 5:24 L3.8- Soaked acid (immature)

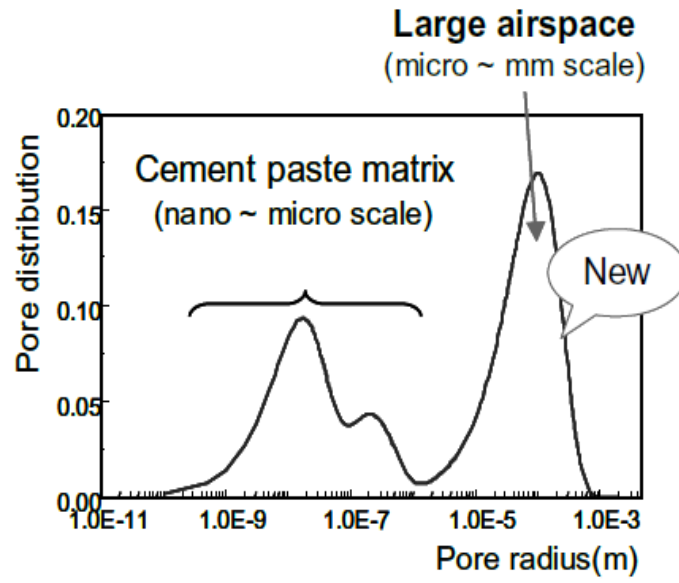


Figure 5:25 Dual pore model

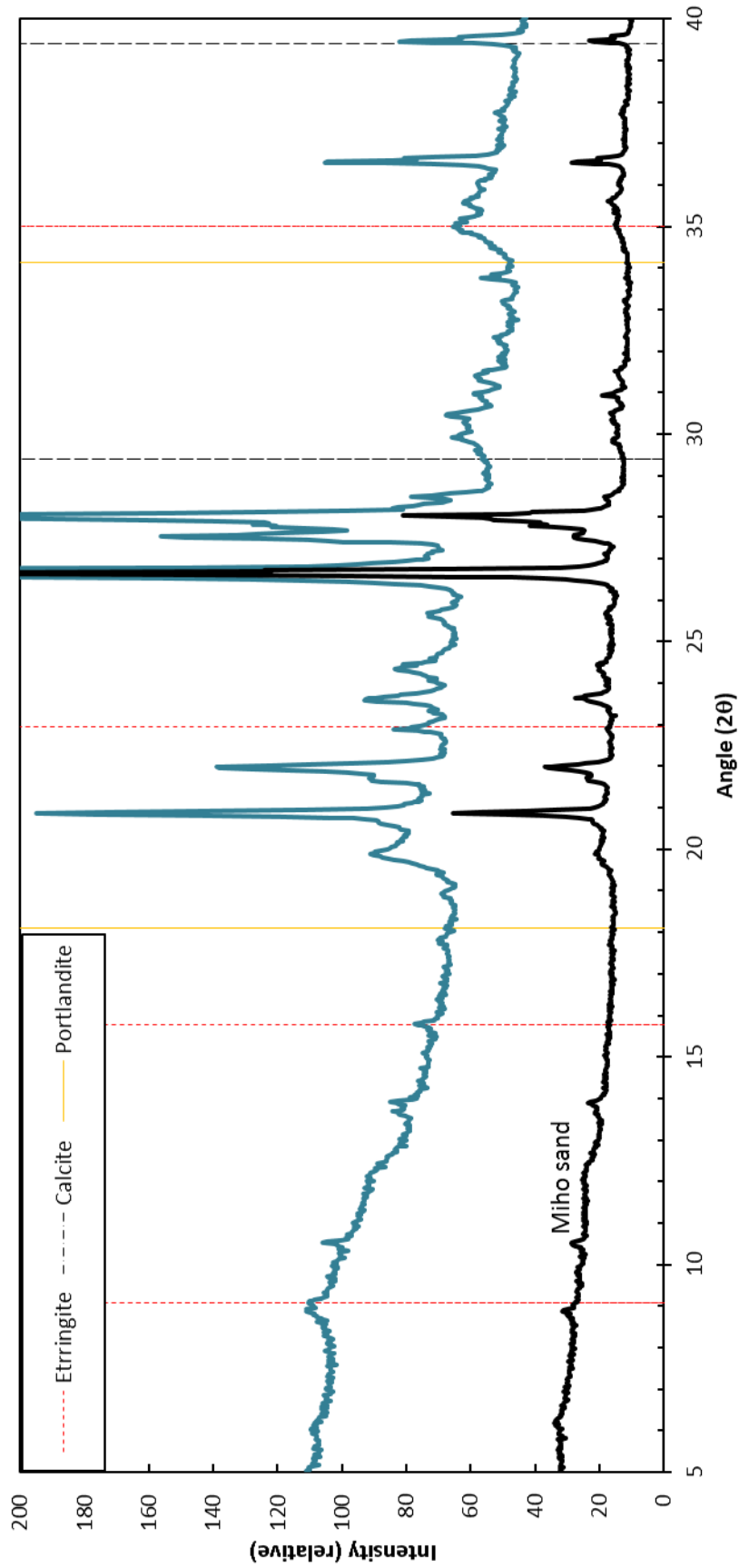


Figure 5:26 XRD results – C 5.3 Sealed-7 days

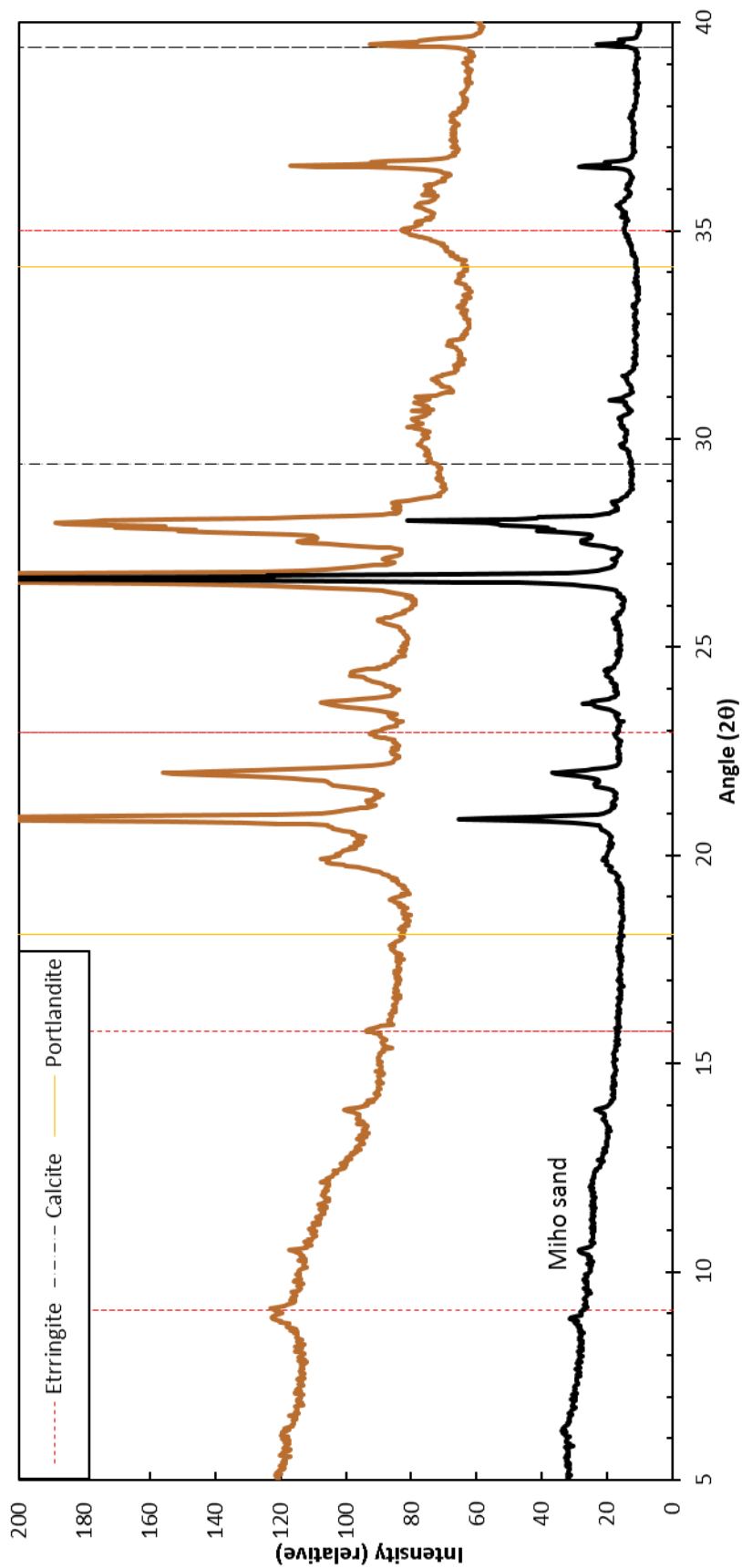


Figure 5:27 XRD results-C5.3 Sealed-28 days

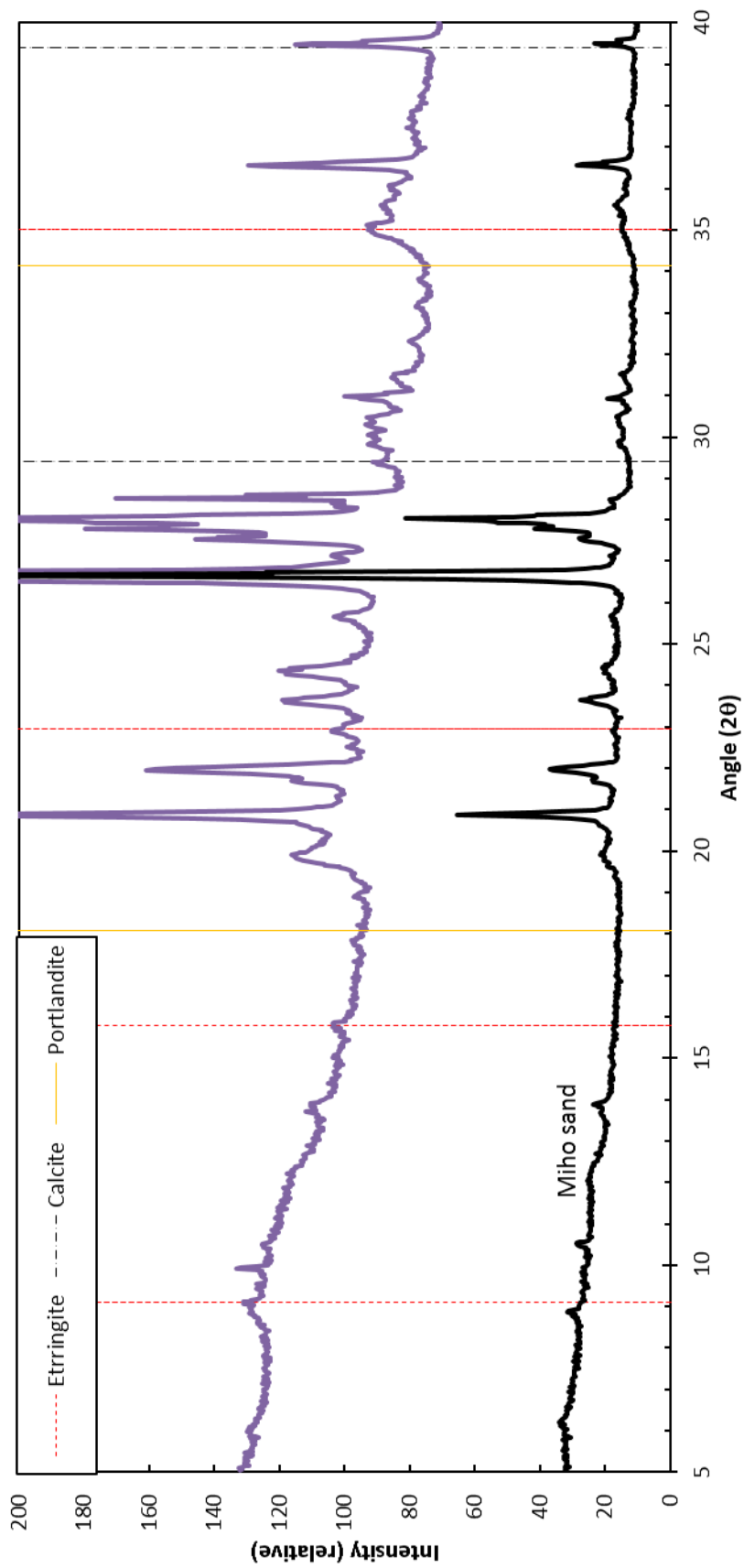


Figure 5:28 XRD results- C5.3 Sealed-672 days

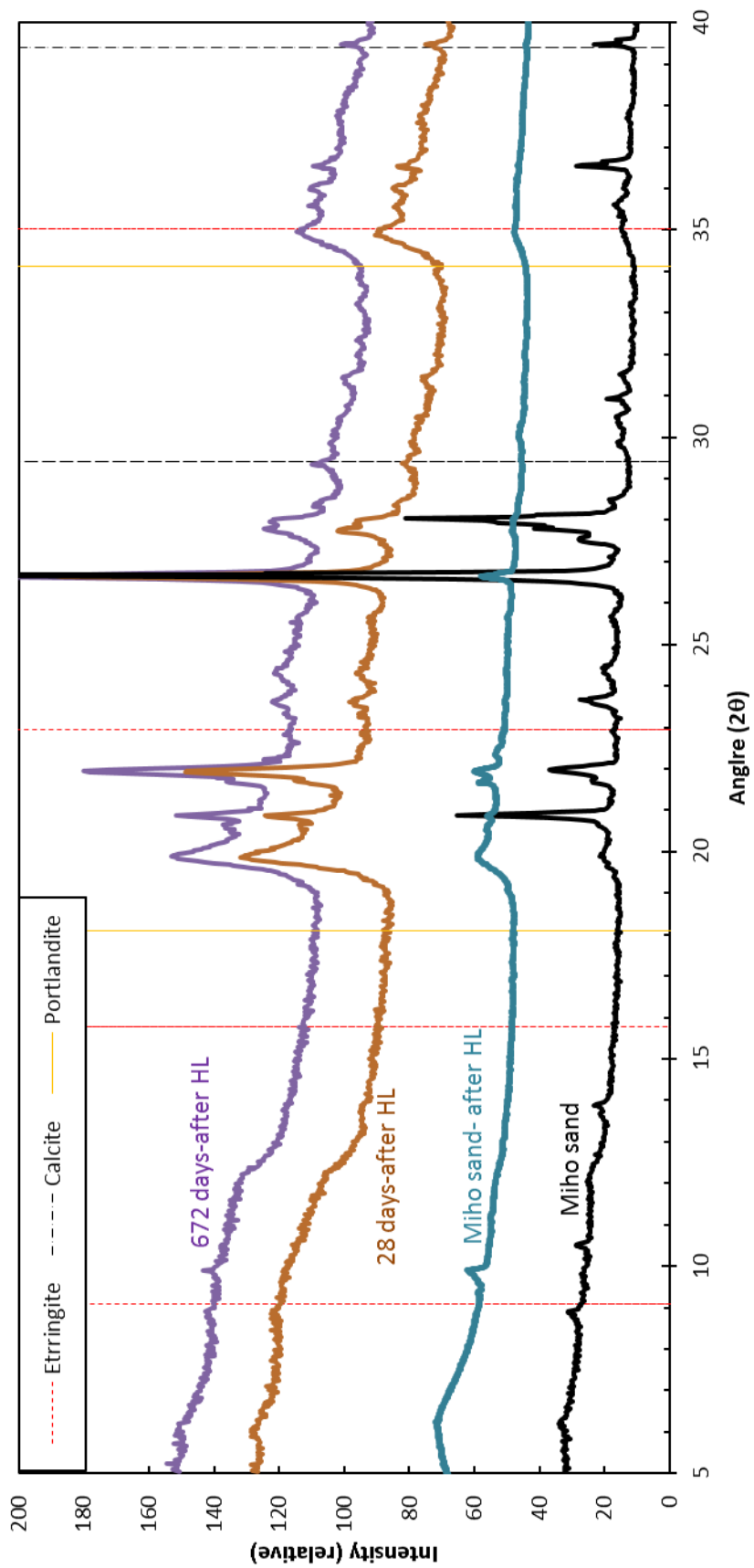


Figure 5:29 XRD results- C5.3 Sealed after applying heavy liquid treatment

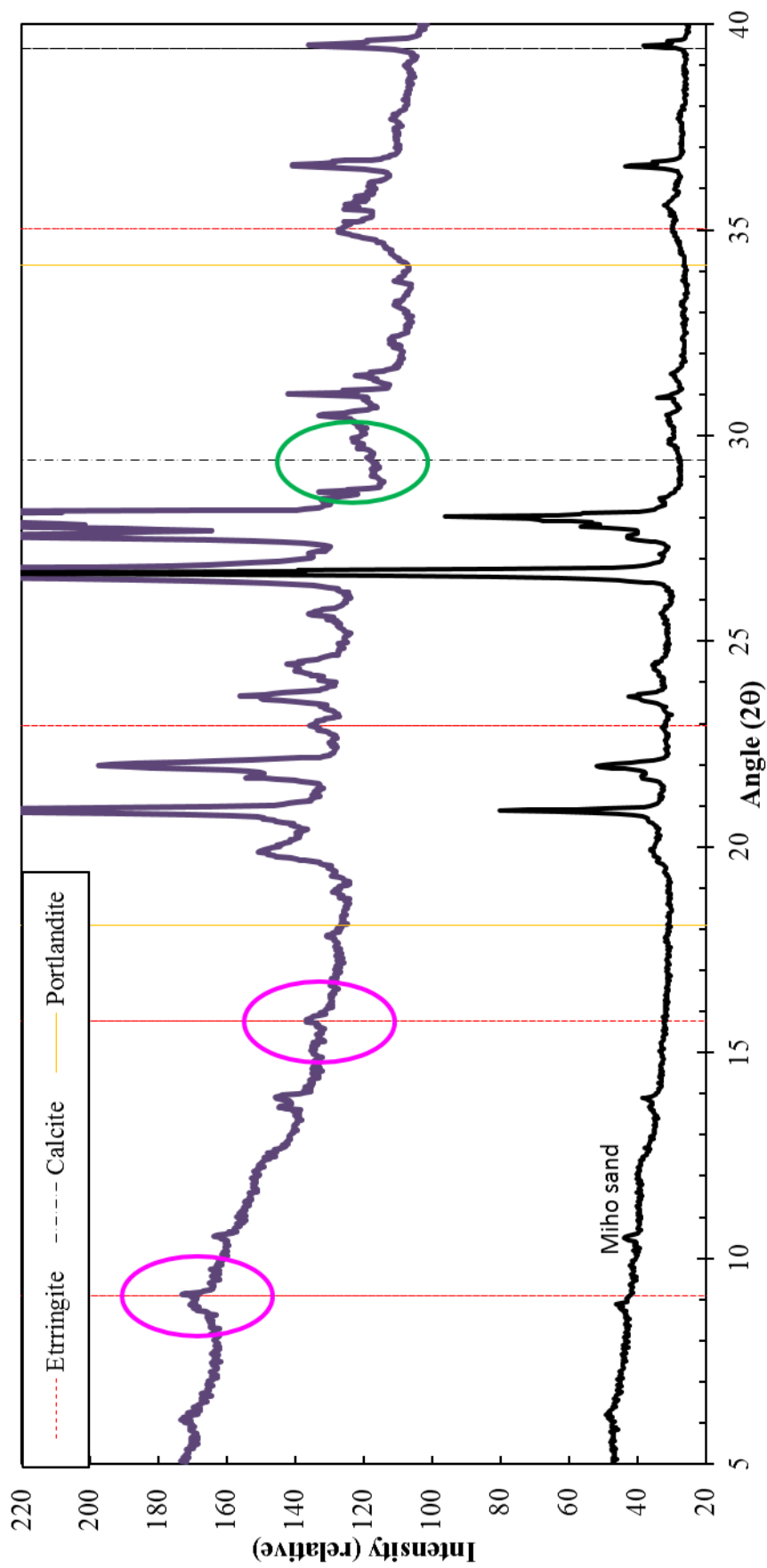


Figure 5:30 XRD results- C5.3 Soaked acid (immature) -672 days(20-25mm)



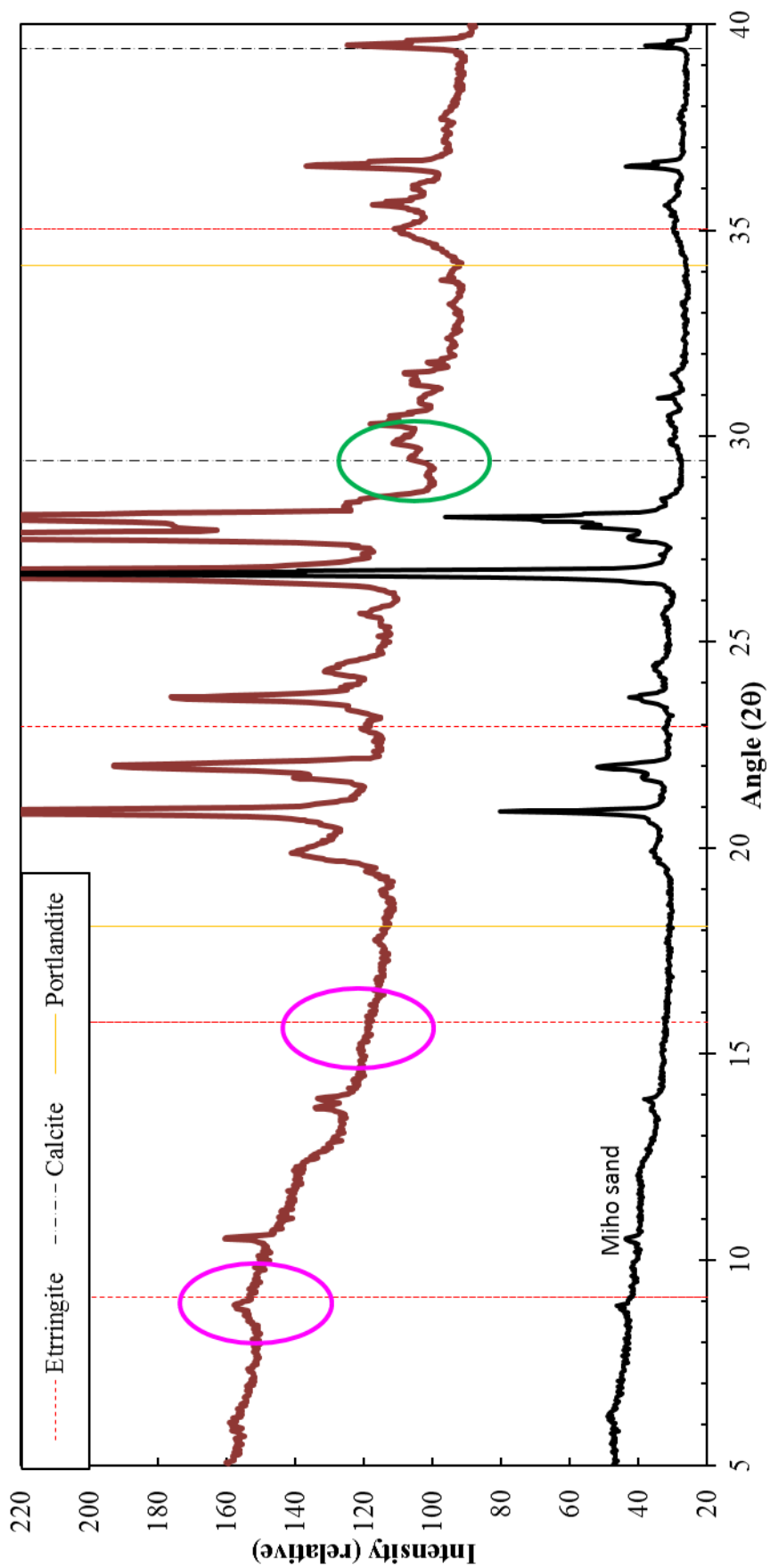


Figure 5.3: XRD results- C5.3 Soaked acid (immature) -672 days (0-5mm)

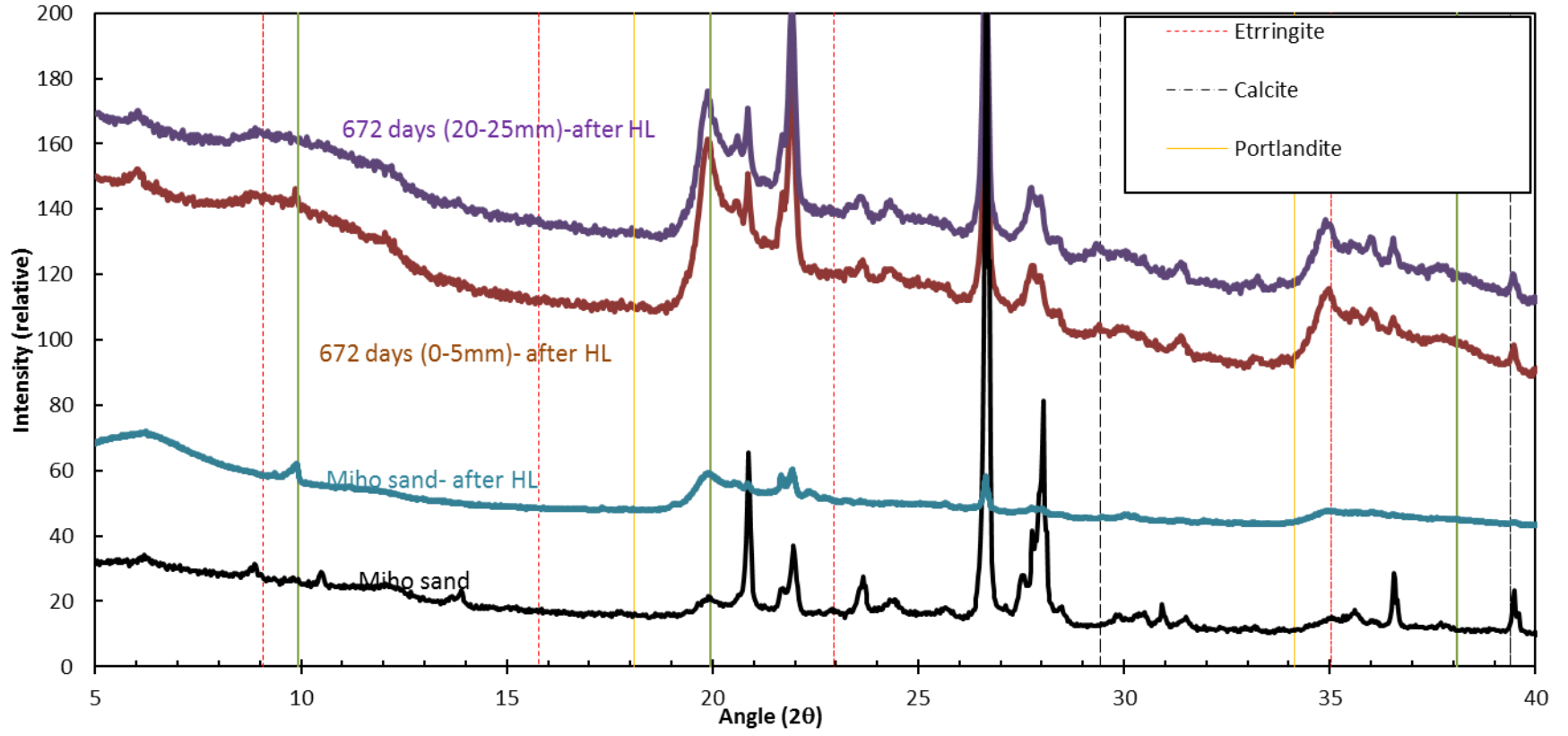


Figure 5:32XRD results- C5.3 Soaked acid (immature) -672 days (0-5mm), (20-25mm)-after heavy liquid treatment

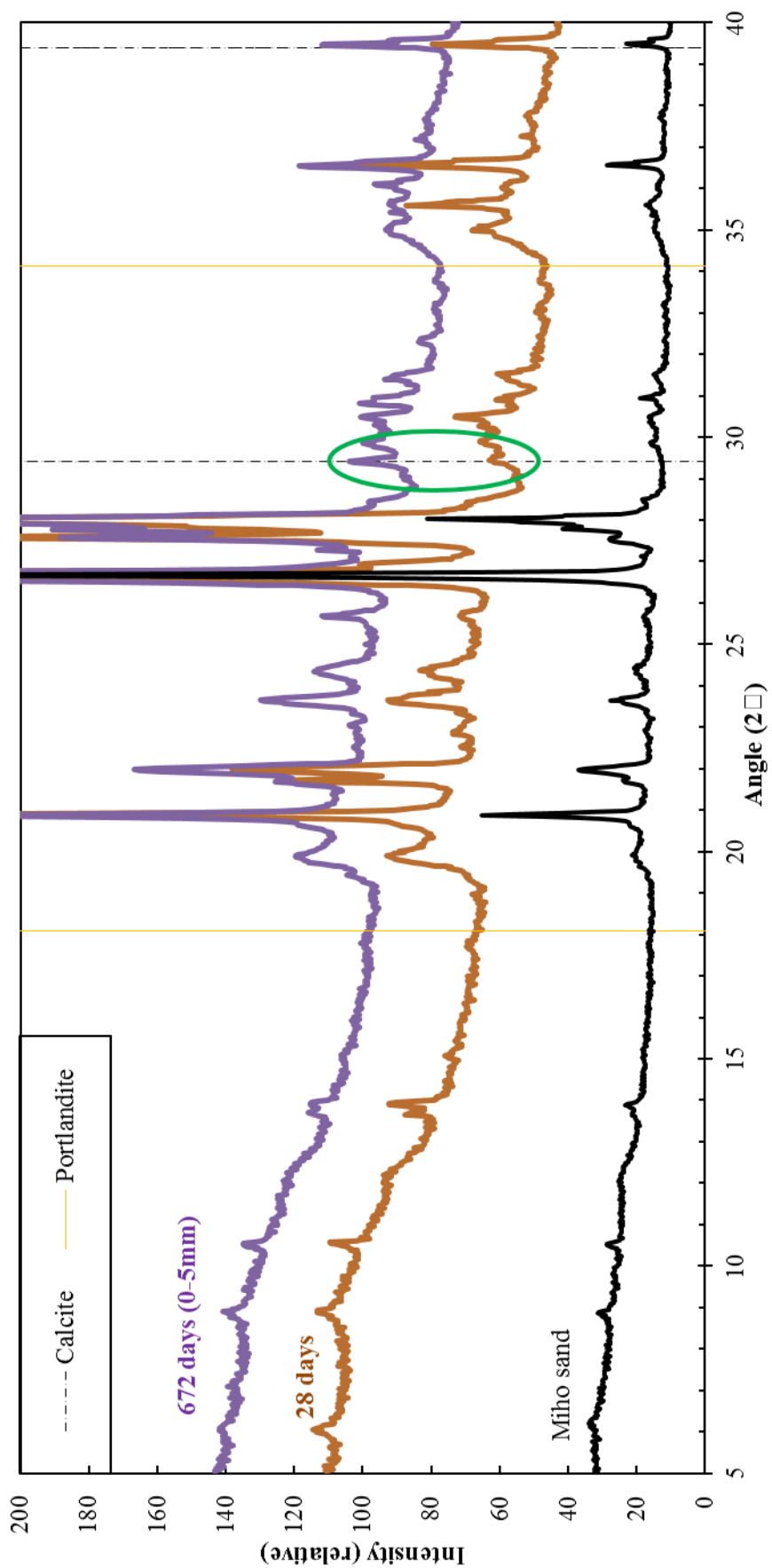


Figure 5:33 XRD results-L3.8 Sealed

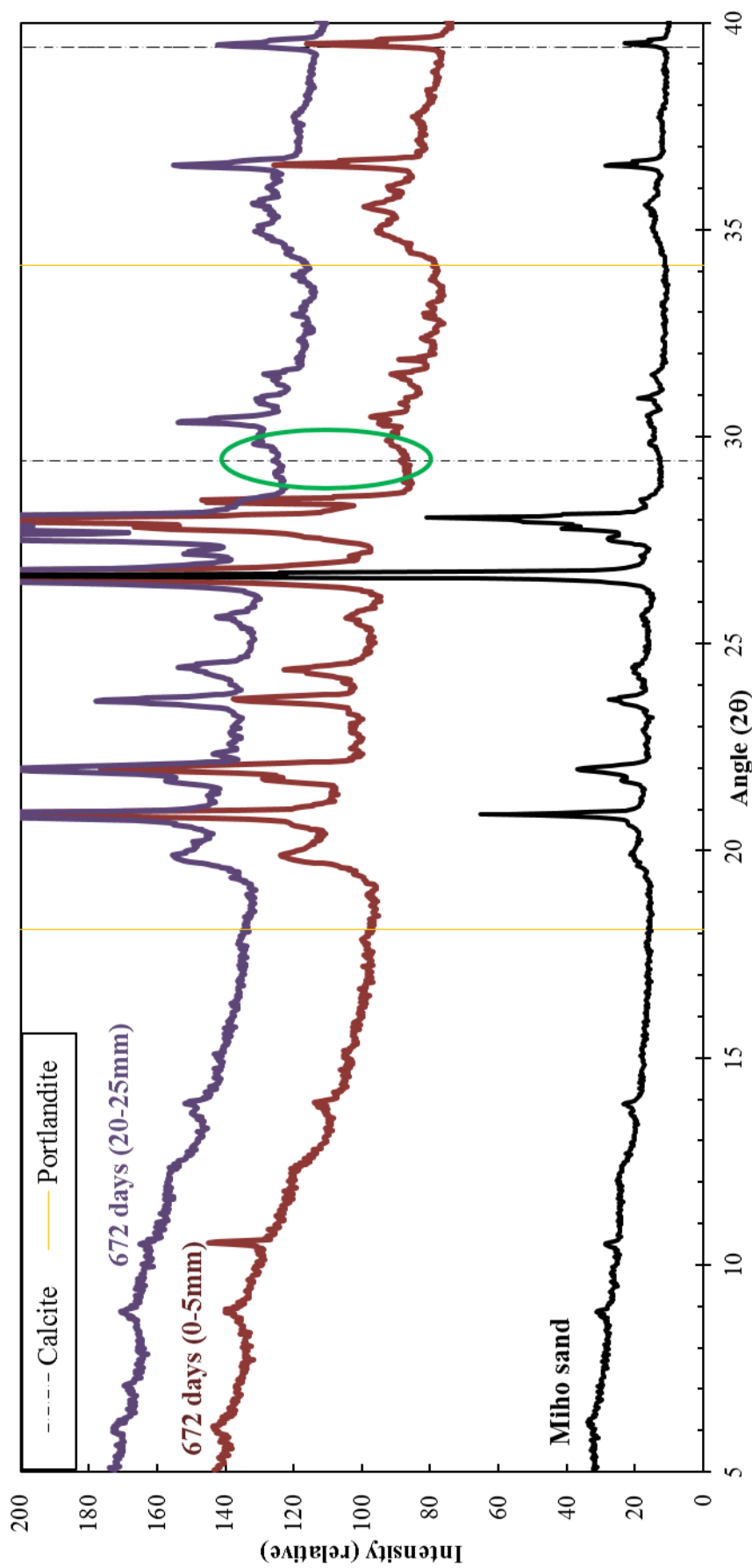


Figure 5:34 XRD results- L3.8 Soaked

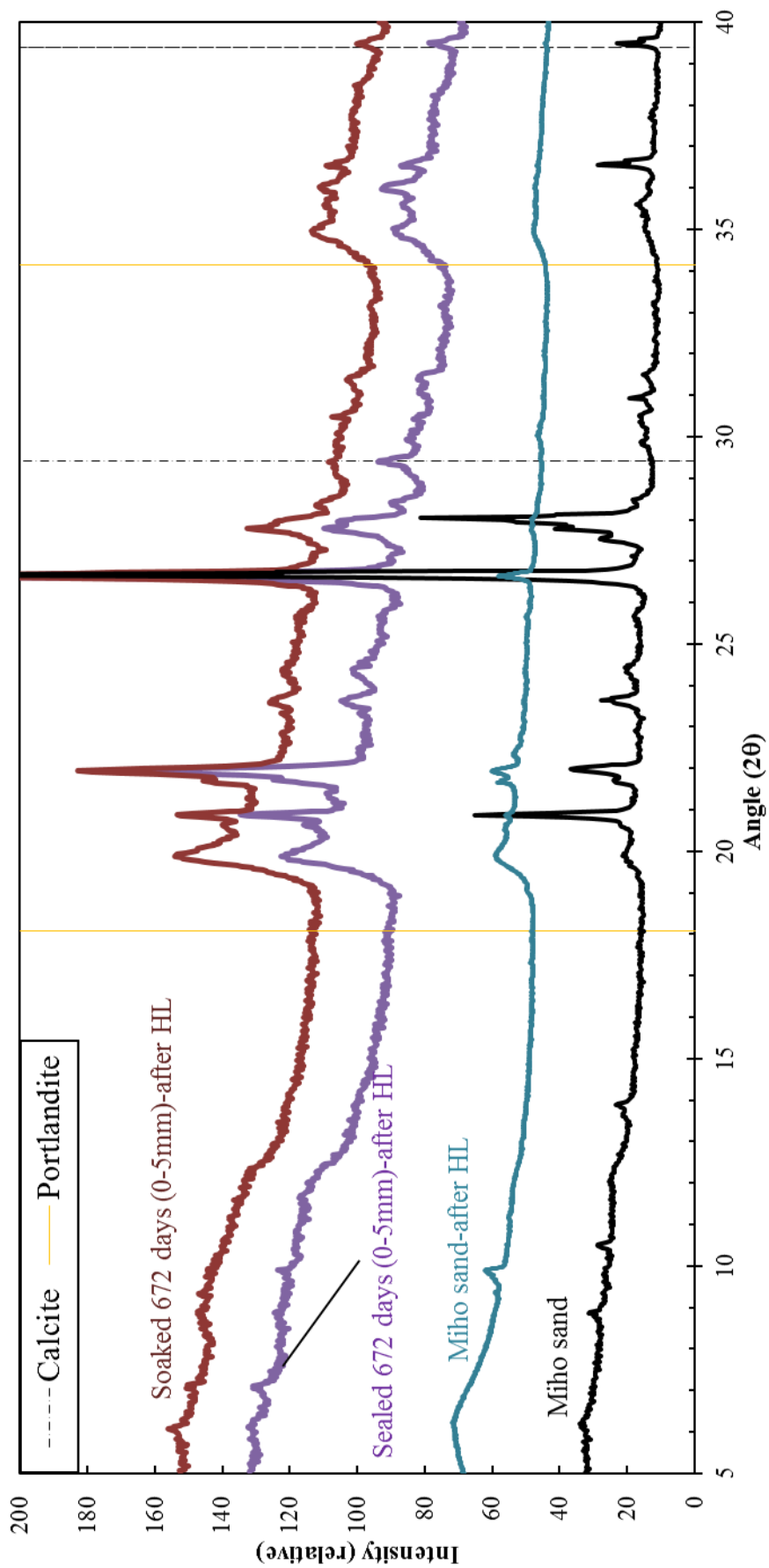


Figure 5:35 XRD results- L3.8 after applying heavy liquid treatment

## **6 Prediction methodology for long term durability of improved surplus soils with low binder contents**

### **6.1 Introduction to the proposed methodology**

In this study, an actual surplus soil called Miho sand was improved as cement treated soil and lime treated soil while using three different binder contents for each type of binder. Miho sand contained 46.3 % of fine and natural water content was 31%. It was classified as muddy soil according to the surplus soil classification. In addition to that, it contained 10 % of amorphous content which was assumed no negative effect was given on the stabilization techniques. Soaking was conducted on artificially made acidic water or pure water with a pH of 4.5 and 7.0. The specimen to soaking water ratio was maintained as 1: 5. However, from the analysis results, it was observed the effect of acidity did not appear in deterioration. Because of that, the results obtained in all acidic water cases used to develop the prediction methodology. The deterioration obtained in lower binder contents could not be evaluated accurately whether it was due to chemical property change or due to physical property change. By considering that fact only the results evaluated from middle and larger binder contents up to 672 days of curing were used to propose the methodology.

The main objective of this methodology was to predict the strength distribution of the soaked specimen after a given soaking period by considering the deterioration mechanism. Because it is important to know the deterioration depth and the strength distribution after a given time for the designers to decide the design strength and the lifetime of the structure.

### **6.2 Definition of parameters**

The proposed model for predicting localized strength distribution is shown in Figure 6:1 which was discussed in detail in Chapter 4. In here the variation of four parameters with time need to be considered.

1. Deterioration depths
  - a.  $D_U$ - Upper bound deterioration depth
  - b.  $D_L$ - lower bound deterioration depth
2. Localized strength ratios
  - a.  $S_U$ - Upper bound localized strength ratio

b.  $S_L$ - lower bound localized strength ratio

In this study, the localized strength ratio was evaluated based on the strength of the sealed specimen. In order to evaluate exact strength at a given time, it required to know the relationship between unconfined compressive strength with a curing period. This was introduced as the fifth parameter in this study. Unconfined compressive strength distribution of a soaked specimen after a given soaking period can be obtained by;

$$\text{Localized strength distribution} \times (UCS)_{sealed(t)} \quad (6-1)$$

In the next sections, it was discussed the relationships of these five parameters with time and the influential factors on those.

### 6.3 Deterioration depths

#### 6.3.1 Cement treated soil

Figure 6:2 and Figure 6:3 shows the relationship between the soaking period and the lower bound deterioration and upper bound deterioration depths respectively. When increase the soaking period deterioration depths gradually increase with a logarithmic relationship with the soaking period. could be used to explain that behavior.

$$y = C + A \ln(t) \quad (6-2)$$

Where

y = deterioration depth (mm)  
 C= constant  
 A= deterioration rate coefficient  
 t = soaking period (days)

Theoretically, the deterioration depth at soaking period is zero should be zero. That made C=0.

#### 6.3.2 Lime treated soil

Figure 6:4 shows the relationship between the soaking period and the upper bound deterioration depth for lime treated soil. In this case, the lower bound ratio was zero up to soaking of 672 days. In lime treated soil also similar relationship as cement treated soil could be observed and the same equation could be used to obtain deterioration depths.

### 6.3.3 Factors influencing deterioration rate coefficient

By considering the above two sections deterioration depths of both improved soils could be explained by the same equation. Figure 6:5 (a) and (b) explains the relationship between binder contents and deterioration rate for cement treated soil and lime treated soil respectively. According to those when increase binder content the deterioration rate become low in both binder types. In the case of cement treated soil when increasing the maturity before soaking clear reduction in deterioration rate was obtained for both upper bound and lower bound cases. In the case of lime treatment, there was no clear effect from maturity before soaking.

## 6.4 Localized strength ratios

### 6.4.1 Cement treated soil

Figure 6:6 shows the relationship between the soaking period and the lower bound strength ratio for cement treated soil. According to that relationship, the strength ratio gradually decreased when increase the soaking period by showing a logarithmic relationship.

$$y = C + B \ln(t) \quad (6-3)$$

Where

y = localized strength ratio  
 C= constant  
 B= localized strength rate coefficient  
 t = soaking period (days)

In this case C=1 and B= (-) B due to the reduction of the strength.

Figure 6:7 shows the relationship between the soaking period and the upper bound strength ratio for cement treated soil. There were three phases in C3.5 immature soaked specimen and 2 phases in C5.3 soaked specimen due to the appearance of internal deterioration and recovery. In the case of C3.5 mature case, only one phase was there. Those phases were changed in accordance to the soaking period and the parameters defined in equation (6-3) could be changed in accordance to the soaking period and the case types as shown in Table 6:1.

### 6.4.2 Lime treated soil

Figure 6:8 shows the relationship between the soaking period and the (a) lower bound strength ratio and the (b) upper bound strength ratio for lime treated soil. In both cases, strength ratio gradually decreased when increasing the soaking period and could explain that relationship by



the same equation (6-3) in accordance with

Table 6:2.

Table 6:1 Summary of constants for  $S_U$  cement treated soil

	C3.5 Soaked (immature)	C3.5 Soaked (mature)	C5.3 Soaked (immature)
$t < 25$	$C=1, B=(-B)$	-	$C=1, B=(-B)$
$25 < t < 333$	$C=0, B=(+B)$	-	-
$333 < t$	$C=1, B=(-B)$	-	-
$25 < t$	-	-	$C=0, B=(+B)$
$t < 168$	-	$C=1, B=0$	-
$168 < t$	-	$C=1, B=(-B)$	-

Table 6:2 Summary of constants for  $S_U$  and  $S_L$  lime treated soil

	L2.5 Soaked (immature)	L2.5 Soaked (mature)	L3.8 Soaked (immature)
$t < 25$	$C=1, B=0$	$C=1, B=0$	$C=1, B=(-B)$
$25 < t < 672$	$C=1, B=0$	$C=1, B=0$	$C=1, B=(-B)$

### 6.4.3 Factors influencing localized strength rate coefficient

The obtained relationships between binder content and the localized strength rate coefficient for cement treated soil and lime treated soil were shown in Figure 6:9 (a) and (b) respectively. In the same figure, the effect of maturity also shown. In the case of cement treated soil variation of the localized strength rate coefficient for lower bound only was shown. When this factor shows positive value, it meant strength increment and when it shows the negative value it was a reduction. However, in the above figures, all rate values were negative values even though it was shown as positive values in the figure.

In the case of cement treated soil lower rate of strength was obtained in C3.5 immature case due to initial deterioration caused by internal deterioration. When increasing the cement content and maturity deterioration was reduced.

## 6.5 Unconfined compressive strength of sealed curing

Figure 6:10 and Figure 6:11 explains the unconfined compressive strength of sealed specimens when increasing the curing period of cement treated soil and lime treated soil respectively. According to that relationship, UCS increase with increase the curing time in a logarithmic scale which can be expressed as

$$y = C + D \ln(t) \quad (6-4)$$

Where

y = unconfined compressive strength (kPa)  
 C= constant  
 D= strength gaining rate coefficient  
 t = curing period (days)

In here, C should equal to the unconfined compressive strength of Mho sand in a saturated state. However, in this, it could measure as 28 kPa with a degree of saturation of 79 %. In addition to that here time was considered as curing period not the soaking period.

### 6.5.1 Factors influencing deterioration rate coefficient

The obtained strength gaining rate coefficient, D was plotted against binder content as shown in Figure 6:12. That coefficient was increased nonlinearly when increasing the binder content.

## 6.6 Summary of parameters and influential factors

Table 6:3 shows the summary of the influential factors on each parameter and the equation derived from the relationships described in this chapter. It could understand that all five parameters could be expressed by a general equation as equation (6-5) by setting the parameters in accordance.

$$y = M + N \ln(t) \quad (6-5)$$

## 6.7 Limitation of the proposed model

This methodology was proposed based on the low binder contents as 3.5 % and 5.3% for cement treated soil and 2.5% and 3.8 % for lime treated soil. For the application of the binder contents more than that model should be calibrated in accordingly as that was a major factor. This empirical model was developed based on two years of data. It is better to extend the model by using more data. The actual surplus soil used here contained fines around 46% and natural

water content was around 31 % and amorphous content of 10 %. This model needs to be improved by using different types of surplus soils for further applications.

Table 6:3 Summary of equations for 5 parameter s in the model

Parameter	Influential factors	Equation	General equation
Deterioration depths $D_U, D_L$	Binder type Binder content Maturity before soaking	$D = C + A \ln(t)$	$Y = M + N \ln(t)$
Localized strength ratios $S_L$	Binder type Binder content Maturity before soaking	$S_L = C + B \ln(t)$	
Localized strength ratios $S_U$	Binder type Binder content Maturity before soaking Soaking period	$S_U = C + B \ln(t)$	
Unconfined compressive strength in sealed condition	Binder type Binder content	$Q_U = C + D \ln(t)$	

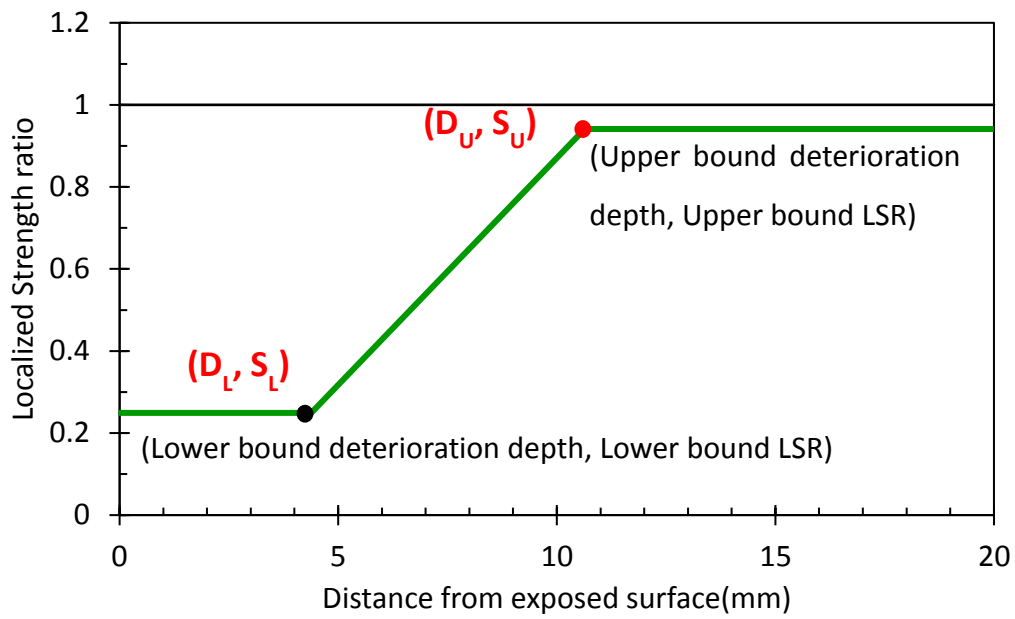


Figure 6:1 General model for Localized strength distribution at a given soaking period

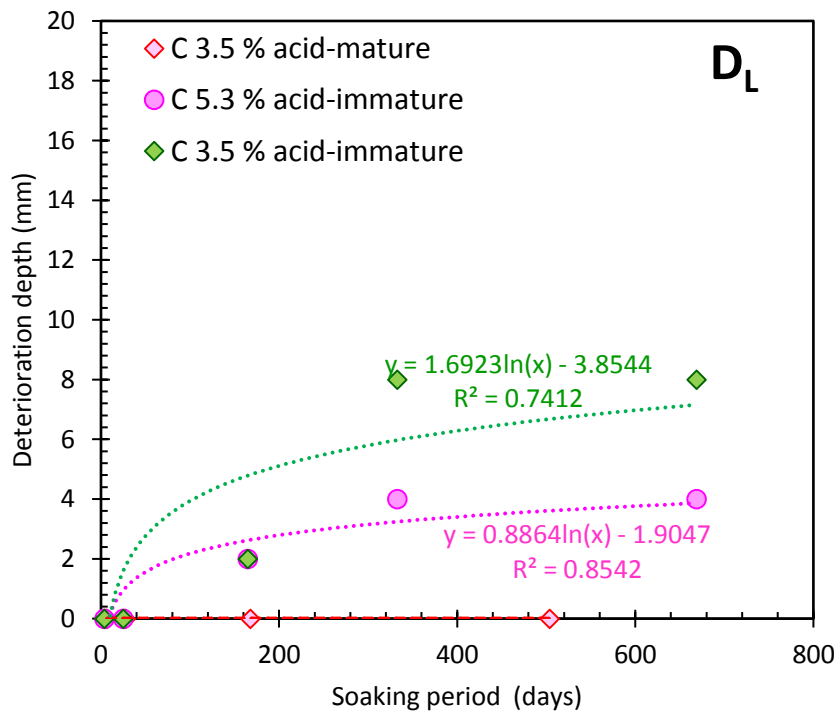


Figure 6:2 Relationship between  $D_L$  and soaking period of cement treated soil

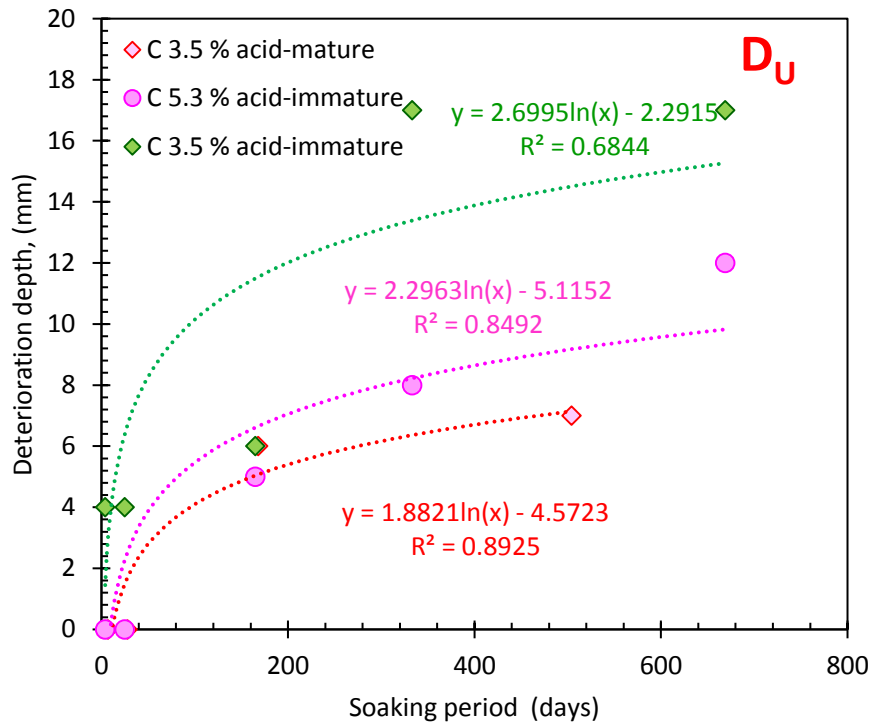


Figure 6.3 Relationship between  $D_U$  and soaking period for Cement treated soil

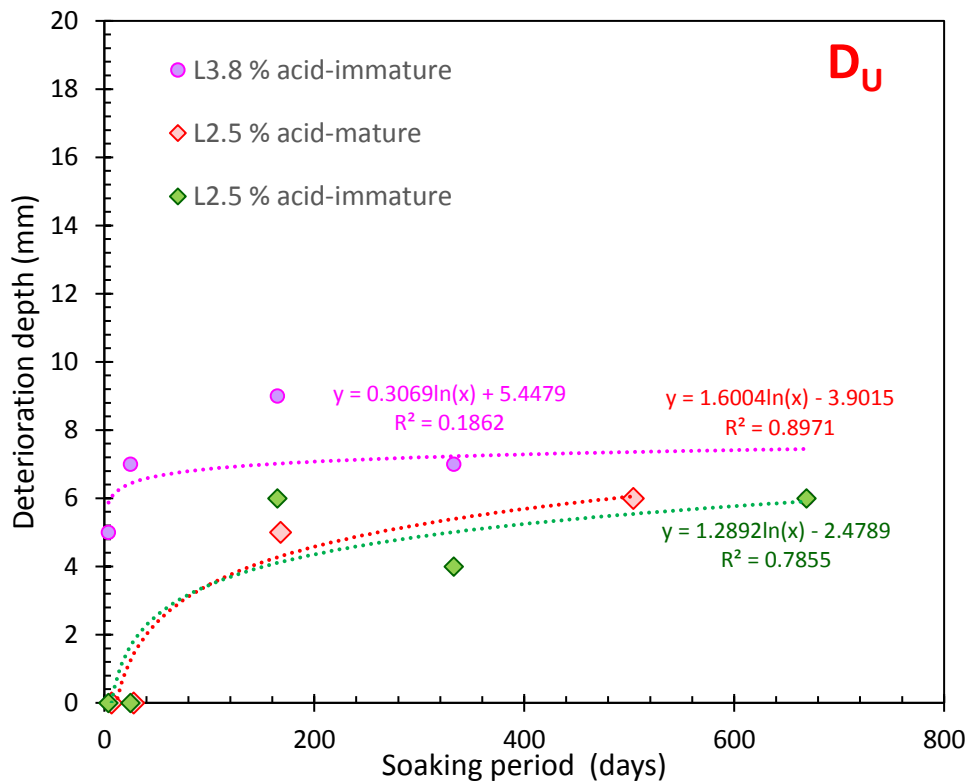


Figure 6.4 Relationship between  $D_U$  and soaking period for Lime treated soil

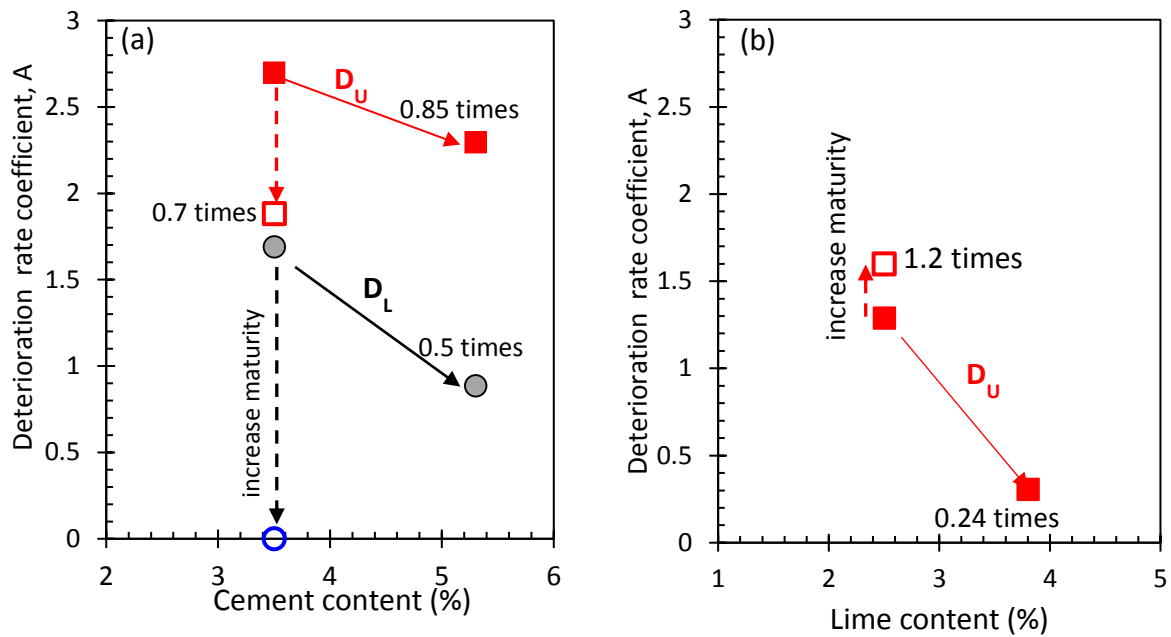


Figure 6:5 Factors influencing deterioration rate coefficient (a) Cement treated soil (b) Lime treated soil

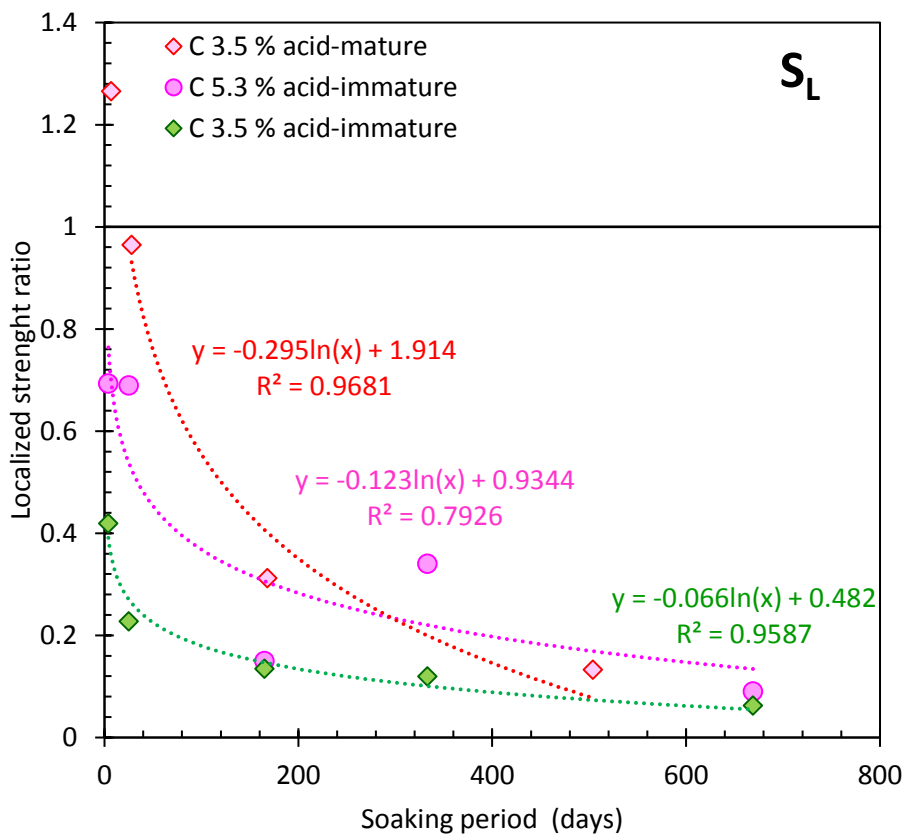


Figure 6:6 Relationship of  $S_L$  with a soaking period of cement treated soil

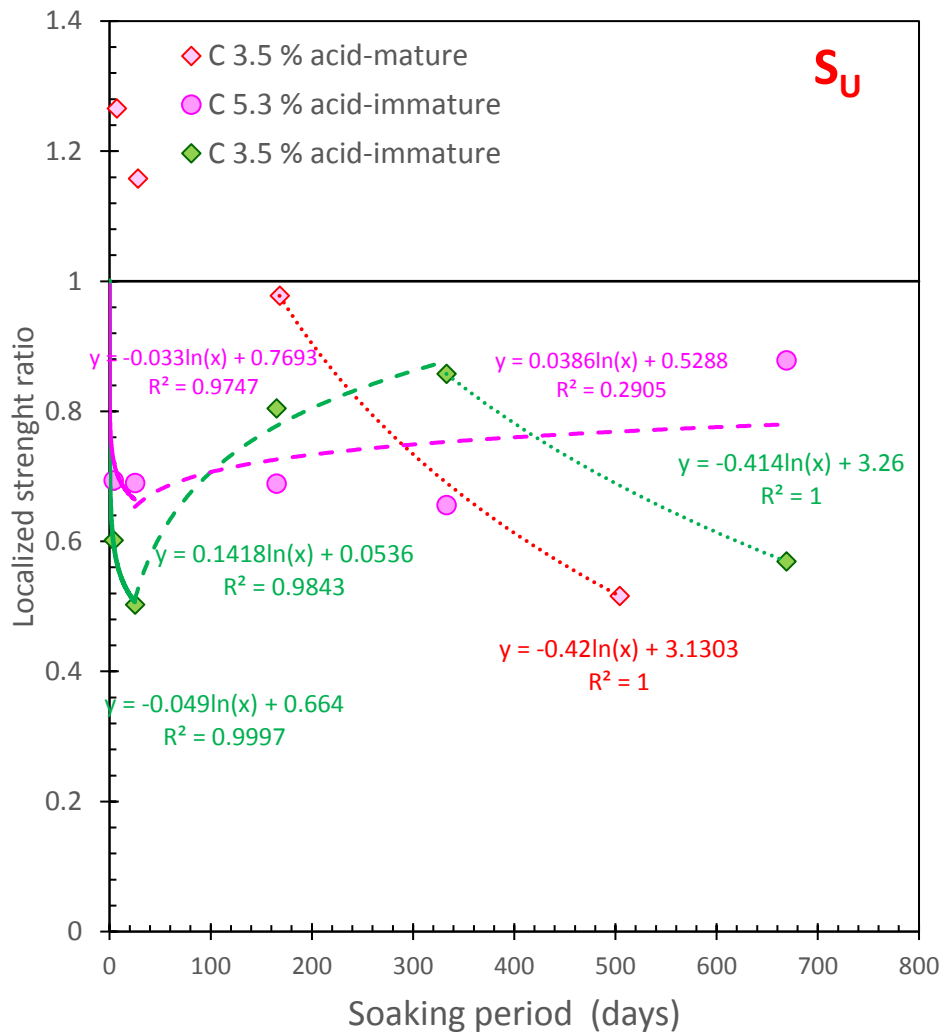


Figure 6:7 Relationship between  $S_u$  and soaking period for cement treated soil

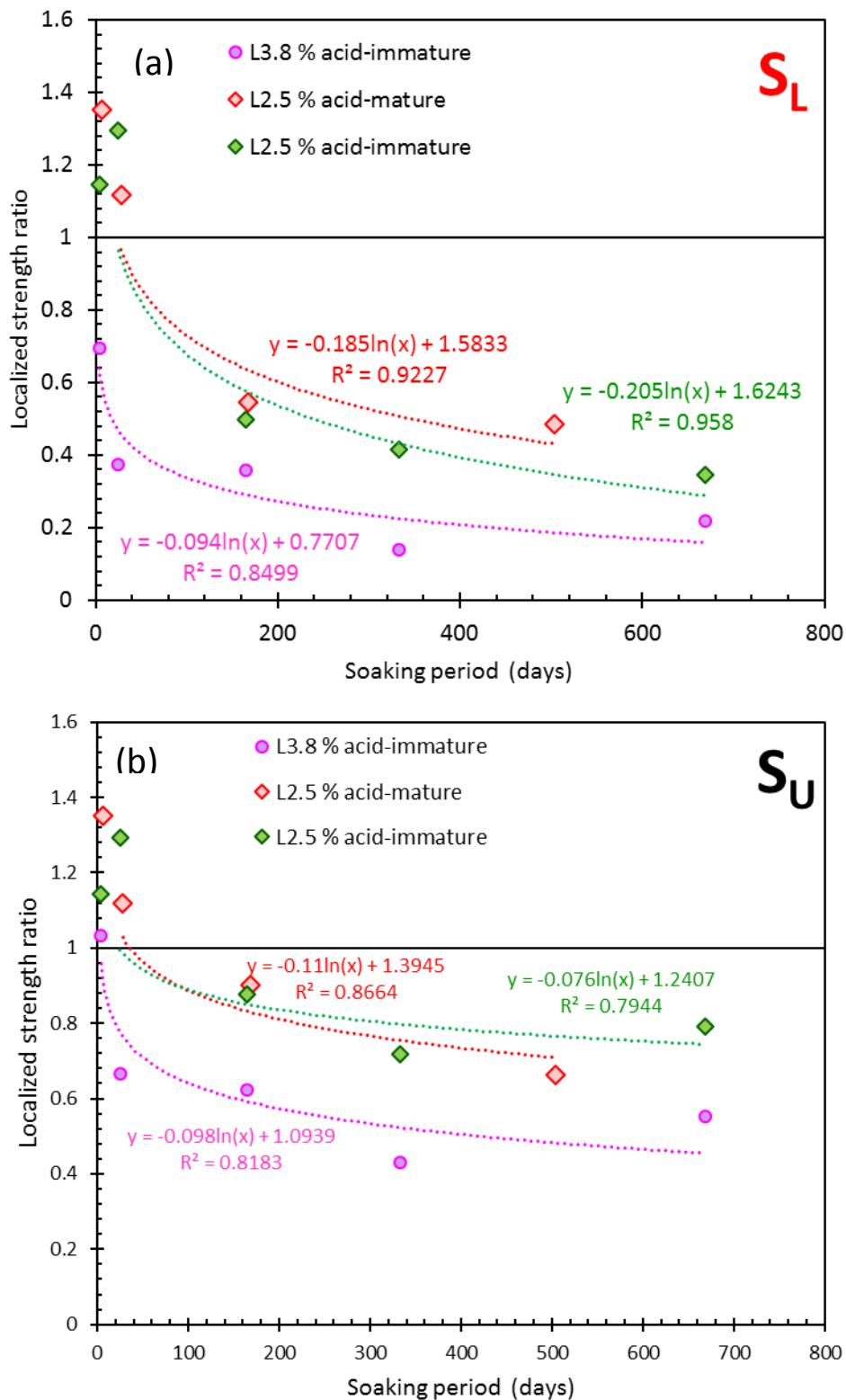


Figure 6:8 Relationships of (a)  $S_L$  (b)  $S_U$  with soaking period for lime treated soil



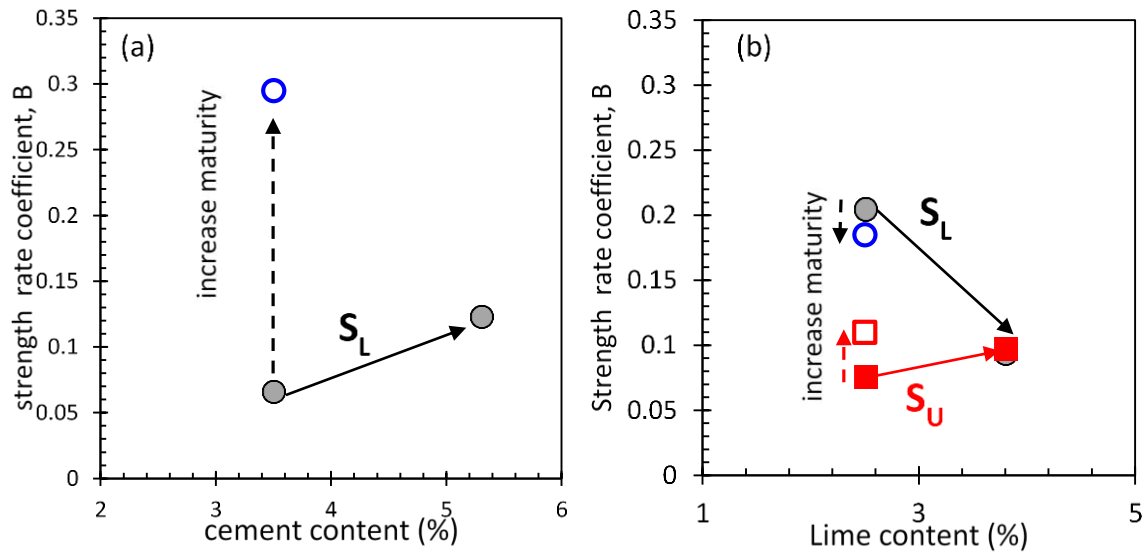


Figure 6:9 Factors influencing localized strength rate (a) cement treated soil (b) Lime treated soil

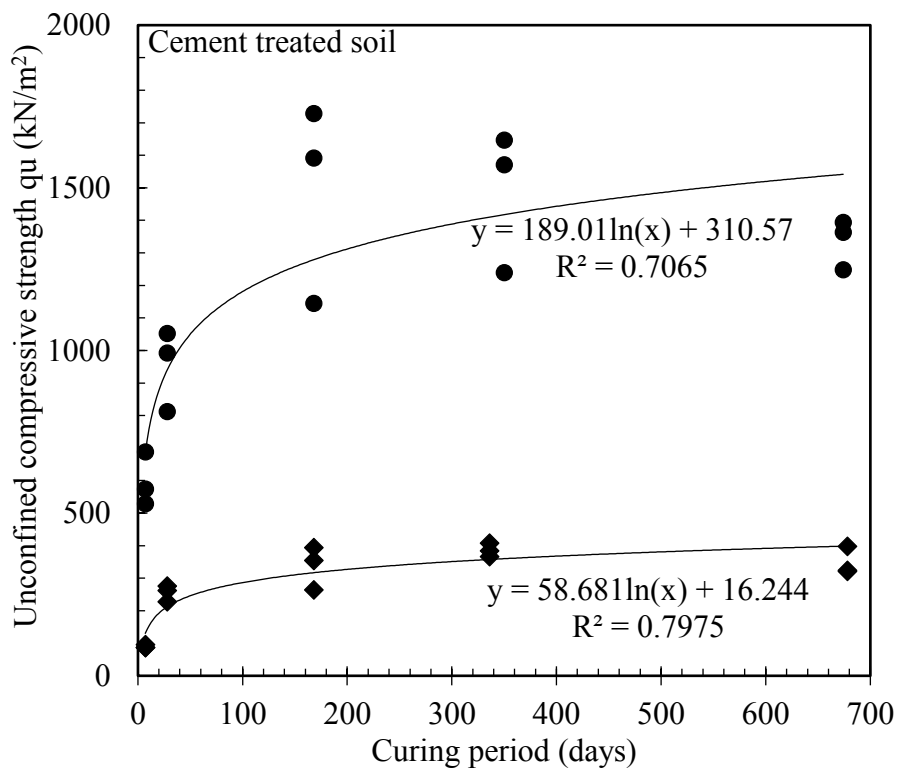


Figure 6:10 Variation of unconfined compressive strength of sealed specimens for cement treated soil

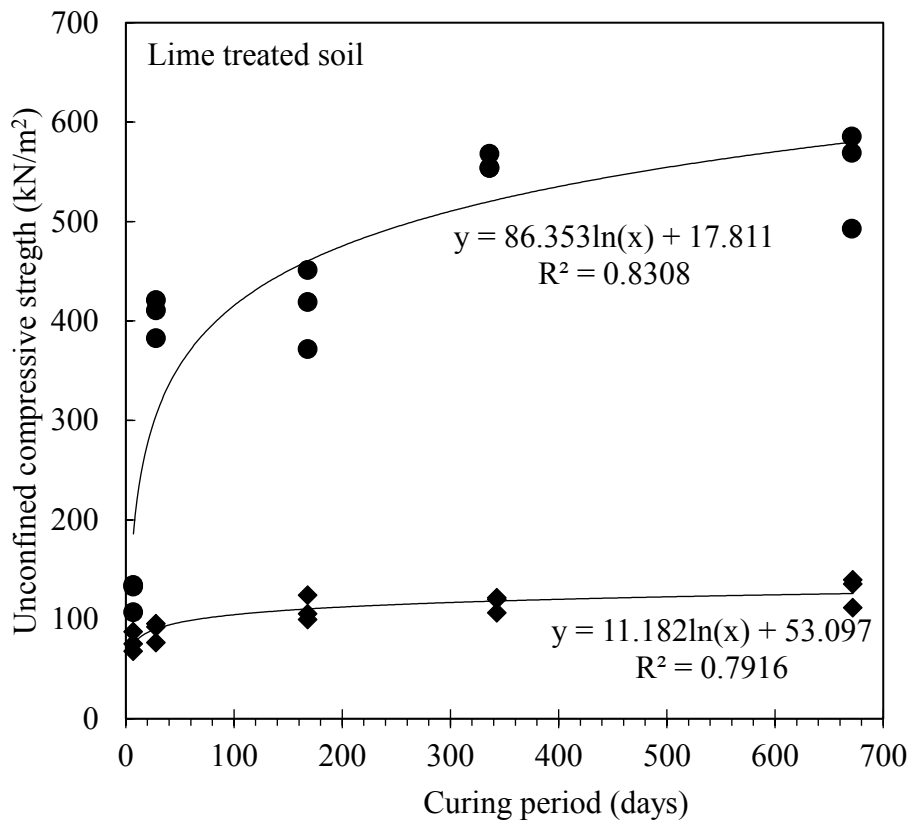


Figure 6:11 Variation of unconfined compressive strength of sealed specimens for lime treated soil

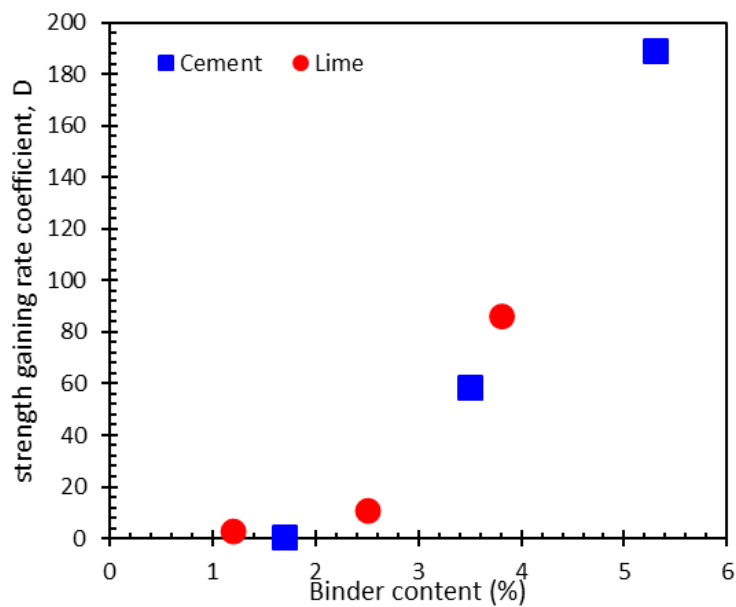


Figure 6:12 Variation of strength gaining rate

## 7 Conclusions and Recommendations

The aim of this study was to understand the long-term behavior of improved surplus soils with low binder content under groundwater by;

1. Evaluating the influential factors on the progression of deterioration.
2. Evaluating the mechanism of deterioration in the aspect of chemical behavior.
3. Proposing a prediction methodology on long term tendency of deterioration.

To achieve these objectives mechanical and chemical tests were conducted on an actual surplus soil called Miho sand after improving with low binder ratios of cement or lime. In here unconfined compression test and needle penetration tests were conducted as the mechanical test. Electron probe microanalyzer (EPMA), X-ray fluorescence spectrometry analysis (XRF) and X-ray diffractometer (XRD) were conducted as the chemical testing. The experiments were conducted under two curing conditions as sealed and soaked with three different binder contents. Under the soaked condition, curing was conducted under two different ways as (immature) pure/acid, and soaked (mature) acid to discuss long term behavior under groundwater in detail. In this study, deterioration was defined as the strength reduction under soaked specimens with respect to the sealed specimen of a given curing period in order to understand the deterioration mechanism clearly.

The first objective was achieved by evaluating unconfined compression test results and needle penetration test results under each curing type of each binder contents. The followings were the findings:

1. From unconfined compression test results, it was found that the evaluated strength ratios of soaked specimens were less than 1 in all cases of both cement and lime treated soil by proving soaking caused for deterioration.
2. Effect of acidity (pH) did not appear in both binder types.
3. In cement treated soil, the progression of deterioration was observed as two stages as primary deterioration up to soaking of 25 days and secondary deterioration from 25 days to 672 days of soaking when improved soil exposed to groundwater in an immature state. The appearance of primary deterioration depended on the cement content and the initial strength (maturity) before exposing to water.

- 
4. In lime treated soil progression of deterioration was appeared as one stage, secondary deterioration.
  5. From needle penetration test results, it was observed a clear reduction in localized strength ratio throughout the specimen when cement treated soil exposed to water in immature state as a result of two actions.
    - (a) Internal deterioration
    - (b) Deterioration driven from the surface

The localized strength ratio of the core of those specimens showed three phases against soaking period. I) internal deterioration (II) recovery from internal deterioration (III) Deterioration driven from the surface. Appearance time and appearance of phase II and III depended on the cement content.

The appearance of Primary deterioration could be explained from internal deterioration. Secondary deterioration was due to the combined effect of recovery from primary deterioration and the deterioration driven from the surface.

6. Deterioration of cement treated soil soaked (mature) and all cases of lime treated soil were due to the deterioration driven from the surface throughout the specimen and caused for not appearing primary deterioration.

The second objective was to evaluate the mechanism of deterioration in the aspect of chemical behavior.

1. The mechanism of internal deterioration could not explain from the Calcium leaching phenomena even though both XRF and EPMA analysis showed a clear movement of Ca ions from the center to the surface of the specimens. It was suggested that internal deterioration was a result of the mobilization of ions from pore water to soaking water. However, the deterioration observed near the surface of cement treated immature specimens were due to leaching calcium ions.
2. In the case of soaked cement treated soil in mature state and all the cases of lime treated soil, Ca leaching was identified as the reason for the deterioration driven from the surface. Ca ratio and the strength ratio throughout the specimen showed a polynomial relationship.
3. XRD analysis was applied to identify the mineral in improved soils. It could find ettringite and Calcite peaks only in cement treated soil. From the soaked specimens, it

was found ettringite had disappeared at the surface. It was suggested that Ca leaching from ettringite also contributed to the strength reduction.

4. the heavy liquid application was not successful for separating small quantities of hydration products from improved surplus soils.

The third objective was to propose a methodology for long term tendency of deterioration.

1. An empirical model was developed to predict strength distribution along with the specimen after a given soaking period based on five parameters:
  - two deterioration depths (upper bound and lower bound)
  - two localized strength ratios (upper bound and lower bound)
  - unconfined compressive strength under sealed condition
2. From detailed analysis on each parameter, it could found all parameters behaved similarly against time in logarithmically and a unique equation could be developed.
3. This prediction methodology was developed for a surplus soil with fine content of 46 %, natural water content of 31 % and amorphous content of 10 %. It is required further verifications with different types of surplus soils.

With reference to the results of this study, the following issues are recommended for further detailed investigations:

1. Effect of soaking water exchange rate on the appearance of internal deterioration.  
In this study, soaking water was exchanged once a week up to one month and then changed it twice a month until six months. It is suggested that the soaking water exchange rate effect on the appearance of internal deterioration and its recovery. Further investigation is required by changing that rate.
2. Effect of pH and the acidity concentration on the appearance of the deterioration.  
In this study pH of acid water was set to 4.5 and the volume ratio of the specimen to water was maintained as 1:5. The effect of acidity on the deterioration might be different when changing that volume ratio. In addition to that, the concentrations of Cl<sup>-</sup> and sulfate ions in the soaking water needs to be accounted for.
3. Verification of the hypothesis on internal deterioration by TG/DTA and XRD.  
The experimental results of this study did not enough to explain the mechanism of internal deterioration. It needs to be verified after reproducing the same results.

4. Study on pore distribution of the specimens to explain ion mobilization or calcium leaching mechanism.

From the observations in this study, it was suggested that the improved surplus soils with low binder contents behaved as a dual model with macropores and micropores. This concept needs to be verified by conducting the mercury intrusion tests.

5. Extension of model parameters based on calcium leaching rate.

From the proposed prediction methodology in chapter 6, it could understand a general equation can be used to explain long term behavior of cement and lime treated soils. It was identified that the mechanism of deterioration of the cement treated matured case and all cases of lime treated soil were due to leaching of Ca ions. Parameters of the model may be possible to improve further using calcium leaching rate.

6. Verification of the prediction methodology

The prediction methodology introduced in this study was for a surplus soil with fine content of 46 %, natural water content of 31 % and amorphous content of 10 %. It is required further verifications in details for different types of surplus soils with different fine contents and amorphous contents by following this study as a base.

Annex A

Data sheet- Quick lime

試 験 成 績 表

御中

宇部マテリアルズ株式会社  
千葉工場



品 名	生石灰 ( 0 ~ 5mm )
-----	-----------------


2016年11月度

試 験 項 目	成 分 ・ 粒 度																				
試 験 報 告	<table border="1"> <thead> <tr> <th>項 目</th> <th>測 定 値</th> </tr> </thead> <tbody> <tr> <td>酸化カルシウム (CaO)</td> <td>94.93 (%)</td> </tr> <tr> <td>不純分 (Imp+MgO)</td> <td>2.24 (%)</td> </tr> <tr> <td>二酸化炭素 (CO<sub>2</sub>)</td> <td>1.65 (%)</td> </tr> <tr> <td></td> <td></td> </tr> <tr> <td></td> <td></td> </tr> <tr> <td>粒 度</td> <td>残 分</td> </tr> <tr> <td>+ 5 (m/m)</td> <td>0 (%)</td> </tr> <tr> <td></td> <td></td> </tr> <tr> <td></td> <td></td> </tr> </tbody> </table>	項 目	測 定 値	酸化カルシウム (CaO)	94.93 (%)	不純分 (Imp+MgO)	2.24 (%)	二酸化炭素 (CO <sub>2</sub> )	1.65 (%)					粒 度	残 分	+ 5 (m/m)	0 (%)				
	項 目	測 定 値																			
	酸化カルシウム (CaO)	94.93 (%)																			
	不純分 (Imp+MgO)	2.24 (%)																			
	二酸化炭素 (CO <sub>2</sub> )	1.65 (%)																			
	粒 度	残 分																			
	+ 5 (m/m)	0 (%)																			
備 考	*不純分とは二酸化けい素(SiO <sub>2</sub> ), 酸化アルミニウム(Al <sub>2</sub> O <sub>3</sub> ) 酸化第二鉄(Fe <sub>2</sub> O <sub>3</sub> ), 酸化マグネシウム(MgO)の合計量																				

## Data sheet- Cement

# 固化材試験成績表

NO.341954

 住友大阪セメント株式会社


平成29年11月度

試験項目		種 類	タフロック3E型 (TL-3E)
容 積		( $\text{g}/\text{cm}^3$ )	3.08
比 表 面 積		( $\text{cm}^2/\text{g}$ )	1420
化 学 成 分	二酸化けい素	[ $\text{SiO}_2$ ] (%)	22.47
	酸化アルミニウム	[ $\text{Al}_2\text{O}_3$ ] (%)	7.33
	酸化第二鉄	[ $\text{Fe}_2\text{O}_3$ ] (%)	2.19
	酸化カルシウム	[ $\text{CaO}$ ] (%)	56.37
	酸化マグネシウム	[ $\text{MgO}$ ] (%)	2.09
	三酸化硫黄	[ $\text{SO}_3$ ] (%)	6.08
	備 考 ※タフロック3E型は大鉄クロム溶出低減型のセメント系汎用固化材、 (特殊土用セメント系固化材) ※試験方法は、JIS B 5201、JIS B 5202 及び JIS X 5204 による。 尚、JIS B 5202 採本体法による。		

お問い合わせその他ご連絡先

住友大阪セメント株式会社

東京支店 固材グループ

〒100-6966 東京都千代田区六番町6番地28

TEL : 03-6211-4829



Japanese Road earthwork structure technical standard

道路土工構造物技術基準・同解説

解表 4-8 日常管理の基準値の目安 (路体)

区分	仕上がり厚さ	管理基準値			施工含水比	
		土砂区分	締固め度 $D_c$ (%)	空気間隙率 $v_a$ (%)		飽和度 $S_r$ (%)
土砂	30cm 以下	粘性土	— (※1)	10 以下	85 以上	(※2)
		砂質土	90 以上 (A, B 法) (※3)	—	—	
岩塊	試験施工により決定	試験施工により決定				

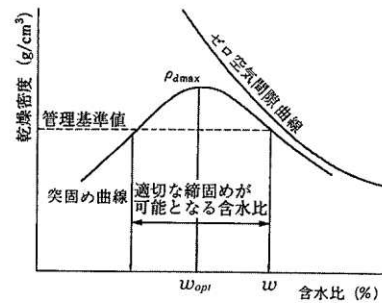
表中のいずれかの基準値を用いて管理を行う。

表中の一は使用不適當

※1：粘性土材料で締固め度管理が可能な場合は、本表の「砂質土」の基準を適用可

※2：締固め度管理の場合は、右図中に矢印で示す範囲、空気間隙率及び飽和度管理の場合は、自然含水比又はトラフィカビリティーが確保できる含水比を目安とする。

※3：突き固めによる土の締固め試験 (JIS A 1210) における突き固め方法の呼び名



解表 4-9 日常管理の基準値の目安 (路床及び構造物との接続部)

施工部位	仕上がり厚さ	管理基準値		施工含水比	
		土砂区分	締固め度 $D_c$ (%)		空気間隙率 $v_a$ (%)
路床	20cm 以下	粘性土	—	8 以下	最適含水比付近
		砂質土	95 以上 (A, B 法) 90 以上 (C, D, E 法) (※1)	—	
構造物接続部	20~30cm	粘性土	—	8 以下	
		砂質土	95 以上 (A, B 法) 90 以上 (C, D, E 法) (※1)	—	

表中のいずれかの基準値を用いて管理を行う。

表中の一は使用不適當

※1：突き固めによる土の締固め試験 (JIS A 1210) における突き固め方法の呼び名

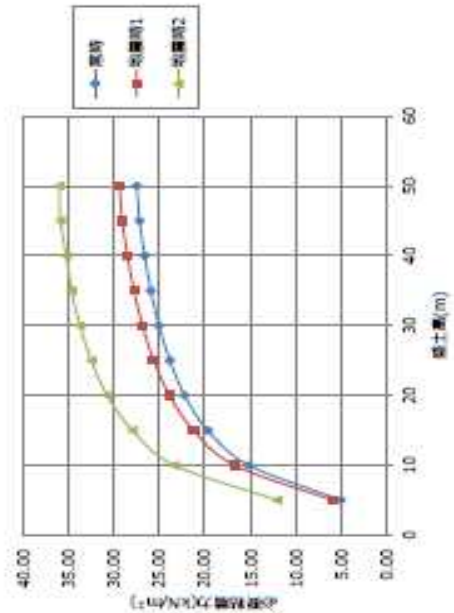
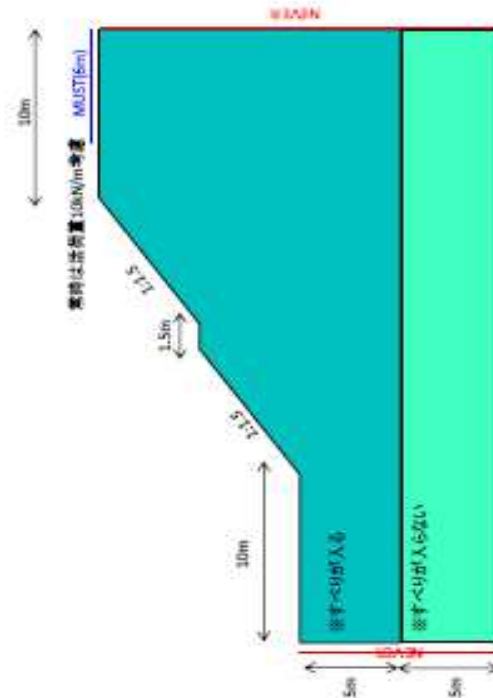
Stability analysis -1

断面形状：段-1断面

【条件】  
 $\gamma = 19 \text{ kN/m}^3$   
 傾斜: 1:1.5  
 $\phi = 15^\circ$   
 級土層 5~50まで10(9)→  
 作用 1.高時  
 2.地震時1 kh=0.12 (L1三層地層)  
 3.地震時2 kh=0.24 (L2三層地層)

【結果】  
 $F_s = 1.2$  活荷重  $10 \text{ kN/m}^2 (L=1.0 \text{ m})$  考慮  
 $F_s = 1.0$   
 $F_s = 1.0$

必要粘着力(kN/m <sup>2</sup> )	作用	
	高時	地震時
5	5.06	6.00
10	15.15	16.73
15	19.67	21.24
20	22.22	23.88
25	23.62	25.60
30	25.03	26.85
35	25.92	27.78
40	26.60	28.48
45	27.16	29.07
50	27.49	29.37

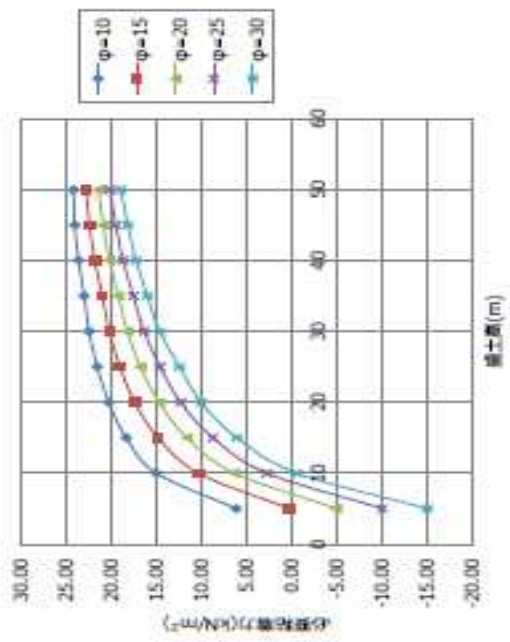
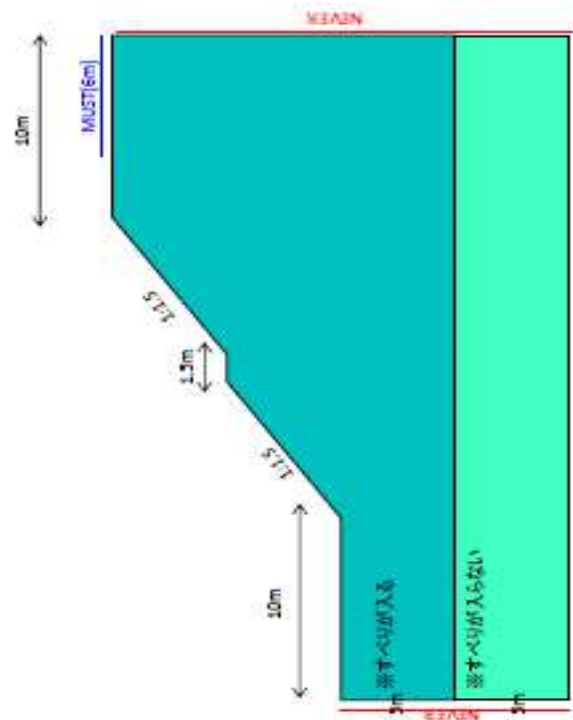


Stability analysis - 2

【条件】  
 $\gamma = 19 \text{ kN/m}^3$      $F_s = 1.0$     断面形状：図-1参照  
 傾斜：1:1.5    小段：1.5m

【結果】

必要粘着力 (kN/m <sup>2</sup> )	内部摩擦角 (deg)				
	$\phi = 10$	$\phi = 15$	$\phi = 20$	$\phi = 25$	$\phi = 30$
5	6.14	0.30	-4.88	-9.98	-14.92
10	14.95	10.32	6.33	2.76	-0.54
15	18.30	14.77	11.59	8.73	6.09
20	20.21	17.34	14.68	12.28	10.04
25	21.49	18.99	16.72	14.55	12.41
30	22.38	20.16	18.17	16.33	14.61
35	22.93	20.93	19.16	17.51	15.96
40	23.53	21.76	20.14	18.63	17.20
45	23.98	22.33	20.82	19.43	18.11
50	24.11	22.74	21.39	20.12	18.89



## Annex B

Cement Content (%)	Curing days	Unconfined compressive strength, $q_u$ (kPa)						
		Curing type			①	②	③	
1.7	7	Sealed	–	Sat	38.06	46.75	47.76	
		Soaked	immature	Acid	23.63	20.48	21.64	
	28	Sealed	–	Sat	50.29	43.16	39.86	
		Soaked	immature	Acid	28.18	23.11	28.71	
	168	Sealed	–	Sat	42.90	36.60	58.30	
		Soaked	immature	Acid	28.79	27.45	24.17	
	336	Sealed	–	Sat	37.18	42.49	53.28	
		Soaked	immature	Acid	28.41	27.99	31.33	
	672	Sealed	–	Sat	41.53	48.33	51.48	
		Soaked	immature	Acid	28.17	31.33	23.91	
	3.5	7	Sealed	–	Sat	86.58	86.82	95.93
			Soaked	immature	Pure	64.67	73.67	69.29
Acid					70.42	67.45	67.28	
28		Sealed	–	Sat	261.55	276.10	227.22	
		Soaked	immature	Pure	155.39	122.59	138.48	
				Acid	137.51	148.11	143.04	
168		Sealed	–	Sat	263.88	394.21	354.08	
		Soaked	immature	Pure	162.62	183.35	164.96	
				Acid	174.67	168.99	154.70	
175		Soaked	mature	Acid	333.62	337.45	308.66	
196		Soaked	mature	Acid	369.36	362.55	341.00	
336		Sealed	–	Sat	383.81	366.08	407.49	
		Soaked	immature	Pure	179.41	163.95	181.09	
				Acid	160.23	172.94	161.94	
mature			Acid	305.64	300.72	315.47		
672		Sealed	–	Sat	321.33	323.65	397.90	
		Soaked	immature	Pure	106.95	103.43	95.23	
				Acid	106.23	116.27	137.10	
Soaked	mature	Acid	184.12	202.58	190.42			
5.3	7	Sealed	–	Sat	528.67	573.47	688.33	
		Soaked	immature	Acid	593.03	646.99	562.26	
	28	Sealed	–	Sat	812.13	1051.98	992.44	
		Soaked	immature	Acid	808.84	967.03	907.16	
	168	Sealed	–	Sat	1591.44	1144.75	1728.12	
		Soaked	immature	Acid	1027.65	1133.18	558.54	
	336	Sealed	–	Sat	1646.28	1570.98	1239.14	
		Soaked	immature	Acid	894.10	1027.10	973.10	
	672	Sealed	–	Sat	1362.74	1247.67	1393.25	
		Soaked	immature	Acid	848.32	793.08	913.13	

Cement Content (%)	Curing days	E <sub>50</sub> (MPa)						
		Curing type			①	②	③	
1.7	7	Sealed	–	Sat	4.81	4.94	5.24	
		Soaked	immature	Acid	3.78	1.66	1.45	
	28	Sealed	–	Sat	3.46	4.11	3.50	
		Soaked	immature	Acid	3.57	4.64	2.78	
	168	Sealed	–	Sat	4.62	3.20	3.54	
		Soaked	immature	Acid	4.43	3.98	2.38	
	336	Sealed	–	Sat	7.44	3.47	5.21	
		Soaked	immature	Acid	4.64	4.04	4.04	
	672	Sealed	–	Sat	3.21	4.13	4.94	
		Soaked	immature	Acid	1.67	5.15	4.64	
	3.5	7	Sealed	–	Sat	14.78	14.39	24.98
			Soaked	immature	Pure	18.72	22.27	14.72
Acid					21.76	13.06	12.95	
28		Sealed	–	Sat	77.76	70.44	62.87	
		Soaked	immature	Pure	24.98	26.77	14.08	
				Acid	29.96	26.90	32.16	
168		Sealed	–	Sat	66.75	105.61	114.91	
		Soaked	immature	Pure	28.48	25.83	24.41	
				Acid	25.89	40.31	29.97	
175		Soaked	mature	Acid	78.56	81.85	41.59	
196		Soaked	mature	Acid	78.19	81.79	83.35	
336		Sealed	–	Sat	75.93	94.04	67.02	
		Soaked	immature	Pure	29.84	19.96	23.76	
				Acid	22.49	25.28	22.65	
			mature	Acid	70.84	60.39	65.57	
672		Sealed	–	Sat	45.80	55.27	66.43	
		Soaked	immature	Pure	19.02	15.46	14.26	
				Acid	16.79	13.25	17.95	
		Soaked	mature	Acid	32.61	28.64	30.39	
5.3		7	Sealed	–	Sat	61.62	160.78	173.19
			Soaked	immature	Acid	214.68	175.84	120.22
	28	Sealed	–	Sat	245.06	128.04	185.16	
		Soaked	immature	Acid	211.58	217.55	245.38	
	168	Sealed	–	Sat	500.74	219.54	473.11	
		Soaked	immature	Acid	245.98	293.55	167.81	
	336	Sealed	–	Sat	557.94	431.86	214.88	
		Soaked	immature	Acid	139.20	206.19	188.94	
	672	Sealed	–	Sat	332.62	217.53	307.09	
		Soaked	immature	Acid	144.29	120.28	150.37	

Cement Content (%)	Curing	water content, w (%)					
	days	Curing type			①	②	③
1.7	7	Sealed	–	Sat	30.00	30.00	29.80
		Soaked	immature	Acid	31.60	31.90	31.80
	28	Sealed	–	Sat	30.00	30.20	30.40
		Soaked	immature	Acid	32.50	33.20	32.70
	168	Sealed	–	Sat	30.00	30.10	29.90
		Soaked	immature	Acid	33.20	33.80	33.30
	336	Sealed	–	Sat	30.77	30.01	30.44
		Soaked	immature	Acid	32.80	33.70	33.00
	672	Sealed	–	Sat	29.71	30.12	29.73
		Soaked	immature	Acid	32.37	31.59	32.22
3.5	7	Sealed	–	Sat	32.10	31.70	31.60
		Soaked	immature	Pure	32.10	32.40	32.40
				Acid	31.90	31.90	32.20
	28	Sealed	–	Sat	31.80	31.50	31.30
		Soaked	immature	Pure	33.00	33.20	32.90
				Acid	33.60	33.10	33.00
	168	Sealed	–	Sat	33.10	32.90	33.40
		Soaked	immature	Pure	35.20	34.80	35.40
				Acid	34.30	34.50	35.30
	175	Soaked	mature	Acid	32.00	32.30	32.50
	196	Soaked	mature	Acid	33.30	33.00	33.80
	336	Sealed	–	Sat	33.73	36.88	33.94
		Soaked	immature	Pure	35.00	33.80	34.60
				Acid	33.70	34.40	33.40
			mature	Acid	33.48	34.30	33.85
	672	Sealed	–	Sat	32.70	33.39	33.64
		Soaked	immature	Pure	34.20	34.74	34.07
				Acid	34.34	32.58	34.82
Soaked	mature	Acid	34.46	34.14	33.49		
5.3	7	Sealed	–	Sat	29.30	27.90	27.80
		Soaked	immature	Acid	32.30	31.50	31.70
	28	Sealed	–	Sat	34.30	33.90	33.80
		Soaked	immature	Acid	34.20	33.70	33.80
	168	Sealed	–	Sat	33.10	33.40	33.70
		Soaked	immature	Acid	34.90	34.80	33.80
	336	Sealed	–	Sat	33.70	33.90	34.10
		Soaked	immature	Acid	34.10	33.20	32.60
	672	Sealed	–	Sat	29.53	31.78	33.58
		Soaked	immature	Acid	34.47	34.47	34.11

Cement Content (%)	Curing days	dry density , $\rho_d$ (g/cm <sup>3</sup> )						
		Curing type			①	②	③	
1.7	7	Sealed	–	Sat	1.43	1.44	1.45	
		Soaked	immature	Acid	1.42	1.41	1.43	
	28	Sealed	–	Sat	1.44	1.43	1.44	
		Soaked	immature	Acid	1.42	1.41	1.41	
	168	Sealed	–	Sat	1.44	1.44	1.46	
		Soaked	immature	Acid	1.41	1.41	1.41	
	336	Sealed	–	Sat	1.40	1.43	1.43	
		Soaked	immature	Acid	1.41	1.40	1.41	
	672	Sealed	–	Sat	1.43	1.43	1.43	
		Soaked	immature	Acid	1.42	1.42	1.40	
	3.5	7	Sealed	–	Sat	1.39	1.40	1.41
			Soaked	immature	Pure	1.39	1.39	1.39
Acid					1.40	1.41	1.40	
28		Sealed	–	Sat	1.39	1.40	1.41	
		Soaked	immature	Pure	1.39	1.41	1.40	
				Acid	1.37	1.39	1.39	
168		Sealed	–	Sat	1.40	1.40	1.39	
		Soaked	immature	Pure	1.39	1.39	1.39	
				Acid	1.38	1.38	1.36	
175		Soaked	mature	Acid	1.41	1.39	1.38	
196		Soaked	mature	Acid	1.40	1.39	1.38	
336		Sealed	–	Sat	1.39	1.35	1.38	
		Soaked	immature	Pure	1.36	1.38	1.38	
				Acid	1.38	1.37	1.38	
			mature	Acid	1.39	1.39	1.38	
		672	Sealed	–	Sat	1.40	1.39	1.39
Soaked			immature	Pure	1.38	1.36	1.39	
				Acid	1.38	1.41	1.37	
Soaked		mature	Acid	1.37	1.38	1.40		
5.3		7	Sealed	–	Sat	1.50	1.53	1.55
			Soaked	immature	Acid	1.42	1.42	1.39
		28	Sealed	–	Sat	1.40	1.42	1.41
			Soaked	immature	Acid	1.37	1.39	1.39
		168	Sealed	–	Sat	1.40	1.40	1.40
	Soaked		immature	Acid	1.38	1.38	1.39	
	336	Sealed	–	Sat	1.40	1.40	1.39	
		Soaked	immature	Acid	1.38	1.39	1.40	
	672	Sealed	–	Sat	1.44	1.42	1.39	
		Soaked	immature	Acid	1.39	1.37	1.38	

Cement Content (%)	Curing days	Degree of Sat ,Sr (%)						
		Curing type			①	②	③	
1.7	7	Sealed	–	Sat	90.40	91.00	92.00	
		Soaked	immature	Acid	93.20	93.80	95.10	
	28	Sealed	–	Sat	91.10	91.20	92.60	
		Soaked	immature	Acid	97.10	97.20	96.30	
	168	Sealed	–	Sat	91.50	91.40	94.40	
		Soaked	immature	Acid	97.40	98.40	98.10	
	336	Sealed	–	Sat	89.11	90.64	91.40	
		Soaked	immature	Acid	96.40	97.90	96.80	
	672	Sealed	–	Sat	89.57	90.64	90.04	
		Soaked	immature	Acid	96.27	94.15	93.33	
	3.5	7	Sealed	–	Sat	91.40	91.90	92.10
			Soaked	immature	Pure	90.90	91.90	92.10
Acid					91.60	93.10	92.70	
28		Sealed	–	Sat	90.80	91.10	92.00	
		Soaked	immature	Pure	94.30	97.10	95.40	
				Acid	93.40	94.20	94.30	
168		Sealed	–	Sat	95.60	95.20	94.70	
		Soaked	immature	Pure	99.70	98.60	99.90	
				Acid	96.50	96.30	96.10	
175		Soaked	mature	Acid	93.60	91.70	91.40	
196		Soaked	mature	Acid	95.40	93.40	95.00	
336		Sealed	–	Sat	94.99	98.27	95.21	
		Soaked	immature	Pure	95.70	93.90	97.00	
				Acid	94.70	95.30	93.70	
			mature	Acid	95.17	96.60	94.82	
672		Sealed	–	Sat	94.25	94.68	95.26	
		Soaked	immature	Pure	95.53	95.17	96.43	
				Acid	95.53	95.17	96.43	
Soaked	mature	Acid	95.29	94.87	95.90			
5.3	7	Sealed	–	Sat	97.11	96.38	99.20	
		Soaked	immature	Acid	94.67	92.22	89.93	
	28	Sealed	–	Sat	98.90	99.54	97.64	
		Soaked	immature	Acid	93.86	95.28	95.69	
	168	Sealed	–	Sat	94.80	95.00	96.20	
		Soaked	immature	Acid	96.50	97.10	95.10	
	336	Sealed	–	Sat	96.40	97.20	96.40	
		Soaked	immature	Acid	94.80	94.30	93.60	
	672	Sealed	–	Sat	89.50	93.96	95.54	
		Soaked	immature	Acid	97.05	95.11	94.89	



Cement Content (%)	Curing days	Failure strain (%)						
		Curing type			①	②	③	
1.7	7	Sealed	–	Sat	1.63	2.32	2.36	
		Soaked	immature	Acid	0.91	1.70	2.15	
	28	Sealed	–	Sat	2.64	2.08	2.06	
		Soaked	immature	Acid	1.29	1.01	1.43	
	168	Sealed	–	Sat	1.52	2.16	2.88	
		Soaked	immature	Acid	1.04	1.17	1.41	
	336	Sealed	–	Sat	0.79	2.07	1.96	
		Soaked	immature	Acid	1.16	0.92	1.35	
	672	Sealed	–	Sat	1.75	1.62	1.48	
		Soaked	immature	Acid	1.82	0.86	0.64	
	3.5	7	Sealed	–	Sat	0.72	0.79	0.62
			Soaked	immature	Pure	0.51	0.50	0.66
Acid					0.50	0.64	0.69	
28		Sealed	–	Sat	0.45	0.53	0.53	
		Soaked	immature	Pure	0.71	0.52	1.03	
				Acid	0.57	0.70	0.55	
168		Sealed	–	Sat	0.83	0.66	0.55	
		Soaked	immature	Pure	0.74	1.02	0.89	
				Acid	0.77	0.55	0.64	
175		Soaked	mature	Acid	0.78	0.53	0.86	
196		Soaked	mature	Acid	0.60	0.57	0.58	
336		Sealed	–	Sat	0.55	0.57	0.68	
		Soaked	immature	Pure	0.96	0.77	0.96	
				Acid	0.84	0.86	0.89	
			mature	Acid	0.60	0.66	0.60	
		672	Sealed	–	Sat	1.01	0.82	0.77
Soaked		immature	Pure	0.72	0.81	0.83		
			Acid	0.78	1.12	0.88		
Soaked	mature	Acid	0.68	0.87	0.80			
5.3	7	Sealed	–	Sat	0.99	0.62	0.53	
		Soaked	immature	Acid	0.39	0.47	0.59	
	28	Sealed	–	Sat	0.62	0.77	0.60	
		Soaked	immature	Acid	0.47	0.48	0.44	
	168	Sealed	–	Sat	0.45	0.89	0.48	
		Soaked	immature	Acid	0.50	0.44	0.58	
	336	Sealed	–	Sat	0.42	0.47	0.87	
		Soaked	immature	Acid	0.76	0.60	0.62	
	672	Sealed	–	Sat	0.81	0.93	0.50	
		Soaked	immature	Acid	0.70	0.88	0.73	

Lime Content (%)	Curing	Unconfined compressive strength, $q_u$ (kPa)						
	days	Curing type			①	②	③	
1.2	7	Sealed	–	Sat	27.68	28.62	28.85	
		Soaked	immature	Acid	24.88	26.34	28.72	
	28	Sealed	–	Sat	28.04	26.62	29.77	
		Soaked	immature	Acid	26.01	23.82	23.38	
	168	Sealed	–	Sat	28.50	32.10	34.00	
		Soaked	immature	Acid		22.49	23.62	
	336	Sealed	–	Sat	32.20	36.89	37.08	
		Soaked	immature	Acid	30.17	24.28	26.18	
	672	Sealed	–	Sat	43.24	42.06	42.36	
		Soaked	immature	Acid	26.43	23.19	22.66	
	2.5	7	Sealed	–	Sat	67.86	75.23	87.53
			Soaked	immature	Pure	83.28	94.41	75.22
Acid					100.78	98.16	99.33	
28		Sealed	–	Sat	95.62	76.53	92.43	
		Soaked	immature	Pure	100.16	126.56	133.25	
				Acid	104.58	100.14	83.65	
168		Sealed	–	Sat	124.10	105.50	99.90	
		Soaked	immature	Pure	79.89	84.80	127.61	
				Acid	125.15	79.75	62.85	
175		Soaked	mature	Acid	96.08	116.01	129.56	
196		Soaked	mature	Acid	108.74	111.50	90.36	
336		Sealed	–	Sat	217.31	157.49	215.70	
		Soaked	immature	Pure	94.70	92.26	112.75	
				Acid	99.60	106.60	111.41	
			mature	Acid	121.70	106.43	119.98	
672		Sealed	–	Sat	135.38	139.68	111.73	
		Soaked	immature	Pure	93.24	89.60	85.43	
				Acid	90.40	92.05	106.61	
Soaked		mature	Acid	110.49	83.44	100.21		
3.8		7	Sealed	–	Sat	134.53	107.07	132.99
			Soaked	immature	Acid	184.58	199.92	198.42
		28	Sealed	–	Sat	420.96	410.88	382.91
			Soaked	immature	Acid	363.14	356.39	384.39
		168	Sealed	–	Sat	371.75	419.07	451.29
	Soaked		immature	Acid	431.99	433.26	426.83	
	336	Sealed	–	Sat	554.00	553.94	568.13	
		Soaked	immature	Acid	390.99	366.12	375.78	
	672	Sealed	–	Sat	492.83	585.51	569.20	
		Soaked	immature	Acid	352.04	343.01	362.10	

Lime Content (%)	Curing	E <sub>50</sub> (MPa)					
	days	Curing type			①	②	③
1.2	7	Sealed	–	Sat	3.97	4.78	4.06
		Soaked	immature	Acid	2.82	2.72	1.68
	28	Sealed	–	Sat	2.03	4.11	3.10
		Soaked	immature	Acid	2.29	3.13	2.12
	168	Sealed	–	Sat	4.91	8.91	4.65
		Soaked	immature	Acid		2.46	1.92
	336	Sealed	–	Sat	6.87	7.36	3.73
		Soaked	immature	Acid	3.10	5.12	3.53
	672	Sealed	–	Sat	5.83	7.23	7.35
		Soaked	immature	Acid	1.68	1.51	2.70
2.5	7	Sealed	–	Sat	18.87	19.39	27.85
		Soaked	immature	Pure	17.51	12.42	16.59
				Acid	19.30	34.32	25.62
	28	Sealed	–	Sat	25.52	28.02	18.53
		Soaked	immature	Pure	35.69	45.57	49.07
				Acid	24.03	35.34	13.25
	168	Sealed	–	Sat	26.23	24.68	23.04
		Soaked	immature	Pure	15.47	18.00	37.50
				Acid	17.55	16.20	9.78
	175	Soaked	mature	Acid	21.92	23.25	30.11
	196	Soaked	mature	Acid	15.19	25.13	13.18
	336	Sealed	–	Sat	33.68	34.01	35.07
		Soaked	immature	Pure	21.25	17.91	28.28
				Acid	26.14	27.29	15.45
			mature	Acid	32.24	25.65	36.98
		672	Sealed	–	Sat	39.55	41.08
	Soaked		immature	Pure	20.16	17.10	21.92
				Acid	15.68	14.35	22.21
Soaked	mature	Acid	19.32	14.72	19.24		
3.8	7	Sealed	–	Sat	22.30	10.02	25.16
		Soaked	immature	Acid	64.20	45.08	61.64
	28	Sealed	–	Sat	150.37	107.99	134.46
		Soaked	immature	Acid	116.44	112.30	97.00
	168	Sealed	–	Sat	45.32	54.90	98.42
		Soaked	immature	Acid	137.66	109.79	99.00
	336	Sealed	–	Sat	190.15	78.66	94.32
		Soaked	immature	Acid	84.61	83.66	81.55
	672	Sealed	–	Sat	114.59	115.50	101.46
		Soaked	immature	Acid	78.67	82.51	83.54

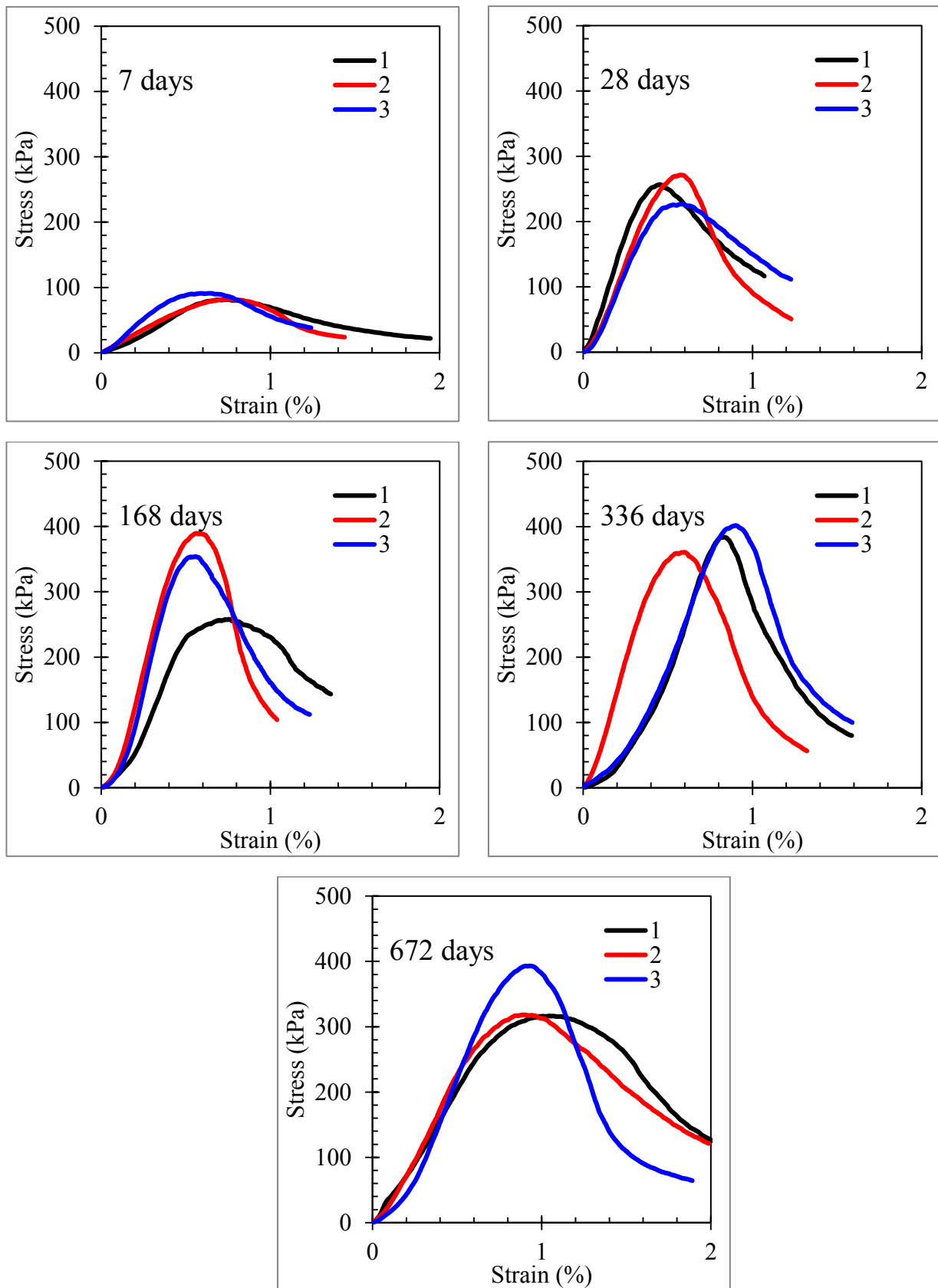
Lime Content (%)	Curing	Failure strain (%)						
	days	Curing type			①	②	③	
1.2	7	Sealed	–	Sat	1.33	1.01	1.40	
		Soaked	immature	Acid	1.53	1.64	3.38	
	28	Sealed	–	Sat	1.69	1.13	1.38	
		Soaked	immature	Acid	1.66	1.32	1.69	
	168	Sealed	–	Sat	0.80	0.71	1.09	
		Soaked	immature	Acid		1.36	1.73	
	336	Sealed	–	Sat	0.97	0.83	1.29	
		Soaked	immature	Acid	1.42	1.04	1.14	
	672	Sealed	–	Sat	1.17	0.87	0.84	
		Soaked	immature	Acid	1.99	1.91	1.41	
	2.5	7	Sealed	–	Sat	0.57	0.55	0.81
			Soaked	immature	Pure	0.77	1.12	0.85
Acid					0.76	0.44	0.54	
28		Sealed	–	Sat	0.56	0.44	0.60	
		Soaked	immature	Pure	0.53	0.43	0.45	
				Acid	0.68	0.54	0.82	
168		Sealed	–	Sat	0.64	0.55	0.67	
		Soaked	immature	Pure	1.02	0.74	0.48	
				Acid	0.94	0.92	1.66	
175		Soaked	mature	Acid	0.62	0.71	0.68	
196		Soaked	mature	Acid	1.11	0.62	0.76	
336		Sealed	–	Sat	1.26	0.92	1.40	
		Soaked	immature	Pure	0.73	0.92	0.57	
				Acid	0.55	0.63	0.98	
			mature	Acid	0.53	0.58	0.49	
		672	Sealed	–	Sat	0.51	0.50	0.76
Soaked		immature	Pure	0.66	0.67	0.57		
			Acid	0.82	0.93	0.67		
		mature	Acid	0.71	0.76	0.68		
3.8		7	Sealed	–	Sat	0.81	1.16	0.89
			Soaked	immature	Acid	0.56	0.73	0.73
	28	Sealed	–	Sat	0.47	0.58	0.48	
		Soaked	immature	Acid	0.47	0.50	0.56	
	168	Sealed	–	Sat	1.04	0.82	0.55	
		Soaked	immature	Acid	0.47	0.54	0.56	
	336	Sealed	–	Sat	0.50	0.82	0.80	
		Soaked	immature	Acid	0.59	0.54	0.59	
	672	Sealed	–	Sat	0.59	0.64	0.71	
		Soaked	immature	Acid	0.56	0.56	0.54	

Lime Content (%)	Curing	water content, w(%)					
	days	Curing type			①	②	③
1.2	7	Sealed	–	Sat	31.40	31.30	31.20
		Soaked	immature	Acid	31.20	31.10	31.10
	28	Sealed	–	Sat	31.50	31.60	31.50
		Soaked	immature	Acid	32.40	32.60	32.70
	168	Sealed	–	Sat	30.80	31.30	30.90
		Soaked	immature	Acid		34.70	34.30
	336	Sealed	–	Sat	30.46	30.09	29.75
		Soaked	immature	Acid	33.40	32.70	33.40
	672	Sealed	–	Sat	30.14	30.78	30.25
		Soaked	immature	Acid	33.70	33.53	34.53
2.5	7	Sealed	–	Sat	31.50	30.80	29.50
		Soaked	immature	Pure	30.70	30.70	31.10
				Acid	30.90	31.50	31.50
	28	Sealed	–	Sat	30.60	31.10	31.00
		Soaked	immature	Pure	32.90	32.60	33.00
				Acid	32.80	32.30	33.20
	168	Sealed	–	Sat	34.30	34.40	34.10
		Soaked	immature	Pure	33.90	35.80	35.30
				Acid	34.60	35.30	35.50
	175	Soaked	mature	Acid	30.10	29.70	30.30
	196	Soaked	mature	Acid	32.20	32.40	32.30
	336	Sealed	–	Sat	27.01	28.15	27.56
		Soaked	immature	Pure	34.00	35.20	34.00
				Acid	32.97	34.09	34.20
			mature	Acid	32.95	33.80	33.47
	672	Sealed	–	Sat	31.78	32.58	32.93
		Soaked	immature	Pure	34.88	34.76	34.87
				Acid	33.08	34.18	33.77
Soaked	mature	Acid	34.64	34.10	35.00		
3.8	7	Sealed	–	Sat	34.20	33.90	34.20
		Soaked	immature	Acid	28.30	28.90	28.50
	28	Sealed	–	Sat	34.00	33.90	33.90
		Soaked	immature	Acid	31.10	30.70	31.00
	168	Sealed	–	Sat	33.10	33.90	34.00
		Soaked	immature	Acid	33.80	33.80	33.50
	336	Sealed	–	Sat	33.10	33.50	33.50
		Soaked	immature	Acid	33.60	34.40	34.20
	672	Sealed	–	Sat	32.91	34.87	32.28
		Soaked	immature	Acid	32.02	32.83	32.25

Lime Content (%)	Curing	dry density, $\rho_d(\text{g/cm}^3)$						
	days	Curing type			①	②	③	
1.2	7	Sealed	–	Sat	1.42	1.42	1.41	
		Soaked	immature	Acid	1.42	1.41	1.43	
	28	Sealed	–	Sat	1.42	1.41	1.41	
		Soaked	immature	Acid	1.40	1.39	1.38	
	168	Sealed	–	Sat	1.42	1.41	1.42	
		Soaked	immature	Acid		1.40	1.39	
	336	Sealed	–	Sat	1.40	1.40	1.42	
		Soaked	immature	Acid	1.41	1.41	1.39	
	672	Sealed	–	Sat	1.41	1.40	1.40	
		Soaked	immature	Acid	1.43	1.41	1.39	
	2.5	7	Sealed	–	Sat	1.41	1.41	1.41
			Soaked	immature	Pure	1.41	1.40	1.39
Acid					1.40	1.40	1.39	
28			Sealed	–	Sat	1.40	1.39	1.41
		Soaked	immature	Pure	1.40	1.41	1.38	
				Acid	1.40	1.41	1.40	
		168	Sealed	–	Sat	1.39	1.39	1.40
Soaked			immature	Pure	1.39	1.37	1.38	
				Acid	1.38	1.38	1.37	
175			Soaked	mature	Acid	1.41	1.40	1.41
196		Soaked	mature	Acid	1.42	1.38	1.39	
336		Sealed	–	Sat	1.40	1.40	1.41	
		Soaked	immature	Pure	1.38	1.37	1.38	
				Acid	1.41	1.38	1.38	
			mature	Acid	1.40	1.38	1.39	
		672	Sealed	–	Sat	1.40	1.40	1.40
			Soaked	immature	Pure	1.37	1.39	1.38
					Acid	1.39	1.38	1.38
			Soaked	mature	Acid	1.37	1.37	1.37
3.8		7	Sealed	–	Sat	1.41	1.41	1.40
			Soaked	immature	Acid	1.42	1.41	1.41
		28	Sealed	–	Sat	1.43	1.43	1.43
			Soaked	immature	Acid	1.40	1.41	1.40
		168	Sealed	–	Sat	1.41	1.41	1.40
	Soaked		immature	Acid	1.38	1.38	1.39	
	336	Sealed	–	Sat	1.40	1.40	1.41	
		Soaked	immature	Acid	1.38	1.38	1.39	
	672	Sealed	–	Sat	1.40	1.39	1.42	
		Soaked	immature	Acid	1.40	1.40	1.40	

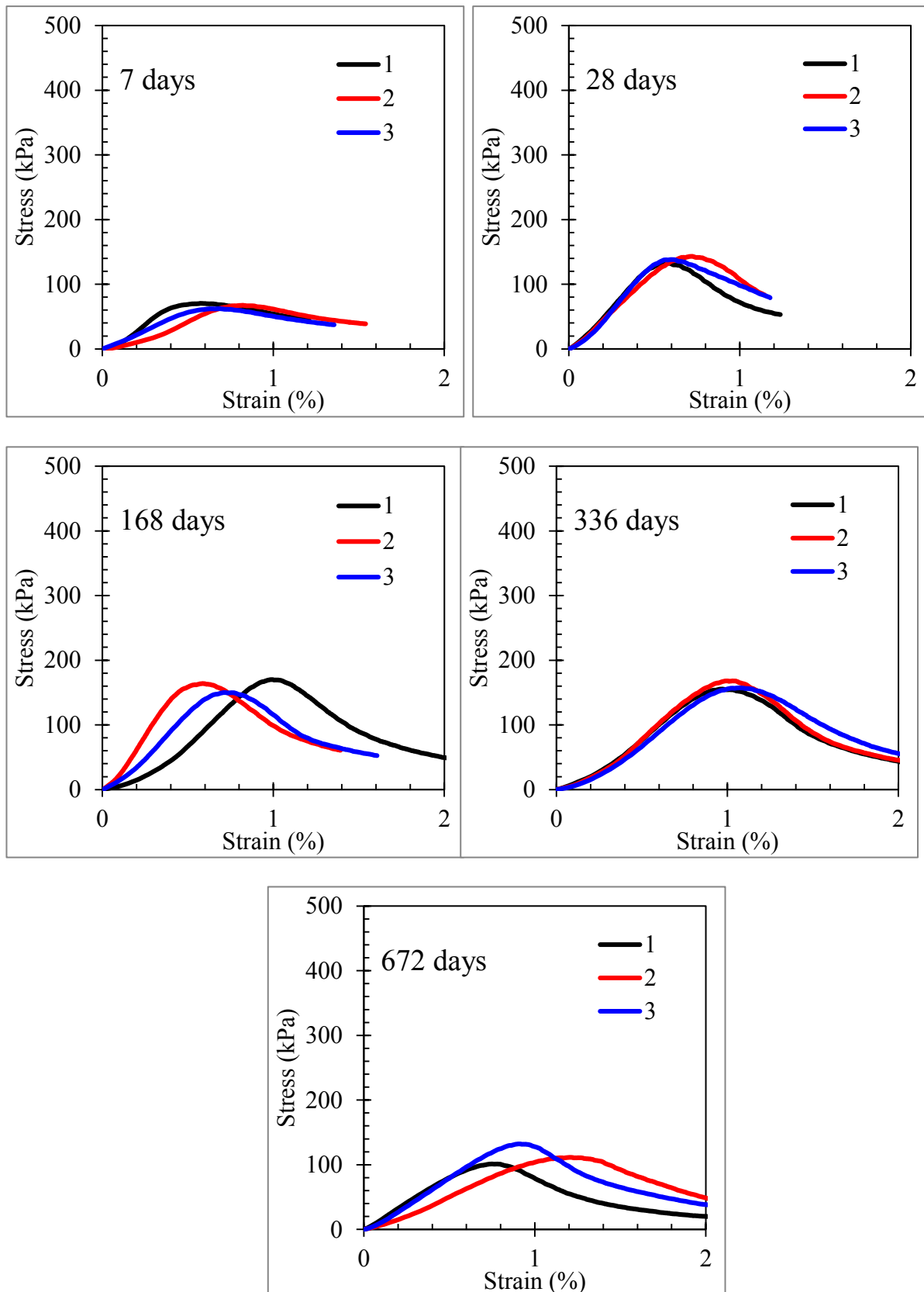
Lime Content (%)	Curing	Degree of saturation, Sr (%)						
	days	Curing type			①	②	③	
1.2	7	Sealed	–	Sat	92.72	92.04	90.83	
		Soaked	immature	Acid	91.25	90.51	93.25	
	28	Sealed	–	Sat	93.30	92.18	91.15	
		Soaked	immature	Acid	92.60	91.60	90.63	
	168	Sealed	–	Sat	91.24	90.68	91.51	
		Soaked	immature	Acid		98.90	96.60	
	336	Sealed	–	Sat	87.49	86.56	87.16	
		Soaked	immature	Acid	97.20	94.50	94.80	
	672	Sealed	–	Sat	87.51	88.15	87.04	
		Soaked	immature	Acid	100.16	97.48	97.61	
	2.5	7	Sealed	–	Sat	91.70	89.16	85.30
			Soaked	immature	Pure	88.93	88.25	88.15
Acid					89.16	89.76	89.29	
28		Sealed	–	Sat	87.02	88.19	89.74	
		Soaked	immature	Pure	94.29	94.12	91.85	
				Acid	93.47	93.29	95.27	
168		Sealed	–	Sat	97.08	97.06	98.21	
		Soaked	immature	Pure	95.30	97.60	97.70	
				Acid	96.70	98.70	97.00	
175		Soaked	mature	Acid	87.20	84.70	88.80	
196		Soaked	mature	Acid	94.30	90.30	91.30	
336		Sealed	–	Sat	77.72	80.23	79.58	
		Soaked	immature	Pure	95.30	95.80	95.30	
				Acid	95.31	95.26	94.62	
			mature	Acid	94.25	94.52	94.25	
672		Sealed	–	Sat	91.74	94.04	94.96	
		Soaked	immature	Pure	95.56	98.12	96.85	
				Acid	92.96	95.82	93.98	
Soaked		mature	Acid	95.41	94.00	95.55		
3.8		7	Sealed	–	Sat	98.71	97.12	96.99
			Soaked	immature	Acid	82.53	83.90	82.29
	28	Sealed	–	Sat	100.00	100.00	100.00	
		Soaked	immature	Acid	88.82	88.05	88.25	
	168	Sealed	–	Sat	95.70	97.00	96.50	
		Soaked	immature	Acid	93.80	93.60	94.20	
	336	Sealed	–	Sat	94.20	95.90	96.30	
		Soaked	immature	Acid	92.90	94.60	95.20	
	672	Sealed	–	Sat	94.03	97.51	94.77	
		Soaked	immature	Acid	90.78	93.22	91.63	

**Cement 3.5 % - Sealed**

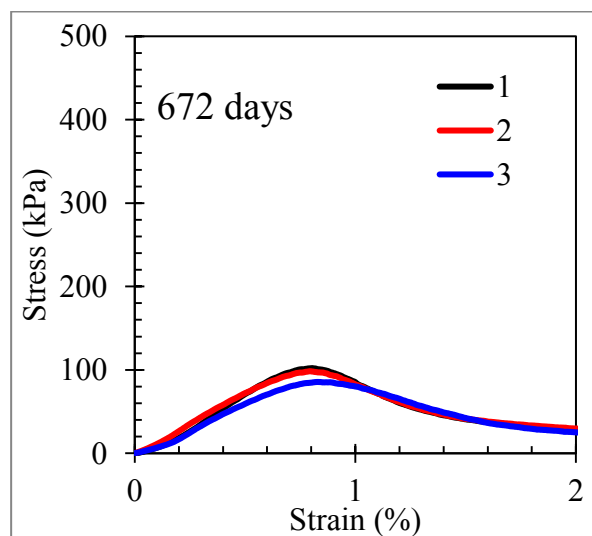
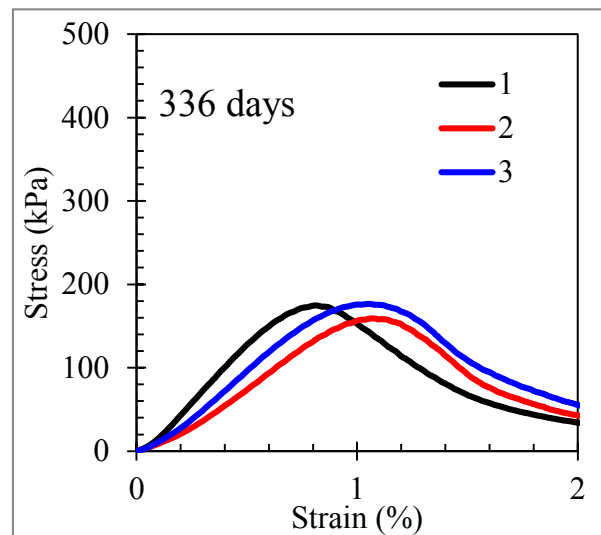
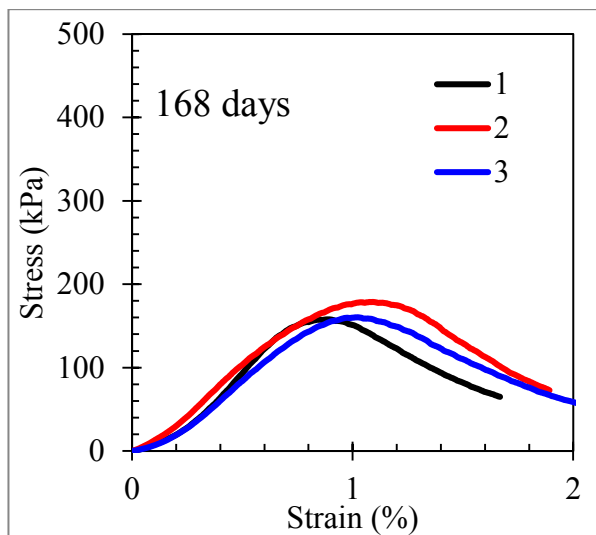
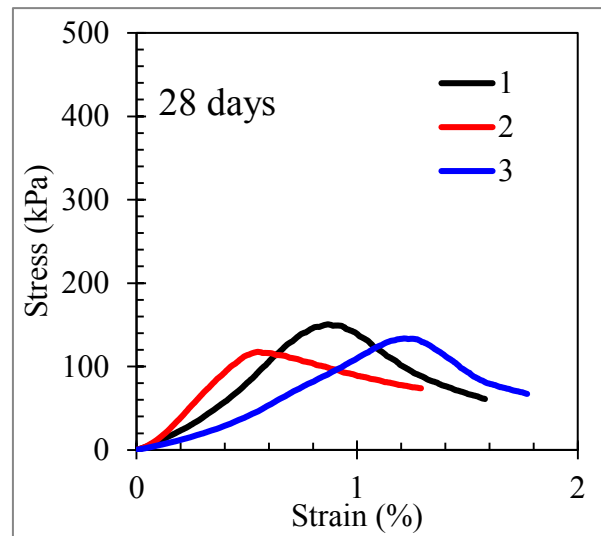
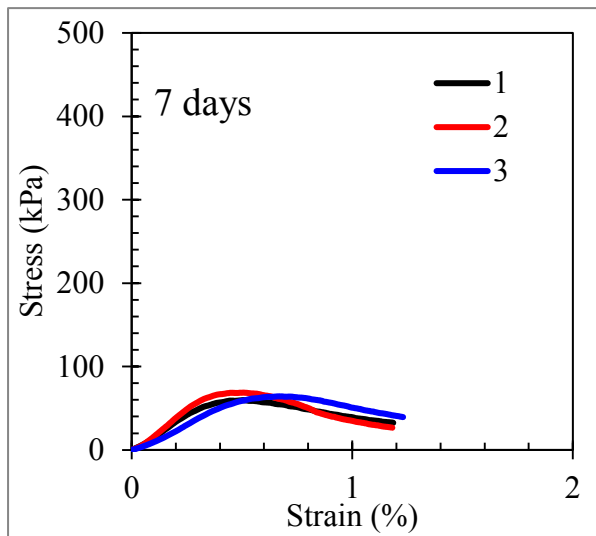




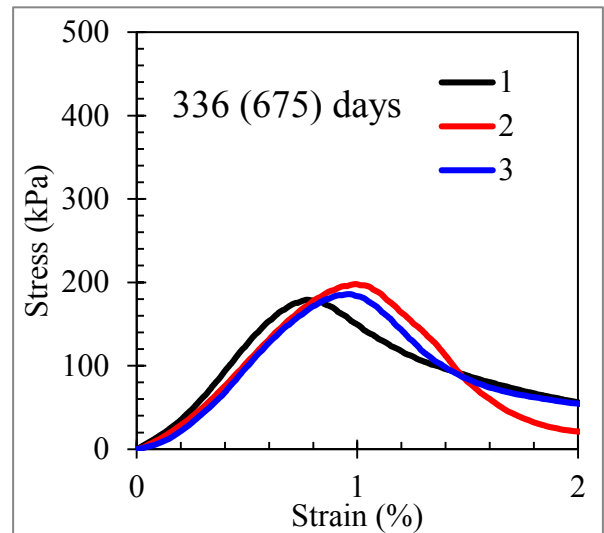
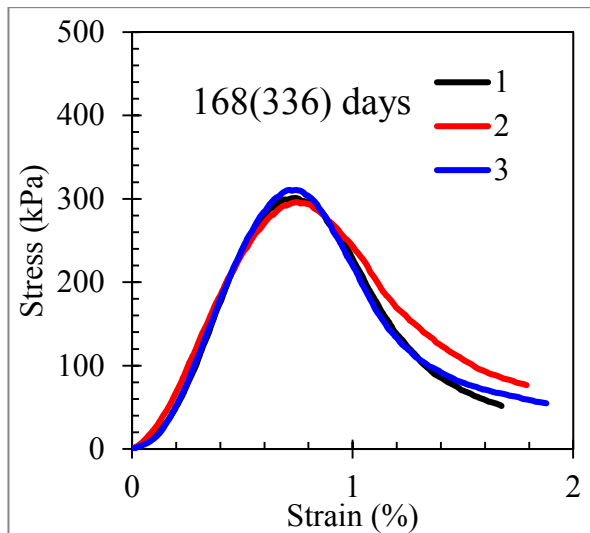
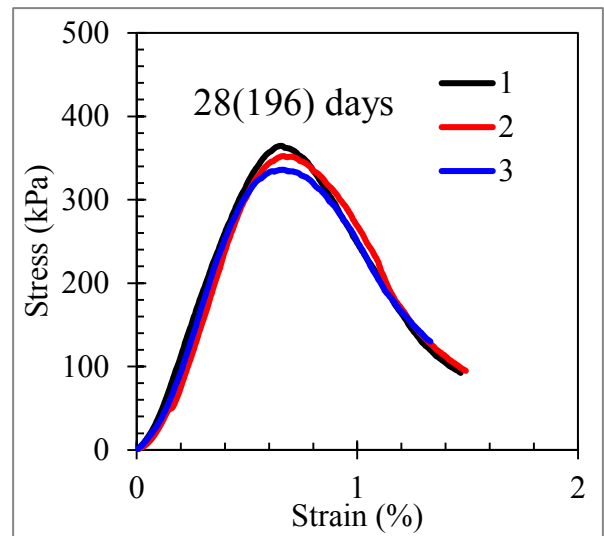
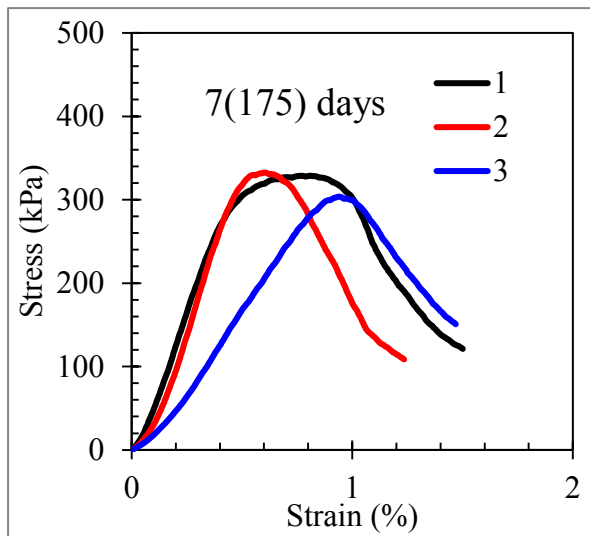
**Cement 3.5 % - Soaked Acid (immature)**



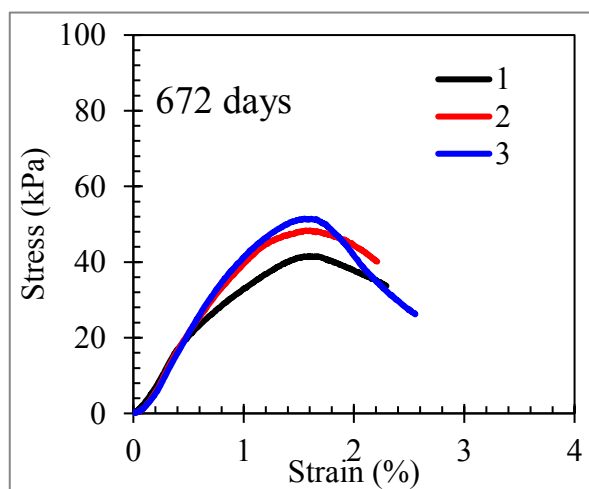
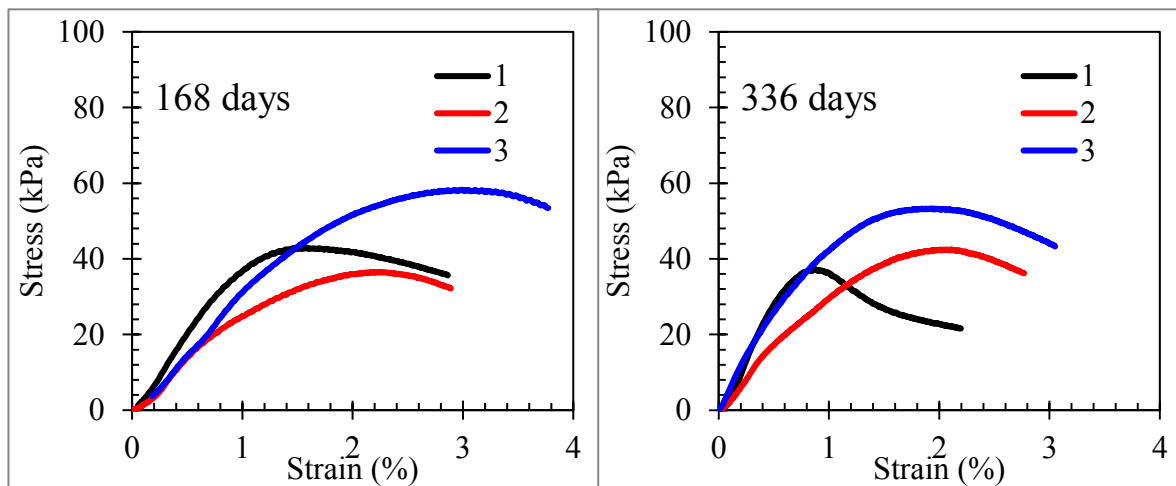
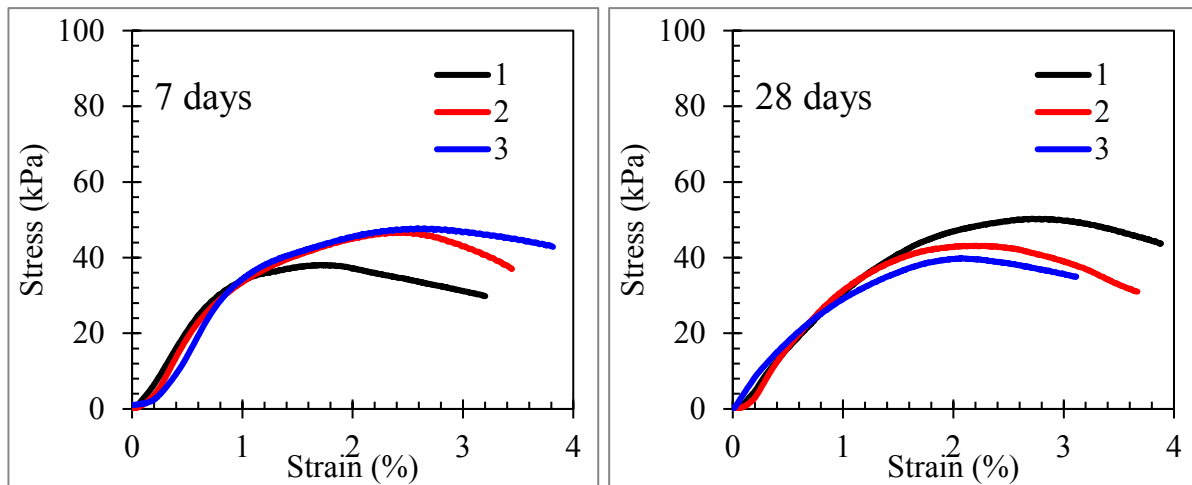
**Cement 3.5 % - Soaked pure (immature)**



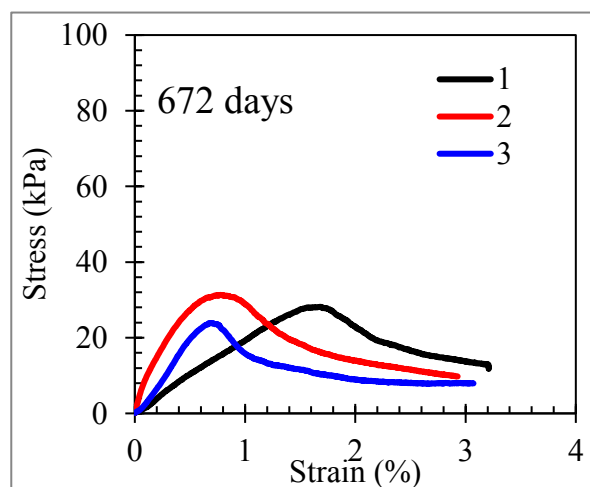
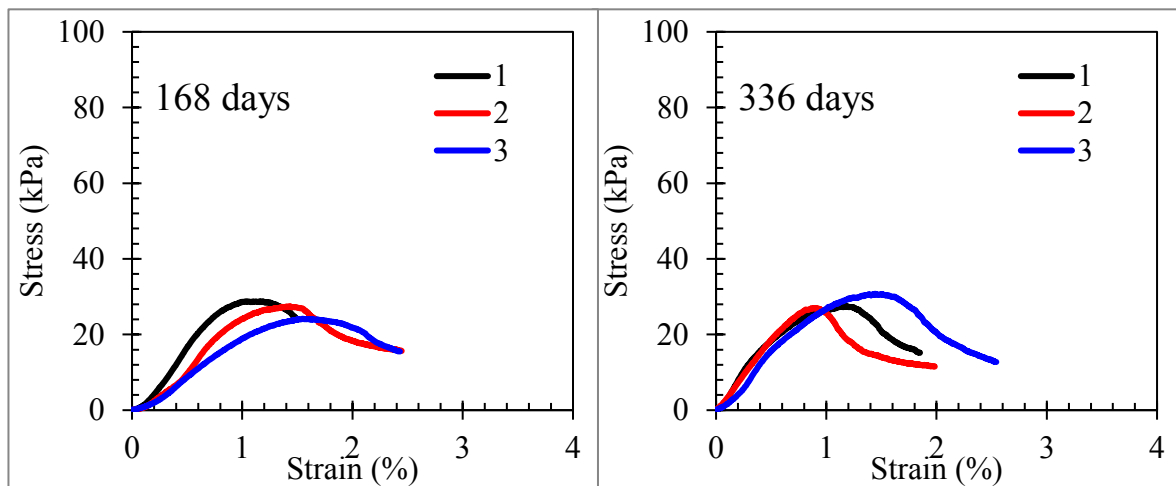
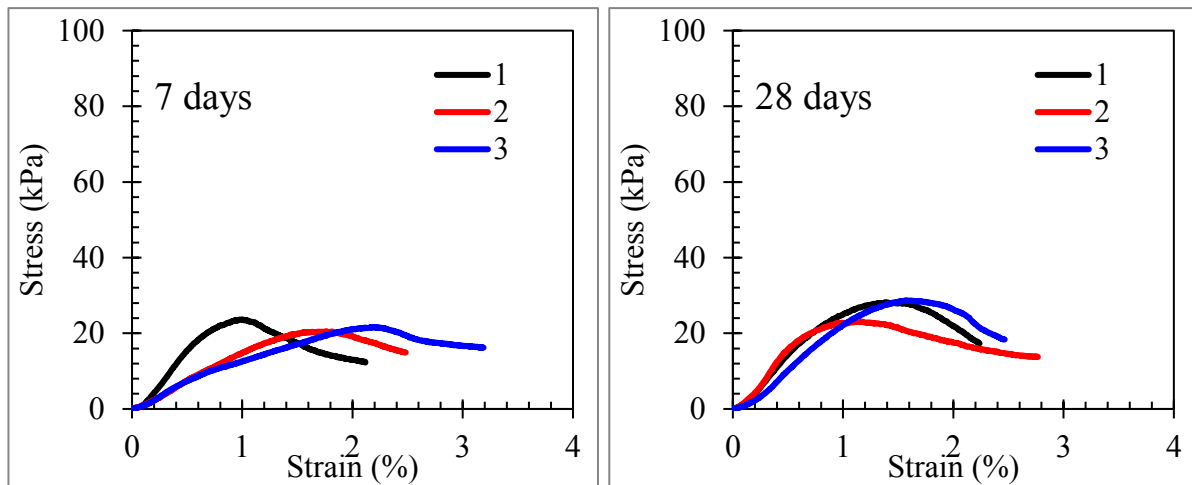
**Cement 3.5 % - Soak acid (mature)**



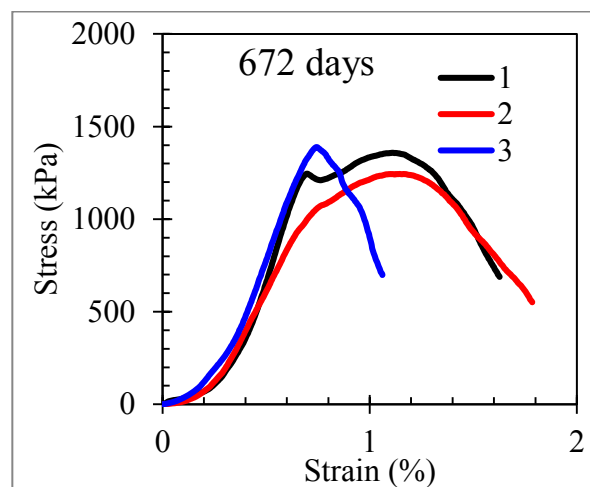
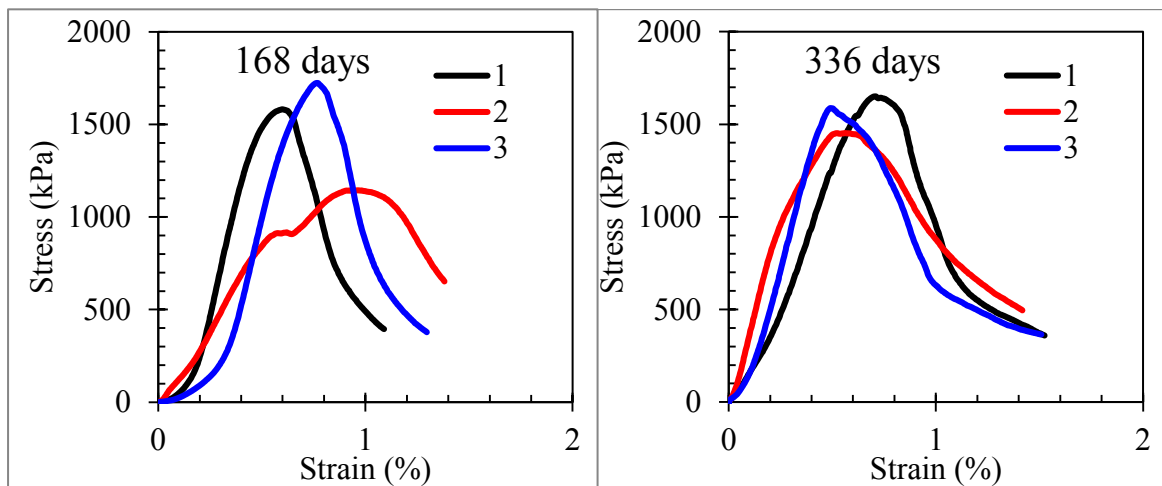
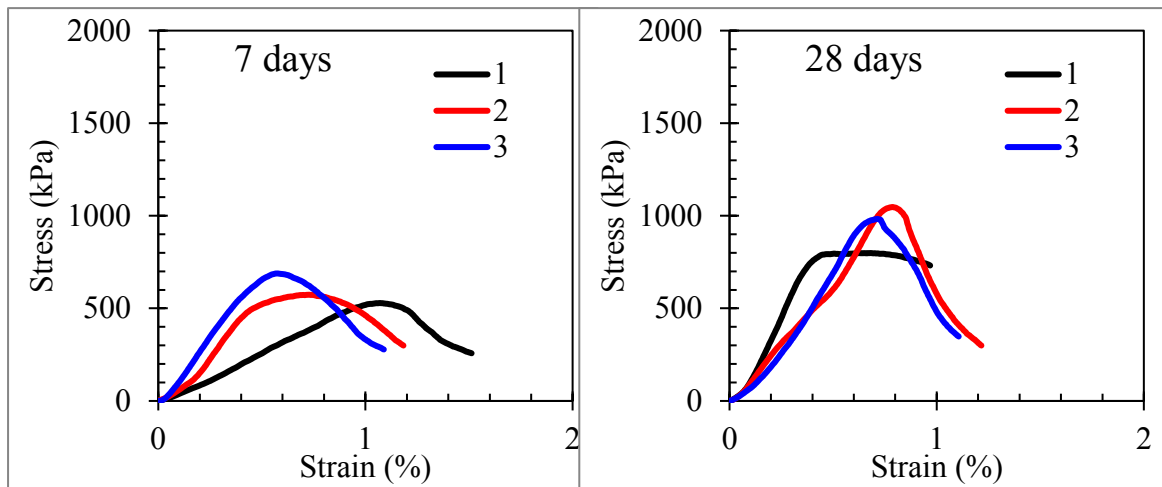
**Cement 1.7 % - Sealed**



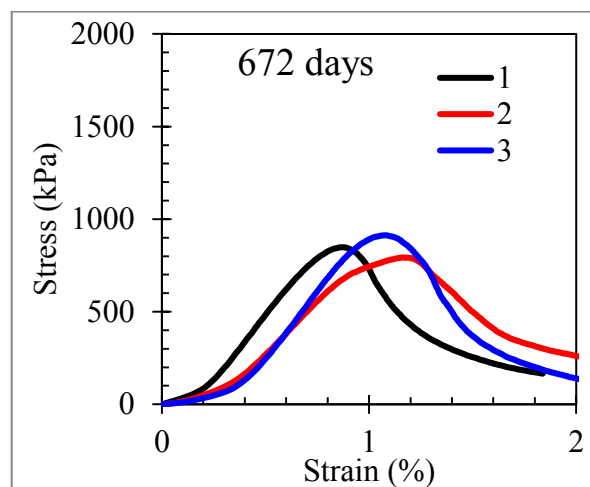
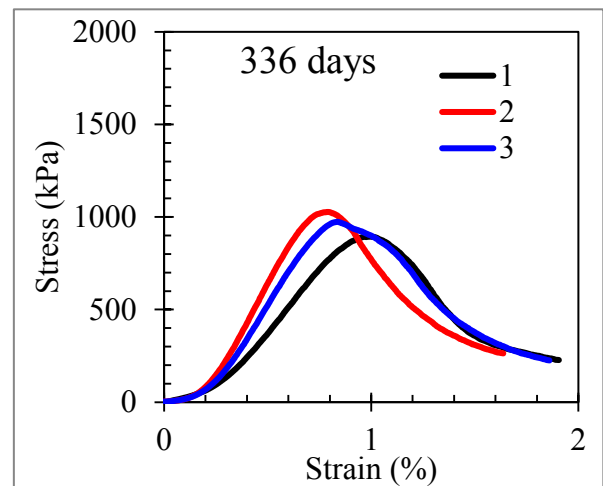
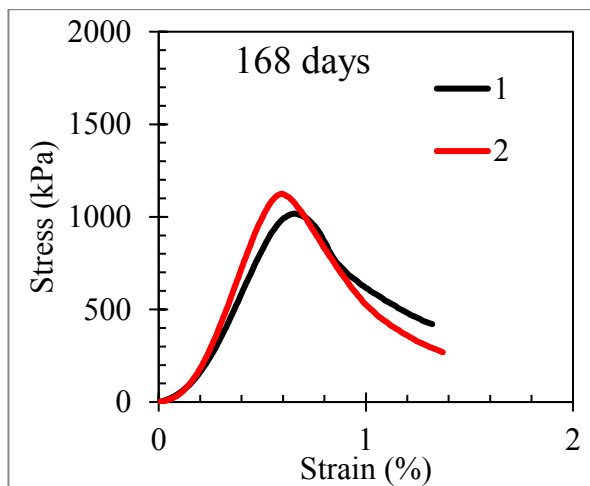
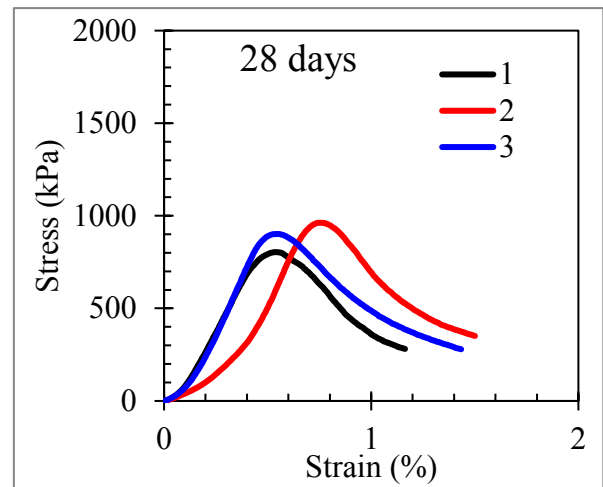
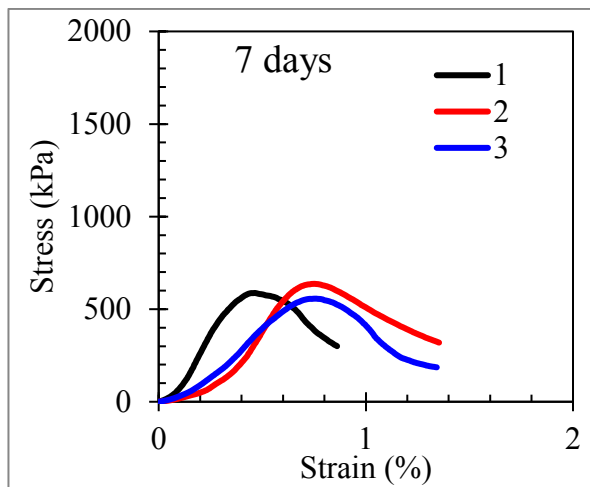
**Cement 1.7 % - Soaked Acid (immature)**



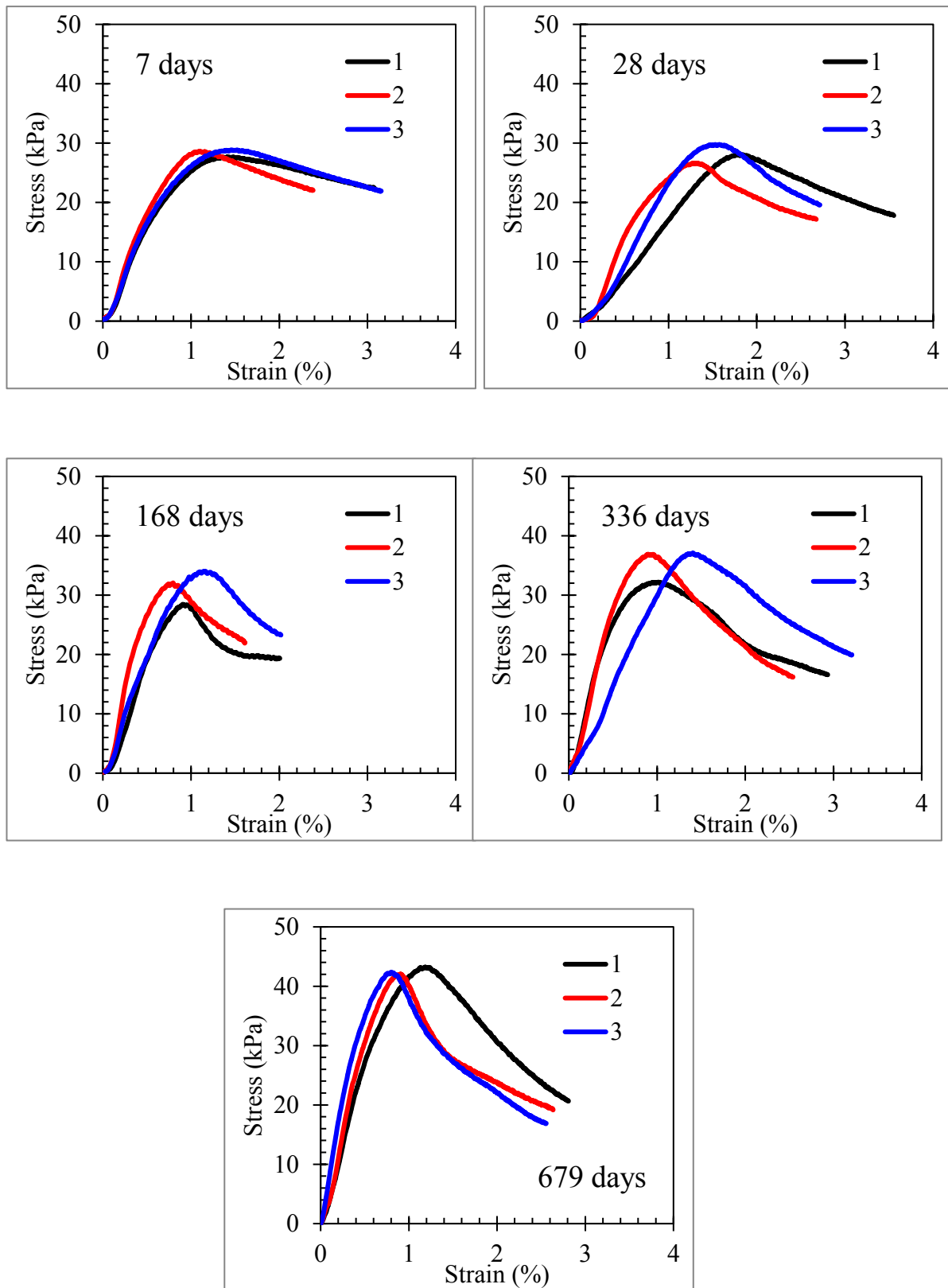
**Cement 5.3 % - Sealed**



**Cement 5.3 % - Soaked acid (immature)**

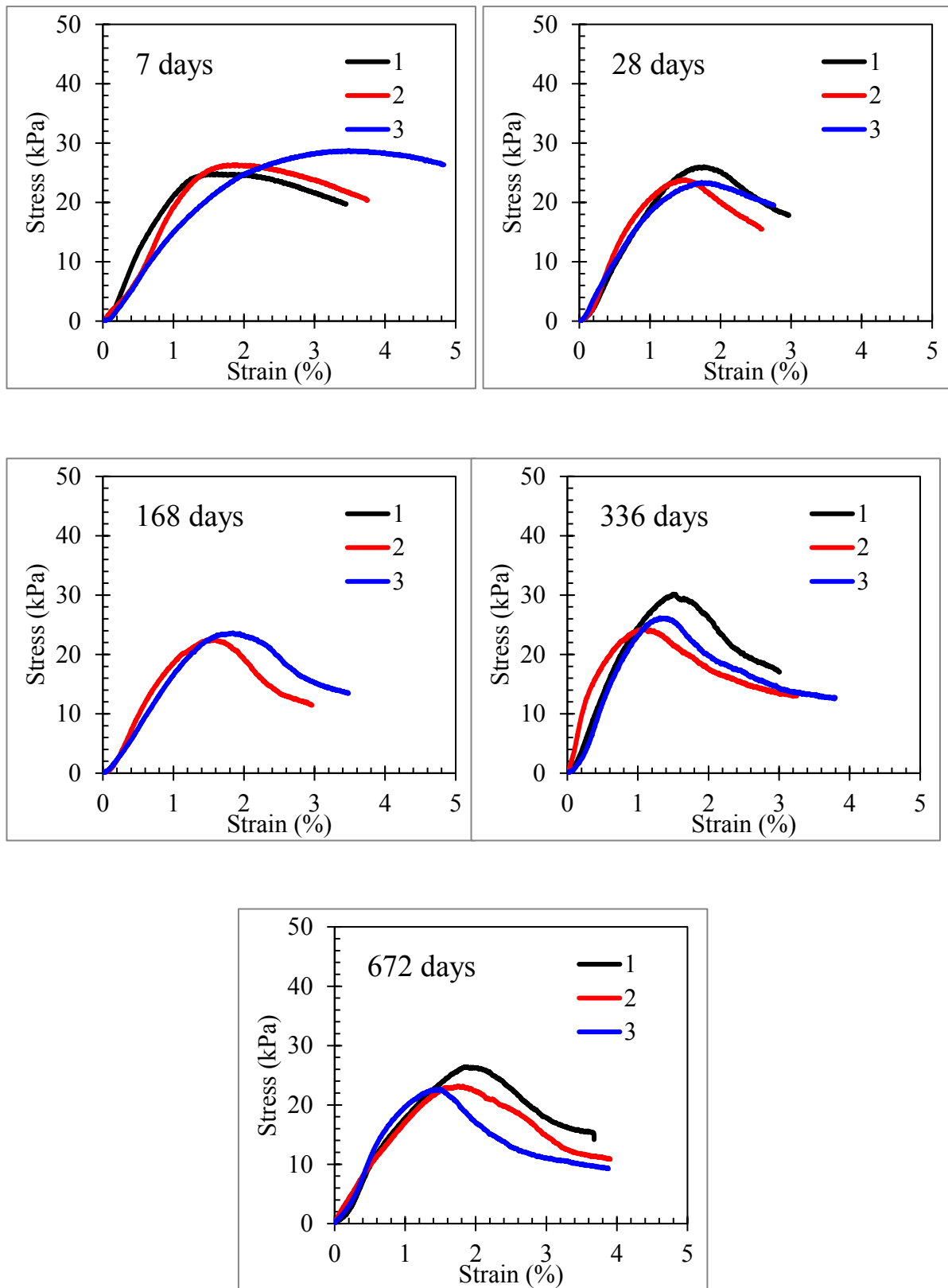


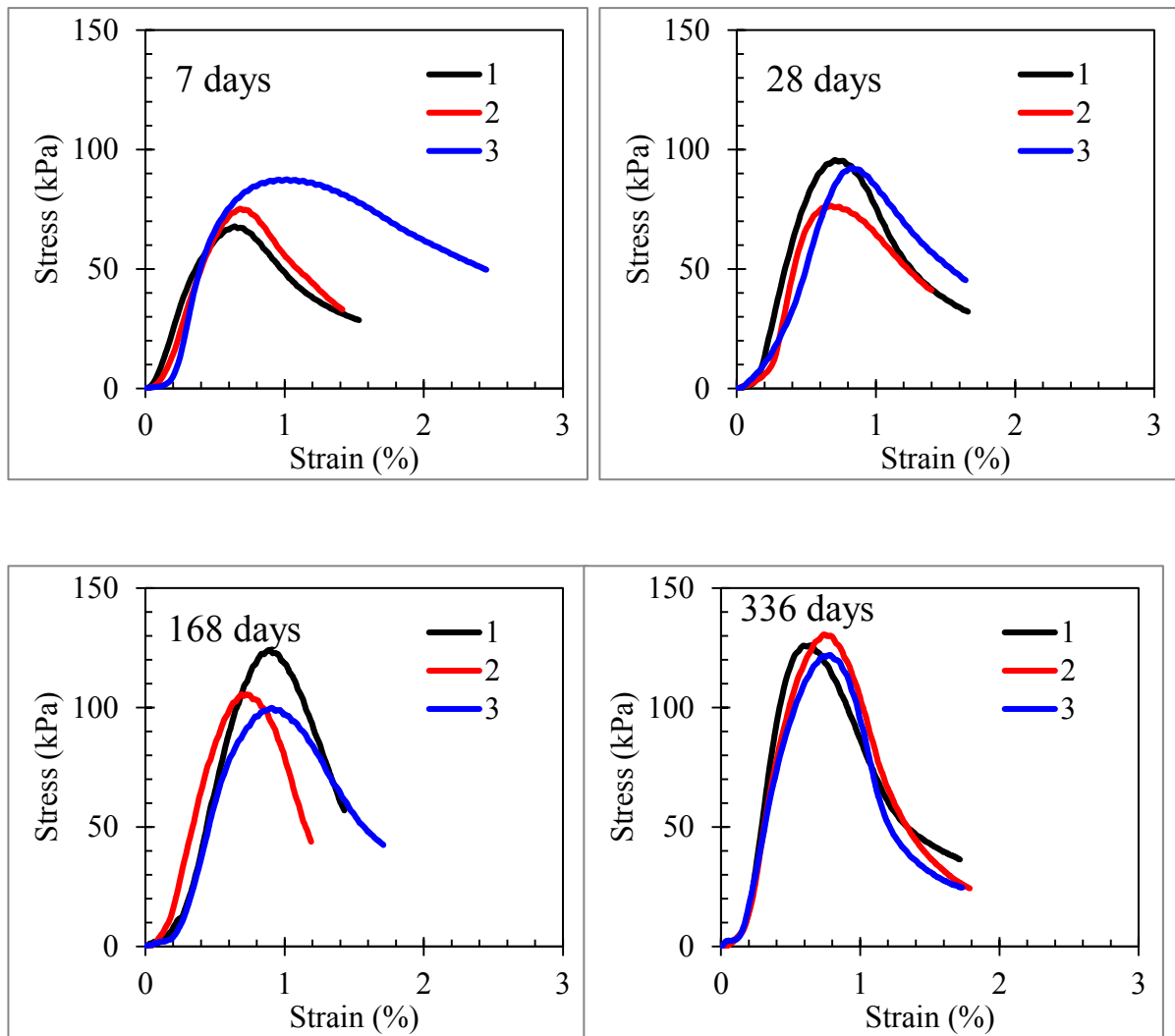
**Lime 1.2 % - Sealed**



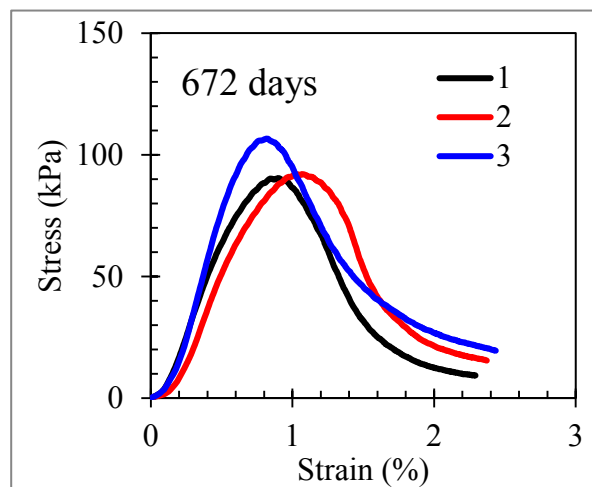
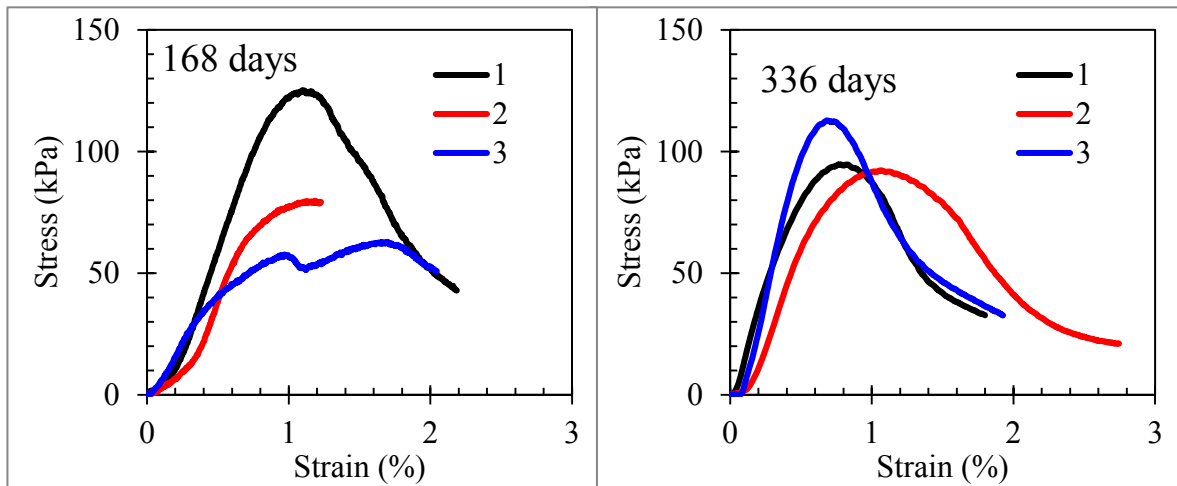
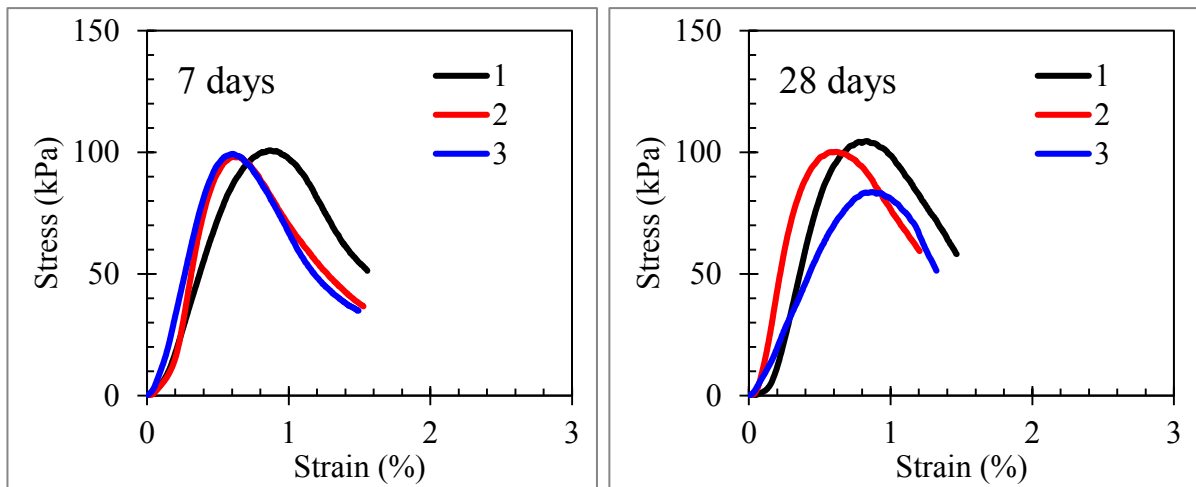


**Lime 1.2 % - Soaked Acid (immature)**

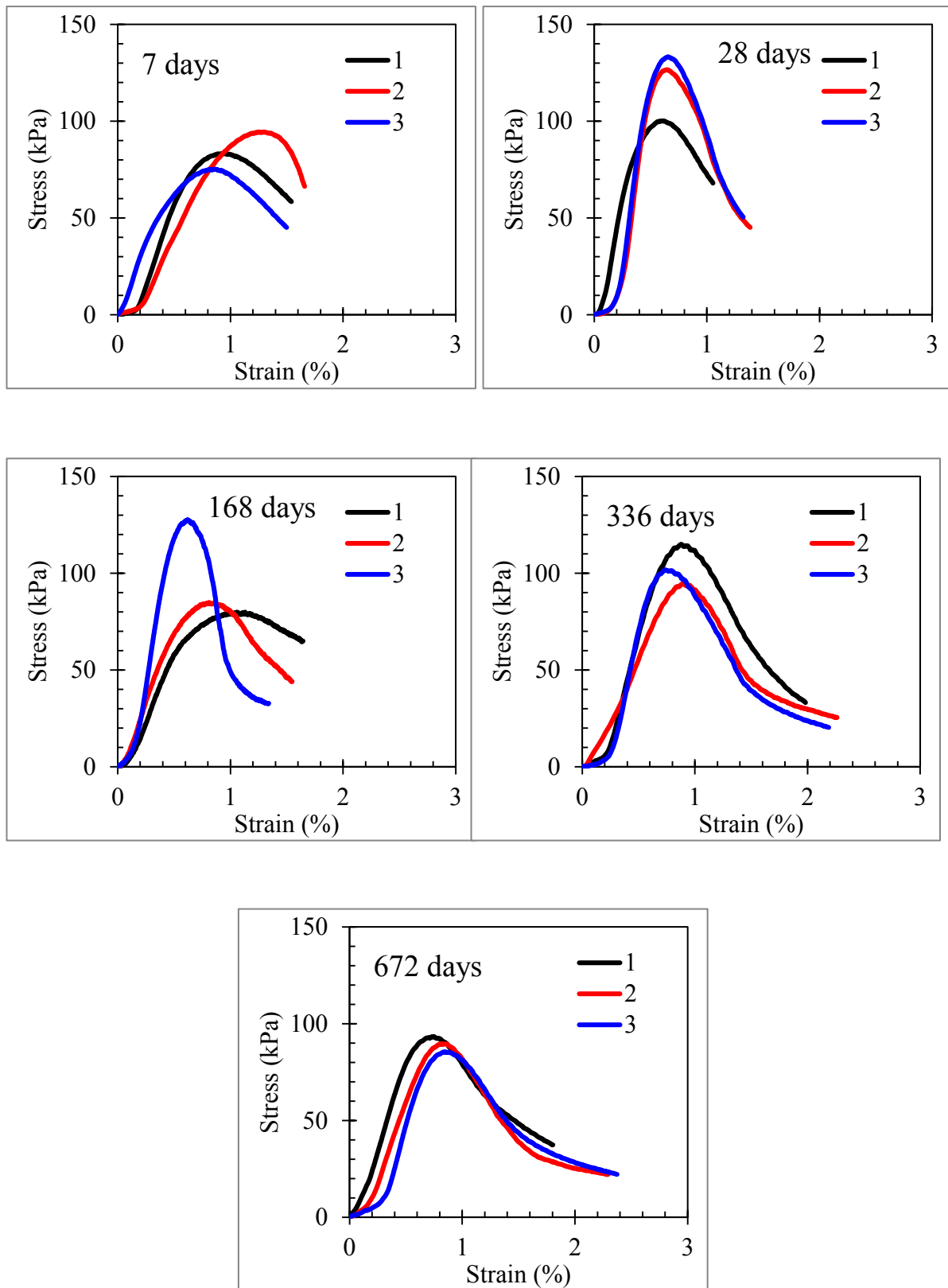


**Lime 2.5 % - Sealed**

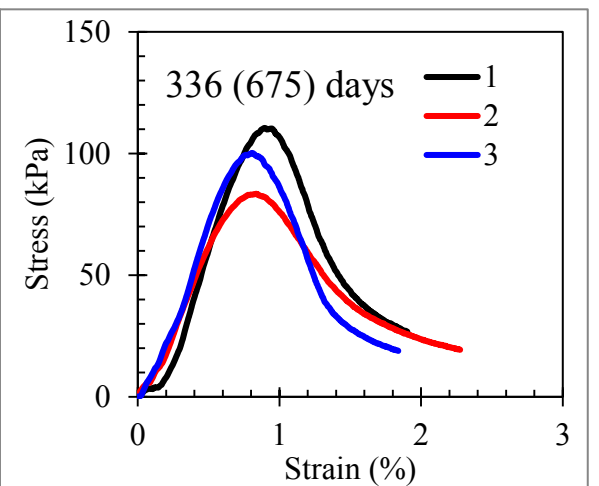
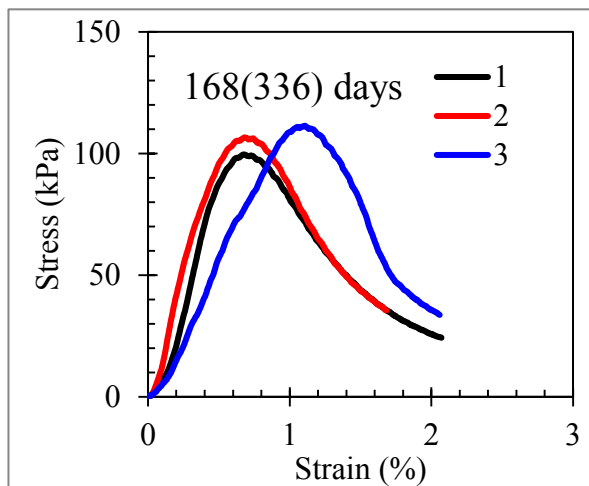
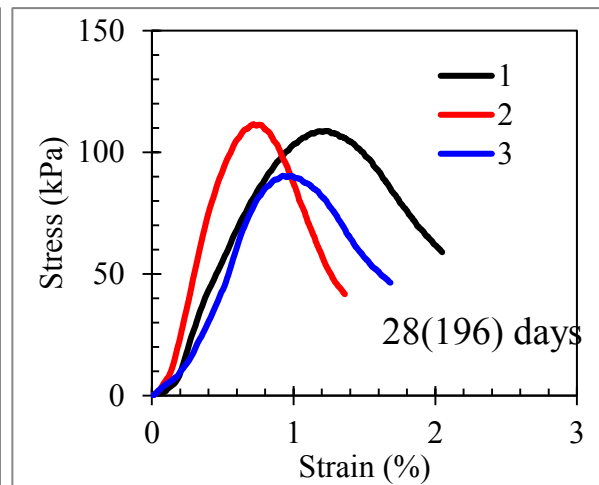
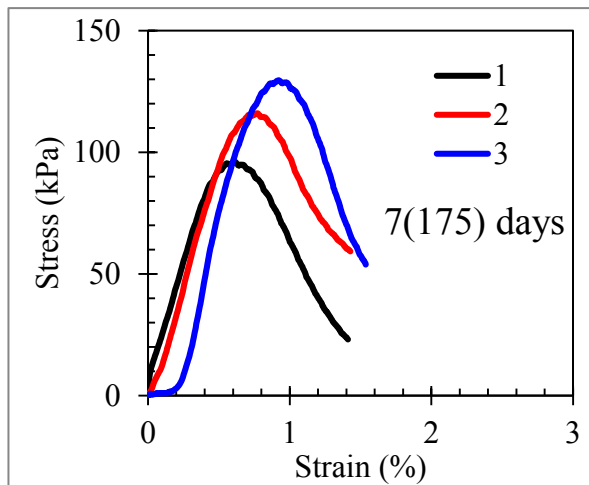
**Lime 2.5% - Soaked Acid (immature)**



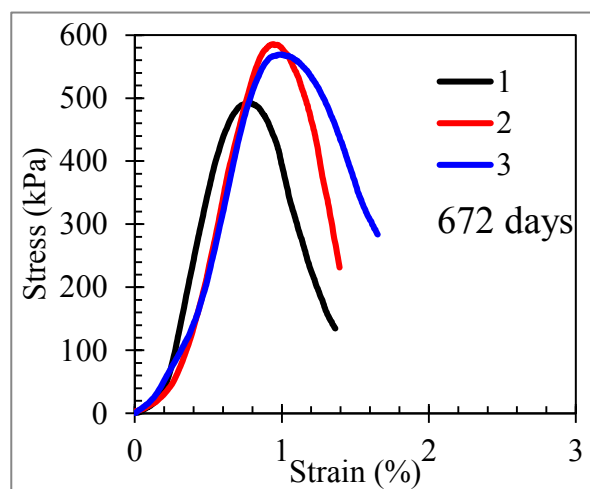
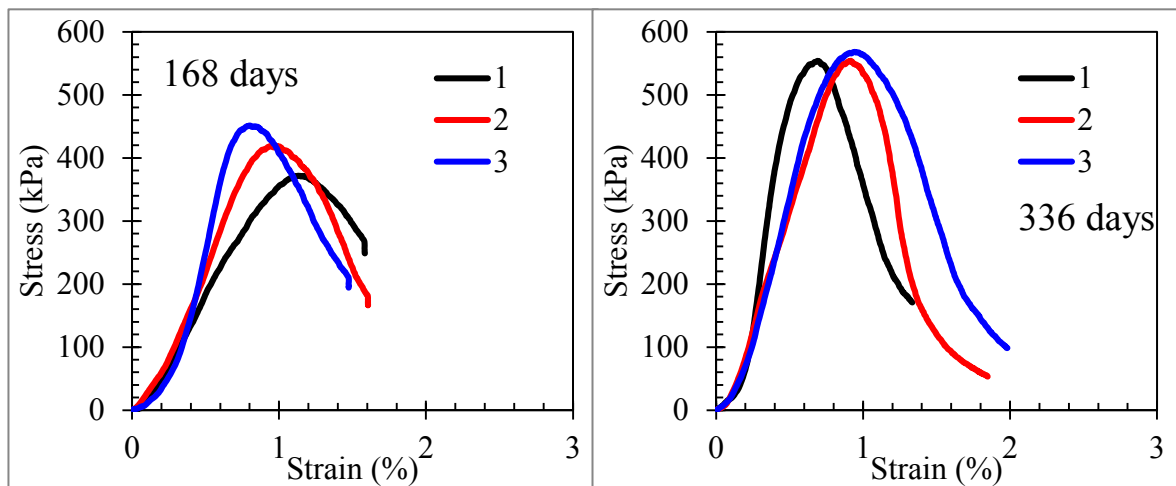
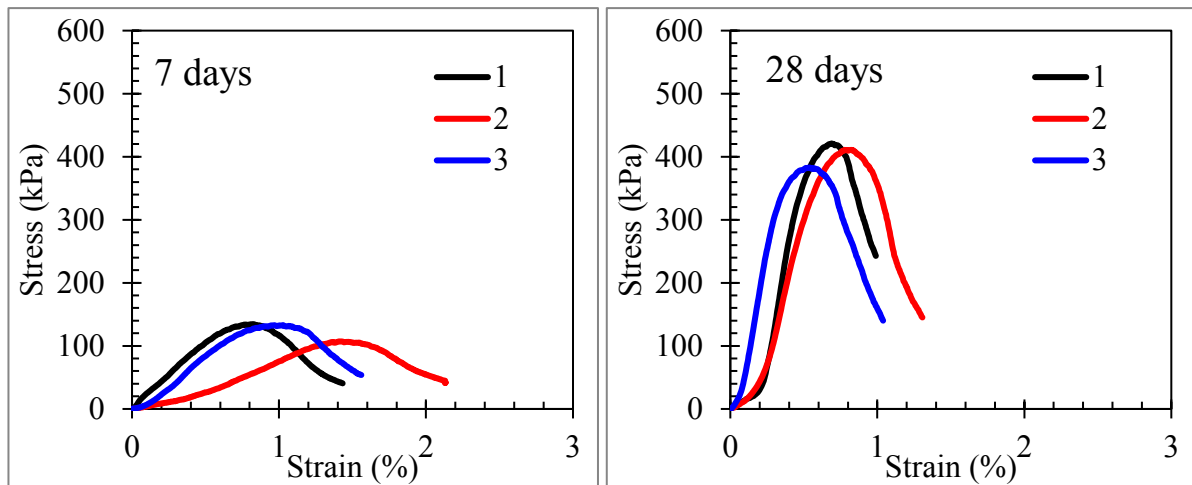
**Lime 2.5 %- Soaked Pure (immature)**



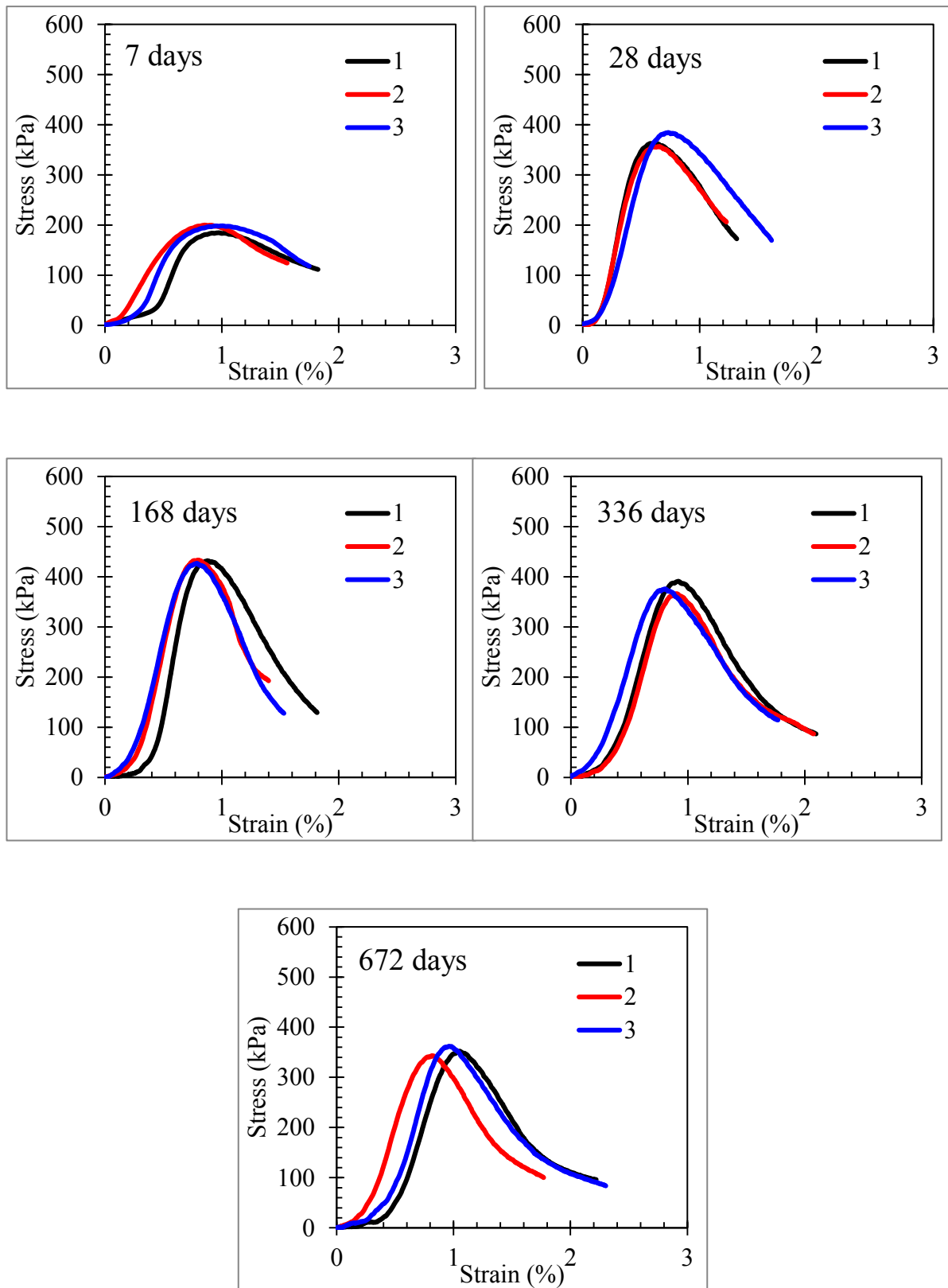
**Lime 2.5% - Soaked acid (mature)**



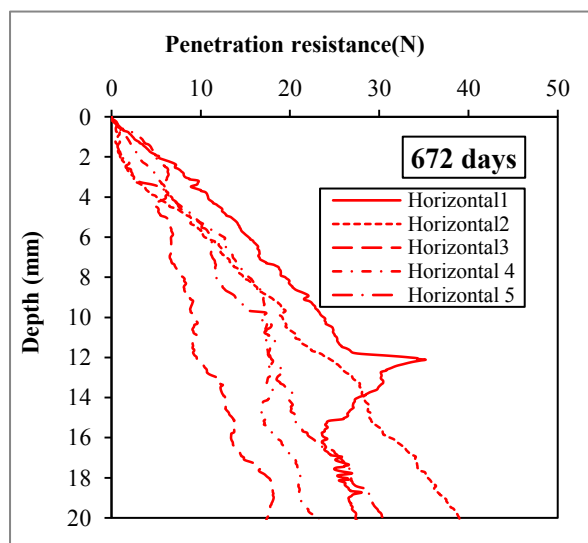
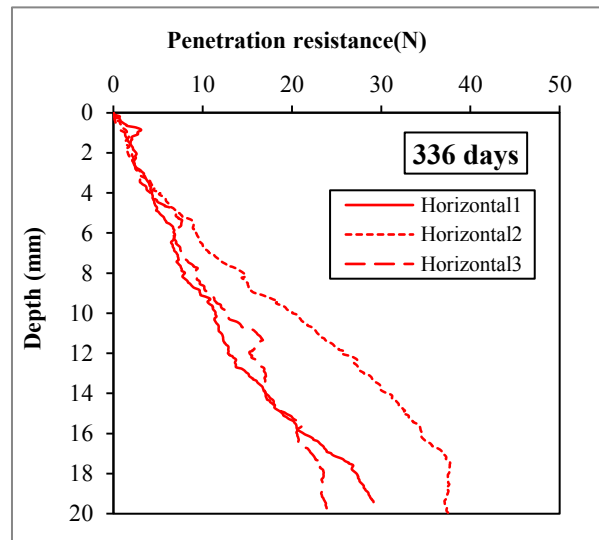
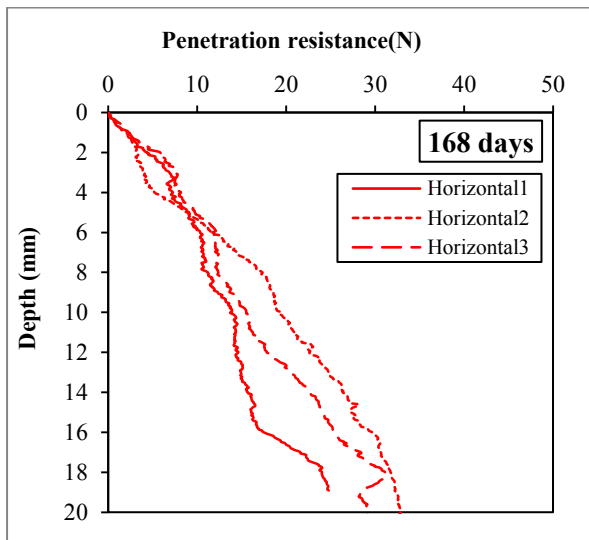
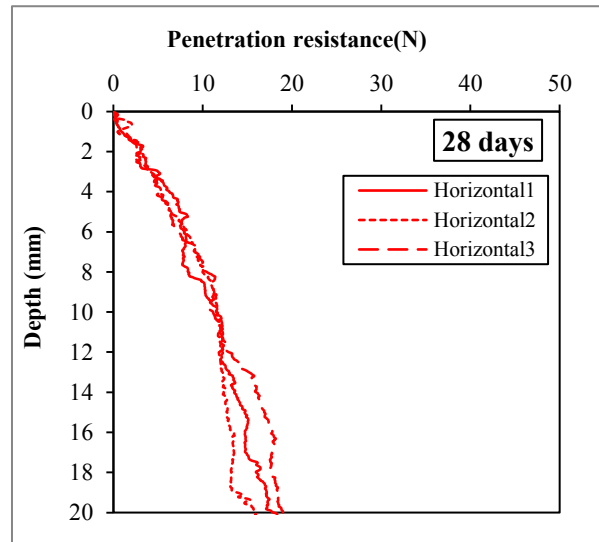
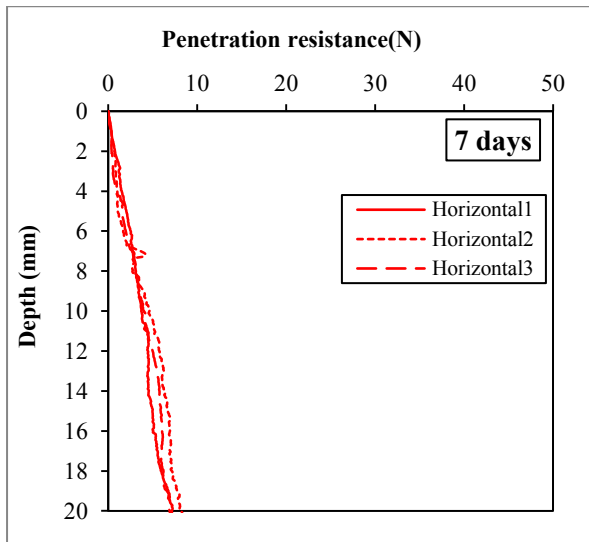
**Lime 3.8 % - Sealed**



**Lime 3.8% - Soaked Acid (immature)**

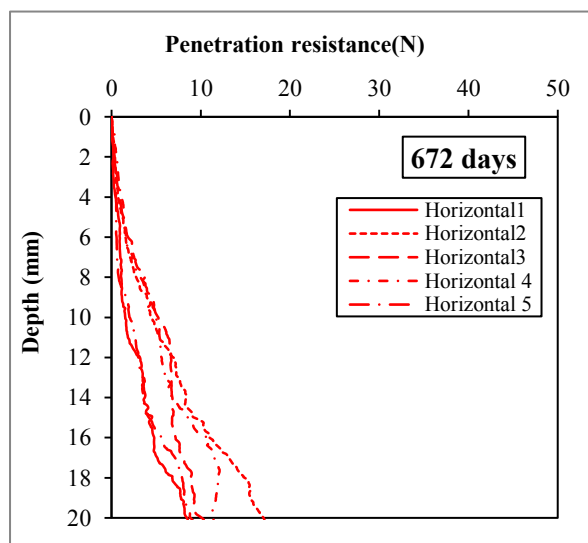
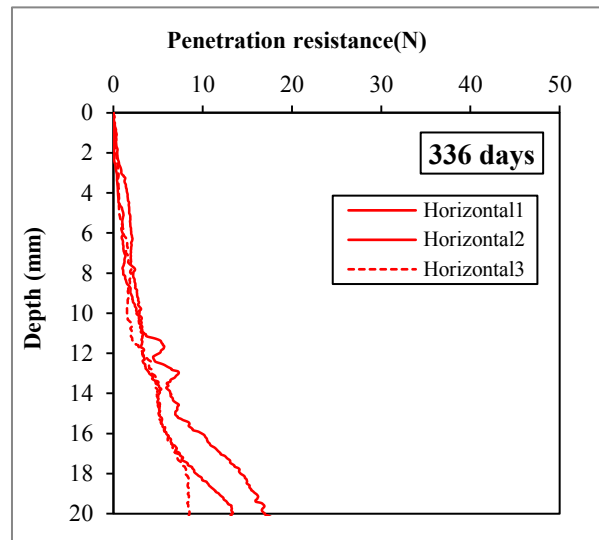
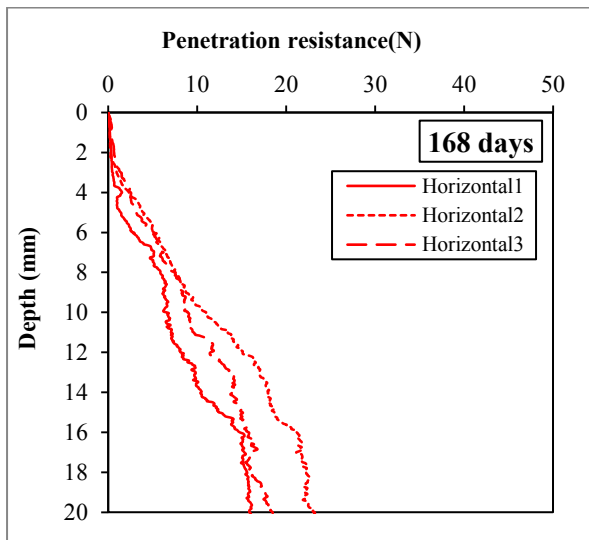
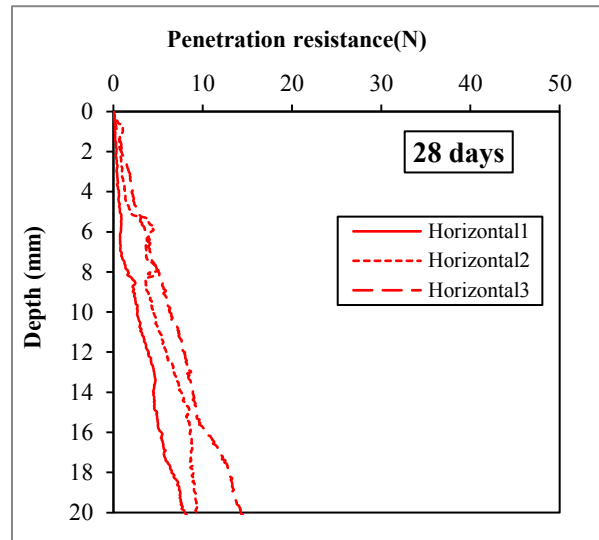
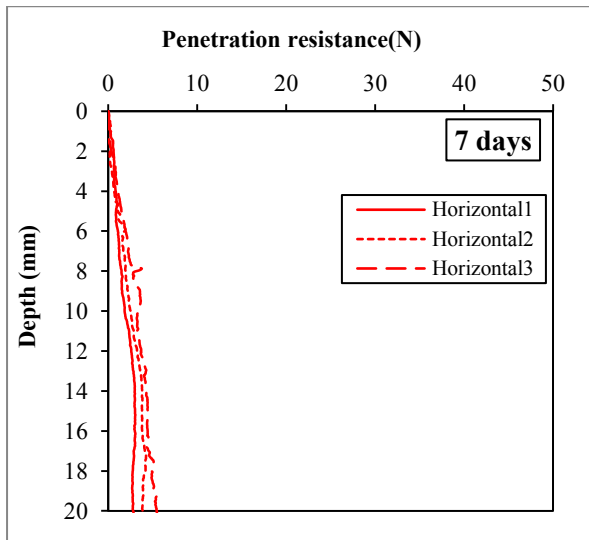


Cement 3.5% - Sealed

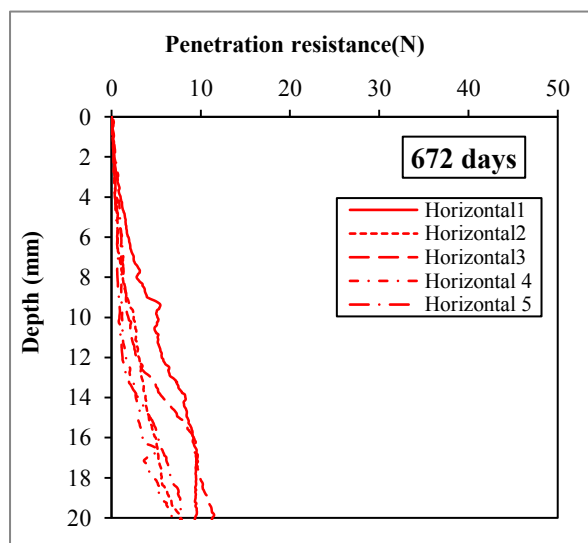
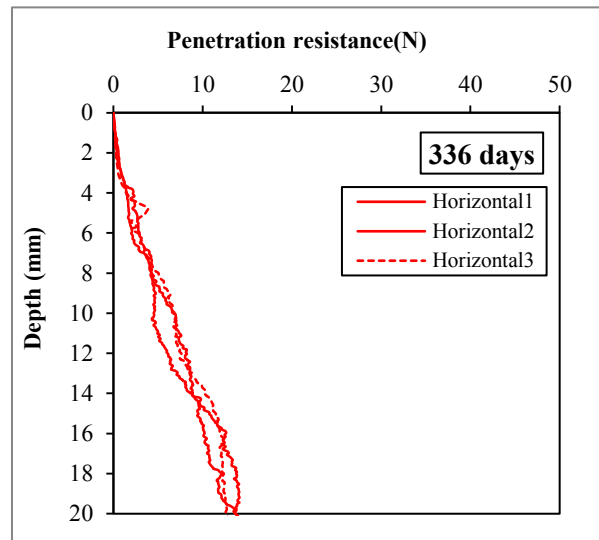
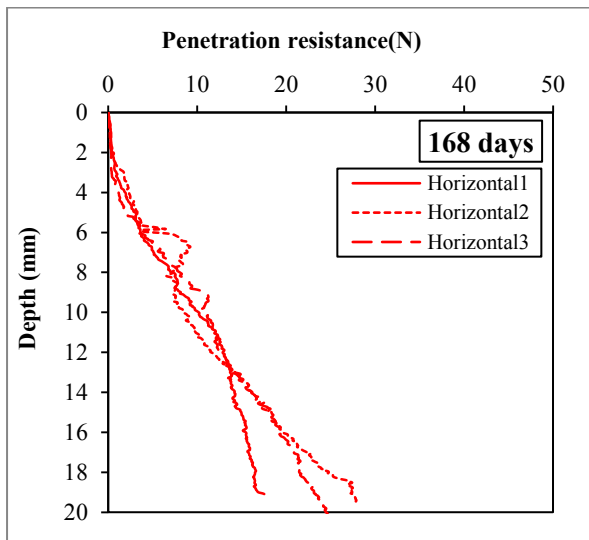
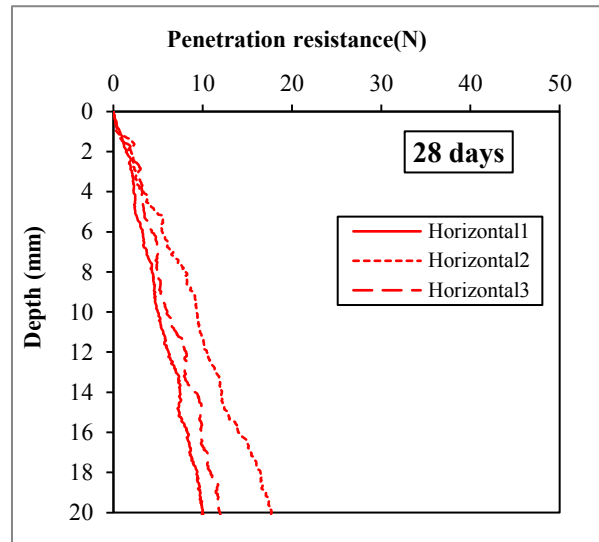
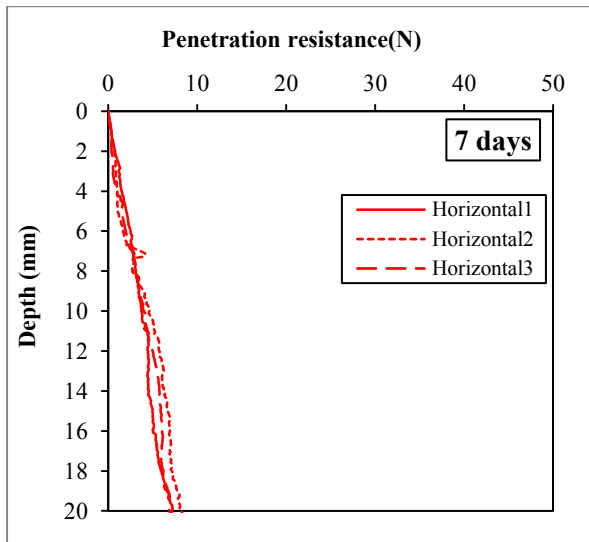




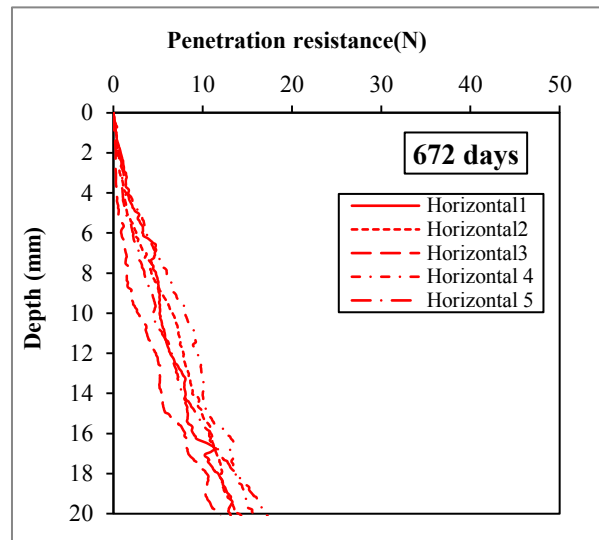
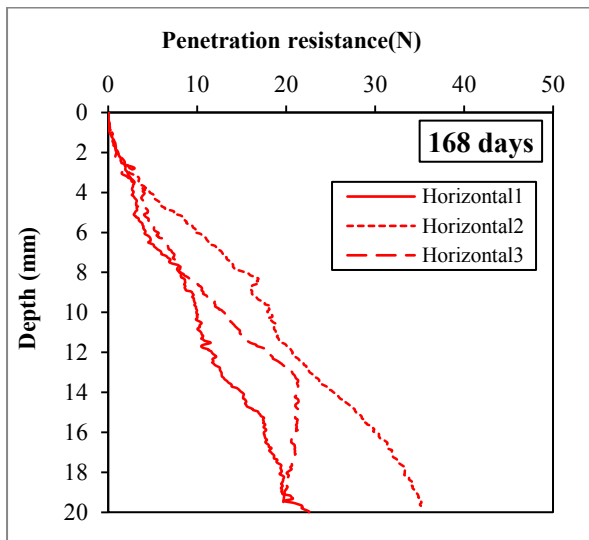
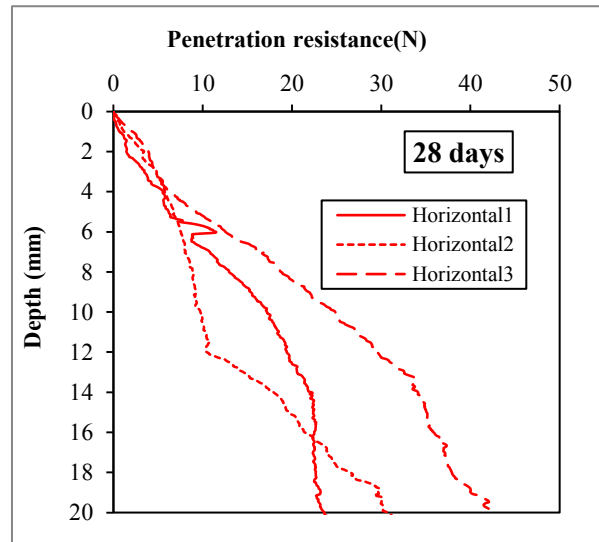
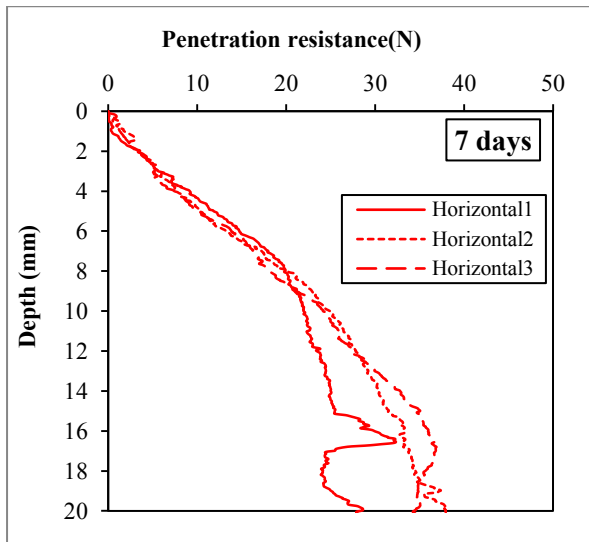
Cement 3.5% - Soaked Acid (immature)



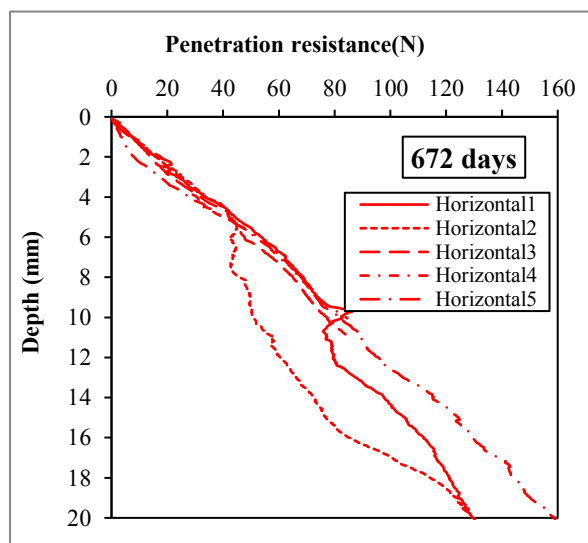
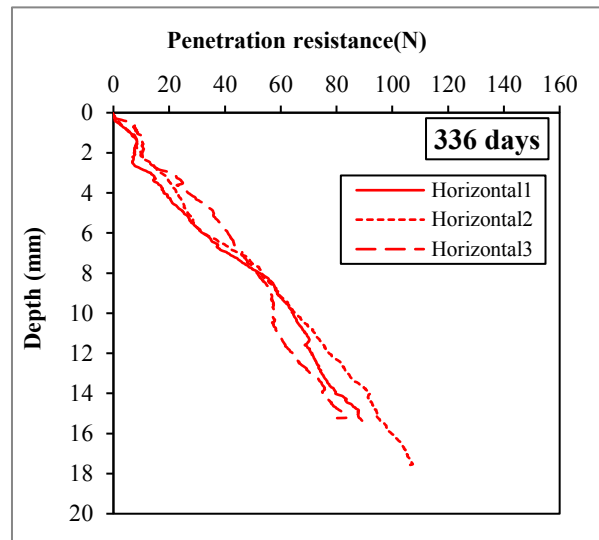
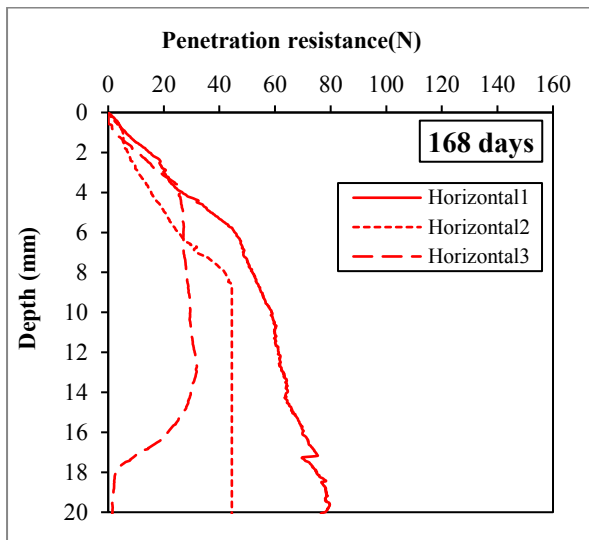
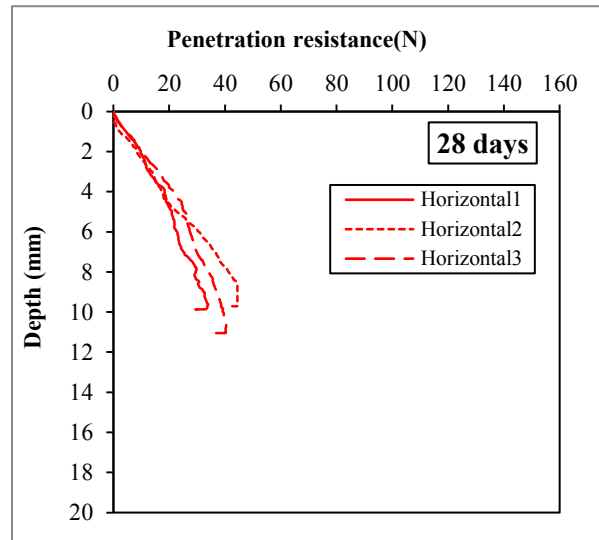
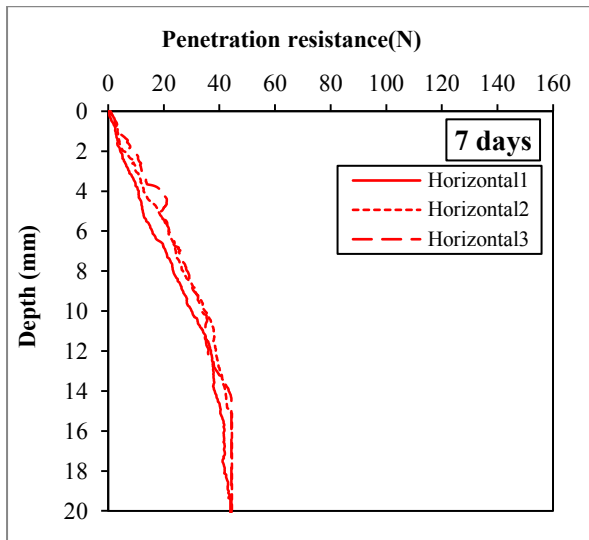
Cement 3.5% - Soaked Pure (immature)



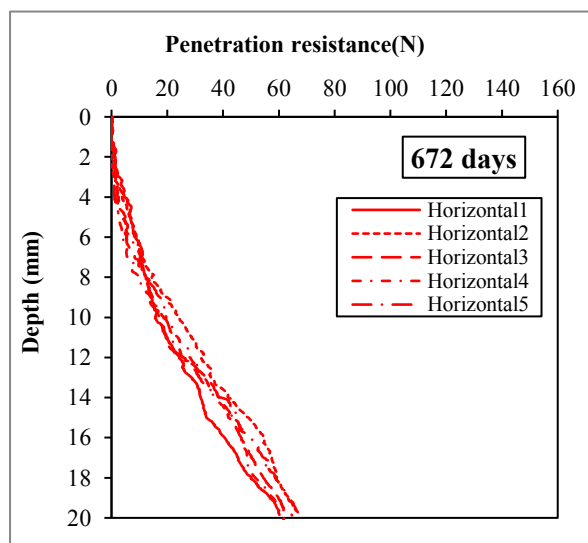
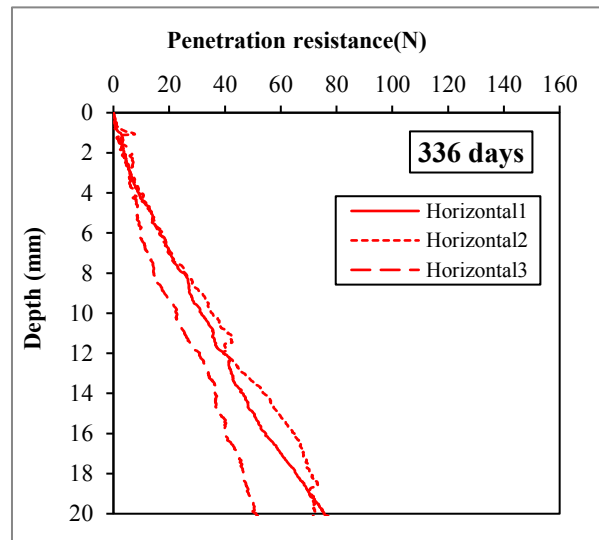
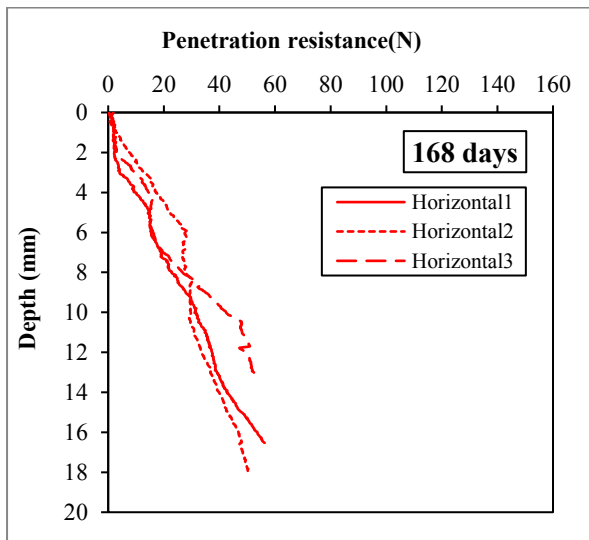
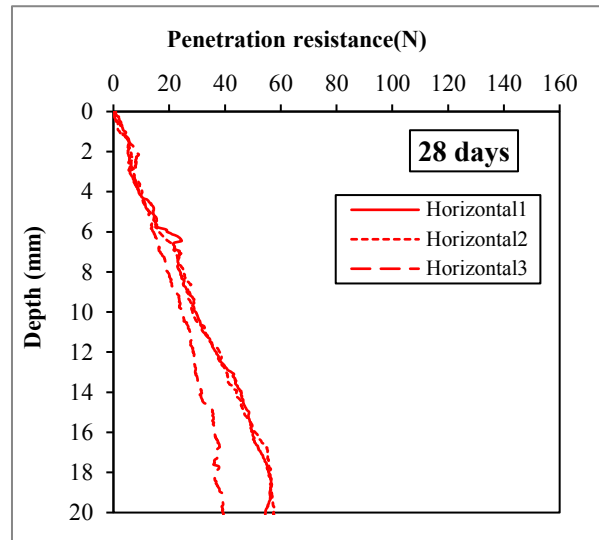
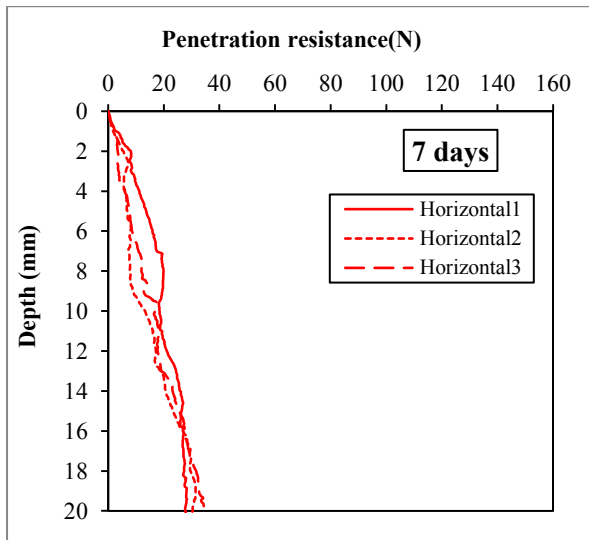
Cement 3.5% - Soaked acid (mature)



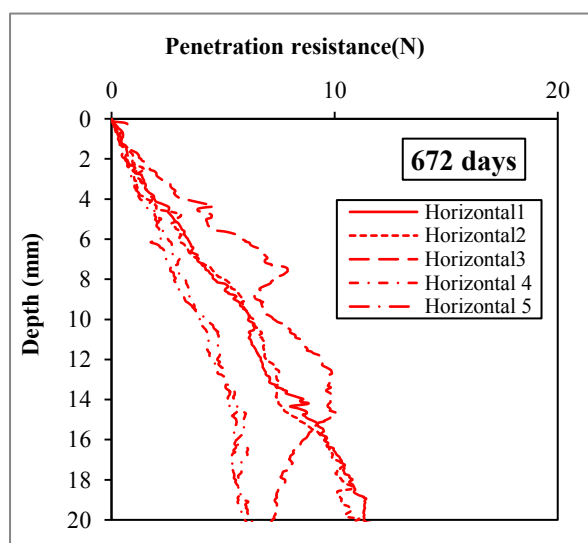
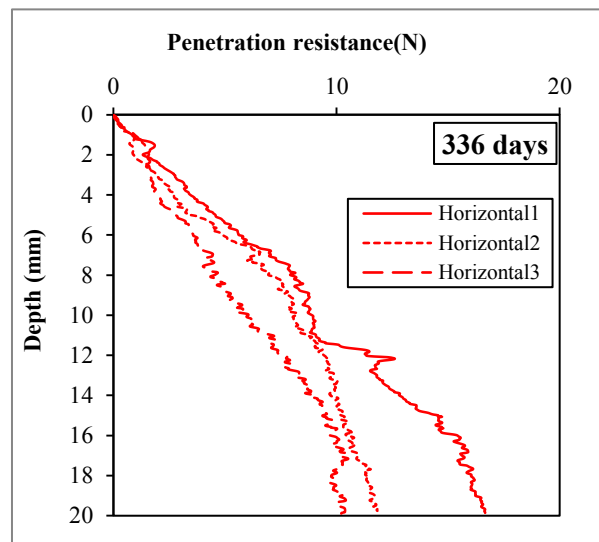
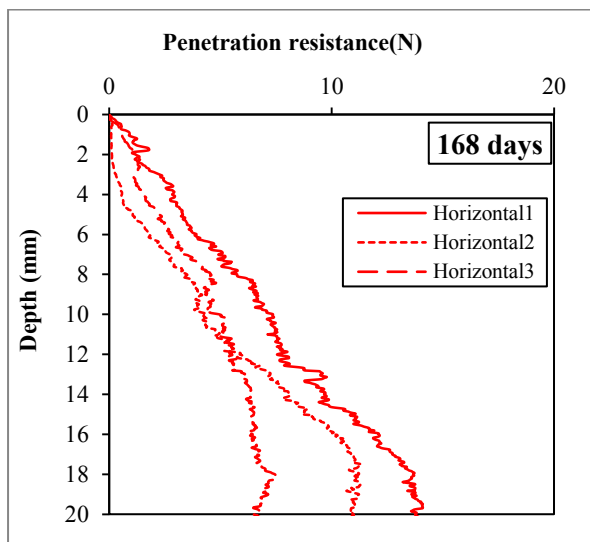
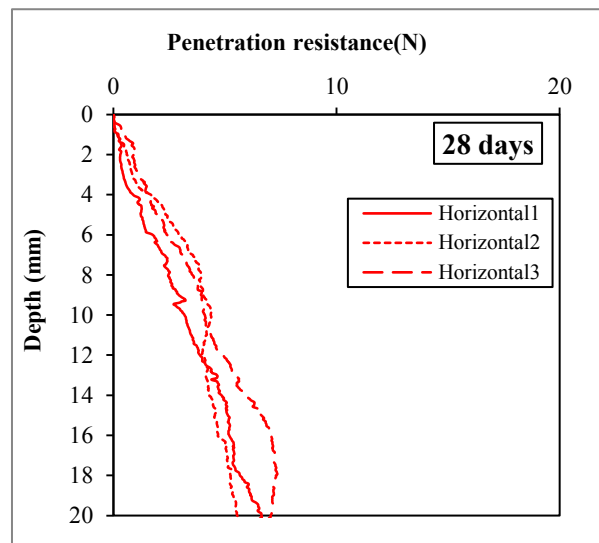
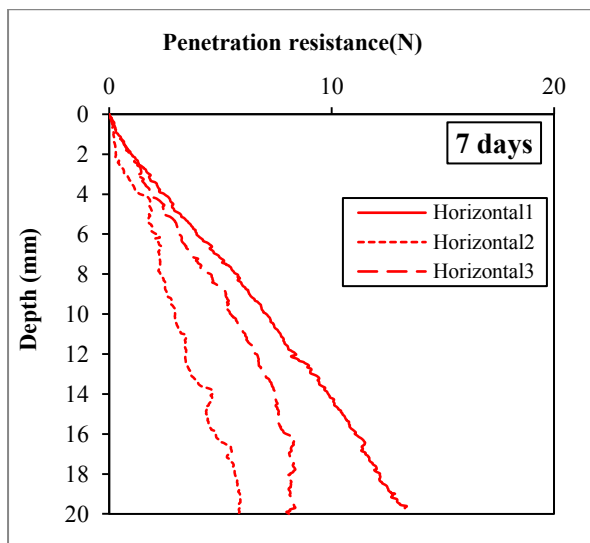
Cement 5.3% - Sealed



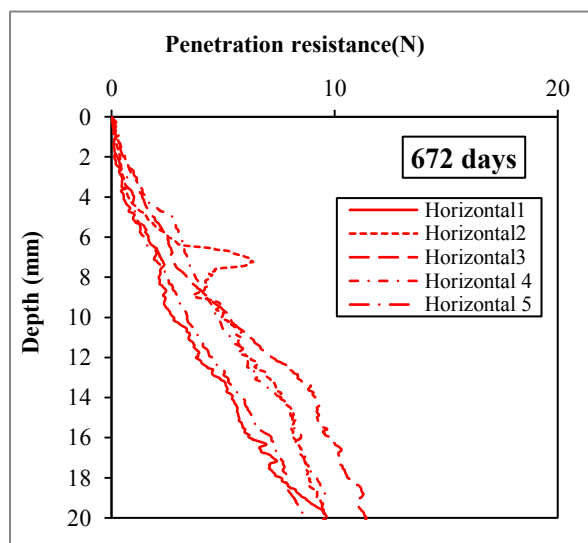
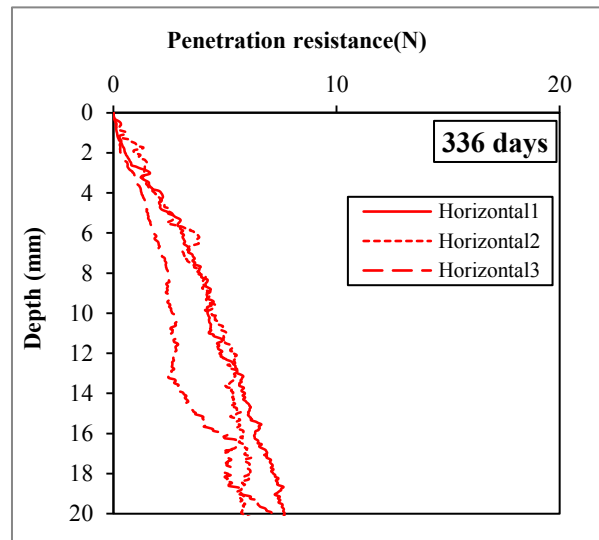
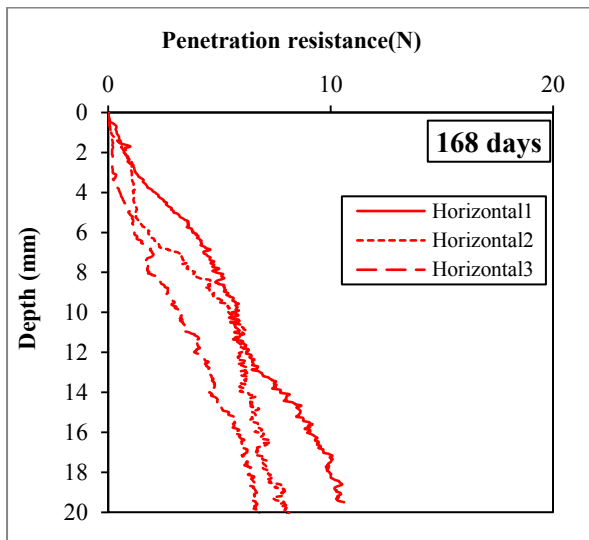
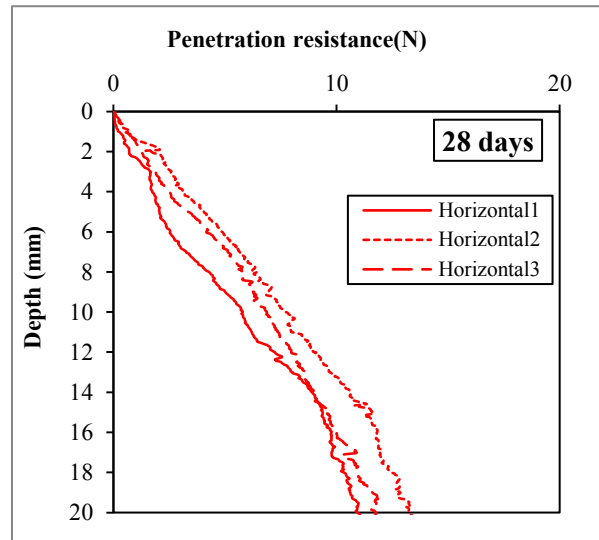
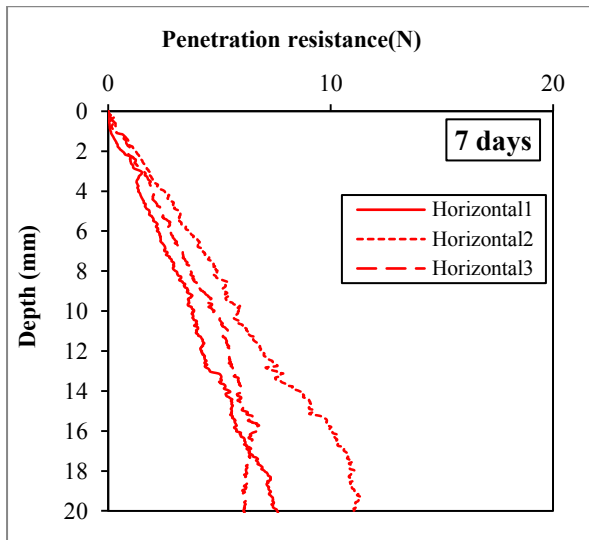
Cement 5.3% - Soak acid (immature)



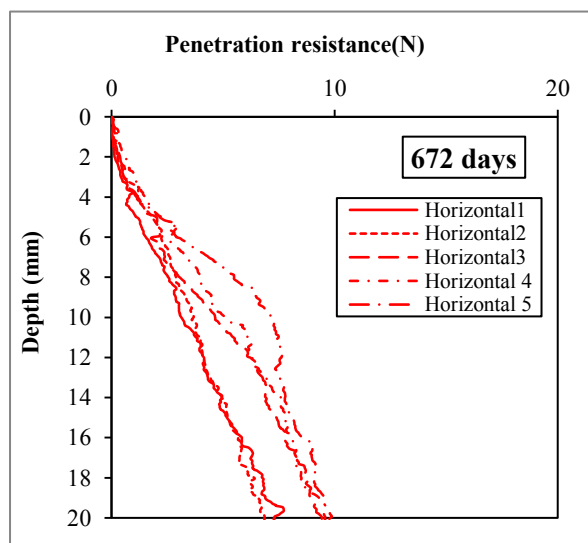
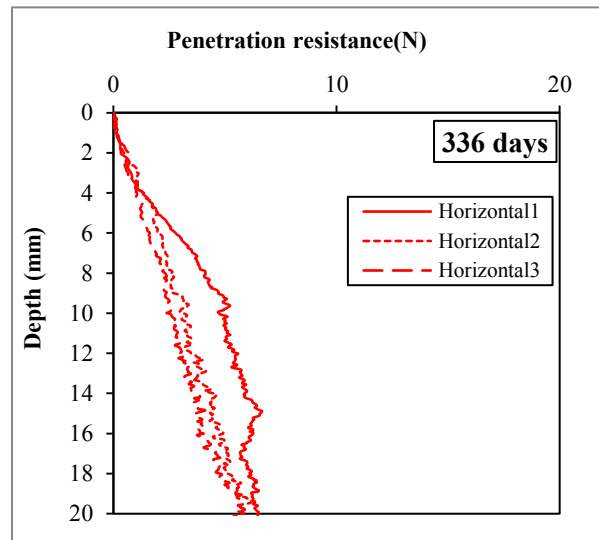
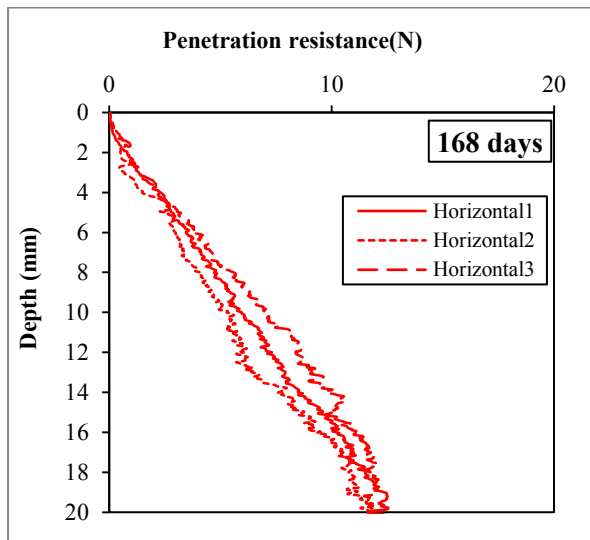
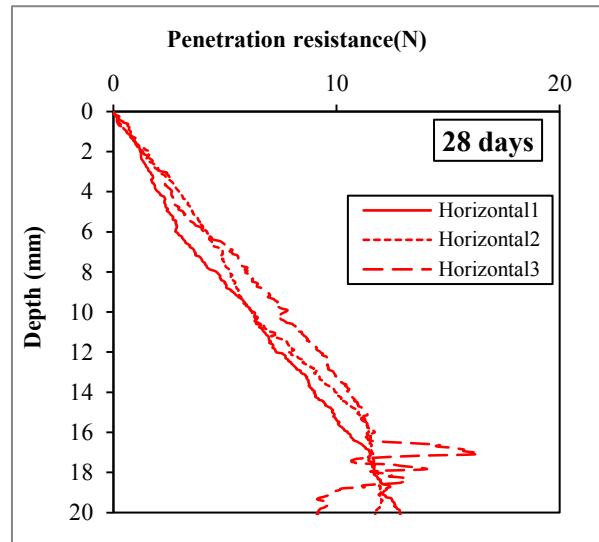
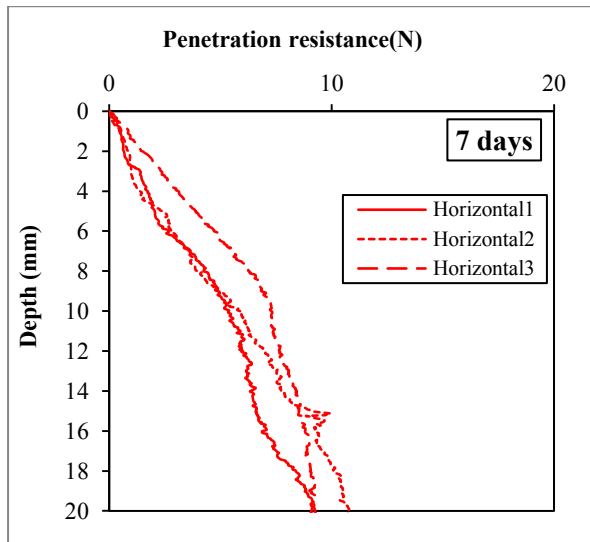
Lime 2.5% - Sealed



Lime 2.5% - Soaked acid (immature)

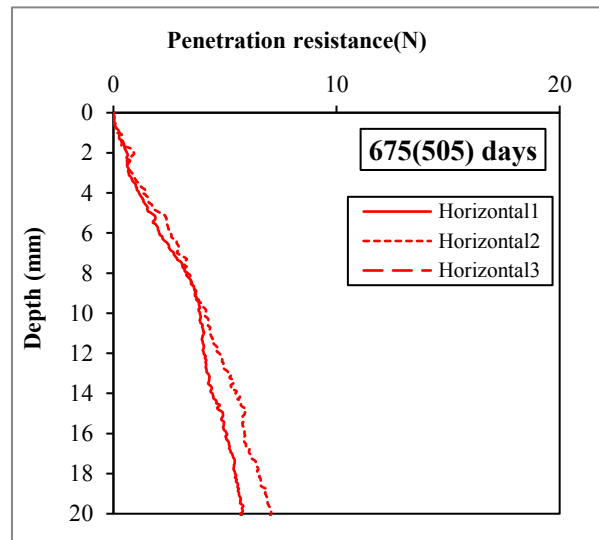
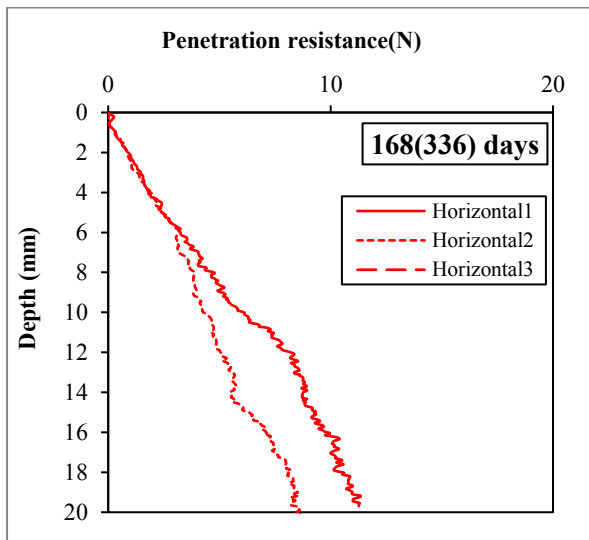
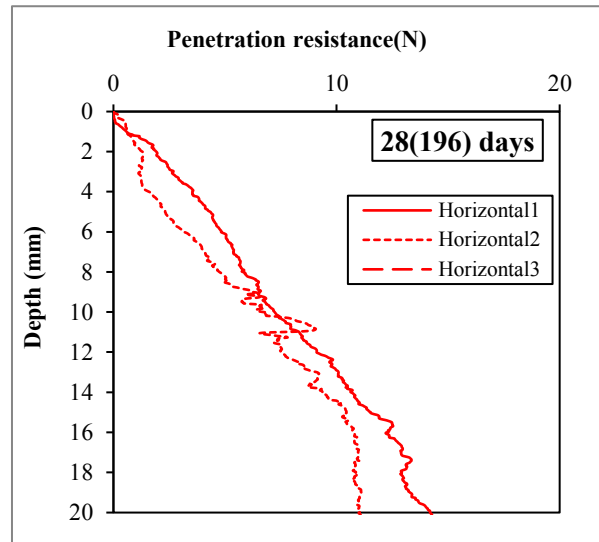
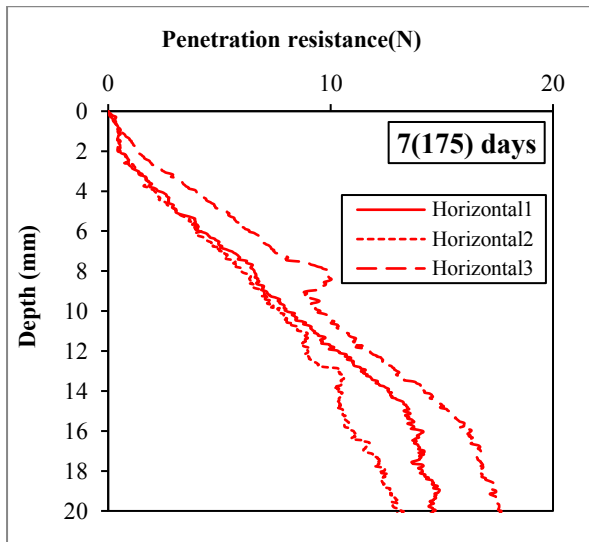


Lime 2.5% - Soaked Pure (immature)

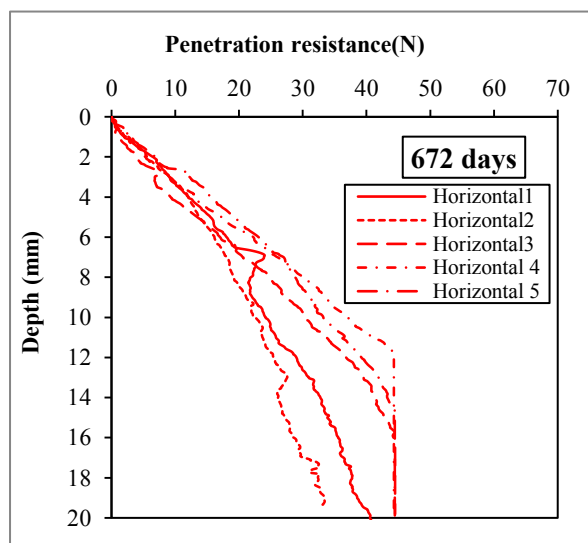
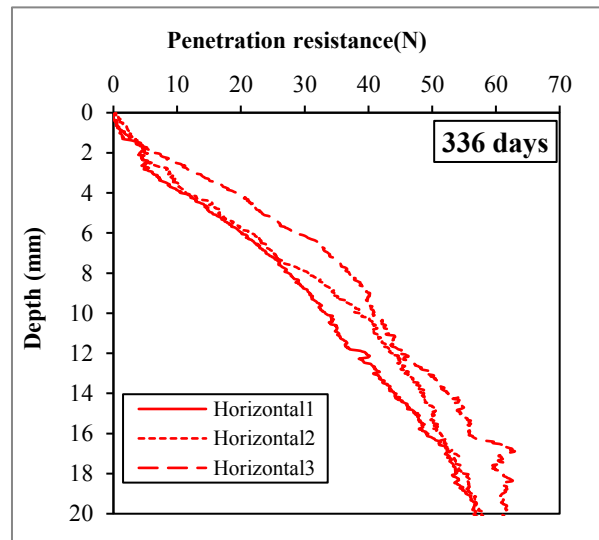
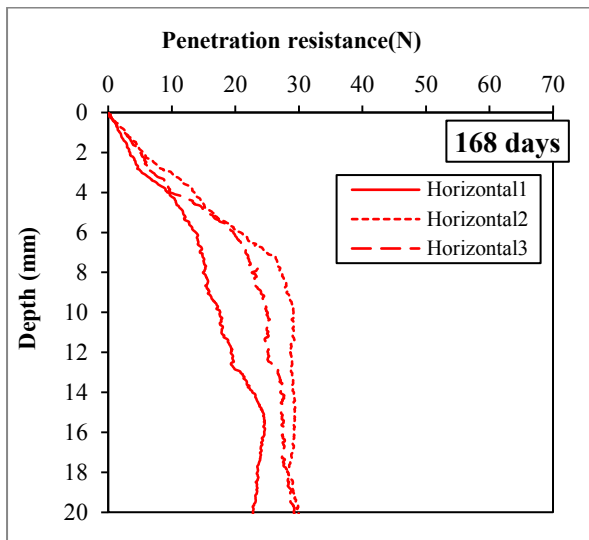
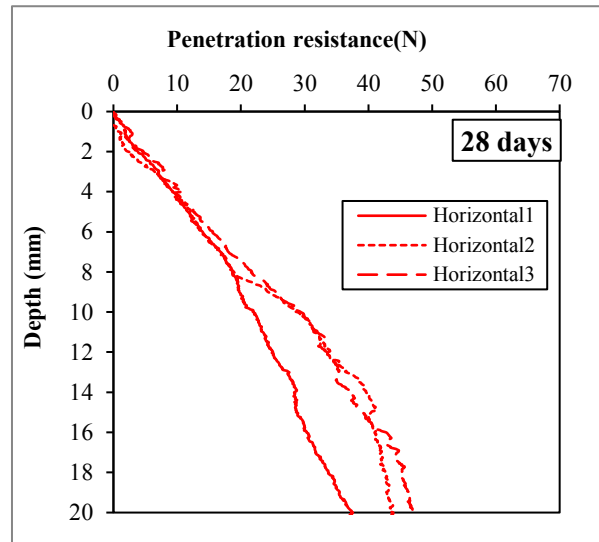
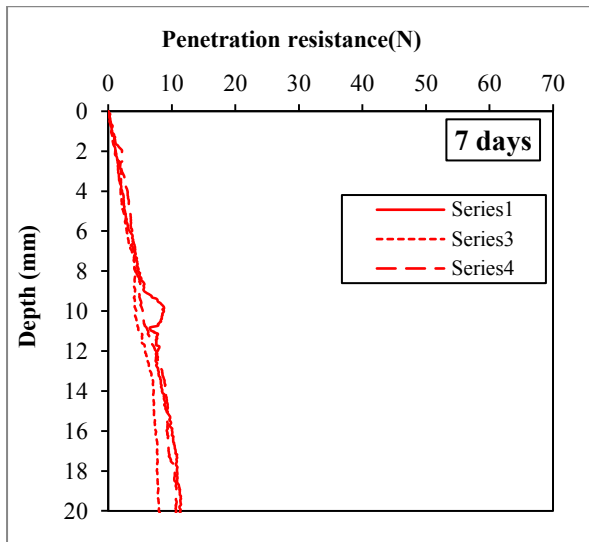




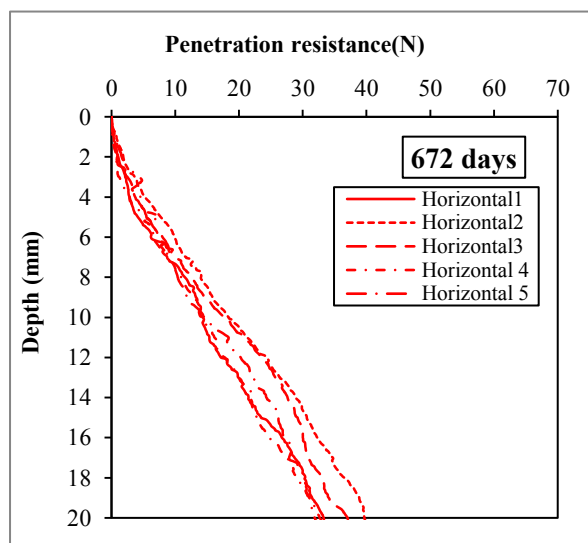
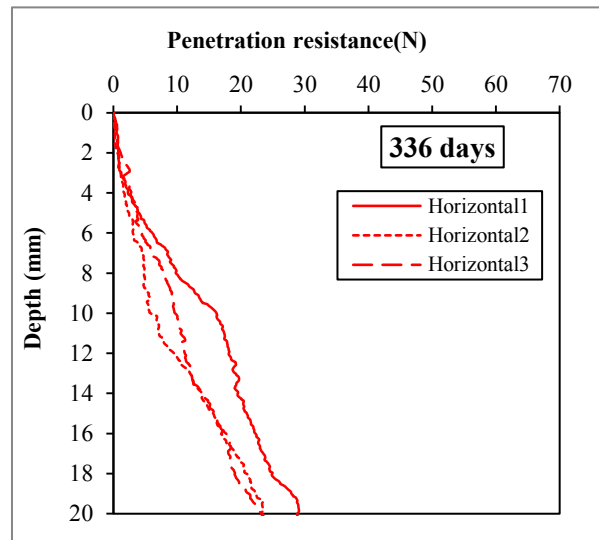
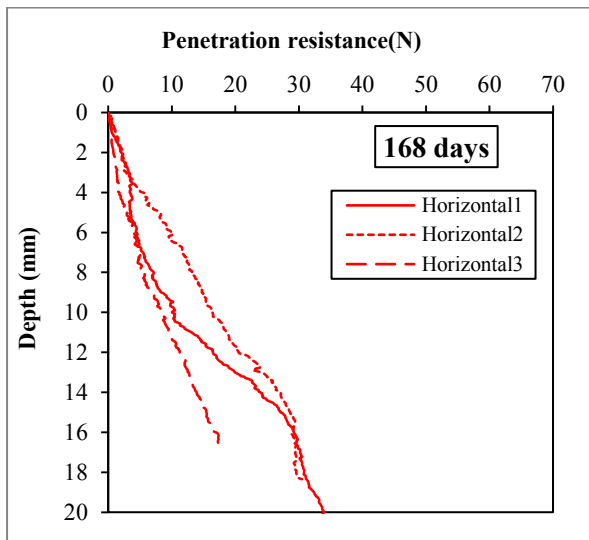
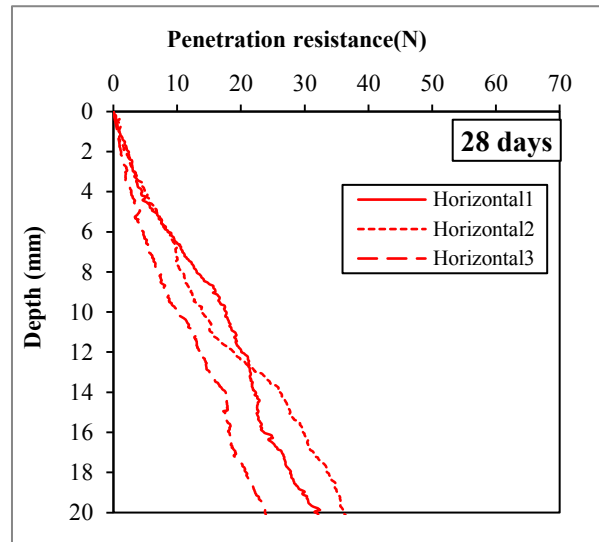
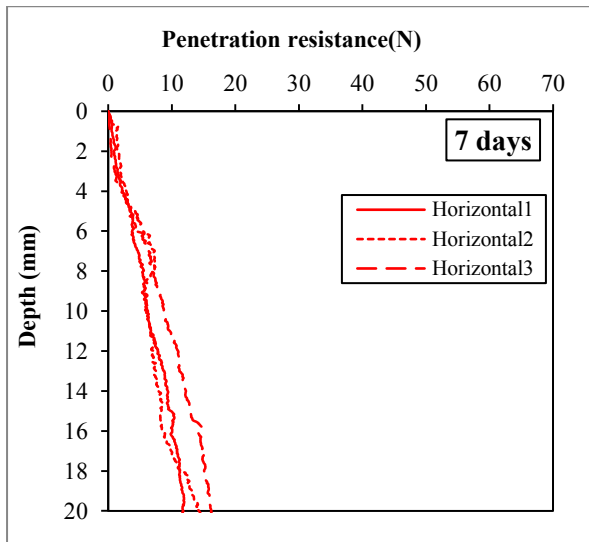
Lime 2.5% - Soaked acid (mature)



Lime 3.8% - Sealed



Lime 3.8% - Soaked acid (immature)



**Annex D-** CaO from XRF analysis

Binder content	Curing type	Depth from surface (mm)	Curing period (days)			
			28	168	336	672
Lime1.2% Seal	Sat.	0-5	3.0853	3.1546	2.9383	3.022
		10-15			2.8412	2.78
		20-25	3.0853	3.039	2.8716	2.873
	Unsat.	0-5	2.9823	3.0921	2.9973	2.881
		10-15			2.8789	2.756
		20-25	2.9823	3.0115	2.9122	2.881
Lime1.2% Soak (immature)	Acid	0			4.892	3.061
		0-5	2.8468	2.836	2.3391	2.235
		10-15			2.6166	2.514
		20-25	2.9219	2.8154	2.5585	2.521
Lime2.5% Seal	Sat.	0-5	4.3896	4.5242	4.8137	4.525
		10-15			4.4766	4.225
		20-25	4.3896	4.4457	4.4691	4.242
	Unsat.	0-5	4.5203	4.721	4.7614	4.527
		10-15			4.4895	4.162
		20-25	4.5203	4.8409	4.5993	4.255
Lime2.5% Soak (immature)	Pure	0			6.7309	7.601
		0-5	4.1285	3.9465	3.2373	2.811
		10-15			3.7492	3.248
		20-25	4.4616	4.2502	3.8437	2.84
	Acid	0			7.6221	7.803
		0-5	4.3007	4.1794	3.1768	2.94
		10-15			3.8049	3.38
		20-25	4.6243	4.3378	4.015	3.511
Lime3.8% Seal	Sat.	0-5	5.7547	6.4147	6.1019	6.117
		10-15			5.9211	5.866
		20-25	5.7547	6.4448	6.1067	6.005
	Unsat.	0-5	5.9258	6.2593	6.3291	6.212
		10-15			6.0267	5.838
		20-25	5.9258	6.271	6.0453	5.848
Lime3.8% Soak (immature)	Acid	0			9.6106	12.92
		0-5	5.3279	4.9703	4.1224	3.767
		10-15			5.1387	4.397
		20-25	6.067	6.0905	5.2951	4.488
Lime2.5% Soak (mature)	Acid	0			8.575	7.352
		0-5	4.4088	4.2643	3.287	3.253
		10-15		4.0991	3.839	3.622
		20-25	4.5896	4.2321	3.974	3.601

Binder content	Curing type	Depth from surface (mm)	Curing period (days)			
			28	168	336	672
Cement 1.7 % Seal	Sat.	0-5	2.7597	2.6451	2.6136	2.732
		10-15			2.6282	2.686
		20-25	2.7597	2.7223	2.6282	2.668
	Unsat.	0-5	2.7343	2.726	2.6634	2.75
		10-15			2.6285	2.785
		20-25	2.7343	2.8191	2.7026	2.687
Cement 1.7 % Soak (immature)	Acid	0			2.4863	2.138
		0-5	2.614	2.3508	2.2594	2.2
		10-15			2.3756	2.337
		20-25	2.7212	2.6249	2.479	2.454
Cement 3.5 % Seal	Sat.	0-5	4.1664	4.0995	4.0106	3.969
		10-15			3.9998	3.966
		20-25	4.1664	4.0853	3.9819	3.816
	Unsat.	0-5	4.1187	4.1972	3.9857	3.983
		10-15			4.0169	3.967
		20-25	4.1187	4.0481	4.0562	3.848
Cement 3.5 % Soak (immature)	Pure	0			5.4065	11.85
		0-5	3.7279	3.7666	2.6316	2.589
		10-15			3.5174	3.176
		20-25	4.1274	4.0147	3.7004	3.349
	Acid	0			7.7134	6.223
		0-5	3.6727	3.4461	2.7557	2.54
		10-15			3.3201	3.095
		20-25	4.0937	3.9436	3.651	3.464
Cement 5.3 % Seal	Sat.	0-5	5.2945	5.543	5.3337	5.276
		10-15			5.3227	5.22
		20-25	5.2945	5.535	5.2153	4.86
	Unsat.	0-5	5.5161	5.4485	5.4372	5.166
		10-15			5.2946	5.181
		20-25	5.5161	5.4057	5.4113	5.076
Cement 5.3 % Soak (immature)	Acid	0			8.631	13.25
		0-5	5.1272	4.561	3.6302	3.186
		10-15			4.8466	4.195
		20-25	5.1207	5.4026	4.9945	4.624
Cement 3.5 % Soak (mature)	Acid	0			5.624	5.397
		0-5	3.7826	3.6276	3.094	2.972
		10-15		3.863	3.546	3.51
		20-25	3.9776	3.8349	3.65	3.626

**Appendix 1- Effect of degree of saturation on the unconfined compressive strength of improved soil**

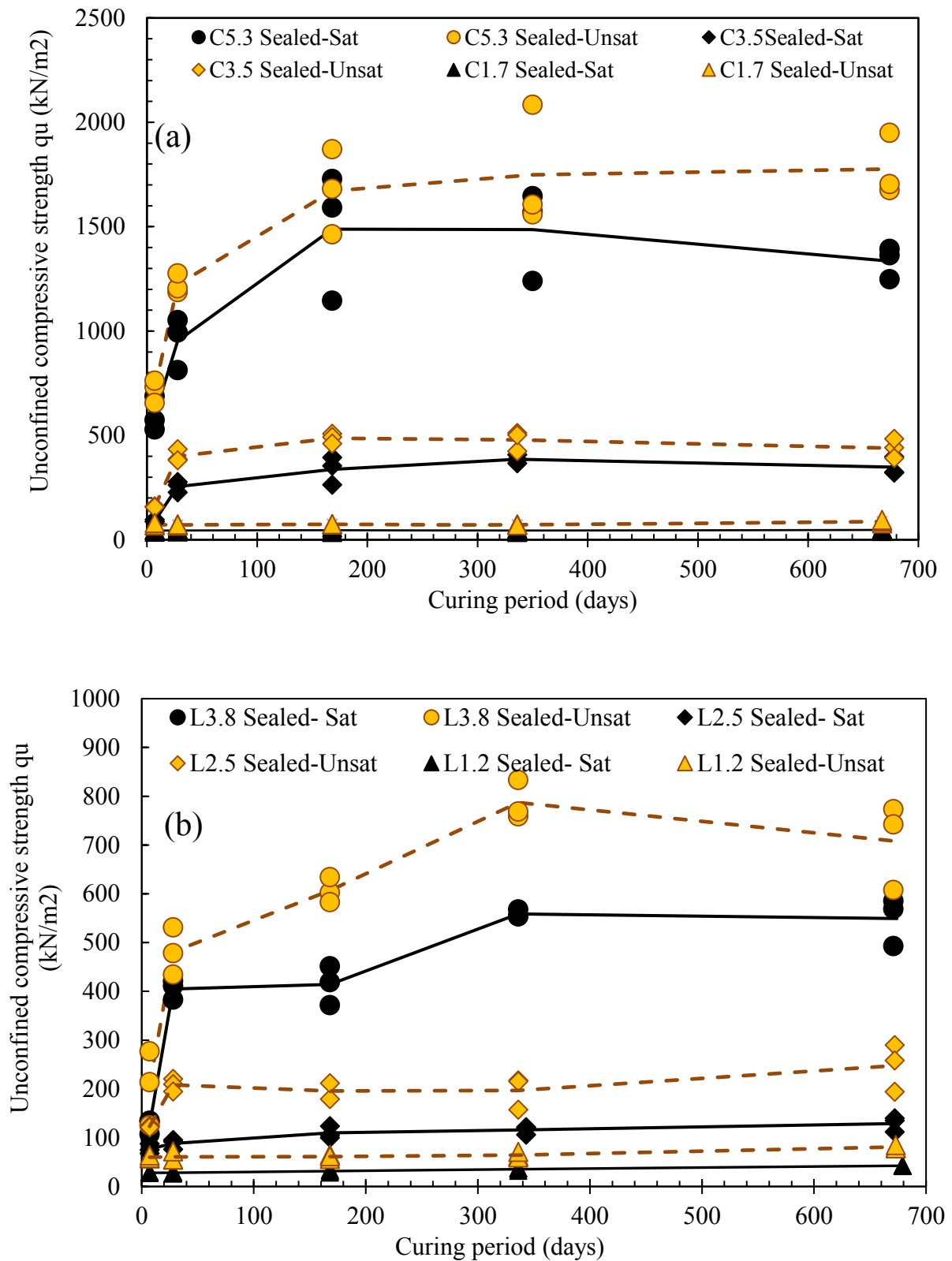
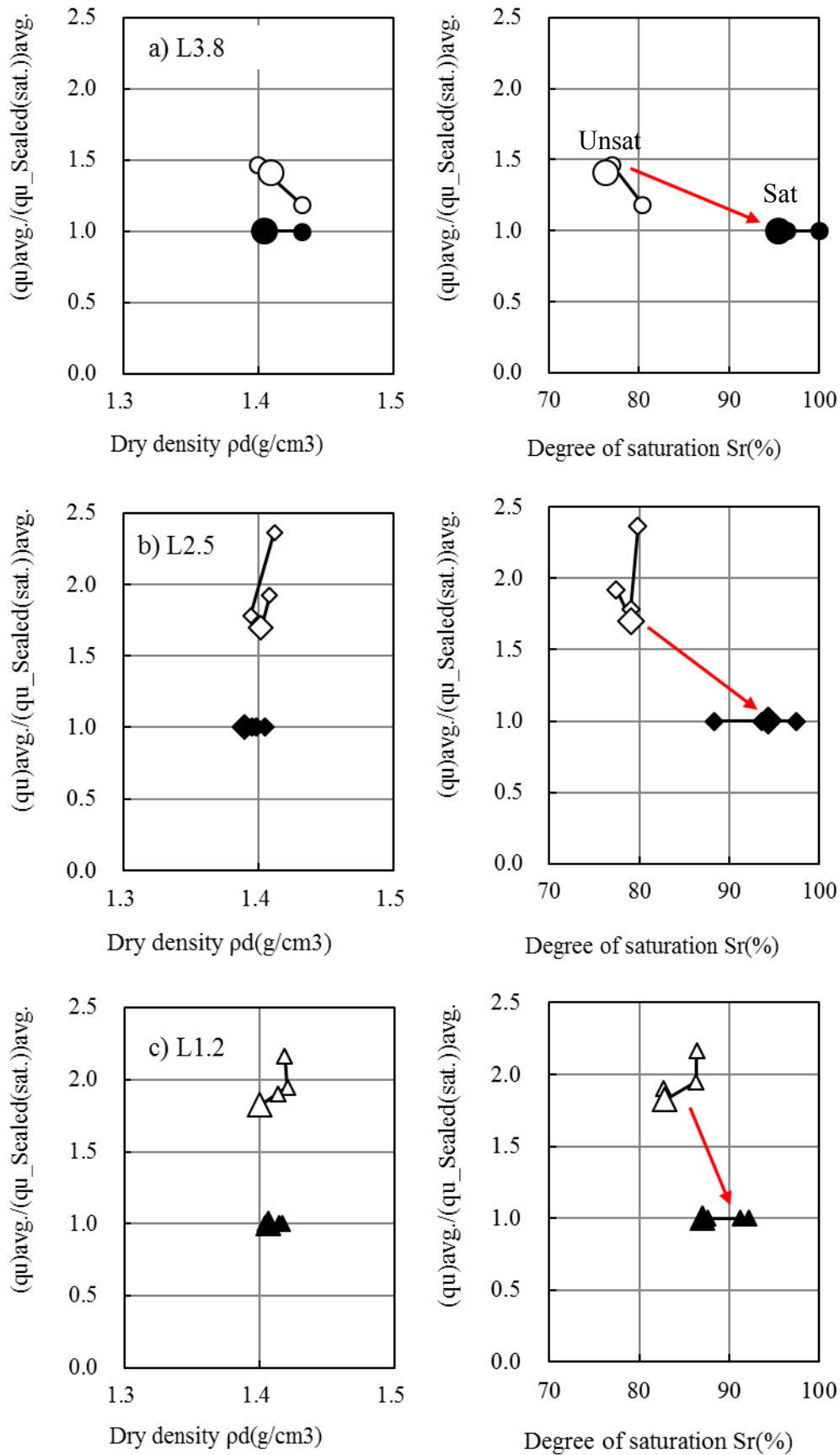
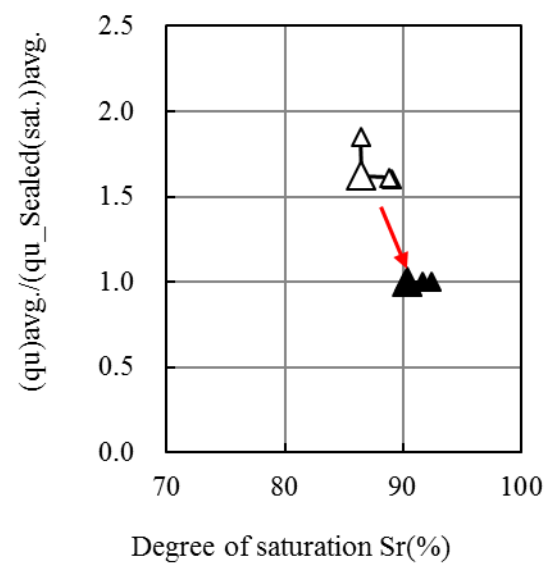
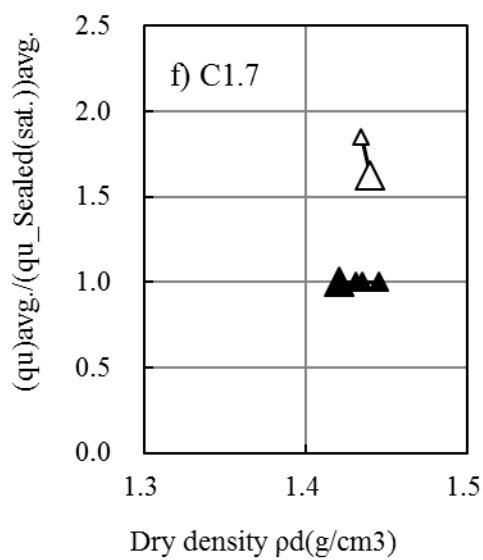
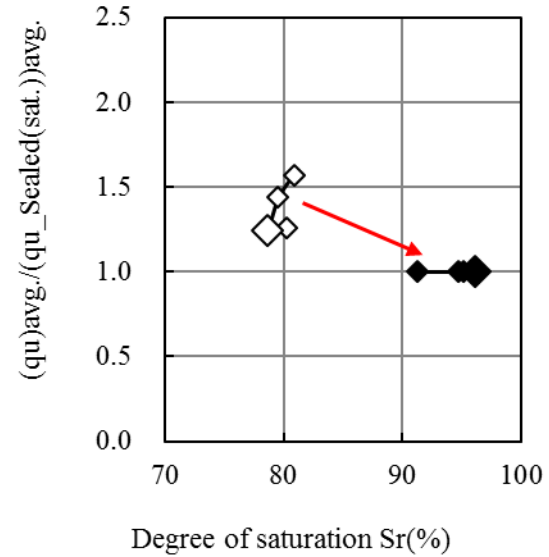
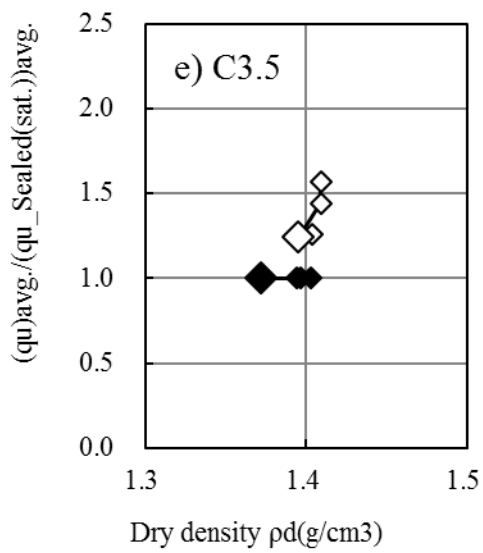
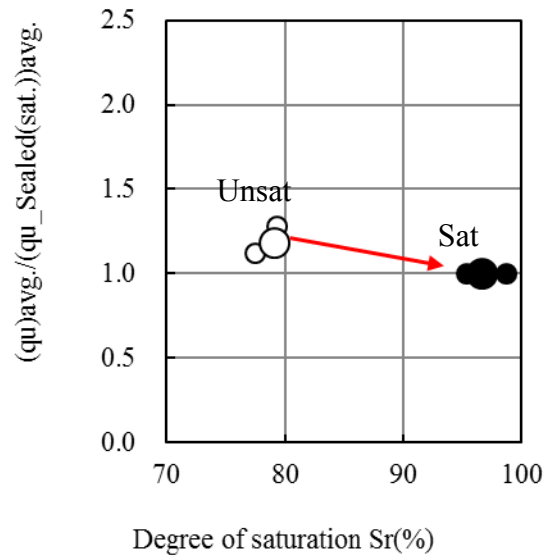
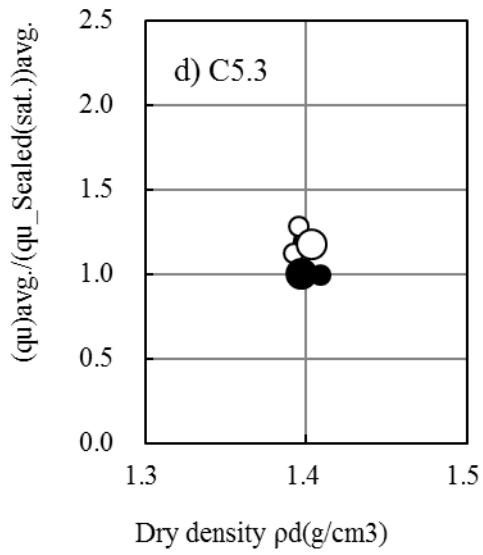


Figure A1:1 UCS results (a) cement treated soil (b) lime treated soil



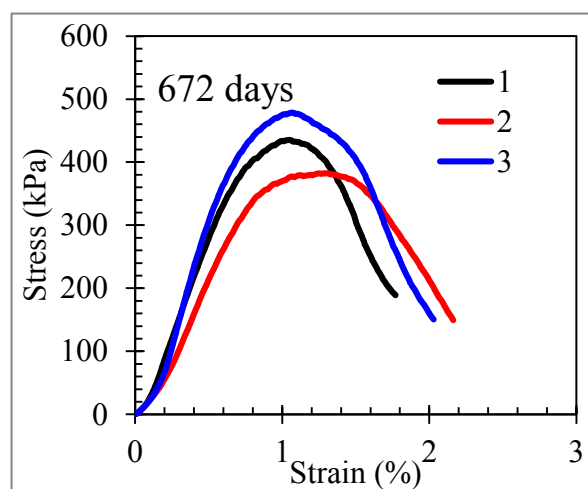
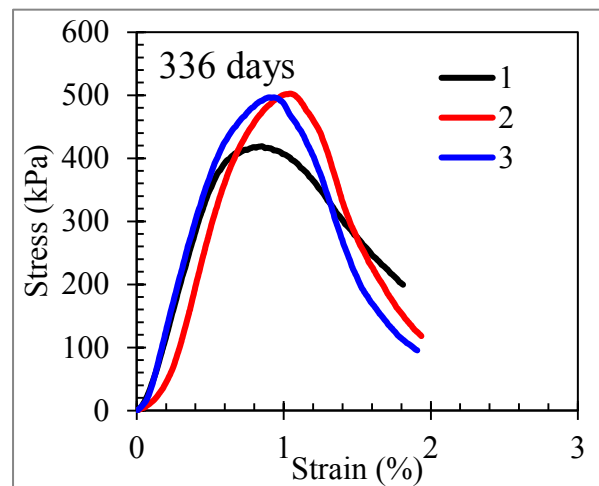
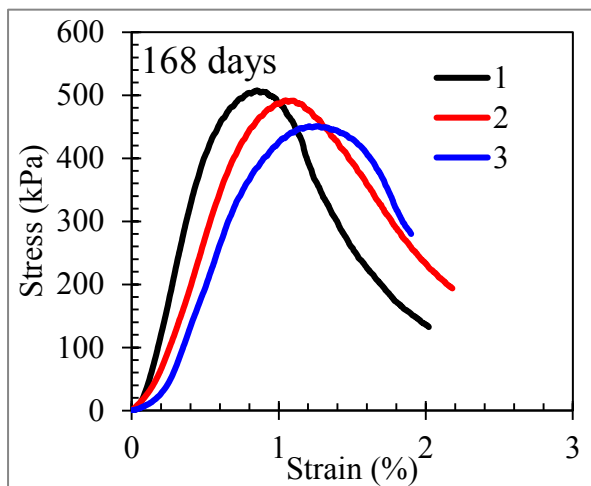
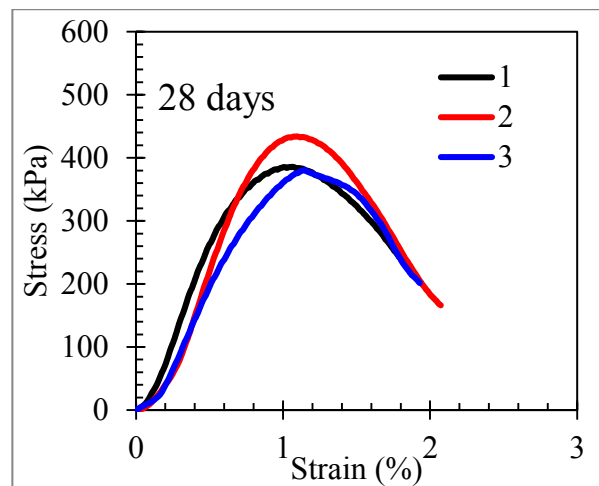
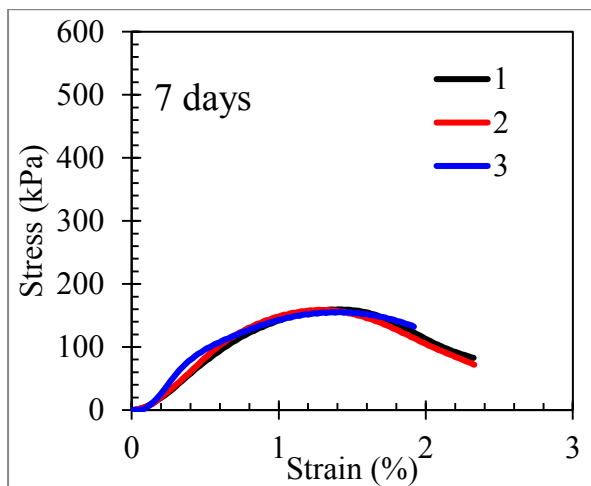




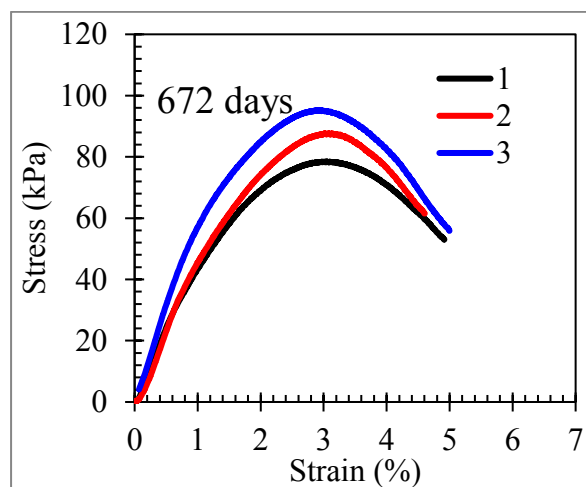
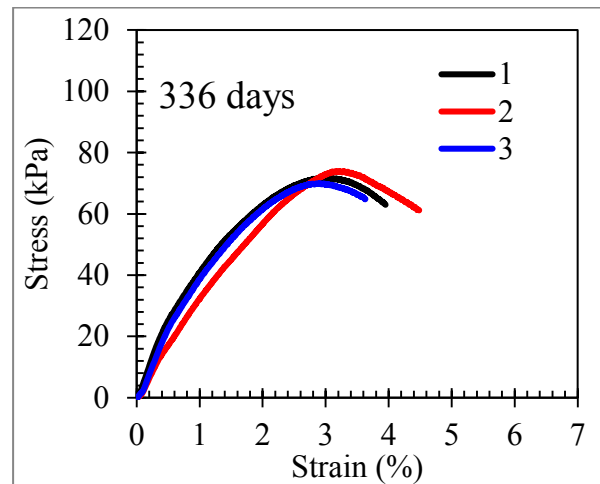
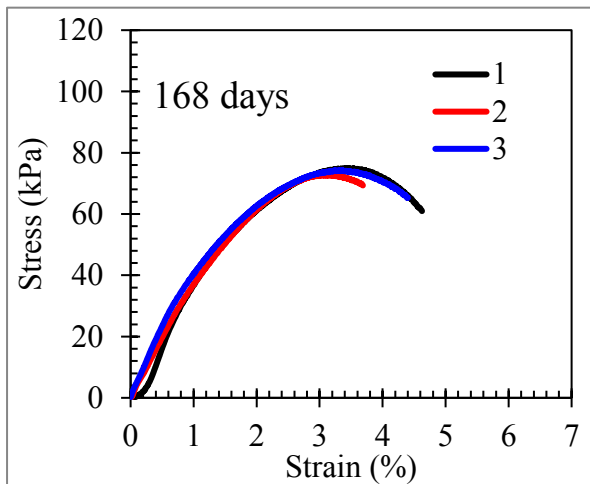
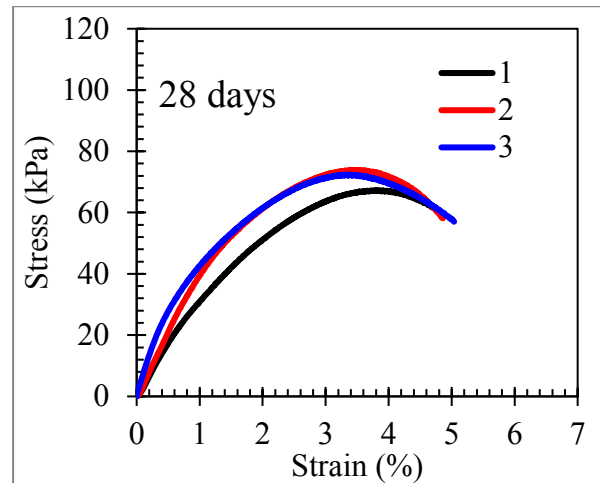
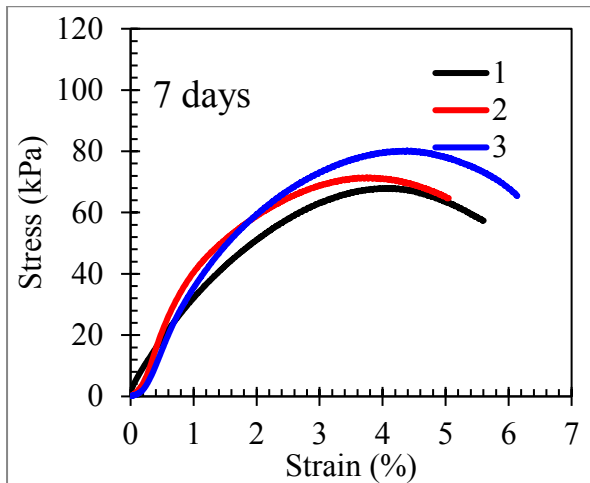
---

In here two sets of specimens were prepared and cured under sealed condition inside a constant temperature room. Saturation was applied on one set of specimens one day before testing (called here after as saturated case) in order to find out the effect of degree of saturation on the unconfined compressive strength. It was found highest  $q_u$  in the unsaturated condition in all types of soils. To identify the effect of changes in physical properties on the difference of the strengths relationships between strength ratio, dry density and degree of saturation ( $S_r$ ) were obtained. The strength ratio was defined as the ratio of the averaged  $q_u$  value in each condition to the averaged  $q_u$  value in ‘Seal(sat)’ condition at a particular curing period. There was no distinct trend on the change in dry density except for C1.7, while exhibiting variations in every sets of specimens. On the other hand, levels of  $S_r$  values in ‘Seal(sat)’ conditions were always higher than those of unsaturated conditions. It was inferred that the  $q_u$  values of ‘Seal(sat)’ were lower due possibly to the decline of the strengths derived from the suction force.

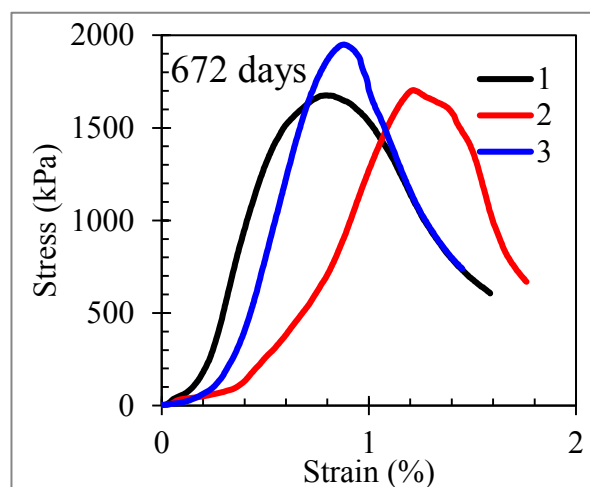
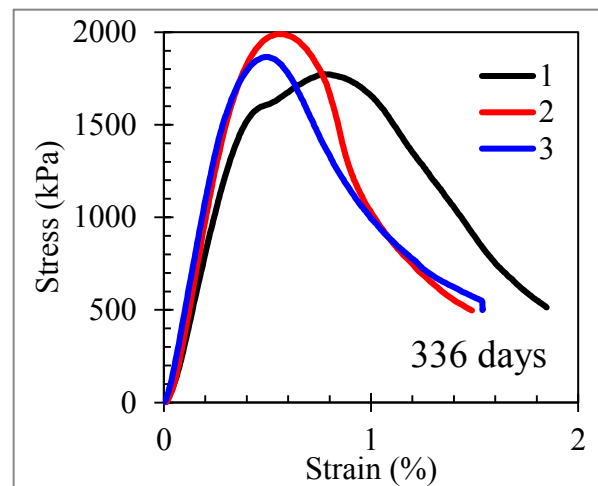
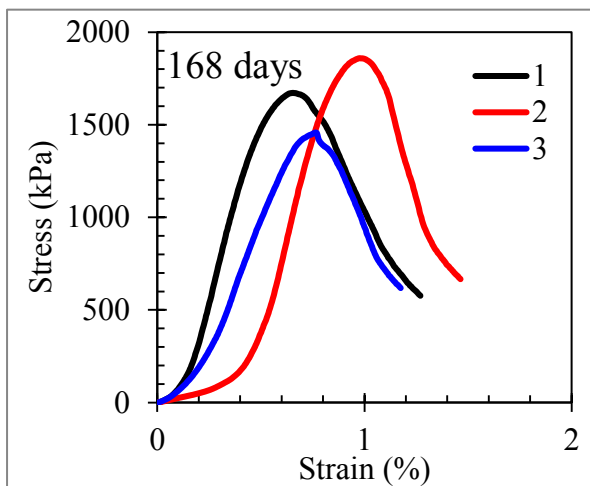
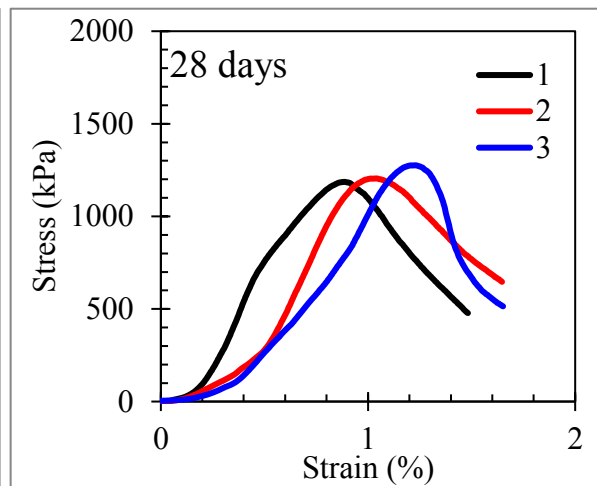
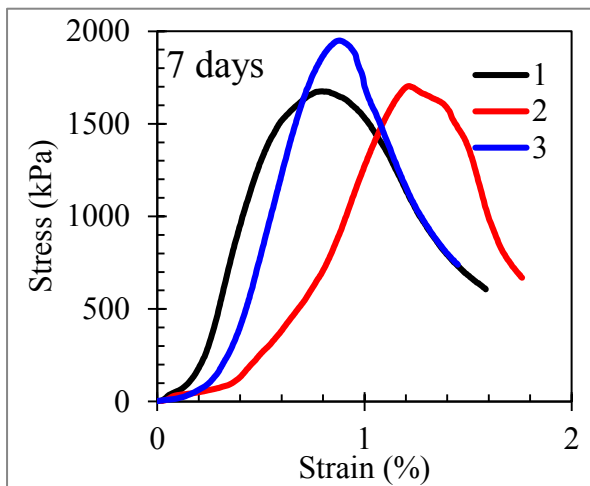
## Cement 3.5 %- Sealed Unsaturated



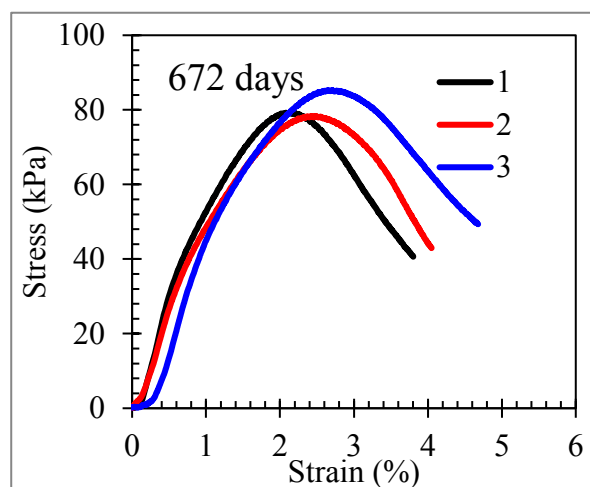
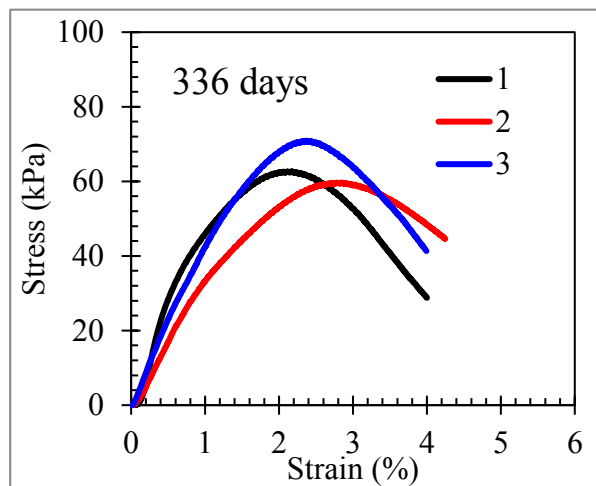
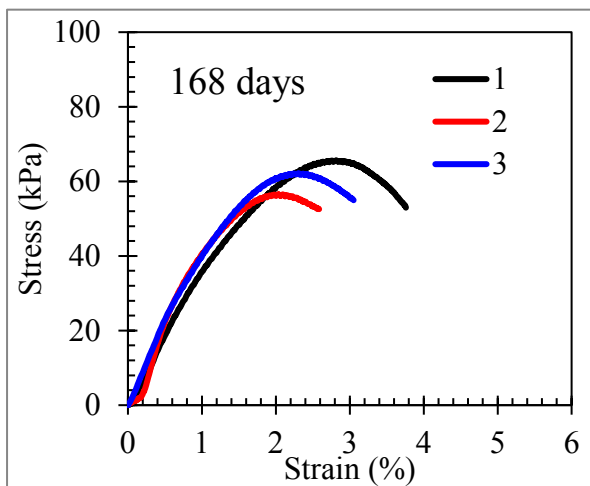
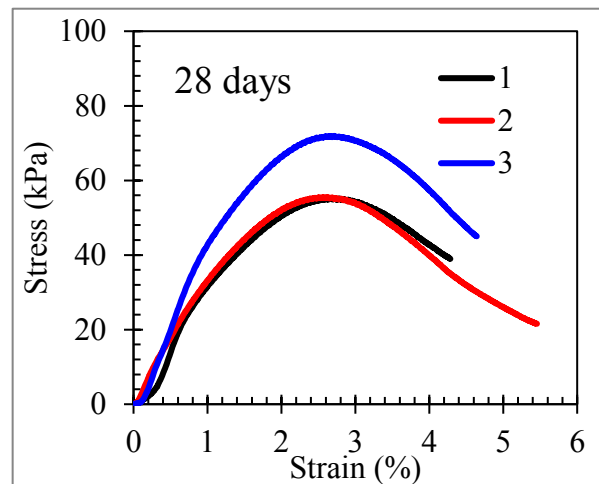
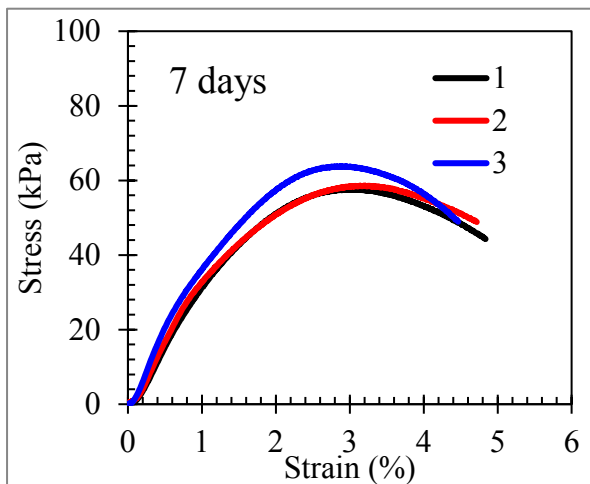
Cement 1.7 %- Sealed Unsaturated



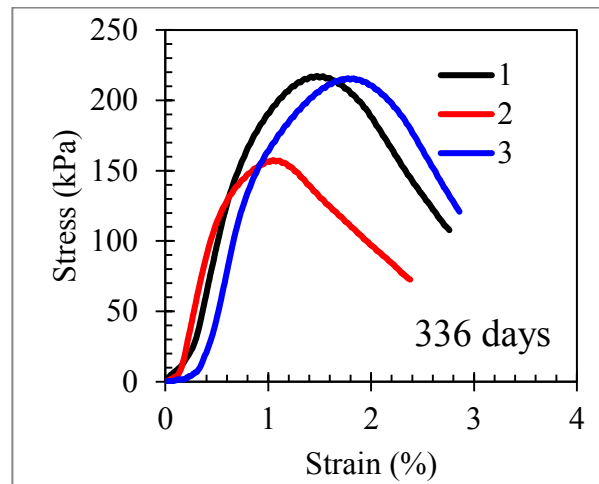
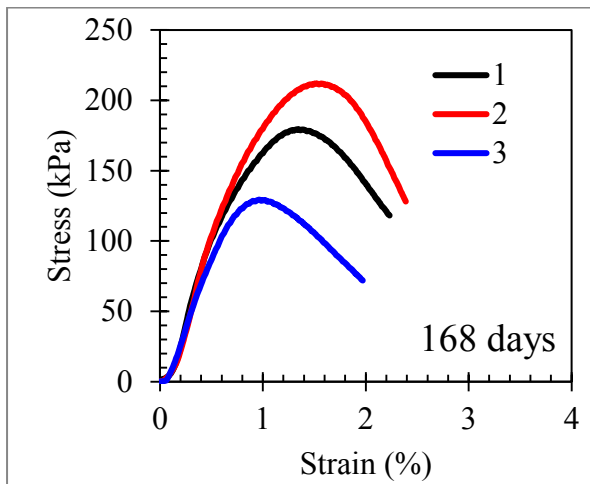
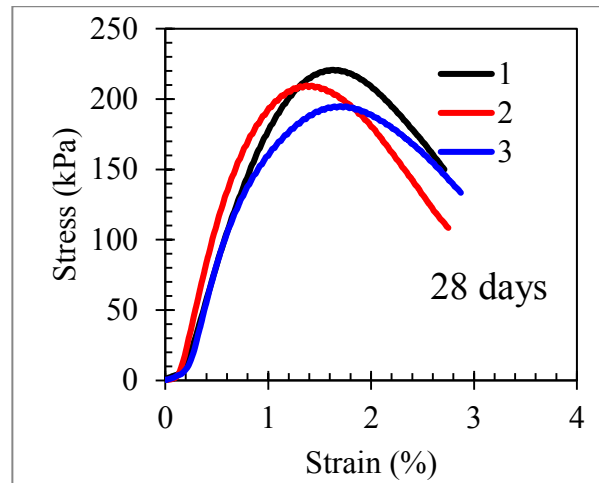
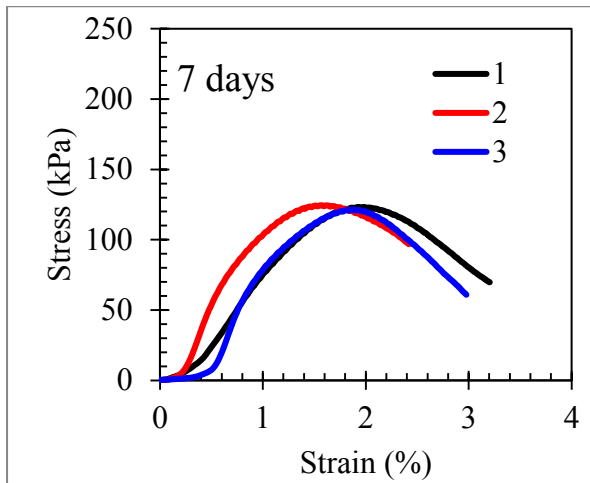
Cement 5.3 %- Sealed Unsaturated



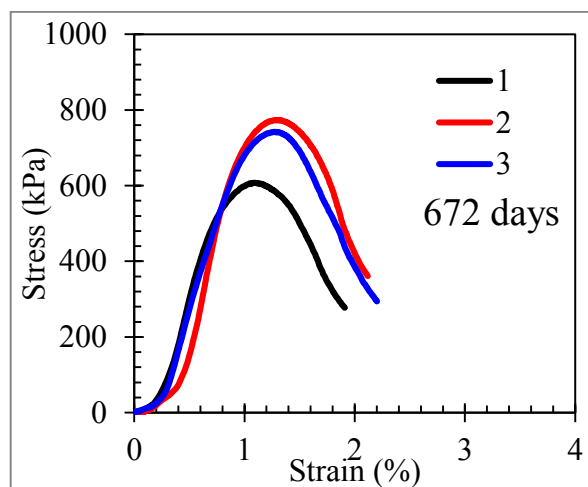
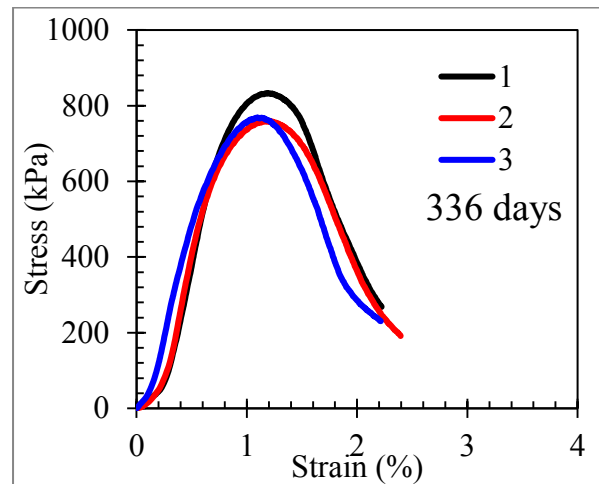
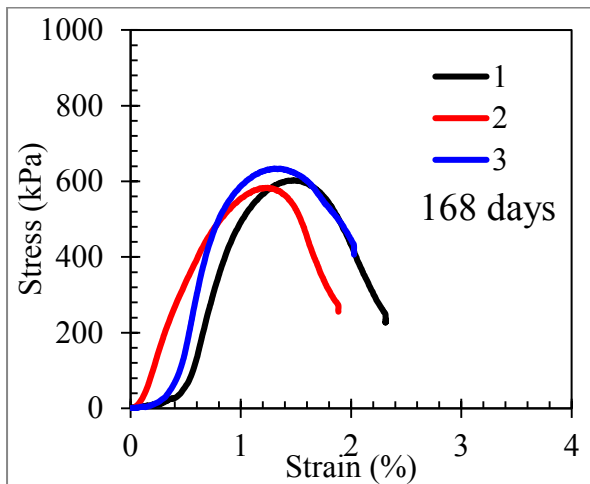
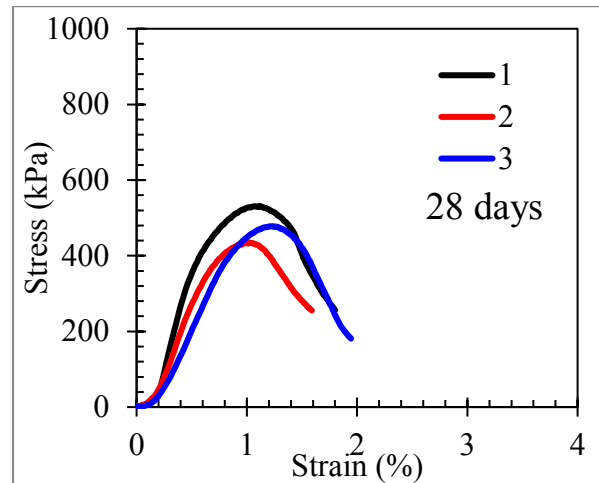
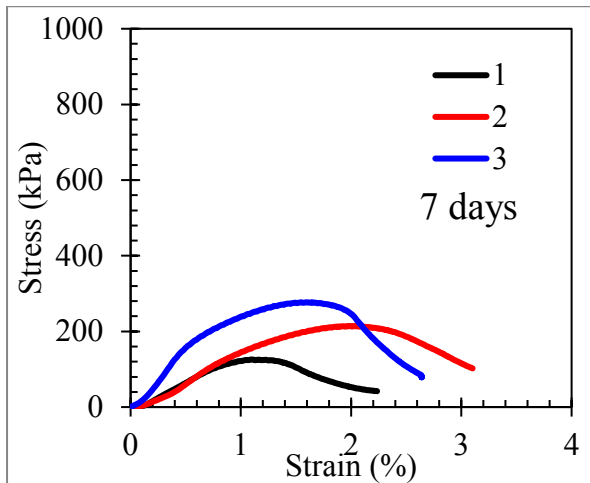
Lime 1.2 %- Sealed Unsaturated



Lime 2.5 %- Sealed Unsaturated



Lime 3.8 %- Sealed Unsaturated



**Appendix 2- Results of needle penetration test-method 2**

	JGS 3431 standard	This study	
		Method-1	Method-2
Needle diameter (mm)	0.84	0.84	0.84
Needle length (mm)	10	30	15
Penetration rate (mm/minute)	20±5	11	11

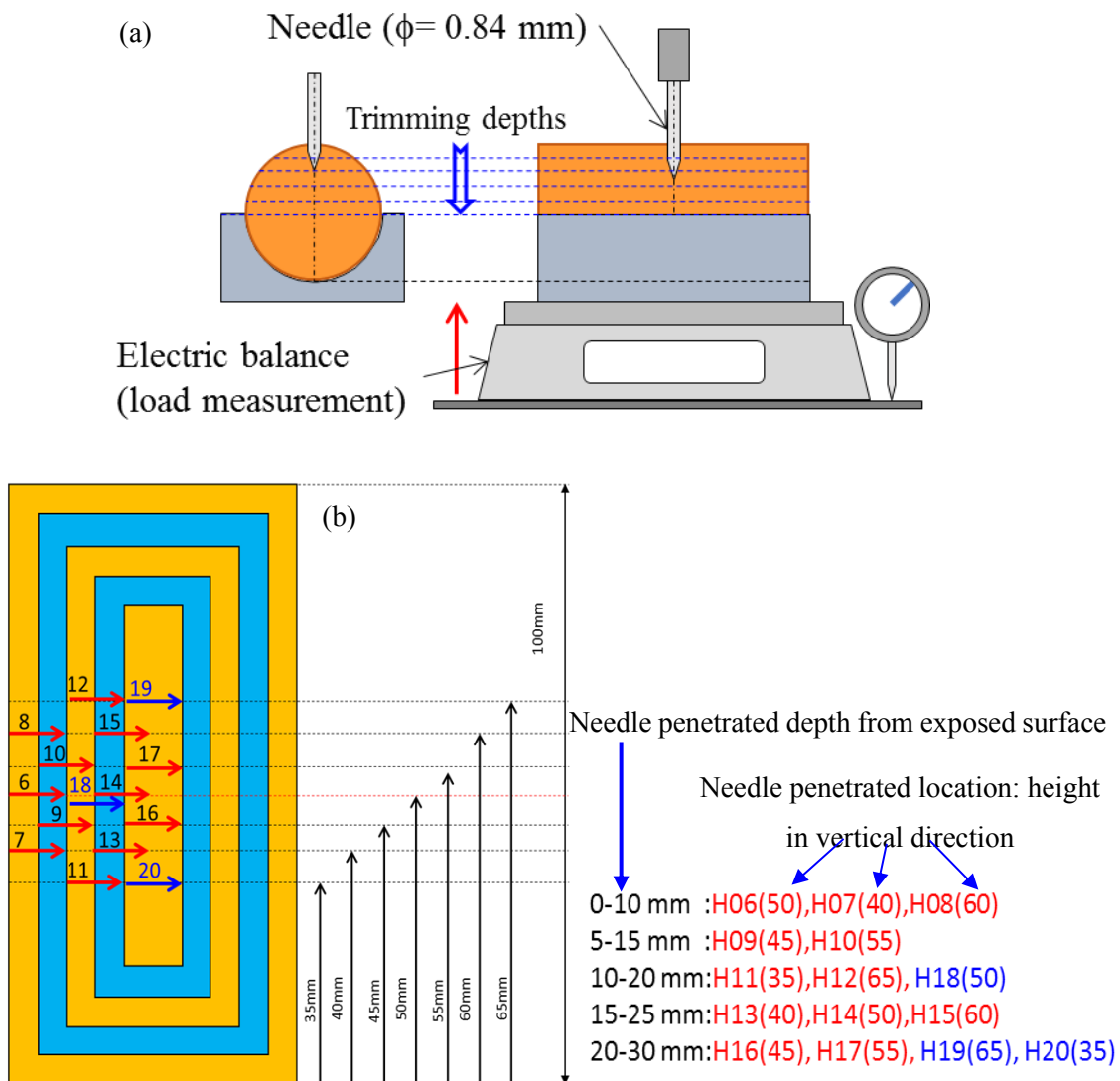


Figure Ap 2:1 Needle penetration test -method 2



In order to understand whether there was a negative effect on the measured penetration resistance in method 1 due to the long length of the needle, method 2 was conducted following standard needle penetration test only after the curing of 672 days as illustrated in (a). In here first, the needle was penetrated 10 mm depth only from one side at three or four different heights of the specimen as shown in (b). After that 5mm depth of the surface layer was trimmed off and another set of measurements were obtained in next 10 mm depth. This procedure was followed to get measurements at depths of 0-10, 5-15, 10-20, 15-25 and 20-30 mm from the exposed surface as shown in Figure Ap 2:1.

From the results, it was found a large scattering of data near the core for most of the cases. It may be due to the difference in local density as shown in Figure Ap 2:2. However, cement treated soil results agreed with method 1 results and followed the same trend. In the case of lime treated soil, a clear difference in the results of two methods was obtained. The reason for that behavior could not be well understood.

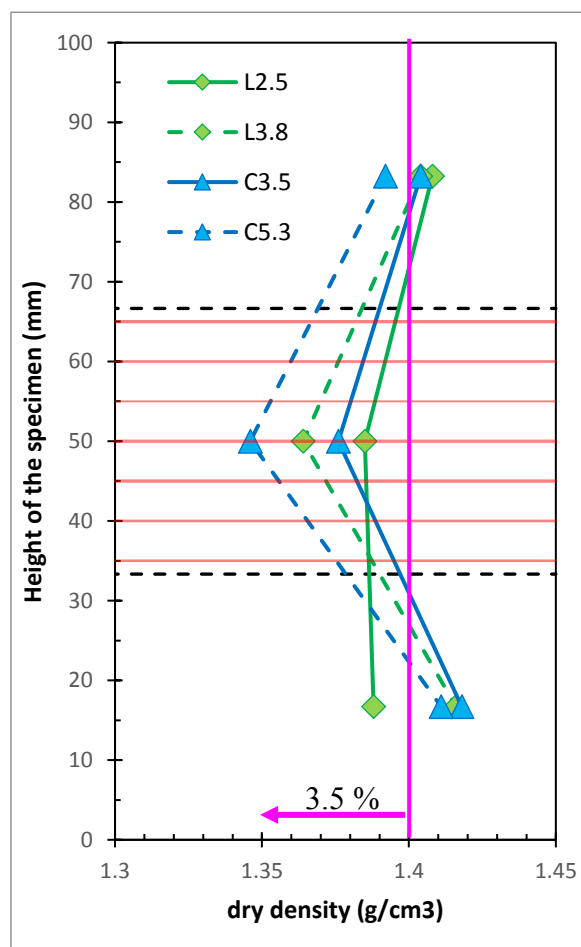
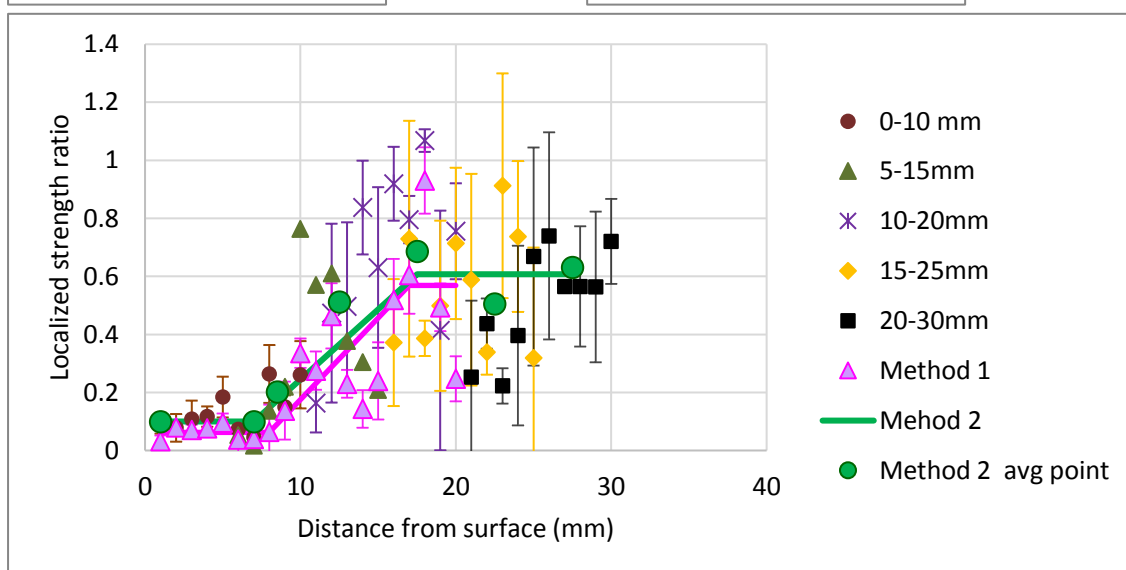
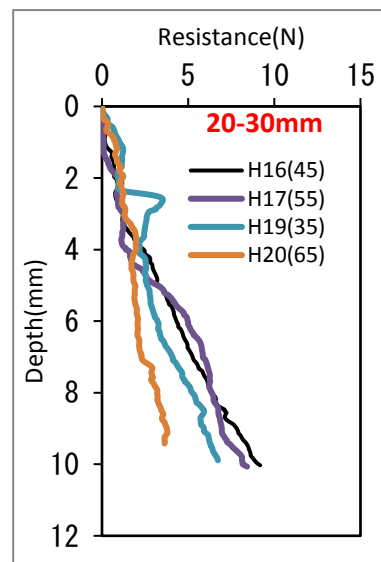
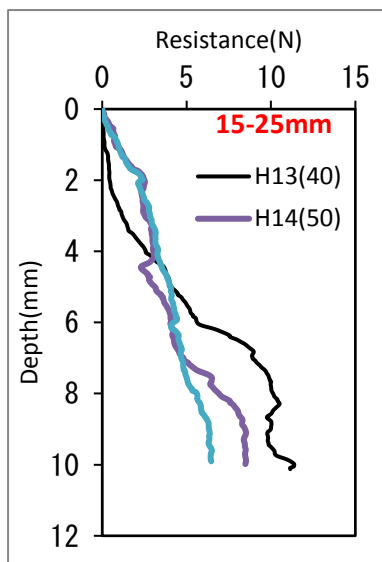
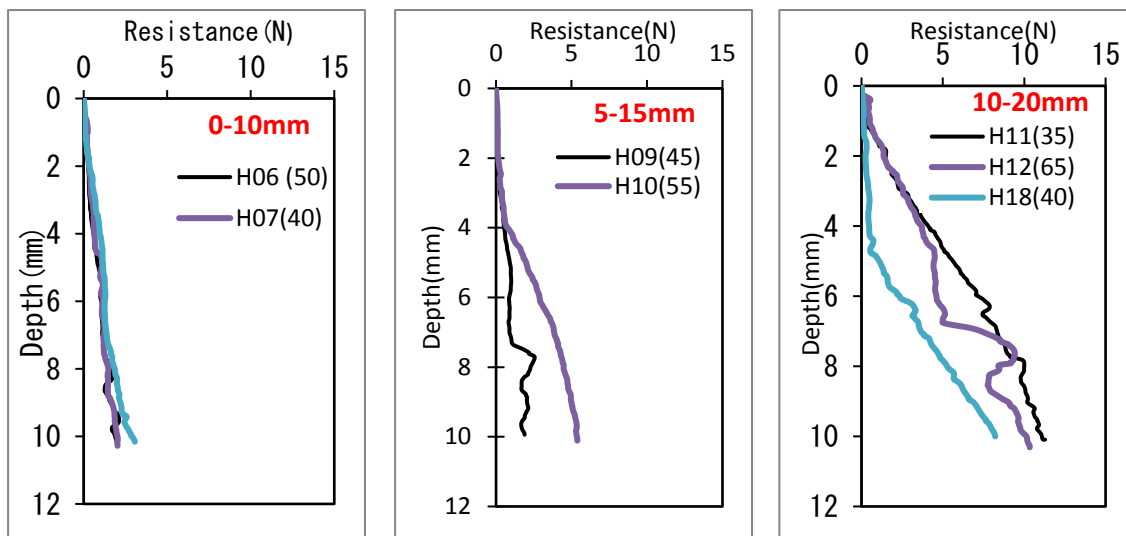
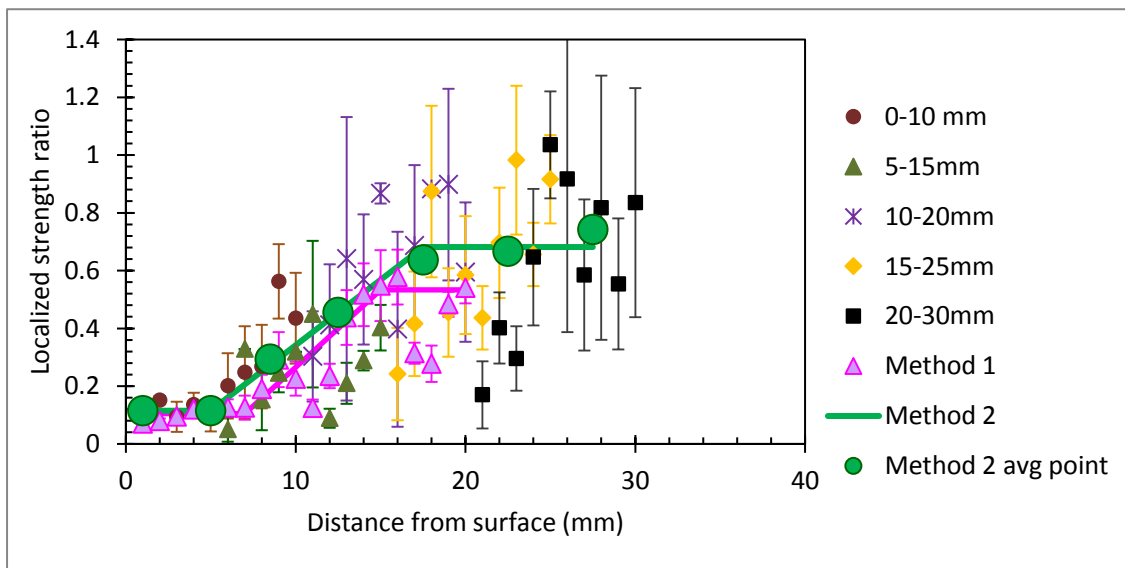
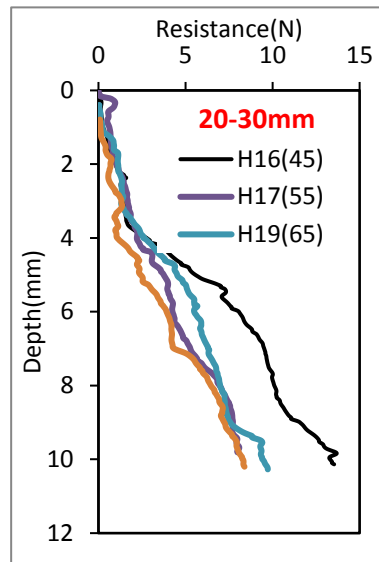
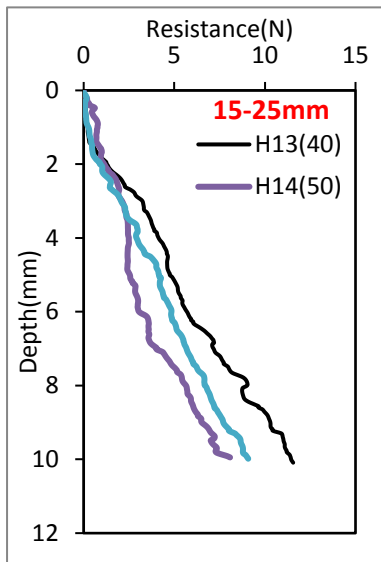
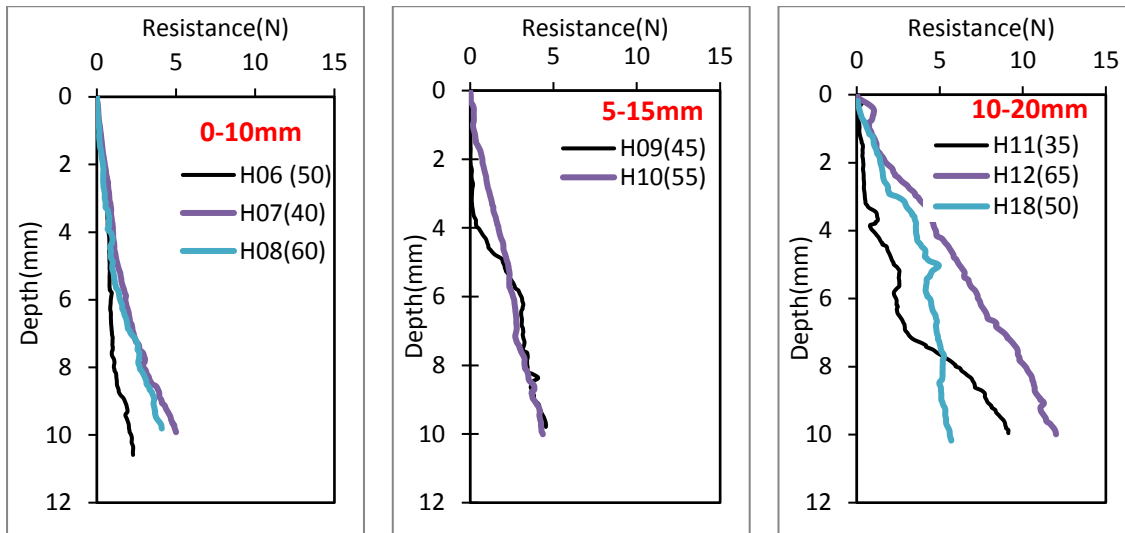


Figure Ap 2:2 Density variation along with depth

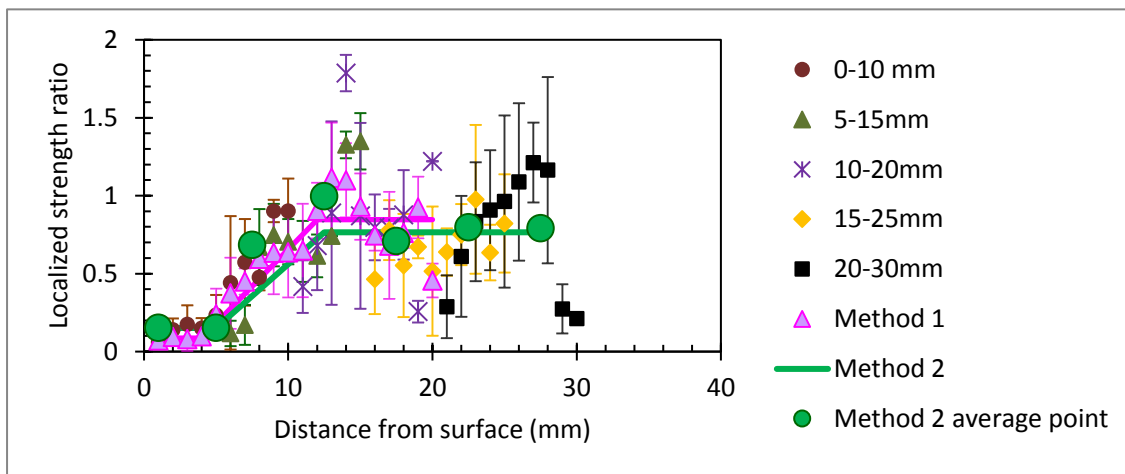
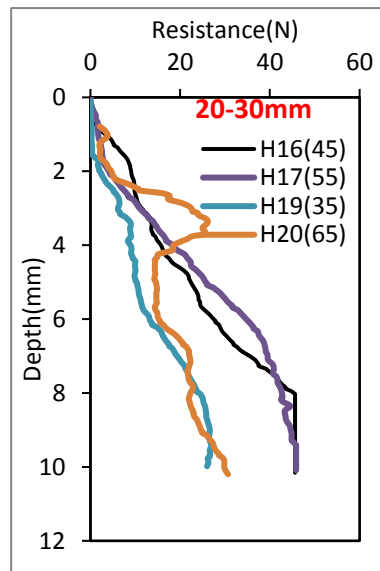
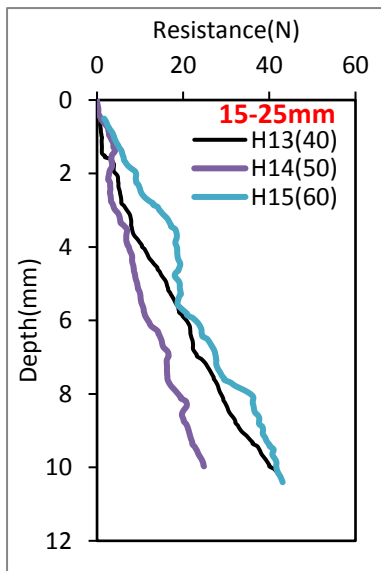
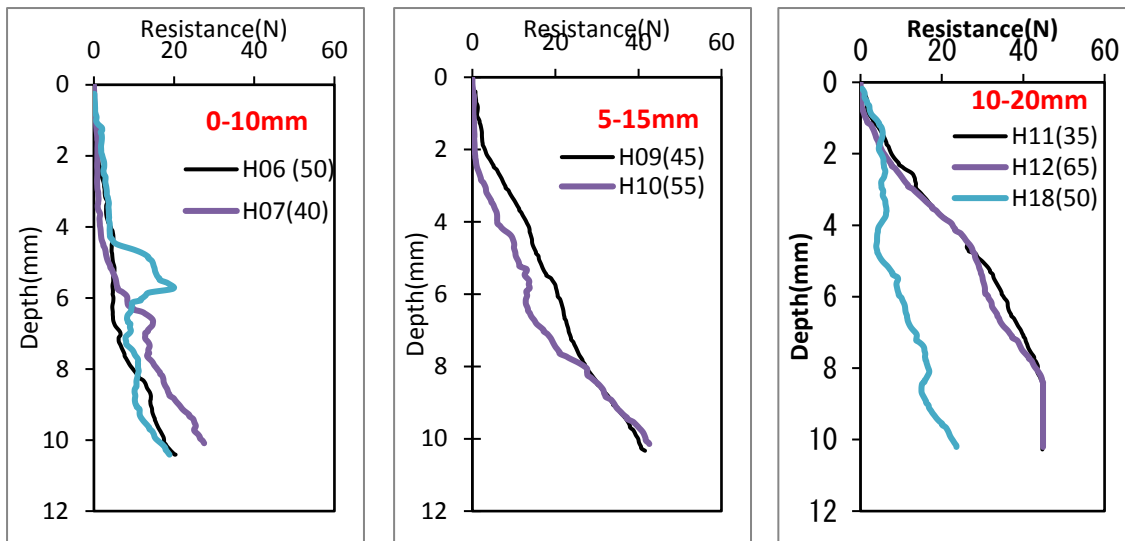
**Cement 3.5% - Soak acid (immature)**



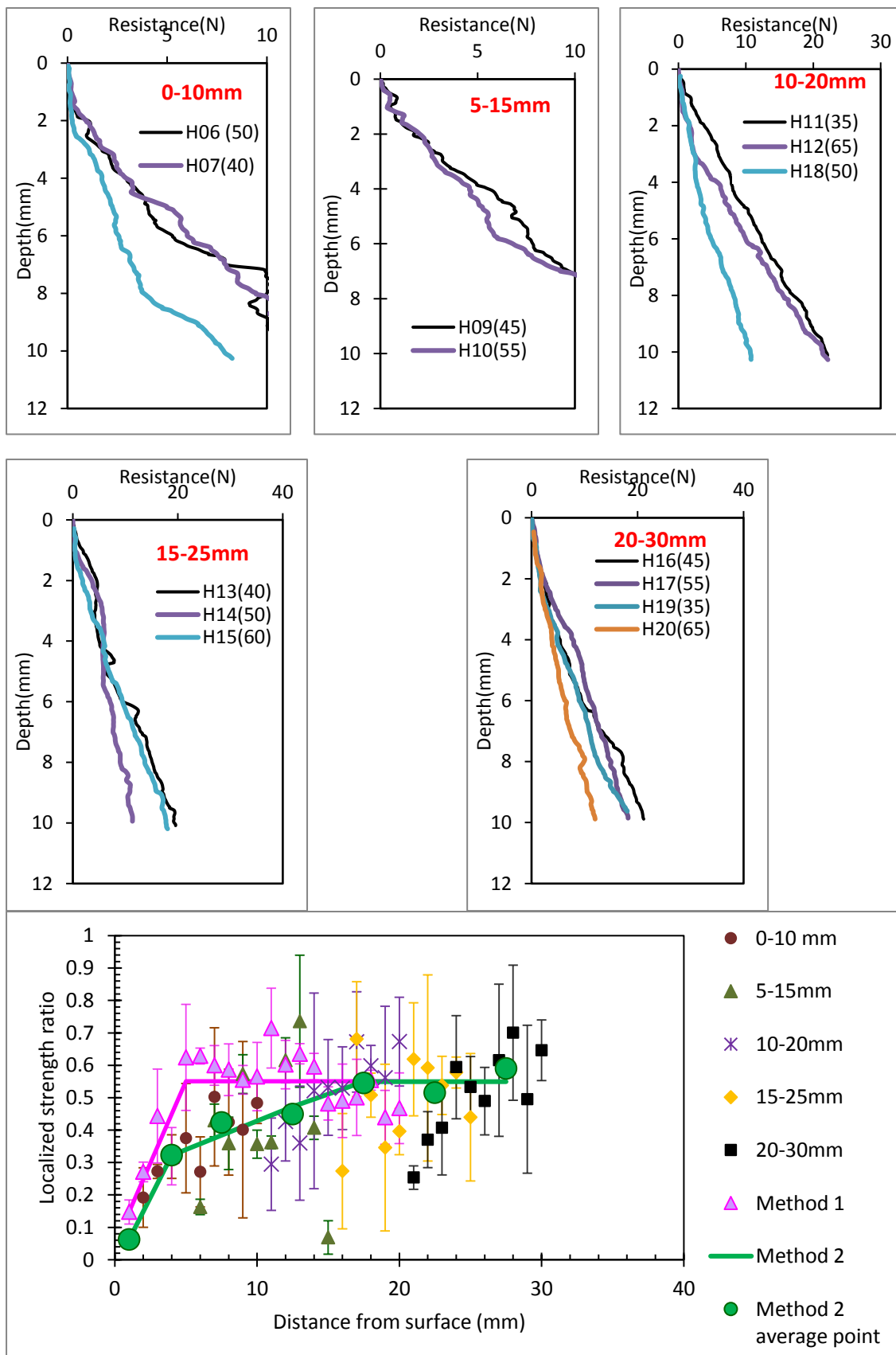
**Cement 3.5% - Soak Pure (immature)**



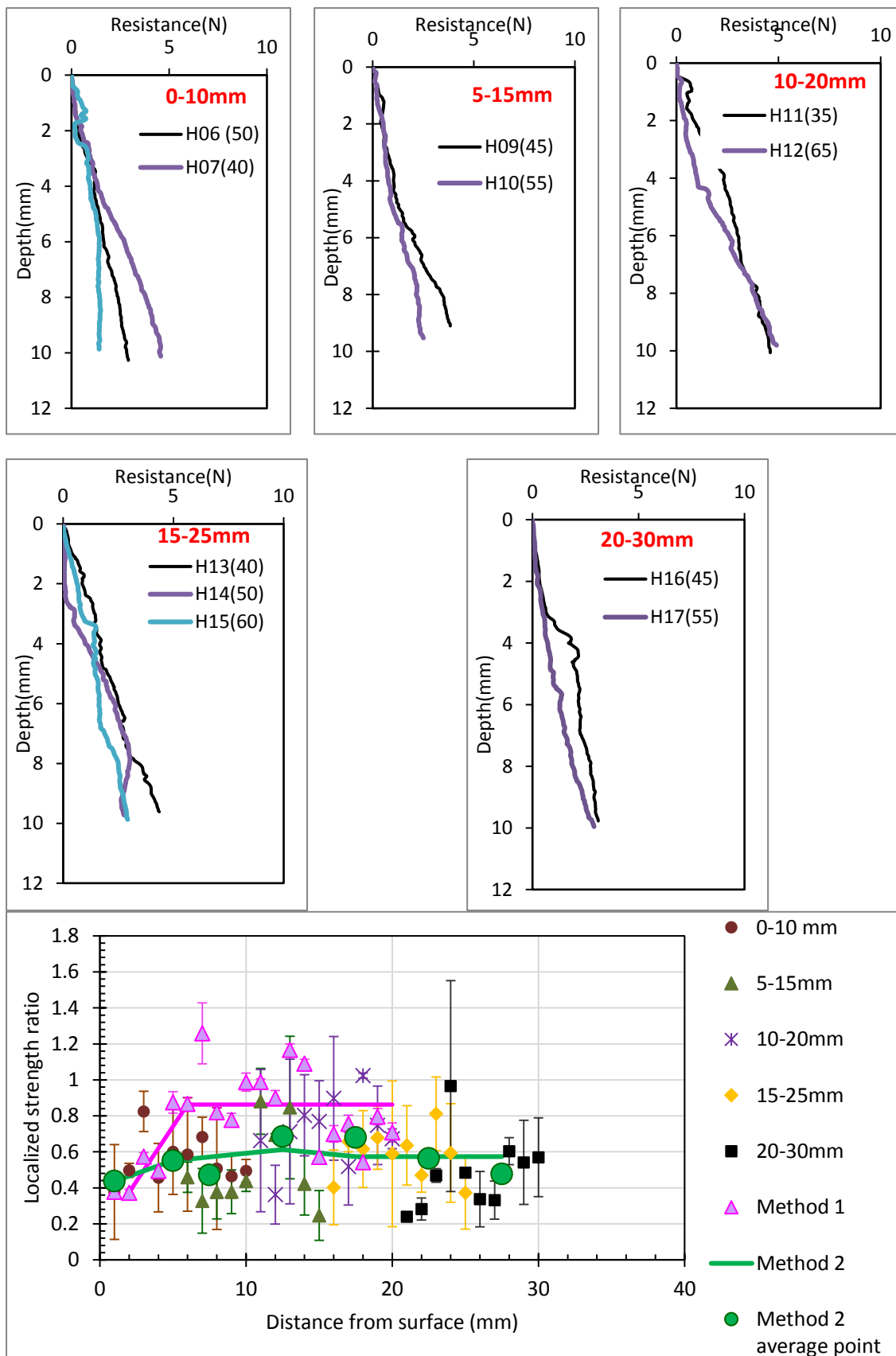
Cement 5.3% - Soak acid (immature)



**Lime 3.8% - Soak acid (immature)**



Lime 2.5% - Soak Acid (immature)



Lime 2.5% - Soak Pure (immature)

